Copyright is owned by the Author of the thesis. Permission is given for a copy to be downloaded by an individual for the purpose of research and private study only. The thesis may not be reproduced elsewhere without the permission of the Author.

# INVESTIGATING *EPICHLOË* ENDOPHYTE TRANSMISSION IN POACEAE HOSTS

A thesis presented in partial fulfilment of the requirements

for the degree of

Doctor of Philosophy

in

Plant Science

at Massey University, Manawatū,

New Zealand

**Wei Zhang**

**2018**

## Abstract

Vertically-transmitted *Epichloë* endophytes are agriculturally important fungi that colonise the aerial plant tissues of cool-season grasses within the Poaceae. Plants colonised by selected strains of *Epichloë* have superior protection from herbivores, thus affirming the important role of these endophytes in New Zealand farming systems. However, the development and marketability of endophyte-based products is often hindered by failures of endophyte transmission. This research investigated: (1) the developmental timing of endophyte colonisation of the seed embryo; (2) the identity of soluble sugars related to endophyte aging during seed storage; (3) the comparative endophyte hyphal density in the shoot apex and florets of high- and low-transmission genotypes; and (4) the molecular mechanisms for endophyte transmission from the inflorescence primordia to the unfertilised ovary.

Through a detailed investigation, utilising confocal microscopy to observe the distribution of *Epichloë coenophiala* strain AR601 in tall fescue (*Festuca arundinacea*), the endophyte hyphal colonisation in the ovary (pre-fertilisation) through to the fully mature seed stage was tracked. Confocal microscopy images revealed that endophytes have colonised the embryo sac before host grass fertilisation.

Tall fescue seeds, either endophyte-free or infected with one of three endophyte strains (AR584, AR605 or common-toxic) were subjected to a 2x2 factorial combination of two factors (accelerated aging or not, and seeds imbibed or not) and the sugar profiles in the seeds were investigated. Trehalose was the sugar that correlated most closely with the loss of endophyte during seed aging. After imbibition, the concentrations of trehalose

significantly declined in the endophyte-infected seed tissues, suggesting that the endophyte-oriented trehalose was utilised during imbibition. In addition, the sugar alcohols mannitol and ribitol were found in high concentrations in endophyte-infected embryo and endosperm tissues. These two sugars, therefore, could be potentially used as indexes to estimate endophyte biomass.

Two experiments were performed to investigate the endophyte hyphal density in the vegetative and reproductive tissues of perennial ryegrass (*Lolium perenne*): namely quantification of the endophyte density in the shoot apex tissues using real-time PCR, and analysis of immunoblot colour intensities of laterally bisected florets from six endophyte-grass genotypes (high-transmission [HT]: genotypes 11, 103, 107; low-transmission [LT]: genotypes 13, 79 and 83) and from three positions (bottom, middle and top) of the spike. The florets were collected at three growth stages (Stage I [unfertilised], Stage II [ten days after Stage I] and Stage III [twenty days after Stage I]). Real-time PCR analysis showed that the HT genotypes generally had higher endophyte densities in the shoot apex tissues compared with the LT genotypes. The immunoblot analysis showed that the immunoblot intensities in genotypes 11, 103, 107 and 13 were significantly higher than the other genotypes at Stage I, while the immunoblot intensities in the three HT genotypes were significantly higher than the LT genotypes at Stage II. However, there were no significant differences in the intensities between any of the genotypes at Stage III. Microscopy confirmed that HT genotypes carried a higher density of endophyte hyphae in the shoot apex tissues and ovaries (Stage I) than the LT genotypes. The data indicated that increased endophyte biomass is one factor that

enhances endophyte transmission from the parent plant to mature seeds in the HT genotypes.

RNA-Seq was used to measure the transcriptional response in two types of tissues (inflorescence primordia and the ovary) in the HT and LT genotypes. This study showed that 102 genes were commonly or exclusively differentially-expressed between the HT and LT genotypes in the inflorescence primordia and/or the ovary. Functional enrichment analyses by agriGO showed that the highly enriched gene ontology (GO) terms between the HT and LT genotypes were involved in serine family amino acid metabolic processes (GO:0009069) and cytoplasmic membrane-bounded vesicle function (GO:0016023) in both the inflorescence primordia and the ovary. More differentially-expressed genes (DEGs) coding for trehalose-6-phosphate phosphatase were induced during development from the inflorescence primordia to the ovary in the HT than the LT genotypes, demonstrating the higher demand for trehalose in the HT than the LT genotypes during endophyte transmission. More genes regulating salicylic acid were significantly repressed while more genes related to jasmonic acid metabolism were significantly induced during development from the inflorescence primordia to the ovary in the HT than the LT genotypes. It is proposed that the lower salicylic acid metabolism and higher jasmonic acid metabolism during development from the inflorescence primordia to the ovary in the HT genotypes might be related to increased endophyte transmission frequencies.

**Acknowledgements**

My sincere thanks go to my Massey supervisor Professor Cory Matthew and AgResearch supervisor Dr. Stuart Card for their unceasing guidance and endless encouragement. I would like to express my special appreciation to Cory because he spent a lot of hours helping me revise my thesis. To my co-supervisor Mr. Craig McGill and advisors Dr. Wade Mace and Dr. Milan Gagic, many thanks for their valuable advice and practical help. I was always inspired by their broad knowledge and motivated by their enthusiasm for research.

I acknowledge funding from the China Scholarship Council, AgResearch, a Sports Turf Bursary, the John Hodgson Pastoral Science Scholarship, and the Seed Tech Services Scholarship which has supported me financially and made it possible for me to focus myself on the study. I also would like to acknowledge Massey University Research Fund for supporting the research in Chapter 6.

I would like to thank Mike Christensen, Dr. Natasha Forester, and Dr. Brian Tapper for their important advice on the setting up of the experiment. Thanks also go to Paul Maclean for his great assistance in the data analysis of the RNA-Seq data, Dr. Christina Moon for her valuable comments on Chapter 6, and also Catherine McKenzie and Dr. Siva Ganesh for their advice on statistical analysis. I also want to thank for their assistance during my research at AgResearch, staff from the Plant-Fungi Interaction Team: Anouck de Bonth, Dr. Christine Voisey, Dr. Linda Johnson, Dr. David Hume, Dr. Richard Johnson, Benjamin Moody, Jaspreet Singh, Dr. Qianhe Liu, Suli Teasdale, Debbie Hudson, Leo Liu, Kati Ruppert, Dr. Wayne Simpson, Yulia Morozova,

and Davood Roodi. I also want to thank Denise Stewart for helping me organise computer access and for helping me complete the thesis process.

Many thanks to my dear friends Ivy Men, Fisher Yu, Lulu He, Xin Wang, Charlene Wang, Liru Zhu, Qinhua Shen, Carrie Sang, Chris Maxwell, Yang Li, Jana Muller in New Zealand and also many friends in China for their encouragement and support during my stay in New Zealand.

Special thanks to Ao Chen, my boyfriend for his endless love and support. Without his tenderness and encouragement, I would never have been able to pursue my PhD.

To my dear parents, thank you for your unconditional support and positive encouragement, even though we are thousands of miles apart. To my other family members and friends in both China and New Zealand, thank you all for your love, patience and support during my studies.

## Publications and Presentations

### Publications

Zhang W, Card SD, Mace WJ, Christensen MJ, McGill CR, Matthew C 2017. Defining the pathways of symbiotic *Epichloë* colonization in grass embryos with confocal microscopy. Mycologia 109(1): 153-161. (Chapter 3)

Zhang W, Card SD, Mace WJ, McGill CR, Christensen MJ, Matthew C 2017. The seed of life - investigating *Epichloë* embryo colonisation. 9th International Symposium on Fungal Endophytes of Grasses and 1st International Symposium on Plant Microbiomes. 28th September-2nd October 2015. AgriBioscience, Melbourne, Australia. (Poster)

### Presentations

McKenzie CM, Zhang W, Card SD, Matthew C, Mace WJ and Ganesh S 2017. To PCA or not to PCA. The International Biometric Society Australasian Region Conference. 26-30th November 2017. Kingscliff, New South Wales, Australia. (Presented by the first author)

## Table of Contents

## Glossary of Abbreviations

| Abbreviation | Full name |
|---|---|
| AA | Accelerated aging |
| ABA | Abscisic acid |
| ANOVA | Analysis of variance |
| Ara | D-arabitol |
| AU | Arbitrary units |
| CDA | Canonical discriminant analysis |
| cDNA | Complementary DNA |
| CMFDA | 5-chloromethylfluorescein diacetate |
| CT | Common-toxic |
| DEGs | Differentially expressed genes |
| DEPC | Diethyl pyrocarbonate |
| DL-ara | DL-arabinose |
| dw | Dry weight |
| ELISA | Enzyme-linked immunosorbent assays |
| Em | Embryo |
| Es | Endosperm |
| FC | Fold change |
| FDR | False discovery rate |
| Fru | Fructose |
| fw | Fresh weight |
| Gal | D-galactose |
| Galacti | Galactinol |
| GC-FID | Gas chromatography coupled with flame ionization detector |
| Glu | Glucose |
| Gly | Glycerol |
| GO | Gene ontology |
| HT | High-transmission (referring to % of host seeds with viable endophyte) |
| HPLC | High-performance liquid chromatography |
| Ino | Myo-inositol |
| KEGG | Kyoto Encyclopaedia of Gene and Genome |
| LSD | Least significant difference |
| LT | Low-transmission (referring to % of host seeds with viable endophyte) |
| Mal | Maltose |
| Man | Mannose |
| Manni | Mannitol |
| MANOVA | Multivariate analysis of variance |
| MPSS | Massively parallel signature sequencing |
| MSTFA | N-Methyl-N-(trimethylsilyl) trifluoroacetamide |
| ng | Nanogram |

Continued on the next page

| Abbreviation | Full name |
|---|---|
| NRPS-1 | Non-ribosomal peptide synthetase |
| nt | Nucleotide |
| PBS | Phosphate-buffered saline |
| PCR | Polymerase chain reaction |
| PDA | Potato dextrose agar |
| pg | Picogram |
| Raf | Raffinose |
| RH | Relative humidity |
| Rib | Ribitol |
| RIN | RNA integrity number |
| RNA-Seq | RNA sequencing |
| RO | Reverse osmosis |
| ROS | Radical oxygen species |
| RPKM | Reads per kilobase per million mapped reads |
| SAGE | Serial analysis of gene expression |
| SAM | Shoot apical meristem |
| SDS | Sodium dodecyl sulphate |
| SEC | Size exclusive column |
| Sor | Sorbitol |
| Suc | Sucrose |
| TEM | Transmission electron microscopy |
| TPIB | Tissue print immunoblot |
| TPP | Trehalose-6-phosphate phosphatase |
| TPS | Trehalose 6-phosphate synthase |
| Tre | Trehalose |
| Xyl | Xylose |
| Xyli | Xylitol |

## List of Figures

## List of Tables

# Chapter 1 Introduction

## 1.1 Background

Many members of the grass family Poaceae have co-evolved with asexual *Epichloë* species, which were previously known as *Neotyphodium* (Leuchtmann et al. 2014). Initially, these asexual *Epichloë* species were considered a serious problem in agriculture as some natural grass-endophyte associations produce secondary metabolites, in particular certain alkaloids, which are detrimental to livestock. Particularly notable are the lolitrems produced in endophyte-infected perennial ryegrass (*Lolium perenne*) that cause the disease known as ryegrass staggers, most often seen in animals grazing ryegrass pastures in late summer (Fletcher et al. 1981). Elimination of the endophyte from forage grasses is not always practical as many of these endophytes also produce bioactive compounds that protect their host plants against insect damage. Instead of eliminating these fungi from these forage grasses, strains of asexual *Epichloë* were identified that are less toxic to livestock whilst maintaining certain advantageous traits, especially insect deterrence. Selection and transfer of these endophytes into improved grass cultivars has resulted in non-toxic pastures with effective insect deterrence against pests, including Argentine stem weevil, black beetle and pasture mealy bug (Popay et al. 1999). Pasture varieties containing selected endophyte strains have received wide acceptance in the market. For example, perennial ryegrass seeds infected by AR1, AR37, Endo5 and NEA2 are commercially available for pasture uses in New Zealand. AR542 is commercialised in combination with improved tall fescue cultivars as MaxQ®/MaxP®, which are used in pastures in the USA and New Zealand. Meanwhile, AR601, a toxic endophyte branded as Avanex®, has been commercialised for use at airports to reduce

bird populations and incidence of bird strike to aircraft, with wide acceptance worldwide (Johnson et al. 2013).

The growth of these fungal symbionts is fully synchronised and highly regulated with that of their grass hosts (Christensen et al. 2008). Lineages of single fungal genotypes are transmitted maternally (vertically) through seeds following fungal colonisation of ovules and seed tissues during host flowering and seed formation (Philipson et al. 1986). With the onset of seed germination, hyphae within the shoot apical meristem start to colonise leaf primordia and auxiliary buds, spreading systemically throughout the above-ground parts of the plant (Christensen et al. 2007). Endophyte survival is firmly tied with that of the plant host, and both within host tissues and within the seed, the fungus is reliant on the plant for oxygen, nutrients, water and activation from dormancy. Many Poaceae genera may be colonised by *Epichloë* fungi at highly variable frequencies, ranging from 1–100% and this is true for those growing in natural grasslands or in managed pastures (Leyronas et al. 2001; Gundel et al. 2009b). Endophyte transmission failures can occur during plant development (failure in colonising seedlings, tillers, spikes, spikelets and seeds) or loss of vitality during seed storage. Poor endophyte transmission during both plant development and seed storage is a great hindrance to the commercialisation of grass-endophyte products. However, little information exists on the factors that are responsible for this transmission failure.

## 1.2 Objectives

There were three main objectives in the work described in this thesis: 1) to investigate the pathways of symbiotic *Epichloë* colonisation in grass embryos; 2) to explore the sugar metabolites associated with the loss of endophyte viability within seeds during

storage; and 3) to understand the molecular mechanisms for the failure of endophyte transmission by using RNA-Seq.

## 1.3 Thesis structure

Seven chapters are included in this thesis:

**Chapter 1** (this chapter) presents general background information and gives an introduction to the entire thesis. The specific objectives and the thesis structure are also included in this chapter.

**Chapter 2** is a literature review that provides an overview of the early awareness of *Epichloë* endophyte and its lifecycle, the status of endophyte technology within pastoral practice, current research, and a review of the published papers related to the research components in this thesis.

**Chapter 3** explores and describes the full pathway of *Epichloë* colonisation from the early embryo sac stage to the mature seed stage using fluorescent dyes and confocal microscopy.

**Chapter 4** investigates the sugar metabolites present within the seed embryo and endosperm tissues in endophyte-free and endophyte-infected grass accessions and in response to accelerated aging and imbibition.

**Chapter 5** compares the endophyte biomass of AR37, an important commercial endophyte strain in New Zealand, within the shoot apex tissues and floral tissues of high- (HT) and low-transmission (LT) perennial ryegrass genotypes.

**Chapter 6** tests the differences in gene expression between HT and LT perennial ryegrass genotypes investigated in Chapter 5. Tissues of both inflorescence primordia and unfertilised ovary were subjected to RNA isolation and sequencing with a high-throughput sequencing platform. The transcriptomic data achieved from sequencing were analysed with the assistance of a biostatistician.

**Chapter 7** is a general summary which collates and synthesises the pieces of component research presented in Chapters 3 – 6 and provides discussion on the research gaps that remain after completion of this PhD research project. Based on the findings from this research, recommendations for future investigation are given.

# Chapter 2 Literature review

## 2.1 Definition of the term endophyte

The term 'endophyte' is derived from two Greek words, ένδο meaning within and φυτος meaning plant (De Bary 1866). There are, however, many definitions within the literature with no consensus so far reached (Hyde et al. 2008). These definitions range from the very literal on the one hand (and therefore used to describe any microorganism found within a plant), to the more refined encompassing only microorganisms that cause unapparent and asymptomatic infections entirely within plant tissues (Wilson 1996; Petrini 1991). Wilson defined endophytes as "Fungi and bacteria which, for all or part of their life cycle, invade the tissues of living plants and cause unapparent and asymptomatic infections entirely within plant tissues, but cause no symptoms of disease." Petrini defined endophytes as "all organisms inhabiting plant organs that at some time in their life, can colonise internal plant tissues without causing apparent harm to the host." Petrini's definition therefore includes other microbial genera such as some green algae, whereas Wilson's does not (Weinberger et al. 2005).

## 2.2 Relevance of forage grasses and *Epichloë* in New Zealand

### 2.2.1 Early awareness of grass endophytes

Plants often form symbiotic relationships with microorganisms, commonly bacteria and fungi but also archaea, oomycetes, protists and viruses (Chanway 1996; Card et al. 2016). Two of the most commonly studied groups of microorganisms that form strong associations with grasses (family Poaceae) are Clavicipitaceous endophytic fungi of the genus *Epichloë* and mycorrhizal fungi (White Jr et al. 1993; Brundrett 2006; Johnson et

al. 2013). *Epichloë* can confer abiotic and biotic stress resistance to their hosts (Clay et al. 1999). Most of the endophytic fungi normally infect the aerial portions of their host grass (Christensen et al. 2002; Christensen et al. 2007). Observations of *Epichloë* species (named *Sphaeria* or *Acremonium* before 1996; while asexual *Epichloë* was named *Neotyphodium* between 1996 and 2013) in pasture grass species, particularly *Lolium* and *Festuca* spp., have been reported since the 19$^{th}$ century and include among others (Vogl 1898; Freeman 1904; McLennan 1920; Sampson 1933). Due to advances in molecular biology particularly in the areas of taxonomy and systematics, the number of known *Epichloë* species has greatly increased in more recent years. *Epichloë* species have been reported to colonise numerous tribes within the subfamily Poöideae and *Epichloë* species display specificity in the host species they can infect (Table 2.1). Also, investigators have become aware of alkaloid secondary metabolites produced by the symbionts, and the roles of those alkaloids in protecting the host from biotic stress. In New Zealand, the most intensively studied associations are between perennial ryegrass and *E. festucae* var. *lolii* while in the USA the most commonly studied association is between tall fescue and *E. coenophiala*. Both these grasses are found within the tribe Poeae. It is generally understood that the grass hosts provide a nutrient supply and shelter, as well as a form of dissemination via seed for the fungus, in return, plant hosts gain protection against biotic and abiotic stresses (Tanaka et al. 2012; Johnson et al. 2013).

**Table 2.1 Currently known endophytes of the genus *Epichloë* and the host grasses that they associate with.**

| Fungal species (and taxonomic groupings) | Natural grass host | Grass tribe | Reference |
|---|---|---|---|
| *E. amarillans* | *Agrostis hyemalis* | Aveneae | (Schardl 2001) |
| *E. aotearoae* | *Echinopogon ovatus* | Poeae | (Moon et al. 2002) |
| *E. australiense* | *Echinopogon ovatus* | Poeae | (Moon et al. 2002) |
| *E. baconni* | *Calamagrostis villosa* | Poeae | (Moon et al. 2000) |
| *E. brachyelytri* | *Brachyelytrum erectum* | Brachyelytreae | (Moon et al. 2000) |
| *E. bromicola* | *Bromus* spp. | Bromeae | (Moon et al. 2000) |
| | *Hordelymus europaeus* | Triticeae | |
| *E. canadensis* | *Elymus canadensis* | Triticeae | (Charlton et al. 2012; Ulrich et al. 2014) |
| *E. chisosa* | *Achnatherum sibiricum* | Stipeae | (Li et al. 2015) |
| *E. clarkii* | *Holcus lanatus* | Poeae | (Moon et al. 2000) |
| *E. cabralii* | *Phleum alphinum* | Poeae | (Mc Cargo et al. 2014) |
| *E. coenophiala* (FaTG-1) | *F. arundinacea* | Poeae | (Moon et al. 2004) |
| FaTG-2 | *F. arundinacea* | Poeae | (Tanaka et al. 2005) |
| FaTG-3 | *F. arundinacea* | Poeae | (Tanaka et al. 2005) |
| *E. danica* | *Hordelymus europaeus* | Triticeae | (Leuchtmann et al. 2013) |
| *E. disjuncta* | *Hordelymus europaeus* | Triticeae | (Leuchtmann et al. 2013) |
| *E. elymi* | *Bromus kalmii* | Bromeae | (Schardl et al. 2005) |
| | *Elymus* spp. | Triticeae | |
| *E. festucae* | *Festuca* spp. | Poeae | (Leuchtmann et al. 2000; Schardl 2001) |
| | *Lolium* spp. | | |
| | *Koeleria* spp. | | |
| *E. festucae* var. *lolii* (LpTG -1) | *L. perenne* | Poeae | (Tanaka et al. 2005) |
| LpTG-2 | *L. perenne* | Poeae | (Tanaka et al. 2005) |
| *E. funkii* | *Achnatherum robustum* | Stipeae | (Moon et al. 2007) |
| *E. gansuensis* | *Achnatherum sibiricum* | Stipeae | (Zhang et al. 2010) |
| *E. guerinii* | *Melica ciliata* | Poeae | (Moon et al. 2007) |
| *E. glyceriae* | *Glyceria striata* | Meliceae | (Moon et al. 2000) |
| *E. hordelymi* | *Hordelymus europaeus* | Triticeae | (Leuchtmann et al. 2013) |
| *E. liyangensis* | *Poa pratensis* | Poeae | (Kang et al. 2011) |
| *E. melicicola* | *Melica dendroides* | Poeae | (Moon et al. 2002) |
| | *Phleum pratense* | Poeae | (Moon et al. 2002) |
| *E. mollis* | *Holcus mollis* | Poeae | (Berry et al. 2015) |
| *E. occultans* | *L. multiflorum* | Poeae | (Moon et al. 2000) |

Continued on the next page.

| Fungal species (and taxonomic groupings) | Natural grass host | Grass tribe | Reference |
|---|---|---|---|
| *E. pampeana* | *Bromus auleticus* | Bromeae | (Iannone et al. 2009) |
| *E. sibiricum* | *Achnatherum sibiricum* | Stipeae | (Zhang et al. 2010) |
| *E. schardlii* | *Phleum alpinum* | Poeae | (Tadych et al. 2014) |
| *E. siegelii* | *L. pratense* | Poeae | (Moon et al. 2004) |
| *E. sinofestucae* | *F. parvigluma* | Poeae | (Chen et al. 2009) |
| *E. stromatolongum* | *Calamagrostis epigeios* | Poeae | (Ji et al. 2009) |
| *E. sylvatica* | *Brachypodium sylvaticum* | Brachyelytreae | (Moon et al. 2000) |
| *E. tembladerae* | *Poa huecu* | Poeae | (Iannone et al. 2009) |
| *E. typhina* | *F. arundinacea* | Poeae | (Alderman et al. 1997; Moy et al. 2000; Schardl et al. 2005) |
| | *Poa* spp. | Poeae | |
| | *Phleum pratense* | Poeae | |
| | *Dactylis glomerata* | Dactylidinae | |
| *E. typhina* var. *canariense* | *Poa nemoralis* | Poeae | (Moon et al. 2000) |
| *E. uncinata* | *F. pratensis* | Poeae | (Leuchtmann et al. 2014) |

LpTG-2: *L. perenne* taxonomic grouping 2;

FaTG-2&3: *F. arundinacea* taxonomic groupings 2 & 3.

### 2.2.2 Historical account of perennial ryegrass and tall fescue breeding in New Zealand

Perennial ryegrass and tall fescue, together with their microbial endophytes, were imported into New Zealand from Europe in the 1800s (Siegel et al. 1985; Stewart 2006). The grasses arrived intentionally while the microorganisms, including *Epichloë* spp. arrived unintentionally as their very existence was unknown at the time. The original perennial ryegrass germplasm from Europe was winter-dormant, and therefore unable to exploit the opportunity for some winter growth in the milder climate of New Zealand (Stewart 2006). By selection within a population of plants collected from Hawkes Bay (later known as the 'Hawkes Bay Ecotype'), elite germplasm was developed in the 1930s at Palmerston North. This was initially known as New Zealand certified ryegrass, and was released for sale in 1936 and possessed enhanced traits including increased yield, plus improved winter and spring growth characteristics. New Zealand certified ryegrass was renamed 'Grasslands Ruanui' in 1964 (Easton 1983). Through hybridisation with Italian

ryegrass (*Lolium multiflorum*), which exhibits high winter growth, the world's first hybrid ryegrass cultivar, named 'Grasslands Manawa' was developed and released for sale in 1943. 'Grasslands Manawa' was later backcrossed with perennial ryegrass to produce a hybrid cultivar named 'Grasslands Ariki' which exhibited a higher winter productivity than 'Grasslands Ruanui'. A further step-change occurred when the 'Mangere' ecotype (a perennial ryegrass ecotype from the farm of Mr Trevor Ellett in South Auckland), was identified as having superior productivity and summer performance compared to 'Grasslands Ruanui' and 'Grasslands Ariki'. Subsequently, two new perennial ryegrass cultivars, 'Grasslands Nui' and 'Ellett', were released in 1975 and 1980, respectively. Further cultivars were later produced from the 'Mangere' ecotype, including among others 'Yatsyn 1' and 'Bronsyn', which were the foundation for the modern New Zealand ryegrass cultivars (Stewart 2006). Since the 1980s, late-flowering ryegrass cultivars have been developed and have been particularly popular with New Zealand farmers as the period of leafy herbage growth in spring has been extended by some weeks into the early summer. More recently, the introduction of Spanish germplasm has improved the summer performance of these cultivars, especially in warm temperatures or under periods of moisture deficit (Lancashire 2006). Plant breeders also developed the technology for doubling the chromosome number of natural diploid perennial ryegrass (2n = 14) to form tetraploids (4n = 28). Tetraploids generally have larger tillers than diploids, reflected in their larger cell size, which results in leaves that have greater water-soluble carbohydrates (WSC), and are more palatable to animals and so provide improved animal uptake and production (Charlton et al. 1999). However, tetraploids are regarded in industry circles as being somewhat less persistent than diploids (Anderson 1973) and yield trials by a collaborative consortium of New Zealand seed companies

(New Zealand Plant Breeding and Research Association 2016) indicate that tetraploids are not higher yielding than diploids, so their use or not comes down to farmer preference.

Tall fescue was first introduced into New Zealand from Europe in the 1880s (Anderson 1982), but was not widely used as a pasture species due to its unpalatable texture. In the first half of the 20$^{th}$ century, tall fescue became established in the Midwest of the USA as the primary pasture species because of its natural adaptation to both warm summer and cold winter temperatures, as compared with species like perennial ryegrass. As a result, farmers and extension workers in areas of New Zealand, where perennial ryegrass struggled to cope with local climate conditions, became interested in tall fescue as an alternative forage grass. One of the first cultivars trialled in New Zealand was a British cultivar named 'Aberystwyth S170' which subsequently demonstrated a high drought tolerance with resistance to grass grub (Watkin 1975). Later, the cultivar 'Grasslands Roa' was developed by government scientists at D.S.I.R. Grasslands Division (now AgResearch Ltd.) and released for sale in 1982. 'Grasslands Roa' was sold without endophyte and was the main tall fescue cultivar used in New Zealand until 1994 (Brock 1983), when it was superceded by the Grasslands cultivars 'Easton' and 'Flecha' (European [Continental] and Mediterranean types, respectively), and cultivars developed outside of New Zealand, such as 'Jesup', bred in the USA and 'Tower', bred by DLF Seeds Ltd. After this time period, a step-change occurred in the development of new grass cultivars in New Zealand and the USA, with the discovery and applied use of selected *Epichloë* grass endophyte strains that could be introduced into elite germplasm

and supply additional beneficial traits to the grass. These symbiotic fungi had the capacity to enhance cultivar performance, even more than plant breeding.

From 2002, grass-endophyte associations such as the product Jesup MaxQ®, a combination of the tall fescue cultivar 'Jesup' and the endophyte strain AR584, became available to farmers. The European and Mediterranean types of tall fescue differ primarily in their physiological responses to summer moisture deficit (Assuero et al 2001). Of the two types, European tall fescue is the more commonly used in New Zealand with cultivars of this type able to grow throughout the year with greater activity during summer (Milne 2001). Mediterranean tall fescue cultivars are more suited to dry climates than European types (Burnett 2006), and have been bred to enhance pasture production in lower rainfall regions (Clark et al. 2009). Tall fescue is generally regarded as having slower establishment but deeper rooting depth, compared to perennial ryegrass, and the latter trait is a factor in the moisture deficit tolerance of tall fescue (Kemp et al. 1999).

### 2.1.3 Role of *Epichloë* endophyte in New Zealand pastoral agriculture

The presence of selected *Epichloë* strains within elite grass germplasm can improve the biotic and abiotic stress tolerance of both perennial ryegrass and tall fescue, and this discovery has been especially relevant in New Zealand. The associations, specifically between *E. festucae* var. *lolii* with perennial ryegrass and *E. coenophiala* with tall fescue are now positively impacting New Zealand pastoral agriculture with new endophyte strains contributing approximately $200 M NZD per annum to the New Zealand economy (Johnson et al. 2013), and with endophyte-infected ryegrass pastures producing more digestible dry matter to grazing livestock than endophyte-free pastures

(Easton 1999). Researchers in New Zealand first became aware of these endophytic fungi in the 1940s, and considered their presence benign (Neill 1940; Cunningham 1958). The same fungi were then recognised as being detrimental to livestock, when some endophyte-grass associations were found to produce toxic alkaloids (Easton et al. 1996). A few years later, indole diterpene alkaloids (lolitrems) were found to be responsible for ryegrass staggers (a neurological disorder in grazing animals) in New Zealand (Fletcher et al. 1981). Awareness of the potential for animal toxicosis was the reason for the release of 'Grasslands Roa' tall fescue as an endophyte-free variety. However, the endophyte-free cultivars of perennial ryegrass were found to be susceptible to insect attack, notably by Argentine stem weevil (*Listronotus bonariensis*). A further scientific breakthrough was made when the presence of the endophyte and the insect deterrent properties of the alkaloid peramine were discovered. This secondary metabolite benefits its host grass by conferring deterrence against this insect pest (Rowan et al. 1986a; Rowan et al. 1986b). This finding provided the logical impetus for the creation of an endophyte programme that could discover and characterise endophytes that could be used for the development of artificial grass-endophyte associations with low or no animal toxicity while deterring insect pests (Johnson et al. 2013).

A well-structured discovery pipeline has evolved at AgResearch Ltd. over many years within the currently named Plant-Fungal Interactions Team (de Bonth et al. 2015). The pipeline starts with the collection of suitable wild grass germplasm usually in the form of seed selected and obtained via international gene-banks and/or collection expeditions to locations of interest. Published methods are then used to identify the presence of endophyte within this germplasm before simple sequence repeat (SSR)

analysis can identify genetically unique strains not currently present in the AgResearch culture collection. These unique strains are then further characterised with respect to their molecular diversity, secondary metabolite profiles and bioactivity. Candidate endophyte strains are then selected for inoculation into elite grass cultivars and populations from subsequent plant generations are evaluated through specifically designed agronomic and toxicological screens (Johnson et al. 2013; Card et al. 2014a; de Bonth et al. 2015). Although it may take more than 10 years to identify an endophyte strain that may offer commercial potential, the AgResearch pipeline (in association with Grasslanz Technology Ltd., the commercialisation arm of AgResearch), has produced commercially successful products in ryegrass including AR1 and AR37. AR1 induces no ryegrass staggers while deterring Argentine stem weevil and other insect pests through the production of the alkaloid peramine (Johnson et al. 2013). Incorporating AR1 into elite ryegrass cultivars also increased milksolids per hectare by 8%, compared with the common-toxic endophyte strain (Bluett et al. 2005). AR37 is an endophyte strain originally sourced from French germplasm that produces epoxy-janthitrems, compounds that play a role in decreasing insect activity (by inhibiting their feeding) while having minimal adverse animal production effects (Thom et al. 2013). They are also suspected of being a cause of a form of ryegrass staggers, however, on average the symptoms are less severe and less frequent than those experienced with forage containing the common toxic endophyte (Johnson et al. 2013). Further grass endophyte products exist in the New Zealand pastoral industry and include NEA2 and related strains (owned by New Zealand Agriseeds Ltd.) which can be artificially associated with both diploid and tetraploid perennial ryegrass cultivars to give a spectrum of insect resistance (Popay et al. 2011). More recently at least two other companies have entered the

commercial market with their own strains of proprietary endophyte sold with ryegrass or tall fescue cultivars. The presence of selected *Epichloë* endophyte strains in pasture grasses is now seen by many as being a necessary component of forage swards including newly sown ryegrass pastures (Bouton et al. 2002). Today over 70% of ryegrass seed used in New Zealand contains one of several selected endophyte strains (Card 2015).

Finally, infection of a host grass by asexual *Epichloë* species can also offer many other benefits that have been little researched to date. Examples include resistance to fungal pathogens (Chynoweth et al. 2012) and tolerance to abiotic stresses including drought (Secks et al. 1999; Gundel et al. 2006; Nagabhyru et al. 2013; He 2016), low soil nitrogen (Bacon 1993), salt (Reza Sabzalian et al. 2010; Yin et al. 2014), and heavy metals (Liu et al. 1996; Malinowski et al. 1999; Ren et al. 2011).

### 2.1.4 Role of *Epichloë* in bird and animal deterrence

Another innovation developed in New Zealand that incorporates endophyte technology is AVANEX®, a product brand that includes two types of grass-endophyte association, both turf-types, one in tall fescue for use as a wildlife deterrent at airports (mainly birds) and the second in ryegrass, as a wildlife deterrent for sports fields and recreational areas (Pennell et al. 2015; Pennell et al. 2017b). The tall fescue association is with the cultivar Jackal, infected with the endophyte *E. coenophiala* strain AR601 and the second is a perennial ryegrass cultivar, Colosseum, infected with the endophyte *E. festucae* var. *lolii* strain AR95. The mechanism behind wildlife deterrence of AR601-grass associations involves the production of relatively high amounts of multiple alkaloid compounds. Ergovaline has been implicated in the inducement of an avoidance behaviour in a range of mammals and birds while loline alkaloids reduce insect numbers, thus indirectly

making the area less attractive to insect-feeding species (Miller et al. 2017). A reduction in bird numbers at several New Zealand airports and thus a reduced risk of bird collisions with aircraft, has been reported (Pennell et al. 2011; Pennell et al. 2017a). As a result, AVANEX® is gaining international adoption for use in airports and recreational areas.

## 2.3 Life cycles of asexual and sexual *Epichloë* species

*Epichloë* species can be categorised into three groups according to their life cycle, namely Type I, Type II and Type III (Clay et al. 2002). Type I endophytes only disseminate horizontally (i.e via spores) while Type III endophytes only spread vertically (i.e. with transmission between plant generations via hyphal infection of seed) while Type II endophytes can disseminate both horizontally and vertically (Chung et al. 1997; Gundel et al. 2011a).

The vertical transmission path of these fungi and their distribution within their host grass is illustrated in Figure 2.1. Specifically, within mature seed, epichloid hyphae colonise two main locations; within the embryo tissues (including the scutellum, coleoptile, plumule, radicle and coleorhiza tissues, as well as between the embryo and the endosperm [previously referred to as the 'infection layer']) (Philipson et al. 1986) and between the aleurone and pericarp layers (Figures 2.1A) (Christensen et al. 2009; Card et al. 2011). The hyphae between the aleurone and pericarp layers are remnants of fungus left over from the colonisation of the nucellus layer and are not involved in transmission since the endosperm will be degraded upon germination (Latch 1982). Instead it is believed that the hyphae in this layer provide protection for seeds during germination by carrying a store of secondary metabolites including alkaloids that deter certain insects, mammalians and birds from eating the seed (Ball et al. 1997). Recent

studies have confirmed that endophyte-infected perennial ryegrass seed can have high concentrations of ergovaline, chanoclavine and peramine present many years after the endophyte has died (Mace et al. unpublished). Mycelia are deposited between the embryo and endosperm within the infection layer (Figures 2.1B) (Card et al. 2011). The hyphae between the embryo cells extend into the leaf primordia after seed germination, and few hyphae are found in the radicle or in mature roots. In the seedling, a network of hyphae is typically found concentrated in the seedling meristem regions (Figures 2.1C), and hyphae originating from this meristematic zone colonise leaf laminae, forming filaments that are long and parallel to the leaf axis. In mature tillers, the network of highly branched hyphae meristematic region remains (Figures 2.1D) (Musgrave et al. 1984; Easton 1999), and as the buds develop, these provide the opportunity for hyphae to grow into each axillary bud and colonise the new plant tillers. In individual tillers, from the leaf base upwards, the hyphae are orientated longitudinally along the leaf axis but sometimes branched (Hinton et al. 1985; Christensen et al. 2007). Hyphae extend by intercalary growth among enlarging plant cells and cease branching and elongating when their host plant stops growing while remaining metabolically active (Christensen et al. 2007). Upon vernalisation, each vegetative grass meristem has the potential to become a reproductive meristem. In this case the mycelium which was located in the vegetative meristem is already embedded in the reproductive meristem tissues as they develop and will usually extend further into the maturing inflorescence and subsequently into the plant ovaries. In endophyte-infected ovaries, endophyte hyphae can be identified among ovary wall cells, nucellus cells and stigma cells (Figures 2.1E). In this way, the endophyte will transmit to the next generation (Christensen et al. 2007, 2009) after fertilisation.

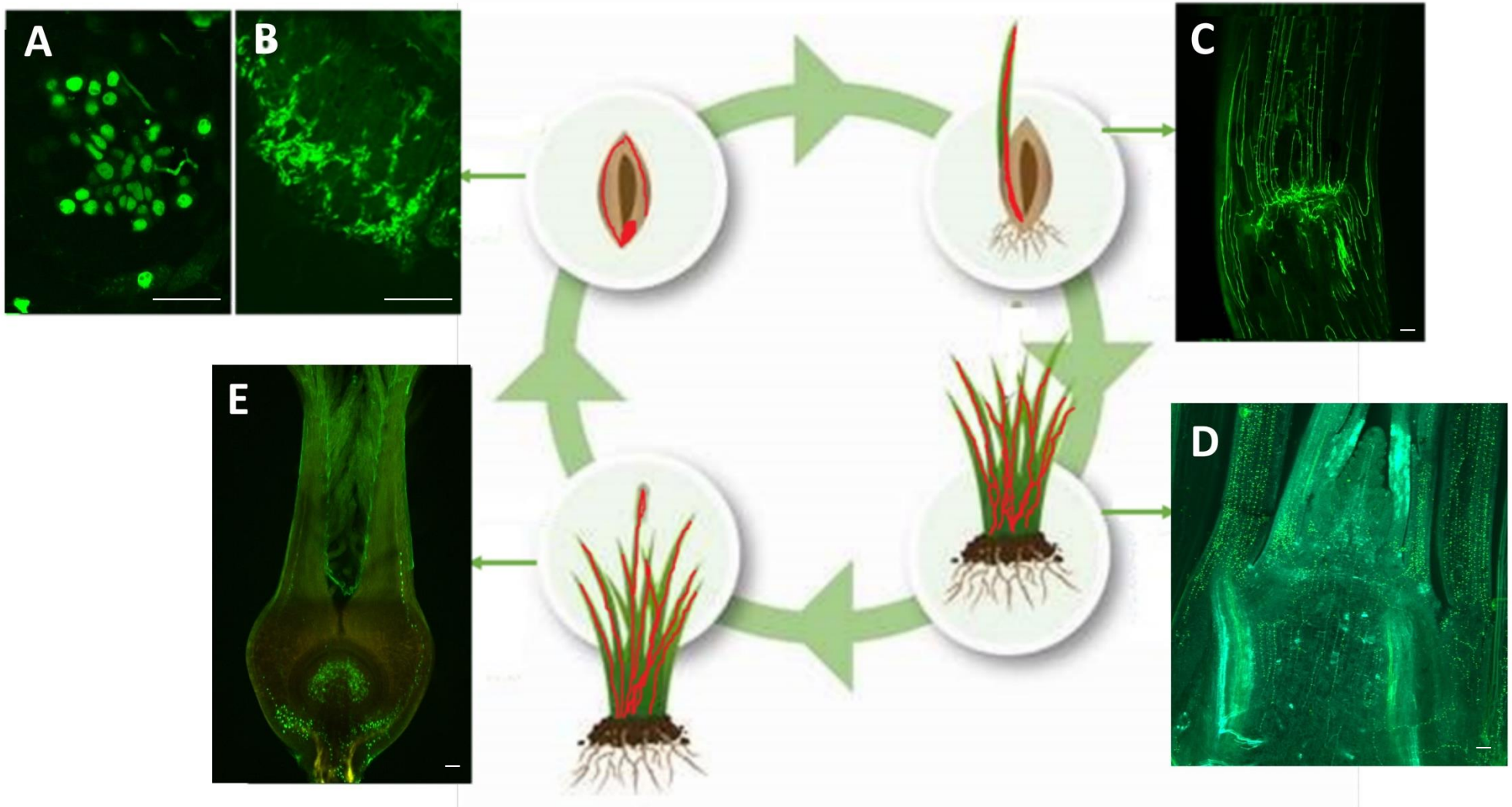
A
B
C
D
E

**Figure 2.1 The lifecycle of asexual *Epichloë* species.** The red colour indicates the locations of asexual *Epichloë* species. This lifecycle figure was modified from the figure from PGG Wrightson Seeds Ltd. (http://www.pggwrightsonseeds.com/), and the confocal images were taken by the author. A. Confocal image of a cross section of a mature seed embryo showing viable filamentous epichloid hyphae in embryo axis of seed which was stained with CMFDA; B. Confocal image of the back side of a dissected seed embryo showing viable epichloid hyphae in the 'infection layer' (between embryo and endosperm), stained with CMFDA; C. Confocal image of a longitudinal section of a seedling showing GFP-labelled epichloid hyphae. D. Confocal image of a longitudinal section of the meristematic zone of the apex of a vegetative tiller with the epichloid hyphae stained with aniline blue and Alexa Fluor 488. The dots on the filamentous hyphae show the hyphal septa. E. Confocal image of a longitudinal section of an endophyte-infected unfertilised ovary with the epichloid hyphae stained with aniline blue and Alexa Flour 488. The dots are the hyphal septa stained with Alexa Flour 488. Each microscopy image is shown enlarged in Figures A2.1 to A2.5. Scale bar = 50 µm.

Some *Epichloë* spp. cause grass choke disease, where spore forming mats, or stromata, are formed around the immature inflorescence of their host (Chung et al. 1997). These stromata are self-incompatible and therefore heterothallic mating must occur between stromata of opposite mating types for the life cycle to continue (Schiestl et al. 2006). This is mediated by a particular genus of fly (*Botanophila* spp.), which is attracted to these fungal structures for feeding and egg laying. After the transfer of spermatia of an opposite mating type, asci are formed within the perithecia. These ascospores are ejected and mediate horizontal transmission via the infection of grass ovules, thus eventually infecting the mature seeds and completing the sexual life cycle (Leuchtmann et al. 1994; Schiestl et al. 2006; Bultman et al. 2008).

## 2.4 Status of endophyte technology in pastoral practice: research needs

### 2.4.1 Biology of transmission

Only a few published manuscripts have addressed the process of endophyte infection via the embryo. Freeman (1904) used light microscopy and documented an asymptomatic fungus (probably *E. occultans*) colonising ovaries and embryo tissues of

*Lolium temulentum*, reporting that the hyphae were found throughout the upper end of the ovule and stopped at the antipodal end of the embryo sac. However, conflicting conclusions are reported in the literature on the timing of embryo colonisation by *Epichloë* endophyte hyphae during host floral development (Philipson et al. 1986; Majewska-Sawka et al. 2004). Philipson et al. (1986) used transmission electron microscopy (TEM) to investigate fungal development during flowering and concluded that endophyte hyphae accumulated adjacent to the large lateral antipodal cells in the ovaries and subsequently gained entry to the embryo sac, suggesting that fungal hyphae were present at a very early stage of embryo development. In contrast, Majewska-Sawka and Nakashima (2004) used an *in situ* immuno-localisation of fungal proteins to locate the endophyte and concluded that endophyte hyphae colonised the nucellus tissue heavily but were never found in the embryo sac and the integuments, while endophyte hyphae in the infection layer entered the scutellum when the embryos were mature. Given these conflicting conclusions, there is a need to elucidate the timing of *Epichloë* infection of the seed embryo, using advanced tissue staining and microscopy techniques.

### 2.4.2 Obstacles in the development of endophyte seed products

In the host plant, there are four critical growth stages for the vertical transmission process of asexual *Epichloë* endophytes: germination (between seed and seedling), tillering (between seedling and vegetative tiller), flowering (between vegetative tiller and developing inflorescence) and fecundity (between developing inflorescence and seeds) (Clay et al. 1989; Clay et al. 2002; Gundel et al. 2008; Wang 2014). Endophyte transmission failure can happen at any of these four points in the transmission cycle

(Afkhami et al. 2008). Gundel et al. (2011a) considered that the failure of endophyte transmission can be divided into two categories, pre-zygotic and post-zygotic transmission. Pre-zygotic transmission failure represents a lack of dissemination of the fungus from the vegetative plant to the seeds while post-zygotic transmission failure refers to endophyte death during seed storage (Gundel et al. 2008).

#### 2.4.2.1 Pre-zygotic transmission failure

Although asexual *Epichloë* species provide many benefits to the pasture industry worldwide, transmission of the endophyte from vegetative tissues to seed is sometimes imperfect. Many endophyte strains have been successfully inoculated into new host species or cultivars, but there is also substantial evidence of genetically based host-endophyte incompatibilities which result in reduced growth of endophyte mycelia in the host plant or poor between-tiller transmission of endophytes (Latch et al. 1985; Saikkonen et al. 2010; Simpson et al. 2012; Card et al. 2014c). In a few cases, the endophyte infection rate in seed can reach 100% in some pasture species (Leuchtmann 1993; Clay et al. 2002). In general, all grass-endophyte associations including natural and artificial (or novel) associations are far from perfect. For the New Zealand forage seed industry, however, novel associations with an imperfect transmission cycle, resulting in a low frequency of endophyte-infected seed creates problems when developing a product that must have a high level of efficacy to be successful (Rolston et al. 2007). Therefore, a research need is to further elucidate the mechanisms of vertical endophyte transmission. As with other plant-microorganism associations, pre-zygotic endophyte transmission is mediated by the host/endophyte genetic background and the environment the two symbionts are growing in, both in natural grasslands and in

managed pastures (Groppe et al. 1999; McCallum et al. 2001; Korb et al. 2003; Gibert et al. 2013).

2.4.2.1.1 Host/endophyte genetic background

Both the host and the endophyte genetic background influences their ability to form compatible associations (Rudgers et al. 2010). These have obviously taken many millennia of evolution with the association dating back over 40 million years (Schardl et al. 2008) and therefore host specificity seen with many novel associations should be expected. However, no genetic component responsible for low endophyte infection frequency has been identified to date (Easton, pers. comm.). Since asexual *Epichloë* species are maternally (vertically) transmitted, the endophyte infection is dependent on the presence of endophyte mycelium in the female parent with no contribution from the pollen donor (do Valle Ribeiro 1993). Many researchers have undertaken ecological surveys of *Epichloë* presence within natural grasslands, but few have investigated the genetic or physiological mechanisms behind the often variable infection frequencies within populations. However, it should be pointed out that the nature of out-crossing in perennial ryegrass and tall fescue mean that different genotypes within the population would be expected to have different transmission performance.

2.4.2.1.2 Environmental factors

Environmental factors are another group of key factors that can alter endophyte transmission efficiency. With respect to the various stages in the transmission cycle (germination, tillering, flowering, fecundity; Section 2.3), there is the possibility any one environmental factor can affect one particular transmission stage or several

transmission stages. Gundel et al. (2011a) proposed that the most sensitive part of the lifecycle with respect to inhibiting endophyte transmission would be the floral differentiation and anthesis stages. The factors potentially affecting endophyte transmission include resource supply (nutrients, water), environmental cues (temperature, light, photoperiod, vernalization), abiotic stresses ($CO_2$ level, Uvb, ozone, flooding, drought, herbicide), and biotic stresses (insect herbivores, grazing herbivores, diseases) (Gundel et al. 2011a).

Gundel et al. (2011b) showed that high nutrient levels significantly improved the spike-to-seed transmission frequency compared with low nutrients levels. Under conditions where one or more resources were in limited supply, this led to a decrease in endophyte infection frequency or even the complete loss of the endophyte (Novas et al. 2007) and therefore the metabolic cost of endophytes to their hosts under resource-limiting conditions may be one trigger for reduced transmission rates (Cheplick 2007).

Temperature has also been shown to be a significant variable in governing the endophyte infection frequency in *E. coenophiala*-infected tall fescue throughout the year with lower endophyte infection frequencies observed in cold seasons compared to warmer ones (Ju et al. 2006). Freitas et al. (2017) showed that the endophyte transmission frequency of *E. festucae* var. *lolii* strain AR501 in perennial ryegrass was significantly higher in a cold temperature regime (day/night 12/6˚C) compared to a warm regime (day/night 25/16˚C).

Flooding decreased vertical transmission rate in asexual *Epichloë* and exotic grass associations in natural pastures (Gundel et al. 2009b). In southern Patagonia, the

incidence of endophyte infection in populations of *Phleum alpinum* and *Bromus setifolius* was, respectively, negatively and positively correlated with the rainfall (Novas et al. 2007). Lewis et al. (1997) evaluated *Epichloë* infection rates for ryegrass collected from 523 sites across Europe and correlated infection rates with climatic data for a subset of 255 samples from France. These authors reported a highly significant correlation between endophyte occurrence and high summer evapotranspiration and with high summer water deficit, and concluded that groups of *Lolium* populations with a high level of infection were located mostly in Mediterranean regions, where stress from summer drought is common.

$CO_2$ had differing effects on pre-zygotic transmission in different studies. A growth chamber experiment showed that elevated $CO_2$ (ambient + 300 ppm, 396 ± 3 ppm in ambient $CO_2$ plots) led to higher endophyte infection frequency in an *E. coenophiala* - tall fescue association (Brosi et al. 2011). By contrast, Marks et al. (1990) reported that an elevated $CO_2$ (ambient + 300 ppm) in the controlled chambers did not alter the interactions between perennial ryegrass and its endophyte symbiont, *E. festucae* var. *lolii*.

In addition to climatic factors, a few studies have investigated the effect of mammalian or insect-mediated herbivory on endophyte infection frequencies in grass swards. Gwinn et al. (1998) observed that high and medium grazing pressure significantly increased the infection levels of *E. coenophiala* in tall fescue. In the same plant-endophyte association, Clay et al. (2005) found over a 54-month study in field plots in Bloomington, Indiana, that the endophyte infection frequency for tillers in the sward increased over time by approximately 10% from a starting point of 50% infection rate,

in plots where fencing and insecticides were used to control grazing and insect predation. Where plots were unfenced or water was applied in place of insecticide, the increase in tiller infection over time was numerically slightly greater (~ 12%), but not significantly so. However, in unfenced plots receiving no insecticide, the increase in endophyte-infected tillers during the experiment approached 30% ($p < 0.04$). These authors therefore conclusively demonstrated that subjecting host grasses to herbivory changed the host-endophyte competitive dynamic and increased the rate of endophyte infection. Similar effects of grazing on the endophyte infection frequencies were also found in associations between *E. festucae* var. *lolii* and perennial ryegrass (Jensen et al. 2004; Granath et al. 2007). Moreover, it has also been demonstrated that, compared with non-grazed sites, grass tillers from grazed swards had significantly higher hyphal biomass per unit dry weight of plant tissue, which might also be a possible mechanism for high transmission from a host plant to seed of the next generation (Koh et al. 2007). However, in contrast with the above studies, grazing decreased endophyte transmission in an *E. occultans*-Italian ryegrass population (Garcia Parisi et al. 2012). Intense grazing decreased the endophyte infection frequency in 'preferred' species more heavily defoliated by animals while the endophyte infection frequency in less-preferred species remained constant. This suggests that high grazing intensity could weaken the relationship between the endophytes and their hosts, making them even more vulnerable to further grazing (Hernández-Agramonte et al. 2016). However, another possibility is because of the different plant-endophyte associations used in the above studies.

2.4.2.1.3 Transcriptomic profiling studies on plant-endophyte symbiosis

The transcriptome is defined as the complete set of mRNA transcripts in a cell at a specific developmental stage or a physiological condition (Wang et al. 2009). Transcriptomic profiling studies have been used to comprehensively compare the changes of gene expression of plants when responding to biotic and abiotic stresses and stimuli. There are two approaches to quantifying the transcriptome, one is hybridization-based, and the other is sequence-based (Liu et al. 2007). The hybridization method mainly refers to cDNA (complementary DNA) microarrays. cDNA microarrays are capable of profiling gene expression patterns of tens of thousands of genes in a single experiment. This is accomplished by incubating fluorescently labelled cDNA with microarrays (Malone et al. 2011). The protocol for quantifying the transcriptome using cDNA microarrays is simple but this method has its limitations. Since cDNA microarrays must rely on the existing genome sequence, making the sequencing task difficult for species for which a reference genome is not yet available, or cross-pollinated species like perennial ryegrass or tall fescue.

Sequencing-based methods include SAGE (serial analysis of gene expression) (Velculescu et al. 1995), MPSS (massively parallel signature sequencing) (Brenner et al. 2000) and high throughput RNA-sequencing. These techniques do not require a prior knowledge of the genes to be analysed but each of them has a different strategy. For the SAGE technique, a short sequence tag of 10 nucleotides (nt) adjacent to the 3'-most NlaIII restriction enzyme site is extracted from each expressed sequence. Then the tags are concatenated for high throughput sequencing analysis and tag counts are used to analyse the abundance of their corresponding transcripts. Similarly, MPSS also relies on

the production of short tags next to the 3'-most DpnII restriction enzyme site. However, compared with SAGE, more tags can be produced from the MPSS technique due to the in vitro cloning of cDNA molecules on the surface of microbeads. Recently, the development of high-throughput DNA sequencing methods has provided a new method for mapping and quantifying gene expression. This approach, termed RNA sequencing (RNA-Seq), has advantages over earlier approaches and has revolutionised the way eukaryotic transcriptomes are analysed (Nagalakshmi et al. 2010). In general, a population of RNA is converted to a library of cDNA fragments with adaptors attached to one or both ends. Each molecule is then sequenced in a high-throughput manner to obtain short sequences by single-end sequencing or pair-end sequencing. The reads are typically 30–400 bp. After sequencing, the resulting reads are either aligned to a reference genome or assembled de novo to produce a genome-scale transcription map (Wang et al. 2009).

Numerous studies have been performed on the transcriptomic profiles of *Epichloë* species and their hosts over the past ten years. Earlier studies used microarray-based gene expression profiling to identify host genes whose expression changed in response to the presence of endophyte. Felitti et al. (2006) generated two cDNA-based microarrays based on the available genome resources. One of these is the Nchip™ microarray which allows the interrogation of 3,806 *E. coenophiala and E. festucae* var. *lolii* genes; the other is the EndoChip™ microarray which incorporates 4,195 *E. coenophiala and E. festucae* var. *lolii* genes and 920 *E. festucae* genes. Dinkins et al. (2010) used the Wheat Genome Array and GeneChip® Barley Genome Array on the RNA of endophyte-infected and endophyte-free tall fescue, and found that only 14-15% of

the genes in endophyte-infected and endophyte-free pseudostems were present on the wheat chip, and 17-18% of genes present on the barley chip. However, this study also showed that the endophyte infection can influence the host gene expression in the pseudostem tissues. A SOLiD$^{TM}$-SAGE quantitative transcriptome study on *Festuca rubra* (red fescue) revealed that over 200 plant genes involved in a variety of physiological processes were differentially-expressed in endophyte-infected plants compared with endophyte-free counterparts. Meanwhile, the most abundant differentially expressed genes (DEGs) of the endophyte were for coding secreted proteins and the second most abundant were for a secreted antifungal protein (Ambrose et al. 2012). Recently, with the development of RNA-Seq, transcriptomic studies have been more widely used on *Epichloë* species due to their higher sensitivity than microarrays. Dupont et al. (2015) examined the expression profiles in the pseudostem tissues between *E. festucae* var. *lolii*-infected and endophyte-free perennial ryegrass by RNA sequencing, and found that endophyte infection induced over one-third of host genes, especially those related to host development, trichome formation and cell wall biogenesis. Dinkins et al. (2017) showed, using RNA-Seq, that 478 genes were differentially expressed in at least one tissue type (leaf blade, pseudostem, crown and root) in *E. coenophiala*-infected tall fescue compared with endophyte-free counterparts. Gene ontology results from this study revealed that these DEGs were mostly related to response to chitin, respiratory burst (rapid release of reactive oxygen species) during defence responses, and intercellular signal transduction. From the comparison of results of the two studies just described, it would appear that different functional sets of genes were expressed in perennial ryegrass and tall fescue when infected with endophytes.

Therefore, RNA-Seq is an efficient approach in comparing gene expression among samples of divergent genetic backgrounds or under different environmental conditions. Since the endophyte transmission frequencies vary in different host genotypes, the RNA-Seq technique could be used to identify the genes that are differentially expressed between endophyte-host genotype combinations with high or low transmission performance. Follow-up work could then be done on verifying which genes are responsible for manipulating the endophyte transmission.

#### 2.4.2.2 Post-zygotic transmission failure

As well as transmission failure between tillers or to the inflorescence and ovules during plant development, loss of endophyte can happen during seed storage. When this occurs, commercialisation is severely hindered. In New Zealand, commercial licence agreements specify that > 70% of certain endophyte-infected seeds (AR1, AR37, AR542) must contain viable endophyte (Easton et al. 2007; Rolston et al. 2007). In endophyte-infected seeds, loss of endophyte viability precedes the loss of seed viability during seed storage which can be highly problematic for marketing endophyte-infected seed products (Hume et al. 2005; Gundel et al. 2009a; Hill et al. 2009; Gundel et al. 2011a). In natural grasslands, the mortality of the fungus in the dispersed seeds is a major factor responsible for imperfect endophyte transmission in the wild populations since only viable endophytes in a seed can transmit from the mature seed to the seedling through germination (Ravel et al. 1997). Compared with the research on transmission of *Epichloë* species in planta, more research has been done on transmission during seed storage (Gundel et al. 2011a). Any factors that interfere with the survival of endophytes during storage can directly influence the transmission efficiency.

It is well understood that temperature and moisture are two key environmental parameters that modify the endophyte longevity in seeds during storage (Rolston et al. 1986). Neill (1942) reported that the endophytes lost viability in perennial ryegrass and tall fescue seeds after 12 to 18 months of storage under ambient conditions. Either high moisture or high temperature decreased the endophyte viability in seeds very quickly. Welty et al. (1987) reported that in tall fescue seeds, the endophyte infection frequency dropped to around 80% after 18 months of storage under 10°C and 6.4% relative humidity (RH). However, the endophyte infection frequency dropped to zero after only 5 months when seed was stored at 30°C and 21.8% RH. Hume et al. (2013) suggested that the endophyte-infected seeds should be stored under controlled storage facilities where the preferred conditions are ≤ 5°C and ≤ 30% RH to retain longevity. However, the longevity is also believed to depend on seed species, cultivars and endophyte strain. Seeds from the *E. uncinata*-meadow fescue association were found to have extended endophyte viability while stored under a regime of ≤ 5°C and ≤ 30% RH, and these specifications are regarded as optimum for commercial use. Storing seeds in paper bags in the freezer was an optimal method for preserving endophyte viability and seed germination (Bylin et al. 2016). Also, Kirkby et al. (2011) found that burying seed significantly decreased the endophyte infection rates of *E. occultans* in Italian ryegrass seeds. This observation may indicate one of the mechanisms for the variable endophyte infection rates in natural stands. That is, if endophyte-infected seeds which fall and are buried are more prone to loss of endophyte viability during seed dormancy, these would further develop into endophyte-free seedlings, thus decreasing the overall endophyte infection frequencies. In the Margot Forde Forage Germplasm Center (New Zealand's national gene-bank of grassland plants, Palmerston North, New Zealand), endophyte-

infected seeds are stored in paper bags below 0°C and 30% RH, some ryegrass lines infected with AR1 can maintain viability for up to 14 years (Hume et al. 2011).

In addition to the environmental factors, the endophyte viability in stored seeds is also linked to the genetic background of both plants and endophytes (Wheatley et al. 2007). In a study of the same endophyte strains in different hosts, it was reported that the viability percentage of *E. coenophiala* strain AR542 decreased more slowly in tall fescue cultivar Flecha than cultivars Jesup and Advance, at room temperature, while for different endophytes in the same host, AR584 had greater viability than AR542 in Jesup after 18 months seed storage (Hill et al. 2009).

2.4.2.2.1 Proposed mechanisms for the post-zygotic transmission failure

Dormancy refers to an organism's ability to enter a reversible state of low metabolic activity when faced with unfavourable environmental conditions (Hilhorst 2007). By entering a dormant state, organisms can dramatically decrease their energetic expenditure. Lennon & Jones (2011) discuss various types of dormancy including spores or related structures where respiration is near zero but there is an energy cost to create the resting structure, and reduction of the metabolic rate but with ongoing energetic needs for cell maintenance and survival. The second case is clearly more relevant to understanding endophyte dynamics during seed storage, and likely involves the synthesis of specialised enzymes and machinery to deal with the accumulation of waste products. However, dormancy is not a cost-free strategy since organisms must allocate resources to cell maintenance and survival (Morita 1982). Therefore, despite uncertainty about the precise metabolic details of endophyte survival during seed storage, *Epichloë* species must have some requirement for nutrients or other substrates,

and for cytoplasmic homeostasis, for the endophyte hyphae to survive. Compared with the environment experienced by endophyte hyphae between cells of plant tissues, the nutrient circulation that could be exploited by hyphae in dry seeds is minimal. *Epichloë* species would be expected to be more metabolically active under conditions of high moisture and warmer temperature conditions typical of plant active growth (which result in more rapid depletion of nutrients endophyte cells), compared to low humidity and low temperature conditions typical of seed storage. There is little research on nutrient exchange between endophytes and their hosts, neither is there available research on the apoplastic solutes which are necessary for nutrition of the endophyte hyphae, especially for endophyte in stored seeds (Richardson et al. 1992). Therefore, a potential avenue for future research is the comparison of the nutrient profiles of endophyte-free and endophyte-infected seeds during storage.

Two groups of storage carbohydrates are commonly recognised in fungi: short-chain carbohydrates such as trehalose (α-$_D$-glucopyranosyl-[1-1]-α-$_D$-glucopyranoside) and polyols; long-chain carbohydrate glycogen (Nehls 2008). Trehalose is a common disaccharide in microorganisms and is also present in plant tissues. Trehalose is plentiful in plant symbioses with fungi and bacteria, as well as acting as a compatible osmolyte, stabilising and protecting proteins and membranes in microorganisms against heat, cold and oxidative stress conditions (Bell et al. 1992; Benaroudj et al. 2001; Tibbett et al. 2002). Research has shown that trehalose/mannitol metabolism is necessary for fungal carbon metabolism in ectomycorrhizal symbiosis (Nehls et al. 2010). There is some evidence suggesting that the trehalose in yeast does not function primarily as a reserve but rather as a protection agent to maintain the structural integrity of the cytoplasm

under environmental stress conditions (Wiemken 1990). The sexual endophyte *E. typhina* is more frequently used for carbon translocation studies since it has reproductive structures (stromata) outside of the hosts, which can be isolated for chemical analysis. Thrower et al. (1973) showed that sucrose is the principal carbohydrate acquired from the host by *E. typhina*, which is concomitantly transformed to mannitol and trehalose by the fungus. Lam et al. (1994) demonstrated that sucrose was not used by the fungus directly but was taken up by a sucrose carrier and was then hydrolysed by cell wall invertase into a hexose, which was then utilised by the fungus. Parallel results were also found in mycorrhizal fungi. Ectomycorrhizas can convert plant-derived carbohydrates to fungus-specific nutrients (López et al. 2007). In the *Myriogenospora atramentosa* (a pathogenic fungus in the family Clavicipitaceae) -Bahia grass association, Smith et al. (1985) supplied $^{14}CO_2$ to the host plants and found that stromata of the fungus accumulated more $^{14}C$-labeled mannitol, arabitol and trehalose (which are not typical plant carbohydrates) but only trace amounts of glucose and sucrose. This study therefore indicates that host sugars were converted to fungal sugar alcohols and trehalose, used by the fungus either as an energy substrate during storage or for lowering the water potential within the fungus, thus favouring diffusion of water from the host to the fungus. Therefore, a consensus from the studies reviewed above is that the *Epichloë* endophytes do not use sucrose or other sugars directly but rather convert plant sugars to the fungus-specific sugars like trehalose, mannitol and arabitol for nutrient supply. Under culture conditions, research has shown that sucrose, trehalose, mannitol and sorbitol were suitable carbon sources for the growth while arabinose, ribose, xylose, galactose, sorbose and rhamnose were not utilised for the growth of *E. coenophiala* (Kulkarni et al. 1986).

Glycogen is a long-chain carbohydrate and a major intracellular reserve polymer in bacteria and fungi (Wilson et al. 2010). In one report on the culture of the fungi *Hizophydium sphaerotheca* and *Monoblepharella elongate*, glycogen accounted for 6% and 8.1% of the dry weight, respectively (Coulter et al. 1977). One function of glycogen is to prevent RNA and protein degradation when bacterial cells are under starvation. Therefore, glycogen provides carbon and energy for cells under stress (Iglesias et al. 1992). Glycogen is also a storage compound in cells of mycorrhizal fungi (Bago et al. 2003). During spore germination of a rice (*Oryza sativa*) blast fungus, *Magnaporthe oryzae*, glycogen reserves in the spores were broken down to provide energy and nutrients for the spore germination (Badaruddin et al. 2013). Christensen (1996) observed glycogen granules in *Epichloë* cells using TEM (El-Bashiti et al. 2005). Glycogen is also present in the seed of maize (*Zea Mays*) and is referred to as phyto-glycogen, although with an indistinguishable structure to fungal or animal glycogen (Morris et al. 1939; Hassid et al. 1941). However, to the writer's knowledge, it is not known whether the structure of phyto-glycogen in perennial ryegrass or tall fescue seeds, if present, is the same as that of the *Epichloë* species. If the structures are similar, it will be challenging to isolate *Epichloë*-oriented glycogen from the *Epichloë*-infected seeds using chemical isolation. From this perspective, microscopy studies to monitor glycogen inside endophyte hyphae would be relevant.

Lipids (present as drops) are another group of compounds present in cells of many microorganisms. Saito et al. (2006) found lipid drops in the hyphae of *Phialocephala fortinii*, which is a dark septate fungal endophyte infecting roots. The accumulation of lipids by dark septate fungi in the root cortex could serve as a source of energy-rich

carbon reserves to sustain plant cells during drought conditions (Barrow 2003). Christensen et al. (2002) showed that there was an accumulation of lipid droplets in fungal hyphae of old leaf sheaths rather than young ones, which indicates one aspect of the aging process in endophyte mycelia.

## 2.5 Potential questions and approaches for the research in this thesis

### 2.5.1 Timing of embryo colonisation by *Epichloë* species

Conflicting evidence exists on the timing of *Epichloë* embryo colonisation, and no consensus has yet been reached. Two of the most often cited reports include Philipson et al. (1986) who show by TEM the presence of endophyte within the very early embryo, while Majewska-Sawka et al. (2004), who used immunodetection methods, report that young embryos are never colonised by the fungus, and therefore endophyte infection must occur at a late stage in seed formation. To get a better idea of the transmission mechanism, it is important to understand the pathway of how endophytes colonise the seed embryo. This thesis investigates in Chapter 3, the exact timing of host-to-seed transmission by the use of confocal microscopy (Card et al. 2011; Card et al. 2013), in the hope of resolving the earlier conflicting evidence.

### 2.5.2 Endophyte storage carbohydrates

One possible mechanism for the failure of transmission in *Epichloë* species during seed storage is the depletion of fungus-specific carbohydrates. Use of chemical analysis to explore how metabolite profiles change during seed storage would be relevant to answering this question. In research investigating endophyte transmission in seed storage, artificial aging is a rapid method to mimic the natural aging process; and is useful since natural aging experiments usually last for some years (Cookson et al. 2001).

Tian et al. (2013) concluded that results of exposure to the conditions of 80% RH for seven days or 100% RH for four days predict long-term viability for endophyte-infected seeds. As with natural aging, accelerated aging negatively affects endophyte viability and seed germination rate and vigour (Gundel et al. 2007). In this thesis carbohydrate changes during accelerated aging of seeds with and without endophyte are explored in Chapter 4.

### 2.5.3 Possible relationship between endophyte biomass and transmission

Some studies have reported variation between host genotypes in fungal hyphae density (Cook et al. 2009b), so a hypothesis is that higher fungal biomass within host tissues may increase the success rate of host-to-seed transmission. This question is investigated in Chapter 5 by real-time PCR, optimised to quantify the endophyte biomass in plant tissues.

### 2.5.4 Mechanism for host-to-seed endophyte transmission in planta

Previous research has revealed several DEGs in response to the presence of *Epichloë* species in several grass hosts (Dupont et al. 2015; Dinkins et al. 2017). Recent developments in high-throughput sequencing of mRNA using RNA-Seq mean it is now possible to measure the transcriptional response of grass genotypes, to their endophyte symbiont, and this is reported in Chapter 6 for genotypes selected for high and low endophyte transmission.

# Chapter 3 Defining the pathways of symbiotic *Epichloë* colonisation in grass embryos with confocal microscopy

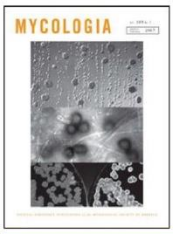

Mycologia

ISSN: 0027-5514 (Print) 1557-2536 (Online) Journal homepage: http://www.tandfonline.com/loi/umyc20

## Defining the pathways of symbiotic Epichloë colonization in grass embryos with confocal microscopy

Wei Zhang, Stuart D. Card, Wade J. Mace, Michael J. Christensen, Craig R. McGill & Cory Matthew

To cite this article: Wei Zhang, Stuart D. Card, Wade J. Mace, Michael J. Christensen, Craig R. McGill & Cory Matthew (2017) Defining the pathways of symbiotic Epichloë colonization in grass embryos with confocal microscopy, Mycologia, 109:1, 153-161, DOI: 10.1080/00275514.2016.1277469

To link to this article: https://doi.org/10.1080/00275514.2016.1277469

View supplementary material

Accepted author version posted online: 09 Jan 2017.
Published online: 22 Feb 2017.

Submit your article to this journal

Article views: 226

View related articles

View Crossmark data

Citing articles: 1 View citing articles

Full Terms & Conditions of access and use can be found at
http://www.tandfonline.com/action/journalInformation?journalCode=umyc20

MASSEY UNIVERSITY
GRADUATE RESEARCH SCHOOL

## STATEMENT OF CONTRIBUTION TO DOCTORAL THESIS CONTAINING PUBLICATIONS

(To appear at the end of each thesis chapter/section/appendix submitted as an article/paper or collected as an appendix at the end of the thesis)

We, the candidate and the candidate's Principal Supervisor, certify that all co-authors have consented to their work being included in the thesis and they have accepted the candidate's contribution as indicated below in the *Statement of Originality*.

**Name of Candidate:** Wei Zhang

**Name/Title of Principal Supervisor:** Cory Matthew

**Name of Published Research Output and full reference:**

Zhang W, Card SD, Mace WJ, Christensen MJ, McGill CR, Matthew C 2017. Defining the pathways of symbiotic Epichloë colonization in grass embryos with confocal microscopy. Mycologia 109(1): 153-161.

**In which Chapter is the Published Work:** Chapter 3

Please indicate either:

- The percentage of the Published Work that was contributed by the candidate:

  and / or
- Describe the contribution that the candidate has made to the Published Work:

Wei Zhang conducted the experiment and wrote the manuscript.

Candidate's Signature — 22 Jan 2018 — Date


24 Jan 2018

Principal Supervisor's signature — Date

# Chapter 4 The impact of endophyte infection, seed aging and imbibition on selected sugar metabolites found in seed embryo and endosperm tissues

## 4.1 Abstract

*Epichloë* endophyte viability often declines at a faster rate than the host seeds. As endophyte-infected seed products are generally stored for periods of time before their sale, this can create problems when trying to deliver a quality product to the end user. This is a major impediment to the commercialisation of endophyte technology. Seed metabolites often change with seed aging and seed imbibition and no reports to date have linked endophyte survival with changes in the seed metabolites during these processes.

This study aimed to investigate the effects of seed aging and imbibition on the sugar metabolites in the endophyte-free and endophyte-infected embryo and endosperm tissues of tall fescue, after separating those tissues by manual dissection. Tall fescue seeds of four endophyte statuses (endophyte-free, AR584, AR605 and common-toxic) were studied. Two treatments: accelerated aging (AA) and seed imbibition were applied to the seeds. Gas chromatography with flame ionisation detection (GC-FID) was employed for analysis of sugar metabolites in the dissected tissues of embryo and endosperm. Results showed that trehalose was the sugar most closely correlated with the loss of endophytes. The concentrations of trehalose were significantly reduced in the endophyte-infected embryo and endosperm tissues with imbibition. This result is consistent with the endophyte-oriented trehalose being utilised by the endophytes with

imbibition. Mannitol and ribitol were two sugars with high concentrations in endophyte-infected tissues of both embryo and endosperm, and could therefore potentially be used as indexes to estimate the endophyte biomass. In addition, the amounts of D-galactose, raffinose and xylose were all elevated in the dry embryo tissues with AA. The concentration of maltose significantly increased in both the endophyte-free and endophyte-infected embryo tissues which might be transferred from the endosperm where starch hydrolyses into maltose during imbibition.

## 4.2 Introduction

Death of *Epichloë* endophytes during seed storage is an impediment to the commercialisation of endophyte technology for the enhancement of forage grass performance. In New Zealand, the endophyte infection frequency in commercialised seed products is expected to be high. For PGG Wrightson Seeds Ltd. (Christchurch, New Zealand) and Grasslanz Technology Ltd. (Palmerston North, New Zealand), an endophyte infection rate of 70% is utilised as an informal standard (Hume et al. 2005).

It has long been established that warm temperatures and high humidity are two key factors causing endophyte death in stored seed lines (Rolston et al. 1986) (Section 2.3.3). The results from the study of Wheatley et al. (2007) showed that at ambient conditions, the longevity of *E. festucae* var. *lolii* in most seed samples of perennial ryegrass remained over 60% for 2 years post-harvest but declined very rapidly afterwards. Even at low temperatures, endophyte infection frequencies drop with time. For instance, Cheplick (2017) showed that of four perennial ryegrass cultivars investigated, the endophyte infection frequency of only one cultivar remained at the original levels after 18 years storage at 4˚C but the infection frequencies in all the cultivars decreased significantly

after 20 years storage. Storing endophyte-infected seeds in paper bags at 0°C and 30% RH has been proved to be suitable for preserving endophyte viability. Under these conditions, the viability of *E. festucae* var. *lolii* strain AR1 in seeds of perennial ryegrass can retain viability levels for up to 22 months (Hume et al. 2011).

Due to the fact that epichloid hyphae experience an environment within host seeds with no obvious source of substrate replenishment, it is logical to expect that maintenance metabolism would eventually exhaust the available stored substrates. In plant tissues, epichloid endophytes are always found within the intercellular spaces, and mainly exist in sink tissues in vegetative organs, such as leaf sheaths and pith, which are regions where sucrose loading from the phloem takes place (Hinton et al. 1985). Nutrients required by endophytes are assumed to be derived from the apoplast with the majority of spaces filled with gases and fluids. The fluids contain various nutrient solutes originating from the host, including several sugars and related carbohydrates derived from photosynthesis, several nitrogenous compounds such as nitrates, nitrites, amino acids and amine, as well as key inorganic ions (Kuldau et al. 2008). There is little research on the specific metabolic substrates that must be present in the apoplast to support fungal growth. The enhanced carbohydrate demand for the endophytes in the green tissues can be accomplished by an increase in plant photosynthesis or nutrient translocation where the endophyte constitutes about 0.2% of the biomass of the infected tissue (Bacon et al. 2000, Tan et al. 2001).

It is a different case for endophyte hyphae within seeds, as there is no photosynthesis occurring, and therefore no nutrient supply from this source. And again there is little research on the nutrition of endophytes during seed storage (Richardson et al. 1992).

Dupont et al. (2015) extracted apoplastic fluid from living pseudostem and leaf blade tissues of perennial ryegrass and found that the apoplast fluid contained more compatible solutes arabitol, threitol, and mannitol in the endophyte-infected than endophyte-free tissues. However, this method cannot be applied to seeds since the seeds are hardened during maturity and there is no apoplastic fluid to collect. To investigate the nutrients required for optimal/increased endophyte survival, an indirect method would be required that compared the sugar profiles between seeds with and without endophyte infection.

This experiment investigates the variation in levels of selected sugars in seed tissues during seed storage, to identify changes during storage, and make deductions about mechanisms of endophyte loss, for future study. Seed hydration (imbibition) processes might be a stressful process for the endophytes inside the seeds. The impact of imbibition on levels of the selected metabolites in endophyte-infected seeds was also quantified in this study. This is believed to be the first study to examine the effects of AA and seed imbibition on the metabolism of soluble sugars in seeds, especially with the involvement of endophytes. The results from this study could shed light on the mechanism of endophyte loss in endophyte-infected seeds during seed storage, which is important for further research and the commercialisation of endophyte products.

## 4.3 Materials and methods

### 4.3.1 Biological materials and chemicals

4.3.1.1 Source of seeds

Seeds of three tall fescue (cultivar Jesup) accessions each containing a genetically unique endophyte strain plus an endophyte-free line of Jesup were used as the plant materials

in this study. Seeds were originally harvested in January 2013 from plots at the AgResearch, Lincoln experimental farm (Canterbury, New Zealand) with seed from replicate plots of the same accession pooled and stored in paper bags at 0˚C and 30% relative humidity (RH) in the Margot Forde Forage Germplasm Centre (Palmerston North, New Zealand) until use.

4.3.1.2 Analytical reagents

The sugar standards of fructose, lactose, mannitol, myo-inositol, sucrose, trehalose, xylitol and xylose used were purchased from BDH Chemicals Ltd. (Poole, England). The glucose standard used was purchased from Thermo Fisher Scientific (Brisbane, Australia). The sugar standards of D-arabitol, DL-arabinose, D-galactose, galactinol, glycerol, maltose, mannose, raffinose, ribitol and sorbitol used were purchased from Sigma-Aldrich (St. Louis, USA). Phenyl β-D-glucoside, MSTFA (N-Methyl-N-[trimethylsilyl] trifluoroacetamide) and pyridine for extraction procedures (see below) were all GC grade and were purchased from Sigma-Aldrich. Methoxyamine hydrochloride (HCl), used as the internal standard, was purchased from Sigma-Aldrich.

### 4.3.2 Experimental design

The experiment was a completely randomised design with three independent factors (4×2×2): plant-endophyte association (accession number [T9892, T9893, T9895, T9896]), AA period (0 d, 4 d), and seed state (dry, imbibed) (Table 4.1). There were three replicates in each treatment. The protocol for seed AA was as follows: seeds were incubated at 40°C for four days in open paper bags above 400 mL tap water within a sealed glass desiccator (25 cm in diameter). This resulted in an environment with close to 100% RH as described by Bylin et al. (2016). After AA, seeds were either kept dry or

imbibed overnight on wet filter papers at 20°C to initiate germination. Embryo and endosperm tissues were analysed separately by dissecting each from their dehulled whole seeds using a scalpel. All the prepared samples (embryo and endosperm tissues) were then stored at –80˚C before concentrations of selected sugars were assessed. To obtain sufficient tissue volume for analysis, embryo tissues from about 250 seeds were dissected and pooled into one sample (5–10 mg dry weight [dw]), while 10 endosperm tissues from the 250 dissected seeds were combined to form a sample of 10–15 mg dw.

**Table 4.1 Seed materials used in this study.**

| Accession number | Endophyte strain | Alkaloid profile | Commercial status |
|---|---|---|---|
| T9892 | Endophyte-free | — | — |
| T9893 | AR584 | Peramine, lolines** | Commercially available in New Zealand, USA, etc. |
| T9895 | AR605 | Ergovaline, lolines** | Commercially available as the product Avanex® in New Zealand. |
| T9896 | Common-toxic* | Peramine, ergovaline, lolines** | — |

* The endophyte strains of tall fescue causing mammalian toxicity was referred to as the common-toxic (formally 'wild-type') strains.
** Johnson et al. (2013).

### 4.3.3 Assessment of seed germination and endophyte infection frequency

Seeds of both AA and non-AA samples from each accession were sown into trays and transferred to a glasshouse and watered as required, with artificial soil mix (composition same as shown in Chapter 3). After eight weeks, when seedlings were at the two- to three-tiller stage of development, seed germination and endophyte infection frequencies were determined for each accession. Germination percentage was calculated as:

$$\%\ \text{seed germination} = \frac{\text{Germinated seedlings}}{\text{Total number of seed sown}} \times 100$$

The endophyte infection frequency was assessed according to the methods of Bylin et al. (2016). In summary, endophyte presence in each seedling (one tiller per plant) was assessed using a tissue-print immunoblot method and the viable endophyte infection frequency calculated as:

$$\%\ \text{viable endophyte} = \frac{\text{Endophyte infected seedlings}}{\text{Germinated seedlings}} \times 100$$

### 4.3.4 Sample preparation for GC-FID analysis

Neutral sugars analysed in this study included DL-arabinose, fructose, D-galactose, glucose, lactose, maltose, mannose, raffinose, sucrose, trehalose and xylose, and the sugar alcohols were D-arabitol, galactinol, glycerol, myo-inositol, mannitol, ribitol, sorbitol and xylitol. The chemical formula and the structures of the analysed sugars were shown in Table A4.1. The sugars were analysed by GC-FID (Shimadzu Scientific Instruments Ltd., Adelaide, Australia). The sample preparation procedure for GC-FID analysis consisted of two steps, an extraction step and a derivatisation step.

#### 4.3.4.1 GC-FID analysis: extraction step

Embryo and endosperm tissues from each sample were stored separately in 2 mL vials (Sarstedt; Nümbrecht, Germany) and freeze-dried for 48 hours using a Flexi-Dry freeze dryer (FTS Systems, Stone Ridge, New York). The weight of the embryo or endosperm tissues was measured with an electronic balance (Precisa; Dietikon, Switzerland) to ± 0.0001 g precision. The samples were ground using a FastPrep-24 (MP Biomedicals; Solon, USA) at a speed of 4 m/s for 10 s and 400 µL of 100% methanol was added. Sugar standards (around 10 mg for each standard) were also prepared in 400 µL of 100% methanol. An internal standard solution (50 µL of 0.2 mg/mL phenyl β-D-glucoside in methanol) was added to each sample. After mixing on the FastPrep at a speed of 4 m/s for 10 s, the samples were extracted for sugars at 70°C for 30 min and allowed to cool to room temperature. The samples were centrifuged at 5000 *x*g for 5 min and the supernatant transferred to 2 mL vials before the addition of 300 µL of chloroform. The mixture was vortexed until fully mixed and incubated at 37°C for 5 min. Six hundred

microliters of Milli-Q water were added to each tube followed by vortexing until fully mixed and centrifuged at 5000 *x*g for 5 min. An aliquot (500 µL) of the aqueous phase from each tube was then transferred into 2 mL glass GC vials (Phenomenex; Torrance, USA) which were then dried overnight in a Savant speed vac concentrator (Model SC100; New York, USA).

4.3.4.2 GC-FID analysis: derivatisation step

Methoxyamine HCl (40 µL of 20 mg/mL in pyridine) was added to the dried aliquot within the GC vial and incubated at 35°C for 90 min. The solution was spun down by centrifuging at 2500 *x*g for 2 min. An aliquot (80 µL) of silylating pre-mix (prepared by adding 145 µL of an alkane standard to a 1 mL ample of MSTFA) was added and mixed by hand-swirling. The solution was incubated at 37°C for 30 min and then centrifuged at 2500 *x*g for 2 min. Eighty microliters of the solution was transferred to a 200 µL glass limited volume insert and placed into a GC vial for further analysis by GC-FID.

**4.3.5 Instrument analysis on neutral sugars or sugar alcohols**

Samples were analysed in a randomised order. Sugars were analysed by GC-FID plus an AOC-20i auto-injector. The GC column was 50 m in length with 0.22 mm internal diameter BPX-70 (0.25 µm film thickness) column (SGE International Pty Ltd., Australia) with a 1 m × 0.53 mm inner diameter deactivated pre-column. The carrier gas was hydrogen at a flow rate of 1.2 mL $min^{-1}$. The initial oven temperature was set at 70°C for 5 min, ramped to 330°C at a speed of 5°C $min^{-1}$, held for 5 min, and then allowed to equilibrate for 6 min at 70°C before the next injection.

### 4.3.6 Determination of sugar concentrations

The sugar concentrations were determined by comparing to an internal standard (Hooper et al. 2009), first calculating a response factor (RF) for each target compound to correct for variation in detector behaviour with compounds of differing molecular weight by using the sugar standard injections, then applying the RF to the GC data to obtain the concentration of each target compound in the seed samples. Peak assignment was based on the retention time of standards (Table A4.2). To obtain RF of each target compound the following equation was used:

$$\text{Response factor (RF)} = \frac{\text{Ax} * \text{Mis}}{\text{Ais} * \text{Mx}}$$

Where:

Ax = Area of the target compound in the standard sample;

Mx = Mass of the target compound in the standard sample;

Ais = Area of the internal standard (phenyl-glucoside) in the standard sample;

Mis = Mass of the internal standard (phenyl-glucoside) in the standard sample.

After obtaining the RF, the mass of each target compound in the seed samples (Mx2) was calculated as a proportion, using the equation:

$$\text{Mx2} = \frac{\text{Ax2} * \text{Mis2}}{\text{Ais2} * \text{RF}}$$

Where:

Ax2 = Area of the target compound in the unknown samples;

Mis2 = Mass of the internal standard (phenyl-glucoside) in the unknown samples;

Ais2 = Area of the internal standard (phenyl-glucoside) in the unknown samples;

Mx2 = Mass of the target compound in the unknown samples.

From target compound mass in each sample calculated in this way, and the original seed sample mass and also the known molecular weight, target compound concentration was then determined (µmol $g^{-1}$ dw).

**4.3.7 Data analysis**

Due to the complexity of the data set, four distinct types of data analysis were explored: (i) a t-test table of concentration fold changes (FC) between pairs of treatments, (ii) a correlation table between analysed sugars and alcohols, (iii) a metabolic pathway analysis, and (iv) various forms of multivariate analysis, including principal component analysis (PCA), canonical correlation analysis (CCA), and multivariate analysis of variance (MANOVA) with canonical discriminant analysis (CDA) performed on 19 analysed sugars and sugar alcohols. All these types of analyses were performed separately for embryo and endosperm tissues.

For the t-test table, statistical differences in the concentration of each sugar metabolite between the two treated groups were analysed using a Student's t-test with Microsoft Excel (Microsoft Corp.; Seattle, USA). For this study, values of $p \leq 0.01$ were considered highly statistically significant, values of $p \leq 0.05$ were considered statistically significant, and values $0.05 < p \leq 0.1$ were considered to indicate a significant trend.

Correlation analysis between all the metabolite data were performed using the Hmisc Package in RStudio (version 0.99.903) (http://cran.r-project.org/web/packages/gplots/index.html). Spearman's correlation coefficient was used to determine the relationship between variables. A correlation matrix was then performed using the 'corrplot' Package in RStudio.

Metabolite-enrichment and metabolite pathway analysis was performed using Metaboanalyst (http://www.metaboanalyst.ca/) (Xia et al. 2015) with *Arabidopsis thaliana* used as the model plant for the pathway analysis. The hypergeometric test from Metaboanalyst was used for over-representation analysis, and pathway topology analysis was performed using 'relative-betweenness centrality'. Pathways of the galactose metabolism pathway and the starch and sucrose metabolism pathway were further analysed due to that more genes analysed in this study were involved in these two pathways. In conjunction with the exploration of these two pathways, the sugars involved were subjected to analysis of variance (ANOVA) and means for those metabolites for the various experimental treatments displayed. Duncan's multiple range test, which is a post hoc multiple comparison test, was used to examine for significant differences among the treatments at the $p < 0.05$ significance level.

Multivariate analysis using PCA or CCA was not included in this thesis. MANOVA and CDA were performed in RStudio; and results for this analysis are reported in Section A4.1. MANOVA was conducted to test the effects of three factors (State [dry, imbibed], Aging [0d, 4d], Endophyte [endophyte-free, AR584, AR605, common-toxic]) on the soluble sugar metabolites in both embryo and endosperm tissues. Wilk's lambda test was used to determine the significance of differences in main effects of the factors and their two-

way and three-way interactions. A CDA ('candisc' package in RStudio) was utilised to separate groups by each experimental factor and the factor two-way or three-way interactions (where statistically significant). In this thesis CDAs are reported using the bivariate correlations between each variable and the relevant discriminant function, often referred to as "structure" coefficients. When the absolute value of the structure coefficient is close to or equal to one (+1 or −1), it means the function holds nearly the same information as the variable. Also available from the CDA output are standardised canonical coefficients that are used to generate the discriminant functions from the original (standardised) variables. It was decided to use structure coefficients rather than the standardised canonical coefficients as many researchers now adopt this approach (Sardouie-Nasab et al. 2014; Nkoa et al. 2015; Gladyshev et al. 2017; Portarena et al. 2017).

## 4.4 Results

### 4.4.1 Seed germination and endophyte infection status

Before AA, the seed germination percentage across the four accessions (T9892, T9893, T9895 and T9896) ranged from 90.6% to 96.9% and the endophyte infection frequency in the three endophyte-infected accessions ranged from 93.0% to 94.6%. After AA, the germination rates slightly changed, ranging from 91.7% to 95.8% in the four accessions. However, the viable endophyte infection frequencies in the three endophyte-infected accessions (T9893, T9895 and T9896), dropped with AA treatment to a range from 57.3% to 62.2% (Table 4.2).

**Table 4.2 Germination percentage (%) and endophyte infection frequencies (%) in non-AA and AA accessions of tall fescue cv. Jesup.**

| Accession | Endophyte strain | Germination (%) | | Endophyte infection frequency (%) | |
|---|---|---|---|---|---|
| | | Non-AA | AA | Non-AA | AA |
| T9892 | Endophyte-free | 95.8 | 95.8 | 0 | 0 |
| T9893 | AR584 | 90.6 | 91.7* | 94.3 | 57.3 |
| T9895 | AR605 | 91.7 | 93.7* | 93.0 | 55.6 |
| T9896 | Common-toxic | 96.9 | 93.7 | 94.6 | 62.2 |

*Higher germination % in AA than non-AA can be attributed to sampling variation.

### 4.4.2 Comparative abundance of the tested neutral sugars and sugar alcohols

Many of the tested sugars in the embryo and endosperm tissues varied greatly in their abundance. Of the eleven neutral sugars analysed, sucrose was present in the largest concentration, in both the embryo and endosperm tissues (Tables A4.3 and A4.4). However, the concentration of sucrose was more than ten times greater in the embryo than the endosperm tissues. Of the eight sugar alcohols detected in the embryo tissues, myo-inositol was present in the largest concentration, followed by galactinol, while in the endosperm tissues the most common sugar alcohols were myo-inositol and glycerol. The concentration of myo-inositol in the embryo samples was over 20-fold that detected in the endosperm samples. There were only trace concentrations of xylitol and xylose in both the embryo and endosperm tissues while only trace concentrations of raffinose could be detected in endosperm tissues, with or without endophyte infection (Tables A4.3 and A4.4).

### 4.4.3 Approaches to data analysis

#### 4.4.3.1 T-test approach to analysis of soluble neutral sugars and sugar alcohols

##### 4.4.3.1.1 Effects of endophyte infection on the soluble sugar profiles in the embryo and endosperm tissues

The concentrations of mannitol and ribitol were higher in all the endophyte-infected samples than their endophyte-free counterparts of all the treatments. Comparing the three endophyte-infected treatments (AR584, AR605 and CT) with the endophyte-free treatment, mannitol and ribitol were significantly higher or had a near-significant trend toward an increase in the endophyte-infected embryo or endosperm tissues in almost all the samples ($FC > 4$, $p < 0.1$) (Table 4.3). Exceptions for mannitol were all from the aged samples, including the dry and imbibed CT-infected endosperm tissues, as well as the imbibed AR605-infected endosperm tissues. Furthermore, exceptions for ribitol were all from the dry samples, including the non-aged, AR584-infected endosperm tissues, as well as aged, AR584-infected embryo and endosperm tissues. For the non-aged (dry and imbibed) samples, the concentrations of trehalose were significantly higher in all the three endophyte-infected than the endophyte-free embryo tissues ($FC > 8$, $p < 0.011$) (Table 4.3A and 4.3C). Trehalose was also significantly higher or displayed near-significant trends toward an increase in the non-aged, dry endosperm and aged, dry embryo tissues ($FC > 2$, $p < 0.1$) (Table 4.3A and 4.3B).

**Table 4.3 Heatmap for the effects of endophyte infection on selected metabolites in the embryo and endosperm tissues with FC (value > 1.0 means more in endophyte-infected than endophyte-free) and significance value[1].**

Down-regulated $p \le 0.01$ $0.01 < p \le 0.05$ $0.05 < p \le 0.10$
Up-regulated $p \le 0.01$ $0.01 < p \le 0.05$ $0.05 < p \le 0.10$

| | | F1 | F2 | F3 | | Mannitol | | Ribitol | | Trehalose | |
|---|---|---|---|---|---|---|---|---|---|---|---|
| | | | | | | FC | p-value | FC | p-value | FC | p-value |
| A | Embryo | Dry | AA- | E- | AR584 | 5.11 | 0.012 | n.a. | 0.089 | 8.58 | 0.006 |
| | | | | | AR605 | 6.10 | 0.025 | n.a. | 0.012 | 8.17 | 0.001 |
| | | | | | CT | 4.02 | 0.001 | n.a. | 0.000 | 10.33 | 0.003 |
| | Endosperm | | | | AR584 | 9.85 | 0.000 | n.a. | 0.253 | 2.69 | 0.068 |
| | | | | | AR605 | 15.26 | 0.003 | n.a. | 0.003 | 3.66 | 0.038 |
| | | | | | CT | 5.20 | 0.006 | n.a. | 0.000 | 5.00 | 0.051 |
| B | Embryo | | AA+ | | AR584 | 7.72 | 0.009 | 1.79 | 0.445 | 17.74 | 0.058 |
| | | | | | AR605 | 8.22 | 0.003 | 7.25 | 0.017 | 6.95 | 0.000 |
| | | | | | CT | 8.41 | 0.003 | 12.58 | 0.008 | 15.51 | 0.005 |
| | Endosperm | | | | AR584 | 8.89 | 0.044 | n.a. | 0.212 | 8.73 | 0.186 |
| | | | | | AR605 | 11.54 | 0.000 | n.a. | 0.001 | 13.38 | 0.367 |
| | | | | | CT | 9.36 | 0.124 | n.a. | 0.016 | 4.59 | 0.284 |
| C | Embryo | Imbibed | AA- | | AR584 | 7.18 | 0.008 | n.a. | 0.004 | 9.46 | 0.003 |
| | | | | | AR605 | 9.65 | 0.034 | n.a. | 0.006 | 8.10 | 0.011 |
| | | | | | CT | 4.90 | 0.001 | n.a. | 0.002 | 9.34 | 0.005 |
| | Endosperm | | | | AR584 | 8.60 | 0.089 | n.a. | 0.013 | 1.13 | 0.844 |
| | | | | | AR605 | 9.88 | 0.089 | n.a. | 0.009 | 2.09 | 0.216 |
| | | | | | CT | 4.65 | 0.049 | n.a. | 0.018 | 1.23 | 0.690 |
| D | Embryo | | AA+ | | AR584 | 54.80 | 0.032 | n.a. | 0.038 | 1.18 | 0.775 |
| | | | | | AR605 | 79.70 | 0.018 | n.a. | 0.010 | 1.19 | 0.756 |
| | | | | | CT | 53.27 | 0.012 | n.a. | 0.056 | 0.98 | 0.973 |
| | Endosperm | | | | AR584 | 51.26 | 0.052 | n.a. | 0.017 | 0.57 | 0.242 |
| | | | | | AR605 | 131.83 | 0.151 | n.a. | 0.051 | 1.10 | 0.745 |
| | | | | | CT | 47.07 | 0.123 | n.a. | 0.092 | 0.73 | 0.177 |

[1]FC was calculated as the ratio of the concentration of individual metabolites in the non-underlined treatment and the underlined treatment in F3. n.a. in the 'FC' column denotes that the denominator was zero (the value from the non-underlined treatment). The meanings of the coloured cells are as above. The full table for the effects of endophyte infection on all the tested sugars is found in Table A4.5. F1 = factor 1, F2 = factor 2, F3 = factor 3, AA- = non-accelerated aging, AA = accelerated aging, CT = common-toxic, E- = endophyte-free, FC = fold change.

4.4.3.1.2 Effects of AA on the soluble sugar profiles in the embryo and endosperm tissues

For the dry embryo tissues, AA resulted in significantly higher or near-significant increases in the concentrations of DL-arabinose (endophyte-free, p = 0.008; AR584, p = 0.003; AR605, p = 0.005; CT, p = 0.022), D-galactose (endophyte-free, p = 0.038; AR584, p = 0.074; AR605, p = 0.084; CT, p = 0.076), raffinose (endophyte-free, p = 0.018; AR584, p = 0.042; AR605, p = 0.006; CT, p = 0.023) and xylose (endophyte-free, p = 0.007; AR584, p = 0.009; AR605, p = 0.052; CT, p = 0.016) in both the endophyte-free and endophyte-infected samples. AA also resulted in significantly lower or near-significant decreasing trends in the concentrations of sucrose in all the endophyte-free and endophyte-infected embryo tissues (endophyte-free, p = 0.070; AR584, p = 0.016; AR605, p = 0.036; CT, p = 0.012), and also significantly lower levels of trehalose in only the endophyte-infected embryo tissues (AR584, p = 0.002; AR605, p = 0.004; CT, p = 0.004). The concentration of trehalose in the endophyte-free dry embryo tissues dropped sharply after AA (FC = 0.15) compared with before AA, but there was no statistical significance (Table 4.4A).

For the dry endosperm tissues, AA caused significantly higher or near-significant increases to concentrations of DL-arabinose (endophyte-free, p = 0.001; AR584, p = 0.063; AR605, p = 0.022; CT, p = 0.030) and significantly lower concentrations of trehalose in both the endophyte-free and endophyte-infected samples (endophyte-free, p = 0.016; AR584, p = 0.021; AR605, p = 0.019; CT, p = 0.037) (Table 4.4B).

In the imbibed embryo tissues, the concentrations of glucose (AR584, p = 0.006; AR605, p = 0.048; CT, p = 0.002) and trehalose (AR584, p = 0.001; AR605, p = 0.003; CT, p = 0.002) were significantly decreased after AA in the three endophyte-infected embryo tissues. It is interesting that the concentration of trehalose was elevated in the endophyte-free embryo tissues, which contrasts with the result in dry embryo tissues (Table 4.4C).

**Table 4.4 Heatmap for the effects of AA on selected metabolites in the embryo and endosperm tissues with FC (value > 1.0 means more in AA+ than AA-) and significance value[1].**

Down-regulated $p \le 0.01$ $0.01 < p \le 0.05$ $0.05 < p \le 0.10$
Up-regulated $p \le 0.01$ $0.01 < p \le 0.05$ $0.05 < p \le 0.10$

| | | F1 | F2 | F3 | DL-arabinose | | Galactose | | Glucose | | Raffinose | | Sucrose | | Trehalose | | Xylose | |
|---|---|---|---|---|---|---|---|---|---|---|---|---|---|---|---|---|---|---|
| | | | | | FC | p-value | FC | p-value | FC | p-value | FC | p-value | FC | p-value | FC | p-value | FC | p-value |
| A | Embryo | Dry | E- | AA- | 2.06 | 0.008 | 2.40 | 0.038 | 1.46 | 0.242 | 2.11 | 0.018 | 0.66 | 0.070 | 0.15 | 0.124 | n.a. | 0.007 |
| | | | AR584 | | 2.89 | 0.003 | 2.88 | 0.074 | 1.51 | 0.025 | 1.83 | 0.042 | 0.71 | 0.016 | 0.31 | 0.002 | 6.64 | 0.009 |
| | | | AR605 | | 2.02 | 0.005 | 2.33 | 0.084 | 1.11 | 0.611 | 2.08 | 0.006 | 0.71 | 0.036 | 0.13 | 0.004 | n.a. | 0.052 |
| | | | CT | | 2.54 | 0.022 | 2.56 | 0.076 | 1.24 | 0.139 | 2.20 | 0.023 | 0.78 | 0.012 | 0.22 | 0.004 | n.a. | 0.016 |
| B | Endosperm | | E- | | 2.52 | 0.001 | 1.70 | 0.023 | 2.03 | 0.182 | n.a. | 0.018 | 0.95 | 0.867 | 0.05 | 0.016 | 6.78 | 0.003 |
| | | | AR584 | | 3.14 | 0.063 | 2.44 | 0.040 | 1.08 | 0.905 | 0.58 | 0.740 | 0.77 | 0.612 | 0.17 | 0.021 | n.a. | 0.164 |
| | | | AR605 | | 2.05 | 0.022 | 1.24 | 0.371 | 0.85 | 0.703 | 1.09 | 0.899 | 0.48 | 0.180 | 0.20 | 0.019 | n.a. | 0.002 |
| | | | CT | | 4.27 | 0.030 | 4.48 | 0.114 | 4.26 | 0.189 | 3.61 | 0.124 | 1.05 | 0.748 | 0.05 | 0.037 | n.a. | 0.016 |
| C | Embryo | Imbibed | E- | AA+ | 0.66 | 0.248 | 1.45 | 0.391 | 0.48 | 0.114 | 0.69 | 0.205 | 1.07 | 0.507 | 2.00 | 0.420 | 1.72 | 0.615 |
| | | | AR584 | | 0.56 | 0.028 | 2.59 | 0.216 | 0.36 | 0.006 | 1.54 | 0.132 | 0.67 | 0.014 | 0.25 | 0.001 | n.a. | 0.138 |
| | | | AR605 | | 0.59 | 0.050 | 1.48 | 0.481 | 0.34 | 0.048 | 1.04 | 0.950 | 0.86 | 0.404 | 0.29 | 0.003 | n.a. | 0.239 |
| | | | CT | | 0.67 | 0.169 | 2.21 | 0.533 | 0.47 | 0.002 | 0.61 | 0.146 | 0.92 | 0.672 | 0.21 | 0.002 | n.a. | 0.423 |
| D | Endosperm | | E- | | 0.74 | 0.184 | 0.78 | 0.234 | 0.86 | 0.526 | n.a. | n.a. | 0.77 | 0.293 | 1.45 | 0.448 | 0.91 | 0.941 |
| | | | AR584 | | 1.31 | 0.507 | 1.25 | 0.559 | 1.00 | 0.986 | n.a. | n.a. | 0.67 | 0.021 | 0.73 | 0.609 | n.a. | 0.372 |
| | | | AR605 | | 0.88 | 0.512 | 0.99 | 0.972 | 0.84 | 0.658 | n.a. | n.a. | 1.04 | 0.910 | 0.77 | 0.522 | n.a. | 0.197 |
| | | | CT | | 1.18 | 0.532 | 1.35 | 0.365 | 1.22 | 0.628 | n.a. | n.a. | 0.67 | 0.247 | 0.85 | 0.550 | n.a. | n.a. |

[1]FC was calculated as of the ratio of the amount of an individual metabolite for the non-underlined treatment and the underlined treatment in Factor 3. n.a. in the 'FC' column denotes that the denominator was zero (the value from the non-underlined treatment). n.a. in p-value means that all the observations in the related treatment were zero. The meanings of the coloured cells are as above. The full table for the effects of AA on all the sugars measured is found in Table A4.6. F1 = factor 1, F2 = factor 2, F3 = factor 3, AA- = non-accelerated aging, AA = accelerated aging, CT = common-toxic, E- = endophyte-free, FC = fold change.

4.4.3.1.3 Effects of imbibition on the soluble sugar profiles in the embryo and endosperm tissues

For the non-aged embryo tissues, imbibition induced significantly higher concentrations of maltose in both endophyte-free ($p = 0.037$) and endophyte-infected embryo tissues (AR584, $p = 0.010$; AR605, $p = 0.047$; CT, $p = 0.048$), as well as significantly decreased concentrations of trehalose in endophyte-infected embryo tissues (AR584, $p = 0.021$; AR605, $p = 0.007$; CT, $p = 0.002$). Galactinol was only significantly reduced in non-aged endophyte-free embryo tissues ($p = 0.020$) (Table 4.5A).

For the non-aged endosperm tissues, the sugars galactinol (AR584, $p < 0.001$; AR605, $p = 0.089$; CT, $p = 0.004$) and trehalose (AR584, $p = 0.022$; AR605, $p = 0.021$; CT, $p = 0.043$) were significantly decreased with imbibition in the endosperm tissues of all the three endophyte-infected strains (Table 4.5B).

For the aged embryo tissues, the sugars which were significantly decreased with imbibition were DL-arabinose (endophyte-free, $p = 0.002$; AR584, $p = 0.003$; AR605, $p = 0.003$; CT, $p = 0.005$), glucose (endophyte-free, $p = 0.017$; AR584, $p = 0.004$; AR605, $p = 0.018$; CT, $p = 0.021$) and glycerol (endophyte-free, $p = 0.035$; AR584, $p = 0.039$; AR605, $p < 0.001$; CT, $p = 0.036$) in both the endophyte-free and endophyte-infected embryo tissues (Table 4.5C).

For the aged endosperm tissues, imbibition resulted in significant decreases in the concentration of DL-arabinose in both endophyte-free and endophyte-infected strains (endophyte-free, $p = 0.007$; AR584, $p = 0.046$; AR605, $p = 0.010$; CT, $p = 0.027$) (Table 4.5D).

**Table 4.5 Heatmap for the effects of imbibition on selected metabolites in the embryo and endosperm tissues with FC (value > 1.0 means more in imbibed than dry) and significance value[1].**

Down-regulated $p \le 0.01$ $0.01 < p \le 0.05$ $0.05 < p \le 0.10$
Up-regulated $p \le 0.01$ $0.01 < p \le 0.05$ $0.05 < p \le 0.10$

| | | F1 | F2 | F3 | | DL-arabinose | | Galactinol | | Glucose | | Glycerol | | Maltose | | Trehalose | |
|---|---|---|---|---|---|---|---|---|---|---|---|---|---|---|---|---|---|
| | | | | | | FC | p-value | FC | p-value | FC | p-value | FC | p-value | FC | p-value | FC | p-value |
| A | Embryo | AA- | E- | Dry | Imbibed | 0.82 | 0.428 | 0.70 | 0.020 | 1.41 | 0.321 | 1.41 | 0.242 | 4.55 | 0.037 | 0.61 | 0.264 |
| | | | AR584 | | | 1.33 | 0.042 | 1.01 | 0.887 | 1.35 | 0.068 | 1.32 | 0.192 | 3.73 | 0.010 | 0.67 | 0.021 |
| | | | AR605 | | | 0.93 | 0.681 | 0.80 | 0.385 | 1.50 | 0.234 | 2.25 | 0.038 | 8.14 | 0.047 | 0.60 | 0.007 |
| | | | CT | | | 1.01 | 0.945 | 0.88 | 0.249 | 1.09 | 0.297 | 1.16 | 0.432 | 4.06 | 0.048 | 0.55 | 0.002 |
| B | Endosperm | | E- | | | 1.13 | 0.508 | 0.27 | 0.129 | 0.74 | 0.517 | 0.47 | 0.045 | 1.34 | 0.386 | 0.49 | 0.146 |
| | | | AR584 | | | 0.81 | 0.358 | 0.29 | 0.000 | 0.44 | 0.415 | 0.81 | 0.551 | 1.29 | 0.049 | 0.21 | 0.022 |
| | | | AR605 | | | 0.84 | 0.376 | 0.37 | 0.089 | 0.74 | 0.520 | 1.20 | 0.551 | 1.57 | 0.112 | 0.28 | 0.021 |
| | | | CT | | | 0.67 | 0.103 | 0.24 | 0.004 | 0.70 | 0.545 | 0.69 | 0.322 | 1.40 | 0.478 | 0.12 | 0.043 |
| C | Embryo | AA+ | E- | | | 0.26 | 0.002 | 0.63 | 0.022 | 0.46 | 0.017 | 0.62 | 0.035 | 3.02 | 0.078 | 8.13 | 0.218 |
| | | | AR584 | | | 0.26 | 0.003 | 0.74 | 0.068 | 0.32 | 0.004 | 0.56 | 0.039 | 1.60 | 0.481 | 0.54 | 0.201 |
| | | | AR605 | | | 0.27 | 0.003 | 0.64 | 0.139 | 0.46 | 0.018 | 0.38 | 0.000 | 3.85 | 0.059 | 1.39 | 0.319 |
| | | | CT | | | 0.27 | 0.005 | 0.66 | 0.092 | 0.41 | 0.021 | 0.53 | 0.036 | 2.19 | 0.077 | 0.51 | 0.012 |
| D | Endosperm | | E- | | | 0.33 | 0.007 | 0.23 | 0.006 | 0.31 | 0.109 | 0.36 | 0.010 | 1.34 | 0.085 | 13.19 | 0.023 |
| | | | AR584 | | | 0.34 | 0.046 | 0.12 | 0.020 | 0.41 | 0.185 | 0.42 | 0.230 | 1.53 | 0.312 | 0.86 | 0.828 |
| | | | AR605 | | | 0.36 | 0.010 | 0.42 | 0.101 | 0.73 | 0.347 | 1.04 | 0.928 | 4.37 | 0.110 | 1.09 | 0.927 |
| | | | CT | | | 0.18 | 0.027 | 0.25 | 0.020 | 0.20 | 0.174 | 0.47 | 0.282 | 1.81 | 0.161 | 2.09 | 0.165 |

[1]FC was calculated as of the ratio of the amount of individual metabolite under the non-underlined treatment and the underlined treatment in Factor 3. n.a. in the 'FC' column denotes that the denominator was zero (the value from the non-underlined treatment). The meanings of the coloured cells are as above. The full table for the effects of imbibition on all the sugars measured is found in Table A4.7. F1 = factor 1, F2 = factor 2, F3 = factor 3, AA- = non-accelerated aging, AA = accelerated aging, CT = common-toxic., FC = fold change.

#### 4.4.3.2 Correlation of sugar concentrations in/between the embryo and endosperm tissues

The correlation matrix revealed several obvious positive correlation groups. In the embryo tissues, sugars in each of the three groups were positively correlated with each other (red squares in Figure 4.1). Firstly, the increases in glucose were correlated with increases in glycerol ($r = 0.73$, Square A in Figure 4.1). Secondly, the increases in galactinol were correlated with increases in trehalose ($r=0.57$, Square B in Figure 4.1). Thirdly, D-galactose, lactose and mannose concentrations were positively related with each other (all $r > 0.59$, Square C in Figure 4.1).

In the endosperm tissues, increases in maltose concentration were positively correlated with the changes in the levels of lactose ($r = 0.87$, Square D in Figure 4.1). Additionally, sucrose, myo-inositol, galactinol and xylitol were positively correlated with each other (all $r > 0.5$, Square E in Figure 4.1). Plus, the increases in D-arabitol were correlated with increases in mannitol ($r = 0.69$, Square F in Figure 4.1) and the concentrations of fructose, glucose, glycerol, D-galactose and sorbitol were all positively related with each other (all $r > 0.5$, Square G in Figure 4.1).

The concentrations of the sugars DL-arabinose ($r = 0.83$), mannitol ($r = 0.69$), ribitol ($r = 0.91$), trehalose ($r = 0.79$) and xylose ($r = 0.65$) in the embryo tissues were positively correlated with the respective sugars in the endosperm (marked red 'Star' in Figure 4.1). The metabolites in the embryo and endosperm tissues were rarely negatively correlated; however, a moderate negative correlation between maltose concentration in the embryo and xylitol concentration in the endosperm was observed ($r = -0.54$). Moreover, concentrations of sucrose in the embryo tissues were negatively correlated with DL-

arabinose and xylose in both the embryo (DL-arabinose: r = -0.55, xylose: p = -0.66) and the endosperm tissues (DL-arabinose: r = -0.55, xylose: r = -0.62).

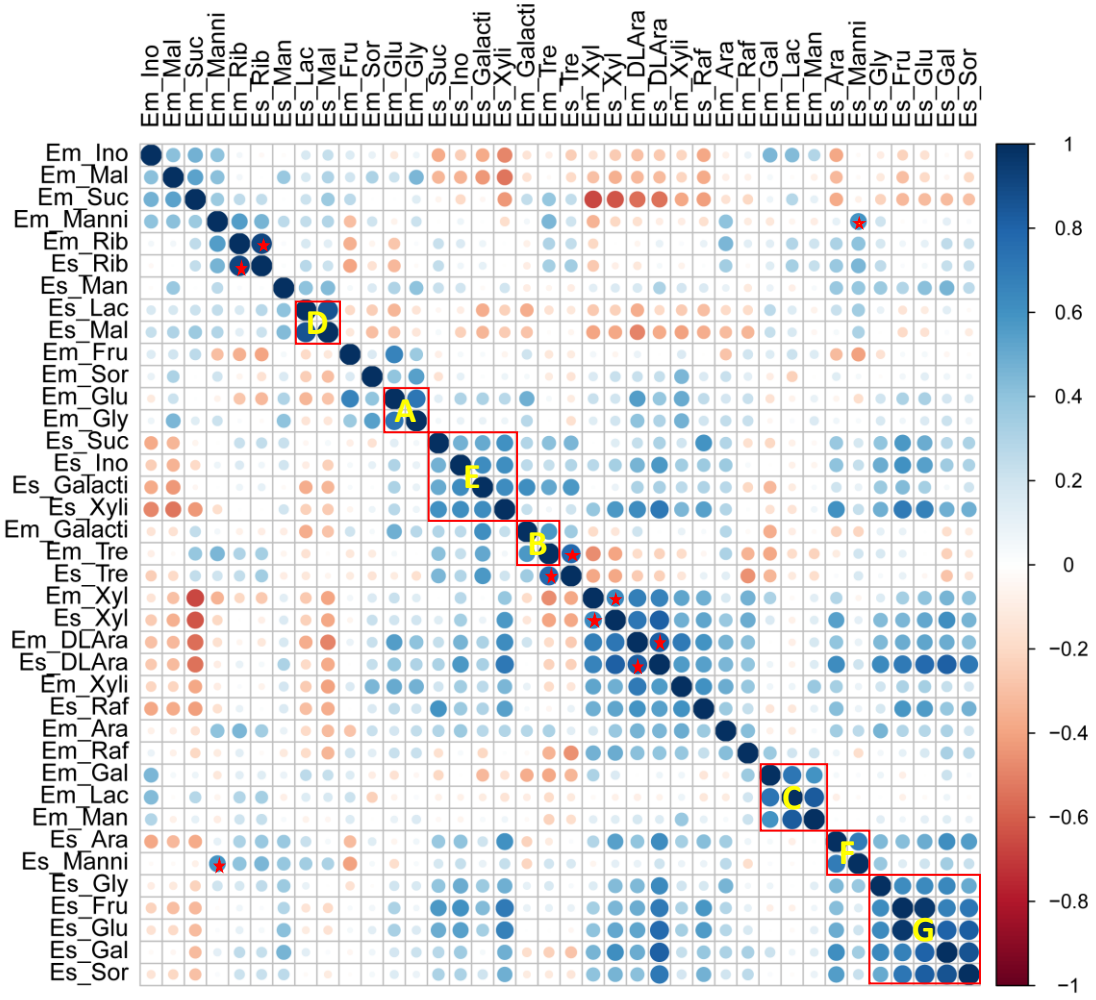


**Figure 4.1 Correlation matrix for concentrations of 19 metabolites in both the embryo and endosperm tissues ordered according to hierarchical cluster analysis between sugars.** The colour scheme indicates the correlation strength as shown by the scale bar (at the right side of the figure) based on Spearman's correlation analysis. Abbreviations: Em = embryo, Es = endosperm. Ara = D-arabitol, DLAra = DL-arabinose, Fru = fructose, Galacti = galactinol, Gal = D-galactose, Glu = glucose, Gly = glycerol, Ino = myo-inositol, Mal = maltose, Manni = mannitol, Raf = raffinose, Rib = ribitol, Sor = sorbitol, Suc = sucrose, Tre = trehalose, Xyli = xylitol, Xyl = xylose.

4.4.3.3 Pathway analysis on the sugars measured in this study

The sugar metabolites analysed in this study were mainly involved in two pathways: galactose metabolism and starch and sucrose metabolism (Figure A4.1). Five sugar metabolites (trehalose, glucose, maltose, sucrose, fructose) analysed in this study were involved in the starch and sucrose metabolism pathway (Figure 4.2A). For all the endophyte-infected accessions, the concentrations of trehalose significantly decreased in both the embryo and endosperm tissues after AA and imbibition treatments, and where AA and imbibition treatments were combined. However, the accumulation of glucose (the product of trehalose degradation) was only observed in endophyte-free, AR584 and CT-infected dry embryo tissues after AA (Figure 4.2B).

**A**

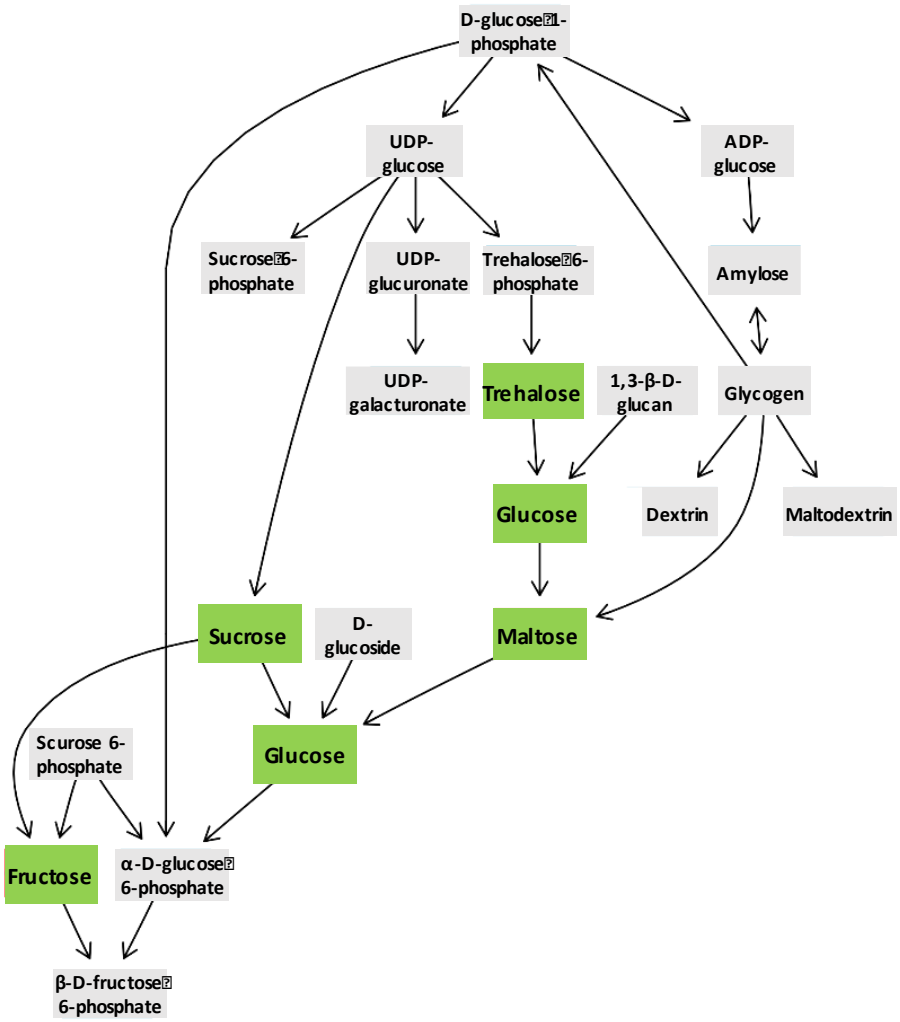
D-glucose 1-phosphate
UDP-glucose
ADP-glucose
Sucrose 6-phosphate
UDP-glucuronate
Trehalose 6-phosphate
Amylose
UDP-galacturonate
Trehalose
1,3-β-D-glucan
Glycogen
Glucose
Dextrin
Maltodextrin
Sucrose
D-glucoside
Maltose
Scurose 6-phosphate
Glucose
Fructose
α-D-glucose 6-phosphate
β-D-fructose 6-phosphate

**B**

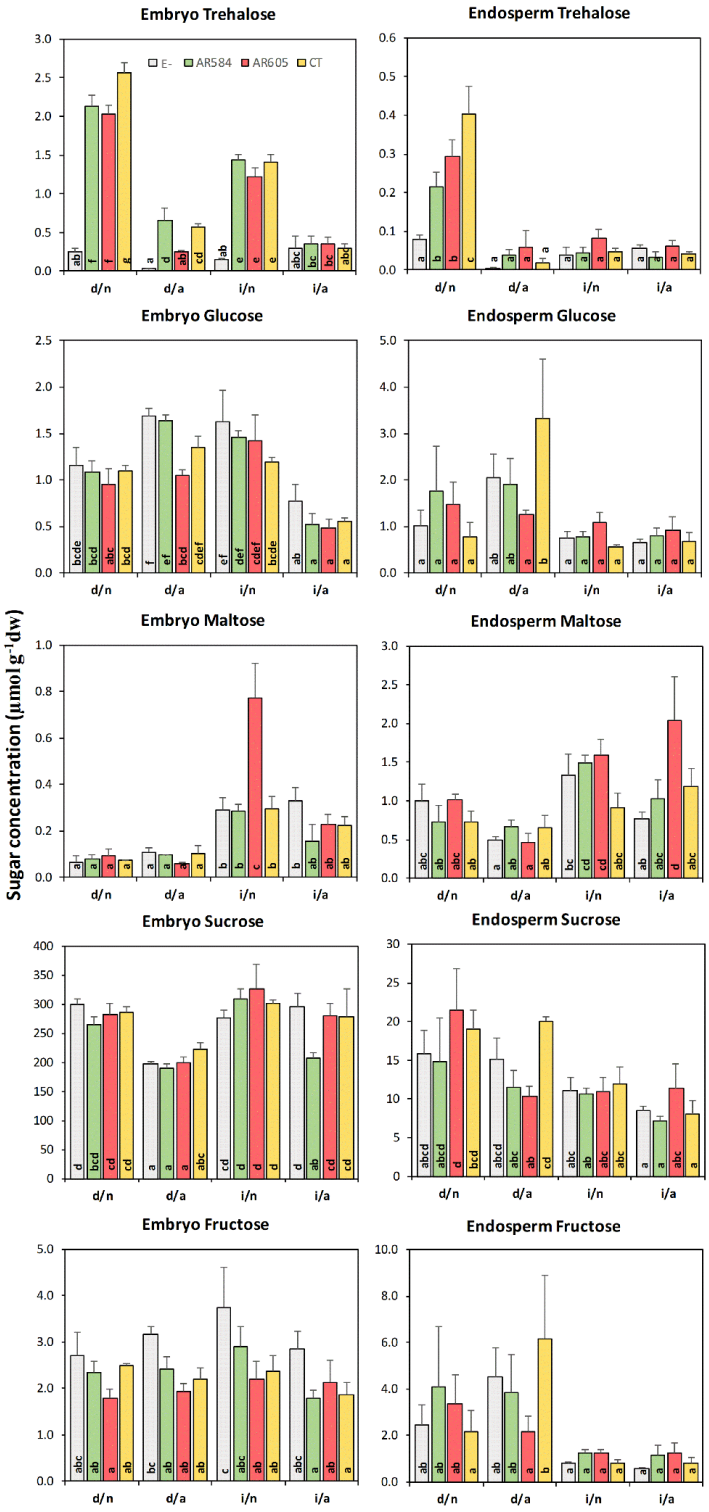


**Figure 4.2 A) Pathway of starch and sucrose metabolism. The pathway was obtained from Metaboanalyst with modification. B) Changes in selected metabolites inside the embryo tissues under different treatments. Each bar chart indicates the amount of each sugar under different treatments.** Different letters inside the bar imply multiple comparisons between different treatments by Duncan's analysis. The x-axis denotes the treatment combinations and the y-axis shows the concentration of each sugar. E- = endophyte-free, CT = common-toxic; d = dry, i = imbibed; n = non-accelerated aging treatment, a = accelerated aging treatment.

In the galactose metabolism pathway, ten sugar metabolites measured in this study (raffinose, lactose, galactinol, sucrose, mannose, D-galactose, sorbitol, myo-inositol, glucose and fructose) were involved (Figure A4.2a). After AA, raffinose was clearly elevated in the dry embryo tissues of all the four seed accessions. With the accumulation of raffinose, a significant decrease in one of its component sugars, sucrose was observed in endophyte-free, AR584- and AR605-infected embryo tissues after AA. The concentration of glucose which is one product when sucrose is catalysed significantly increased in endophyte-free and AR584-infected embryo tissues. However, no significant changes to fructose which is the other product when sucrose is catalysed with respect to AA in both endophyte-free and endophyte-infected embryo tissues. With the significant decreases in galactinol in both the endophyte-free and endophyte-infected embryo tissues, one of its component sugars D-galactose increased but did not reach significance (Figure A4.2b).

Under imbibition treatment, raffinose significantly increased in only CT-infected embryo tissues but there were no significant differences in any of its component sugars (sucrose, fructose and glucose). In terms of AA and imbibition treatments, significant decreases can also be seen in the concentration of galactinol and increased trend in D-galactose (Figure A4.2b). In the endosperm tissues, an obvious trend was the significant decreases in galactinol in all the accessions under imbibition treatment, as well as combined treatments of AA and imbibition (Figure A4.2c).

## 4.5 Discussion

Viable endophyte longevity in stored seeds can be presumed to depend on three factors: (i) storage of reserve carbohydrates (amounts, ratios and types); (ii) enzymes present to mobilise these stored carbohydrates during seed imbibition; and (iii) the level of colonisation by the endophyte of particular seed tissues (hyphae present in the required location and quantity and at the right time). This study investigated the first factor. This research used AA to mimic as closely as possible the physical deterioration processes that would occur during natural aging. AA achieved by creating conditions of biologically high temperature and high humidity has been used in many experiments researching endophyte survival during seed storage (Card et al. 2014b; Missaoui et al. 2015; Bylin et al. 2016). After this AA regime (40°C, 100% RH, 4 days) was applied to endophyte-infected seed accessions, the viability of *Epichloë* dropped sharply while the host seed maintained a high germination rate (Table 4.2). As with previous studies, this study confirmed that endophyte lost viability much sooner than the seed (Gundel et al. 2009a; Hill et al. 2009; Bylin et al. 2016). The reason for including the imbibition treatment in this study was to capture information on metabolite changes in tissues of the seed/endophyte association during the initiation of germination. It has been shown that the imbibition state transition involves substantial reorganisation of cellular components (Larson 1968; Leopold 1980). There are two reasons for extracting embryo and endosperm tissues and analysing them separately: the hyphae of *Epichloë* endophytes are concentrated in or on the embryo tissues (including the embryo axis, scutellum and the 'infection layer' as described in Chapter 3), while the endosperm contains no hyphae but typically hyphae are observed between the aleurone layer and

the seed coat; the hyphae in the embryo tissues are responsible for transmission to the next generation (Christensen et al. 2009).

Prior stored reserves within seeds are needed for the endophytes since there is no consistent nutrient supplied from photosynthesis. There are two major groups of storage carbohydrates in fungi: (i) short-chain carbohydrates such as trehalose, a glucose dimer (α-$_D$-glucopyranosyl-[1-1]-α-$_D$-glucopyranoside] and sugar alcohols (also called polyols, e.g. arabitol, mannitol); and (ii) long-chain carbohydrate present as glycogen (Nehls 2008). The data collected include only selected short chain fungal carbohydrates, and long-chain carbohydrates will not be discussed here.

Of the nineteen sugars analysed in this study, the disaccharide sugar sucrose was found in the highest amounts within the embryo tissues of tall fescue seeds within this study. Sucrose synthesis is regulated and coordinated with starch metabolism and photosynthesis in the green plant tissues (Zhou et al. 2003) and has protective effects on the cell membranes (Crowe et al. 1986) with sucrose levels remaining fairly constant during seed storage (Bernal-Lugo et al. 1992). Myo-inositol was the sugar alcohol that occurred in the greatest concentrations (Nagabhyru et al. 2013). Myo-inositol was reported to be a transient C pool during seed development which contributes to the synthesis of raffinose that accumulates in the mature seeds (Xu et al. 2016). The relatively low concentrations of raffinose in tall fescue seeds shown in this study, probably indicates the genes responsible for the production of enzymes catalysing the conversion of myo-inositol to raffinose were under-expressed.

### 4.5.1 Effects of endophytes on embryo and endosperm sugar profiles

Some studies have investigated sugar alcohols in vegetative tissues with/without endophyte infection. Richardson et al. (1992) showed that myo-inositol was the most abundant sugar alcohol in endophyte-infected leaf blades or sheaths but not in endophyte-free ones in tall fescue. Rasmussen et al. (2008) showed that one genotype of the tall fescue symbiont contained two polyols, D-arabitol and mannitol in the vegetative tissues. The results from this study are consistent with those from the former two studies and show the presence of all three previously noted sugar alcohols (mannitol, myo-inositol and D-arabitol). The amount of mannitol was consistently higher in the three endophyte-infected embryo/endosperm tissues than the endophyte-free counterparts (Tables 4.3, A4.3 and A4.4). Mannitol has been used to quantify the endophyte biomass in plant tissues in several papers (Rasmussen et al. 2008). However, mannitol is not an endophyte-specific sugar. In this study, mannitol was present in comparatively high concentrations in endophyte-free seeds. The presence of a relatively high amount of mannitol in the host tissues might be related to its multiple functions. It has been reported that mannitol can act as an osmolyte and in addition to roles maintaining cell turgor pressure and in energy storage, can also enhance cell membrane stability and protect metabolic machinery during plant dehydration (Chaves et al. 2003; Carvalhais et al. 2011).

The concentration of ribitol was also significantly higher in the endophyte-infected than endophyte-free seeds with, but with ribitol levels nearly zero in endophyte-free seeds (Tables 4.3, A4.3 and A4.4). Moreover, the concentration of ribitol in the endophyte-infected seeds was stable after AA and imbibition treatments. Hence, based on the

present results, ribitol is much more suitable as a 'marker' sugar for the presence of endophyte. The amount of ribitol has been shown to be significantly higher in the leaves of three genera of the family Rosaceae infected with the parasitic fungus of *Gymnosporangium asiaticum* than leaves without infection (Lee et al. 2016). However, the metabolic roles of ribitol are not clearly understood at this point in time.

Mannitol and ribitol were both more abundant in the embryo than the endosperm tissues (Tables A4.3 and A4.4). As discussed previously, the endophyte mycelia are typically observed only in the aleurone layer surrounding the endosperm tissue but are more common in intercellular spaces of the embryo tissues. Therefore, the ribitol and mannitol concentration data for the embryo and endosperm tissues is consistent with the expected endophyte distributions, which are that more mycelium per unit dry weight of host tissue would be concentrated in the embryo than in the endosperm tissues.

### 4.5.2 Effects of AA on embryo and endosperm sugar profiles

AA was associated with a significant decrease in the concentration of trehalose in both dry embryo and endosperm tissues of all the three host-endophyte combinations, and also in dry endophyte-free endosperm tissues (Table 4.4). The decrease in trehalose with AA suggests its importance for maintaining endophyte viability.

Trehalose is a common disaccharide in microorganisms and is also present in plant tissues. It is plentiful in plant symbioses with fungi and bacteria (Elbein et al. 2003). There is some evidence suggesting that trehalose in yeast functions less as a reserve, and more to maintain the structural integrity of the cytoplasm under environmental

stress conditions (Wiemken 1990). Various other authors consider it acts as a compatible osmolyte, stabilising and protecting proteins and membranes in microorganisms against heat, cold and oxidative stress conditions (Bell et al. 1992; Benaroudj et al. 2001; Tibbett et al. 2002). However, other research has shown that trehalose/mannitol metabolism is necessary for fungal carbon metabolism in ectomycorrhizal symbiosis (Nehls et al. 2010). Thrower et al. (1973) showed that sucrose is the principal carbohydrate acquired from the host by *E. typhina*, and that sucrose acquired in this way is concomitantly transformed to mannitol and trehalose by the fungus. Lam et al. (1994) revealed that sucrose was not used by the fungus directly but was taken up by a sucrose carrier and then hydrolysed into hexose units by cell wall invertase, in order to be utilised by the fungus. Related results were also obtained in a study of the mycorrhizal fungus *Glomus etunicatum* in leek roots, which used NMR to show that this fungus could consume glucose and synthesise trehalose and glycogen when glucose was applied exogenously to mycorrhizae (Shachar-Hill et al. 1995). Similarly, in an association between Bahia grass and *Myriogenospora atramentosa* (a pathogenic fungus from the family Clavicipitaceae), when $^{14}CO_2$ was supplied to the host, the fungal stromata accumulated more $^{14}C$-labeled mannitol, D-arabitol and trehalose (which are not typical plant carbohydrates), but only trace amounts of glucose and sucrose (Smith et al. 1985). Evidence suggests that trehalose can act as an energy source. In *Arabidopsis* and yeast metabolism pathways, one molecule of trehalose is broken down into two molecules of glucose by the enzyme trehalase (Müller et al. 1995). Therefore, the above studies appear to show that the epichloid endophytes do not use common plant sugars like sucrose as their primary energy supply, but on receiving these from their host, convert them to fungal-specific sugars like trehalose, mannitol and D-arabitol to support metabolic functions. In support

of this, under culture conditions, it has been shown that sucrose, trehalose, mannitol and sorbitol were suitable carbon sources for growth while arabinose, ribose, xylose, D-galactose, sorbose and rhamnose were not utilised for the growth of *E. coenophiala* (Kulkarni et al. 1986). Considering the above, and the data from the present study, since trehalose is a metabolite with a notable decline during AA, it seems a reasonable deduction for confirmation in future research that endophytes in post-harvest dry seed and prior to imbibition, do not receive any appreciable amounts of plant sugars such as sucrose from their host and consume trehalose already stored in their mycelia during seed formation, for their maintenance metabolism during seed storage. Therefore, exhaustion of trehalose supply can be proposed from the present data as a mechanism for the loss of viability of endophyte mycelia in seeds. However, as noted, the exact roles of trehalose in endophytes during seed storage requires further research.

There are conflicting results on the changes in raffinose levels during seed aging. In the present study raffinose levels significantly increased with AA in both endophyte-free and endophyte-infected embryo tissues. Consistent with the present results, the amount of raffinose increased after seed storage in seeds of pea (*Pisum sativum*) (Lahuta et al. 2007). However, Bernal-Lugo and Leopold (1992) showed that levels of raffinose significantly declined in embryo tissues of aged maize seed. By comparison, no change was found in raffinose levels of soybean seeds during seed aging (Sun et al. 1995). With respect to the effect of endophyte, there was no significant difference in raffinose between endophyte-free and endophyte-infected embryo/endosperm tissues. In peas, although the amount of raffinose declined, its more polymerised stachyose and verbascose steadily increased with seed storage (Lahuta et al. 2007). Since stachyose

and verbascose were not analysed in this study, the changes of these two polysaccharides in the seeds during the AA treatment are unknown. After AA, raffinose significantly accumulated in both endophyte-free and endophyte-infected embryo tissues (Table 4.4A). Consistent with AA-treated embryo tissues in wheat (45°C, 100% RH; Bernal-Lugo et al. 1992), data from this study also exhibited a significantly higher ratio of raffinose:sucrose in aged than non-aged embryo tissues, with no significant differences between endophyte-free and endophyte-infected seeds (Figure A4.3). A hypothesis for future investigation from this data pattern is that increased raffinose:sucrose ratio might be an indication of embryo aging in tall fescue.

Although the concentrations of xylose were lower than 0.1 µmol $g^{-1}$ DW in all samples, xylose levels were significantly higher in both embryo and endosperm tissues for almost all endophyte-infection categories (though not significant in AR584-infected endosperm tissues before and after AA). Also, the concentrations of DL-arabinose increased with seed aging in both dry endophyte-free and endophyte-infected embryo tissues. The sugars xylose and arabinose are components of polysaccharides comprising grass primary cell walls (White Jr et al. 1991). The increase of xylose and DL-arabinose might imply the degradation of seed cell walls with AA. Also, another possibility for the increases in xylose is the induced catalysis of D-xylulose into xylose (Lee et al. 2016).

### 4.5.3 Effects of imbibition on embryo and endosperm sugar profiles

Seed imbibition is a process whereby a seed changes from a dehydrated state to a fully hydrated state and is then able to grow and respond to environmental stimuli (Vertucci 1989). In the present study imbibition induced only significant decreases to the trehalose in the non-aged and dry endophyte-infected embryo (Table 4.5A) and

endosperm tissues (Table 4.5B). This suggests that trehalose was quickly utilised by the endophytes once metabolic processes started during imbibition. After AA, imbibition resulted in a dramatic increase in the level of trehalose in the endophyte-free embryo tissues, compared to a decrease in AR584 and CT-infected and a slight increase in AR605-infected embryo tissues (Table 4.5C). This indicates that trehalose was produced as a side effect of imbibition processes in host embryo tissues at rates exceeding the needs of those host tissues. A trait of trehalose release in host embryo tissues during seed imbibition would presumably assist the endophyte symbiont with comparatively depleted internal trehalose reserves, to revive from dormancy and restore active growth during seed germination.

The functional significance of the observed variations in maltose levels in the present study are at this stage unclear. The amount of maltose increased in both the non-aged and imbibed embryo and endosperm tissues but was only significant in the embryo tissues. It has been shown that maltose has a slight tendency to become a dominant sugar in the endosperm tissues with imbibition (Aoki et al. 2006). It has also been reported that in rice, starch is broken down into maltose during imbibition (Tanaka et al. 1970; Aoki et al. 2006). For example, Nomura et al. (1969) showed that four days after the start of imbibition, α-amylase activity increased rapidly with increased maltose levels detected in the scutellum.

For the aged samples, there were several sugars that were significantly depleted during imbibition in all endophyte-free and endophyte-infected seed lines, including DL-arabinose, glucose and glycerol in the embryo and DL-arabinose in the endosperm tissues (Table 4.5C and 4.5D). It is suggested that depletion of these sugars in seeds

receiving the AA treatment indicates depletion of host reserve carbohydrates during AA, while depletion of trehalose, as indicated above, indicated depletion of *Epichloë* energy reserves. Another possible explanation for the results is that soluble compounds such as glucose and glycerol can be leached during the imbibition process. For example, in barley and *Quercus nigra* seeds, it has been reported that more sugars including glucose and sucrose are leached from aged seeds than from non-aged seeds (Abdul-Baki et al. 1970; Blanche et al. 1990).

### 4.5.4 Use of CDA in this study

Multivariate analysis approaches enable simultaneous analysis of multiple variables under different treatments (Hair et al. 1998). CDA allows identification of a subset of variables that maximises separation between the experimental groups and quantification of the relative contribution of each variable to the between-group separation. CDA is a statistical technique which necessarily compresses data pattern into a lower number of dimensions when the number of variables analysed simultaneously is high. The loss of dimensions arises because the number of output scores is T-1, where T is the number of treatments in the experiment. This means that in the present study a maximum of 3 scores can be produced (when analysing the 4 endophyte statuses or their interactions) whereas there were 19 metabolites measured, and therefore potentially up to 19 dimensions in the data pattern.

CDA has been applied to studies in horticultural research, geographic differentiation, food science, et al. (Dos Reis et al. 1990; Cruz-Castillo et al. 1994; Ding et al. 1999). MANOVA coupled with CDA has been advocated as the method of choice in the analysis of metabolomics data from factorial designed experiments (Johnson et al. 2007).

However, in the present study analysis of the results using MANOVA and CDA allowed only very general conclusions (Section A4.1). For example, there was a three-way interaction (Endophyte x Aging x State) in the MANOVA results on the sugars in the embryo tissues (Figure A4.4, Table A4.8). From the biplot of the three-way interaction of the embryo data, it was seen that fructose level had a large 'loading coefficient' in the endophyte-free embryo tissues while D-arabitol, mannitol and ribitol had larger loading coefficients in the endophyte-infected embryo tissues of all treatments. Since with the presence of a three-way interaction, it is considered that the two-way interactions have moderator variables (Tracey et al. 1989), the MANOVA/CDA method was found to be unsuitable for interpretation of the data from this research. By comparison, the t-test results provided very detailed information about comparisons of pairwise treatment groups and their significance levels for each metabolite analysed in this research.

### 4.5.5 Hypotheses involving loss of functional integrity

Besides resource depletion questions discussed above, many other mechanisms have been proposed to define the physiological changes in the deterioration of orthodox seeds, such as the deterioration of membrane integrity, decreased enzyme activities and lipid peroxidation (Priestley 1986; Wettlaufer et al. 1991; Sun et al. 1993). The most widely investigated is the accumulation of radical oxygen species (ROS) accumulation in cells (McDonald 1999; Bailly 2004). It has been reported that abscisic acid (ABA) and ROS mediated the seed aging process in cotton (*Gossypium hirsutum*), rapeseed (*Brassica napus*), sunflower (*Helianthus annuus*), tall wheatgrass (*Agropyron elongatum*) and wheat (*Triticum aestivum*) (Goel et al. 2003; Lehner et al. 2008; Eisvand et al. 2010; Morscher et al. 2015; Yin et al. 2015). The accumulation of ABA and ROS implies that

oxidative reactions and membrane damage occur in seeds during storage (Pukacka et al. 2007). Such accumulation might also be one of the mechanisms responsible for the aging of endophytes in stored seed. The above discussion on reserve depletion is not intended to be dismissive of the functional integrity hypotheses; rather to explore the evidence for the importance of reserve depletion mechanisms. Clearly, future research will need to explore more fully the importance of both categories of mechanism.

### 4.5.6 Summary, implications and recommendations for future research

In this study, a simple and reliable GC-FID procedure was employed for the separation and quantification of soluble sugars in the embryo and endosperm tissues. Analysis of soluble sugars in the AA-treated seeds, and especially in endophyte-infected seeds, provided an indication of the sugars that contribute to endophyte longevity during seed storage. Analysis of soluble sugars in imbibed seeds in the early stages of germination provided some insights into the metabolisms of soluble carbohydrates in the embryo and endosperm tissues. However, not all the seed-endophyte associations reacted consistently in their observed sugar profiles to the effects of AA and imbibition. A better understanding of the metabolic pathways implicated in this research (galactose metabolism pathway, starch and sucrose metabolism pathway) requires more extensive investigation of the associated intermediate compounds and the related metabolic enzymes in seed components. More work such as investigating the encoding genes can also be conducted as a sequel to the results of this study (for example the activity of the trehalose-6-phosphate synthase gene TPS).

# Chapter 5 Investigating the relationship between endophyte density in host tissues and endophyte transmission frequency to seed at flowering

## 5.1 Abstract

Real-time PCR has been used for quantifying the presence of microorganisms in plants or soil. Tissue-print immunoblotting (TPIB) is widely applied in identifying the presence of *Epichloë* endophytes in cool-season grasses, and can also be used for the approximate quantification of endophytes hyphal density within the host, by analysing the immunoblot colour intensity. The present research quantified the endophyte density in the shoot apex using real-time PCR, and also analysed the immunoblot colour intensities of laterally bisected florets from six genotypes (high-transmission [HT]: 11, 103, 107; low-transmission [LT]: 13, 79 and 83) and from three positions (bottom, middle and top) of the spike. The florets were collected at three growth stages (Stage I [unfertilised], Stage II [ten days after Stage I] and Stage III [twenty days after Stage I]). The hypothesis is to compare the endophyte density in the HT and LT genotypes, with the density in shoot apex quantified by real-time PCR and in the florets estimated using the immunoblot intensities. Real-time PCR analysis showed that the relative endophyte DNA density in the three HT genotypes was significantly higher than the LT genotypes 13 and 83 ($p < 0.05$), but had no significant difference from 79. The immunoblot intensities of the florets differed in different genotypes and growth stages, and there were significant interactions between genotype and growth stage. The immunoblot colour intensities in genotypes 11, 103, 107 and 13 were significantly higher than the other genotypes at Stage I, while the immunoblot intensities in the three HT genotypes were significantly higher than the three LT genotypes at Stage II. However, there were no significant

differences among all the genotypes at Stage III. Microscopy confirmed that the HT genotypes carried a higher density of endophyte hyphae in the shoot apex tissues and ovaries at Stage I than the LT genotypes. The data indicate that increased endophyte density in host tissue enhances endophyte transmission from the parent plant to mature seeds in the HT genotypes.

## 5.2 Introduction

The shoot apical meristem, at flowering, changes into a reproductive meristem which is capable of forming floral organs (Bernier et al. 2005), and thus becomes the source of reproductive plant tissues, which the endophyte hyphae must traverse to colonise the seeds (Freeman 1904). The vegetative shoot apical meristem in the tillers of perennial ryegrass and tall fescue is dome-like and repetitively produces leaf primordia and bud primordia, thus creating a succession of repeated units called phytomers (Perreta et al. 2009; Pautler et al. 2013). Upon seed germination, endophyte hyphae within the embryos (including the embryo shoot apical meristem) extend into the leaf primordia and axillary buds within the seed, and then a densely branched mycelium is formed in the shoot apical meristem zones (Philipson et al. 1986; Christensen et al. 2008). It was indicated by comparing endophyte genomic DNA, that the endophyte biomass in the shoot apical meristem of different genotypes differed (Cook et al. 2009b). Therefore, it is hypothesised that the hosts of HT genotypes carried more endophyte than the LT genotypes in the shoot apex regions. When a symbiont in perennial ryegrass and tall fescue, *Epichloë* strains have the potential to infect each spikelet and floret. The research aim is to understand the relationship between endophyte density and its transmission efficiency, in two tissue types: namely the shoot apex and florets.

Real-time PCR has been used for qualifying the density of pathogen or mycorrhizal fungi in plants or soil (Böhm et al. 1999; Mumford et al. 2000; Vandemark et al. 2002; Alkan et al. 2006). This quantitative method has also been used for measuring the density of fungal endophytes in perennial ryegrass (Rasmussen et al. 2007; Zhou et al. 2014) and locoweeds (Cook et al. 2009a). TPIB uses antibodies (or other specific ligands in related techniques) to identify target proteins among some unrelated protein species, which involves identification of protein target via antigen-antibody (or protein-ligand) specific reactions (Magi et al. 2005). TPIB is a practical method for detection of endophyte in pasture tissues, based on the detection of endophyte-specific proteins. This method is widely applied in assessing the presence of endophyte in grass tillers (Hahn et al. 2003). Furthermore, the TPIB method is cheaper and more reproducible than test-tube-based enzyme-linked immunosorbent assays (ELISA) (Hiatt et al. 1999). However, sometimes it is different to ascertain whether there are endophytes in the tissues or not by visualising the immunoblots especially when the endophyte density in host tissues is low. Immunoblotting coupled with intensity analysis is widely used in research studies in areas of biochemistry (Guo et al. 2005; Zhou et al. 2006). This research aimed to assess the differences in endophyte density in the shoot apex and florets of the HT and LT genotypes. Specifically, three genotypes previously observed to have high endophyte transmission to seeds (HT, designated 11, 103, 107) and three genotypes with low transmission (LT, designated 13, 79 and 83) were selected based on previous field experiments conducted at Lincoln in Canterbury and Palmerston North in the Manawatu (Gagic et al. unpublished).

## 5.3 Materials and methods

### 5.3.1 Experiment One

5.3.1.1 Plant materials

Plants of each of the 6 genotypes (HT genotypes: 11, 103, 107; LT genotypes: 13, 79 and 83) from a same population (derived from a cross between a late flowering New Zealand cultivar and a European cultivar) to be studied were individually cloned and cultivated in pots filled with an artificial soil mix (composition as described in the Materials and methods section of Chapter 3). Each genotype was cloned into four pots. The pots were placed outside in a sunny area on the campus of AgResearch Grasslands, Palmerston North, New Zealand, and the plants were watered daily with a sprinkler irrigation system.

5.3.1.2 Endophyte quantification in shoot apex using real-time PCR

Shoot apex of the six genotypes were collected by sampling endophyte-infected tillers approximately 3 cm above their youngest roots. Three biological replicates were collected from three tillers of each genotype. Fungal endophyte density inside the plant tissues was estimated by the relative endophyte genomic DNA to the total genomic DNA (endophyte and plant). Real-time PCR was performed on the extracted total DNA from infected plants using a Roche LightCycler® 480 machine (Roche; Sussex, UK). The presence of endophytes in the sampled tillers was assessed before starting real-time PCR by peeling out the external leaf sheath followed by staining with aniline blue and observing under the light microscope. Samples were put into liquid nitrogen immediately after harvest and then stored in a –80 °C freezer until use. The AR37 culture was grown on cellophane paper on potato dextrose agar (PDA) (Difco Laboratories;

Detroit, USA) plates, from which the genomic DNA was used to generate a standard curve for real-time PCR. Both plant tissue and fungal mycelium were ground to a fine powder under liquid nitrogen with a sterilised pestle and mortar. Plant genomic DNA (with included fungal DNA) was extracted using Geneaid® Genomic DNA Mini Kit (Taipei, China) following the manufacturer's handbook. Fungal DNA was isolated from mycelium using the ZR Fungal/Bacterial DNA MiniPrep™ kit (Zymo Research Corporation; Orange, United States) following the manufacturer's protocol. DNA concentrations of both plant and endophyte tissues were determined with a Qubit Fluorometer using a Quant-iT™ dsDNA HS Assay Kit (Invitrogen; Carlsbad, USA). For quantification of the fungal endophyte within the plants, a standard curve (15, 7.5, 0.75, 0.075, 0.0075, 0.00075 ng of fungal DNA) was prepared from DNA extracted from the endophyte mycelium. Thirty nanograms of plant genomic DNA (with fungal DNA inside) was used for quantification of the fungal DNA. The endophyte density in the shoot apex of the six genotypes was assessed using real-time PCR and is expressed as pg fungal DNA per ng total (plant + fungal) genomic DNA. Each DNA quantification reaction included three parallel reactions. One non-template control with three replicates was used in this analysis in which water was substituted for the DNA. The volume of each reaction mixture was 10 µL which contained the amount of DNA (0.00075-15 ng of fungal DNA or 30 ng of plant DNA), 5 µL of 2X KAPA SYBR® FAST qPCR Master Mix (KAPA Biosystems; Boston, United States), 200 nM each of forward and reverse primer. Primers suitable for real-time PCR were fragments of one endophyte-specific gene, encoding a segment DNA for coding nonribosomal peptide synthetase (NRPS-1) with the product of 153 bp (Miao et al. 2014). The NRPS-1 forward primer sequence was: GTCCGATCATTCCAAGCTCGTT, while the NRPS-1 reverse primer sequence was: TGGTGGGAAGTTCCCTGCAC. The PCR protocol

was: stage 1 (1 cycle), an initial denaturation at 95°C for 3 min; stage 2 (45 cycles), 10 s of denaturation at 95°C and 20 s of annealing at 60°C; and 5 s of extension at 72°C, with single fluorescence detection point at the end of the annealing step in each cycle; stage 3 (1 cycle), a melting curve was generated by holding at 95°C for 5 sec and 65°C for 1 minute followed by 95°C continuous with 5 acquisitions per °C; stage 4 (1 cycle), cooling at 40°C for 30 sec.

Twenty-five genotypes of different infection frequencies were used to validate the correlation between endophyte infection frequency and endophyte density. Since microscopic evidence suggested that endophyte hyphae are concentrated at the very base of the shoot apex tissue, only 1 cm above the youngest roots was collected from the 25 genotypes. Three biological replicates were collected from three different tillers of each genotype. The protocol for real-time PCR was the same as that described above.

5.3.1.3 Confocal microscopy

Vegetative tillers to be analysed by microscopy were randomly chosen. The shoot apex (typically about 3cm from the youngest root) was collected from the selected tillers with a scalpel. The plant shoot apex was longitudinally hand-sectioned using a razor blade. The morphology of *E. festucae* var. *lolii* hyphae in the shoot apex was determined by staining with AlexaFluor-488 (Molecular Probes Inc.; Eugene, USA) and the images were captured using a Leica SP5 DM6000B confocal microscope (Leica Microsystems; Heidelberg, Germany). The staining procedure and microscopy settings followed the protocol described by Becker et al. (2015).

### 5.3.2 Experiment Two

#### 5.3.2.1 Plant materials

The same genotypes (11, 103, 107, 13, 79, 83) were used as in Experiment One. The florets were sampled from endophyte-infected spikes at three stages (Stage I, Stage II and Stage III). Stage I was defined by the criterion that all the spikelets had just fully emerged from the attached leaf sheath. Stage II and Stage III were ten days and twenty days later than Stage I, respectively. The florets at Stage I were unfertilised while the florets at Stage II and Stage III were fertilised. Each spike was equally divided into three regions: bottom, middle and top based on the number of spikelets on each spike. At each stage, two spikelets were collected from the bottom, middle and upper part of each spike. At stage I and stage II, in each spikelet, six florets were collected. At stage III, only five florets were collected from each spikelet because some florets fell to the ground with mature seed. Therefore, 12 florets (10 florets for Stage III) were collected at each position per spike. Three spikes were sampled from each genotype and regarded as three replicates of each stage, for data analysis purposes. Before blotting the florets, the randomly-selected spikes were confirmed to be endophyte-infected by peeling off the outer leaf sheath, staining with aniline blue and then observing under a light microscope.

#### 5.3.2.2 Tissue-print immunoblotting

Each floret was blotted by cutting the base of the florets just above the connection of the ovary and rachilla (Figure 5.1), and printing on the nitrocellulose membranes. Three spikes were randomly chosen for each genotype and processed as three biological replicates. The TPIB procedure followed the protocol of Simpson et al. (2012).

Specifically, the membranes were immersed in blocking solution (Tris [hydroxymethyl] methylamine 2.42 g, NaCl 2.92 g, non-fat milk powder 5 g, 1M HCl 10 ml, made up to 1 litre with reverse osmosis [RO] water, adjusted to pH 7.5). Samples were shaken on an orbital shaker for 2 h, then rinsed five times with fresh blocking solution (2.42 g Tris, 2.92 g NaCl, non-fat milk 5 g powder, 10 ml 1 M HCl, made up to 1 liter with RO water, adjusted to pH 7.5). Aliquots of 12.5 µL primary antibody solution (rabbit anti-endophyte antibody produced by AgResearch and Massey University's Small Animal Production Unit) per 25 mL blocking solution were added to fully immerse the membranes which were then shaken for 15 min at room temperature and afterwards incubated in blocking solution overnight at 4°C. The following day, the membranes were rinsed five times with blocking solution and 6.25 µL secondary antibody (goat anti-rabbit IgG-AP, sc-2034) (Santa Cruz Biotechnology; Santa Cruz, USA) per 25 mL blocking solution was added, and the resulting mixture was then shaken for 2 h at room temperature. Excess antibody was poured off, and the membranes were rinsed with blocking solution before being subjected to staining. Dyes were prepared by separately dissolving 20 mg Fast Red (Sigma-Aldrich) in 12.5 ml Tris buffer (Tris [hydroxymethyl methylamine] 24.2 g in 1 litre RO water adjusted to pH 8.2) and 12.5 mg of naphthol AS-MX phosphate (Sigma-Aldrich) in 12.5 ml Tris buffer per membrane. The membranes were shaken for 15 min at room temperature until red colour appeared on positive immunoblots, then rinsed three times with tap water to stop the colour development.

**Figure 5.1 Illustration of the dissection position (red line) for immunoblotting of a floret at Stage I.** Scale bar = 500 µm.

5.3.2.3 Immunoblot intensity analysis

Immunoblot membranes of the florets were scanned into the computer and saved as a pdf document. Then the pdf document was opened with Adobe Photoshop CC 2014 software (Adobe Systems Inc., San Jose, CA), with which the intensity of each immunoblot on the membranes was analysed. The intensity of the immunoblots in twelve florets (ten florets for Stage III) from two spikelets was averaged as one replicate. The RGB-colour image obtained by TPIB was transformed into a greyscale image and inverted for better intensity discrimination. In greyscale mode, individual pixels can acquire an intensity between 0 and 255. The edges of each immunoblot were selected through the 'Lasso' tool, and the intensity of each immunoblot was estimated by the 'Measurement' tool. The immunostaining intensity of each immunoblot was calculated as the difference in grayscale colour intensity between immune-stained tissue and background greyscale intensity and was expressed as arbitrary units (AU).

5.3.2.4 Microscopy

Randomly chosen ovaries were collected at Stage I and subjected to microscopy analysis. The morphology of *E. festucae* var. *lolii* hyphae on both sides of ovaries was determined by staining with AlexaFluor-488, which specifically stains the chitin in fungal cell wall septa as bright green dots (pseudocolor). The stained samples were observed under an inverted confocal laser scanning microscope (FV10i-w, Olympus; Tokyo, Japan) with 10x objective using FV10i-ASW 3.0 Viewer software (Olympus; Center Valley, Pennsylvania). All images were maximum intensity projections of z-stacks. The stained samples were excited with laser light of 473 nm wavelength.

### 5.3.3 Data analysis

All the data analysis was done with RStudio (version 0.99.903) and the figures created with RStudio and Microsoft Excel 2013. One-way ANOVA was applied on analysing the significant difference in the endophyte density among the six genotypes in Experiment One. Differences among the three factors (genotype, position and stage) and their interactions in immunoblot intensity were analysed using a three-way ANOVA in Experiment Two. Fisher's protected least significant difference (LSD) method was utilised for the multiple comparisons in both Experiment One and Two. A mean separation of $p < 0.05$ was considered statistically significant.

## 5.4 Results

### 5.4.1 Experiment One

Compared with the LT genotypes, the three HT genotypes carried more endophyte DNA in the shoot apex. The relative endophyte DNA density in genotypes 11 (2.29 pg/ng), 103 (1.97 pg/ng) and 107 (3.15 pg/ng) was significantly higher than genotypes 13 (0.95

pg/ng) and 83 (1.14 pg/ng) (Figure 5.2A). Multiple comparisons showed that the endophyte density in plant genotypes 11 and 103 was significantly higher than 13 and 83, and was higher than 79 (1.83 pg/ng), but there was no significant difference when comparing genotypes 11 and 103 with genotype 79. Microscopy images revealed that HT genotypes 11, 103 and 107 had higher endophyte hyphal density than the LT genotypes 13, 79 and 83. Specifically, lines of stained septa (indicating fungal hyphae) extend to the top of the apical meristems in the HT genotypes, but do not do so in LT genotypes (Figure 5.2B).

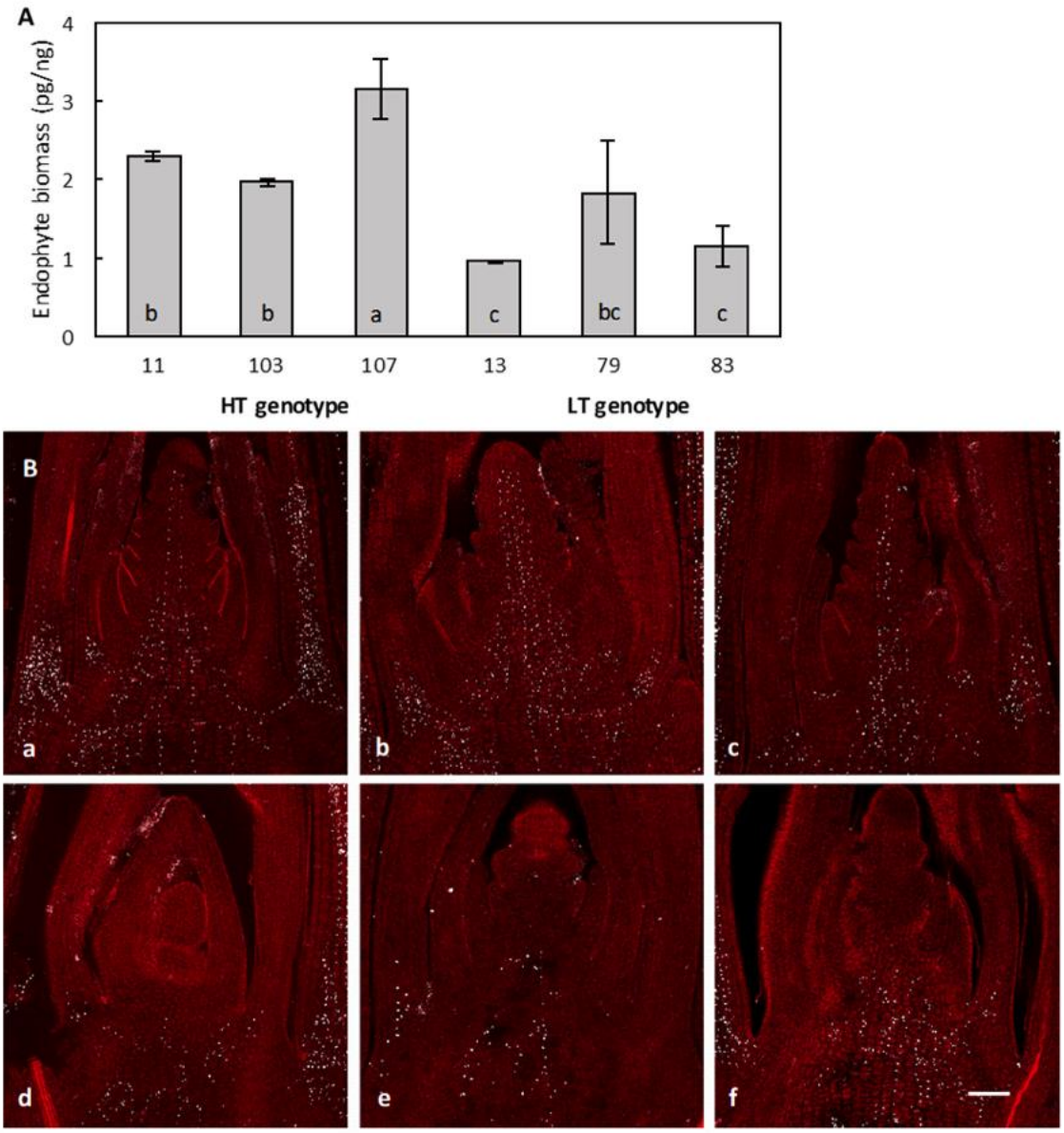


**Figure 5.2 (A) Fungal density (pg fungal DNA/ng plant and fungal genomic DNA) in the shoot apex of HT (11, 103, 107) and LT genotypes (13, 79, 83).** Error bars represent the standard error of the mean. Different small letters on the bars indicate significant differences between the various genotypes at the 0.05 level (ANOVA and Duncan's multiple range test). **(B) Confocal images of Alexa Fluor 488-stained perennial ryegrass shoot apex in six genotypes (11: a; 103: b, 107: c, 13: d; 79: e; 83: f).** The chitin in mycelium septa stained with Alexa Fluor 488 as white dots. Bars = 200 µm.

The same real-time PCR was performed when investigating the hyphal density in the shoot apex tissues of 25 genotypes. Regression analysis between endophyte density and endophyte infection frequency ($p < 0.05$) was detected. Also, genotypes with higher endophyte density tended to have high endophyte infection frequency while genotypes with lower endophyte density could have high or low endophyte infection frequency (Figure 5.3).

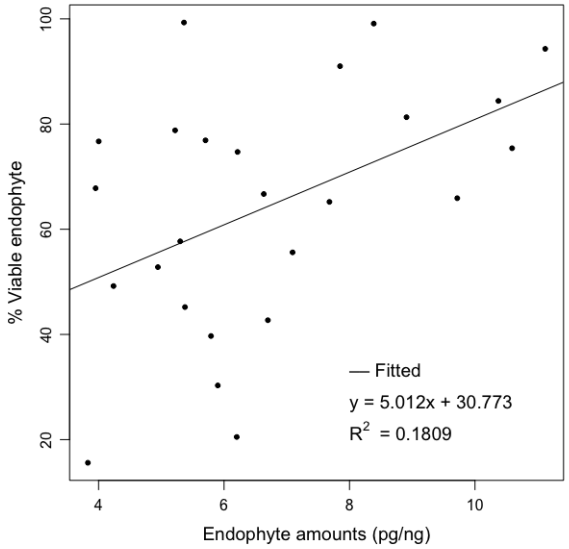


**Figure 5.3 Correlation between endophyte infection frequency (%) and endophyte density (pg/ng) in the shoot apex.** Y-axis denotes the percentage of viable endophyte infection (%) in seeds.

### 5.4.2 Experiment Two

Three-way ANOVA results showed that the main factors genotype ($p < 0.001$), and sampling stage ($p < 0.001$) had a highly significant effect on the immunoblot intensity, while the sampling position of the spikelet ($p = 0.033$) had a significant but smaller effect on the immunoblot intensity. There was also a highly significant interaction between genotype and sampling stage ($p < 0.001$), but there were no other two-way or three-way interactions (Table 5.1).

**Table 5.1 Three-way ANOVA results for the effects of perennial ryegrass genotype (11, 103, 107, 13, 79, 83), spikelet position (bottom, middle and top) and growth stage (Stage I, Stage II and Stage III) on the immunoblot intensity of the florets.** d.f.: degrees of freedom; p-value: probability value.

| Source of variation | d.f. | F value | p-value |
|---|---|---|---|
| Genotype | 5 | 110.41 | < 0.001 |
| Position | 2 | 3.51 | 0.033 |
| Stage | 2 | 72.58 | < 0.001 |
| Genotype x Position | 10 | 0.16 | 0.998 |
| Genotype x Stage | 10 | 32.25 | < 0.001 |
| Position x Stage | 4 | 0.78 | 0.541 |
| Genotype x Position x Stage | 20 | 0.62 | 0.891 |

The immunoblot intensity in the florets from the top of the spike (37.61 AU) was significantly higher than the middle (34.66 AU) and only slightly higher than the bottom (36.49 AU), but the difference among them was minimal. At Stage I, the immunoblot intensity in genotypes 11, 107, 103 and 13 was significantly higher than genotypes 79 and 83. The immunoblot intensity of genotype 103 was significantly lower than genotypes 11 and 107 but still significantly higher than genotypes 79 and 83. At Stage II, there were no significant differences among the three HT genotypes. The immunoblot intensity in the HT genotypes was significantly higher than the LT genotypes (except that there was no significant difference between genotype 103 and 13 in the florets from the top of the spike). No matter which position on the spike the spikelets were sampled from at Stage III, there were no significant differences between any of the genotypes (Figure 5.4).

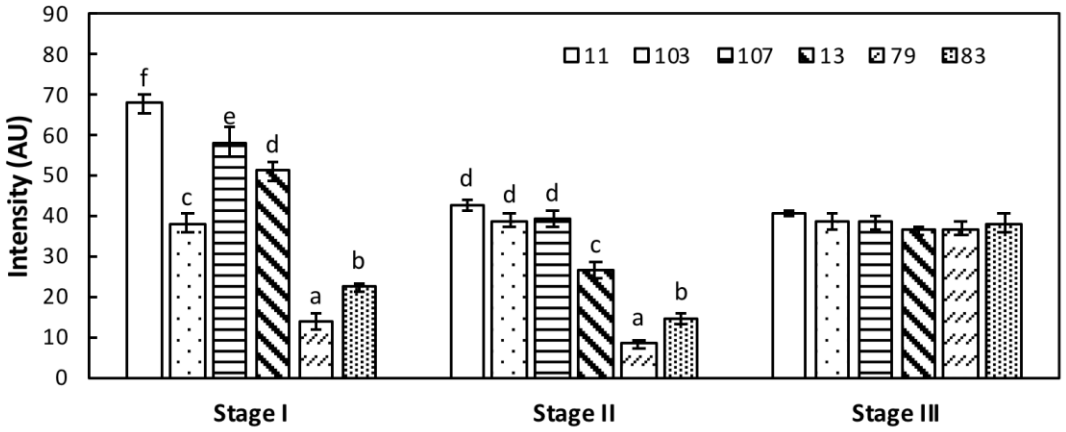


**Figure 5.4 Intensity of tissue-immunoblots on florets from six genotypes (11, 103, 107, 13, 79, 83), measured in units of mean pixel greyscale score.** The florets were sampled at three development stages (Stage I, Stage II and Stage III; Stage I was defined by the criterion that all the spikelets had just fully emerged from the attached leaf sheath, Stage II and Stage III were ten days and twenty days later than Stage I, respectively). Error bars represent the standard error of the mean. Different small letters above the error bars indicate significant differences at p = 0.05, using Fisher's protected least significant difference (LSD) multiple range test. If any letter marked in one treatment is the same as the other, it indicates no significant difference between them.

Microscopy was also used to investigate the hyphal distributions in the ovaries of each genotype. For ovaries at Stage I, the side that would further develop into the embryo of the seed is shown here as 'Side A' (Figure 5.5 I), while the side that would develop into the endosperm of the seed is shown as 'Side B' (Figure 5.5 II). The patterns of hyphal distribution differed on Side A and Side B. On Side A, the endophyte hyphae extended from the bottom of the ovary up to the stigmas. By contrast, on Side B, most of the hyphae were concentrated at the base of the ovary. It is seen in the figures that there were more endophyte hyphae in genotypes 11, 103 and 107 (labelled a, b, and c, respectively) than 13, 79 and 83 (labelled d, e, and f, respectively) on both sides of the ovary (Figure 5.5).

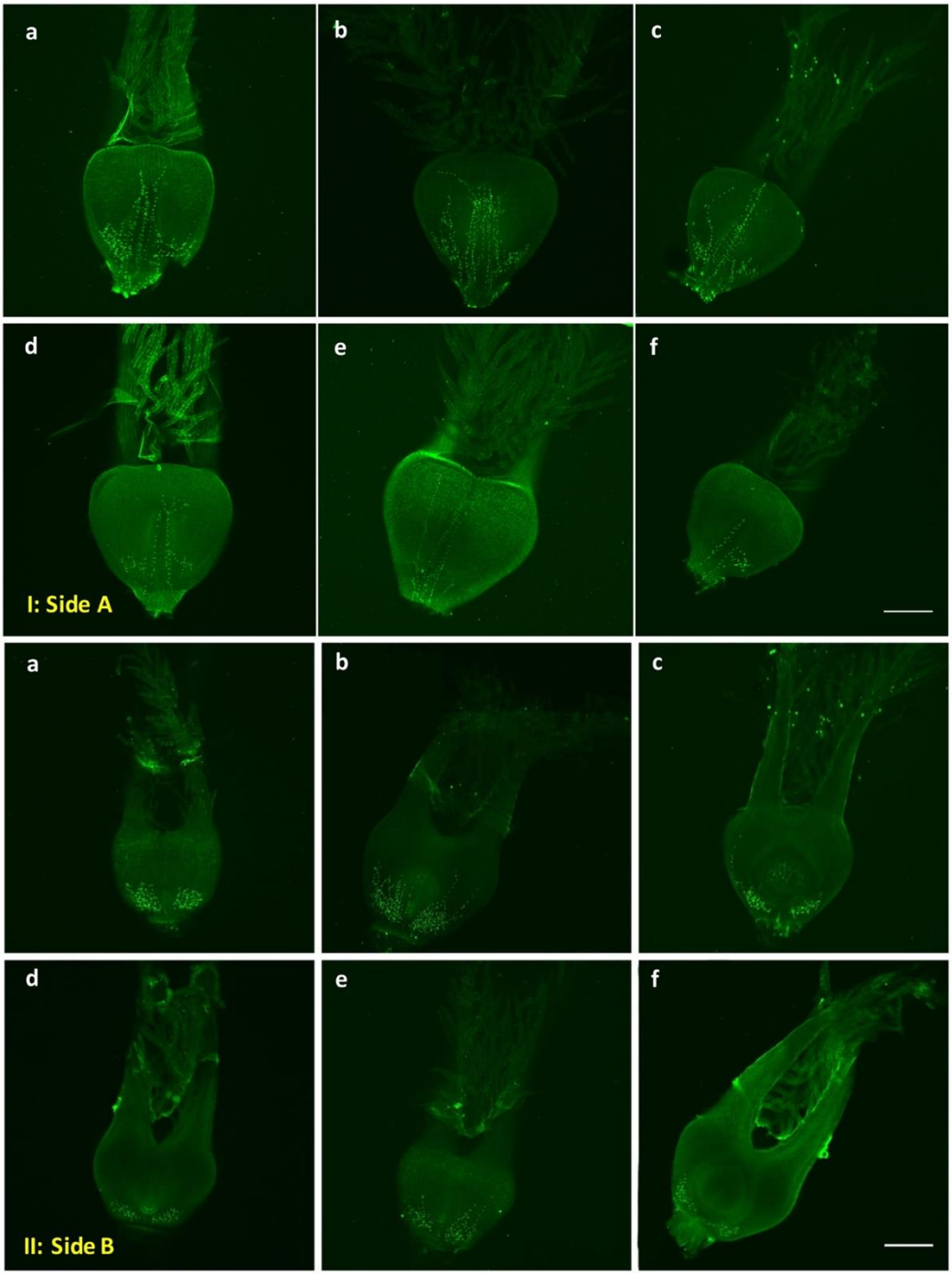


**Figure 5.5 Confocal images of Alexa Fluor 488-stained perennial ryegrass ovaries for: I; Side A (will develop into the seed embryo); and, II; Side B (will develop into the seed endosperm).** Samples were collected at Stage I in six genotypes (11: a; 103: b, 107: c, 13: d; 79: e; 83: f). Hyphae stained with Alexa Fluor 488 as bright green. Bars = 200 µm.

## 5.5 Discussion

The shoot apical meristem is established during plant embryogenesis, and together with cotyledons, hypocotyl, embryonic root and root meristem is a part of the central plant body (Jürgens et al. 1994). Under suitable environmental conditions, developmental signals result in the vegetative apical meristem being converted to an inflorescence meristem. During the development of the inflorescence, the axillary meristems (branch meristems, spikelet meristems and floral meristems) follow patterns that vary between species to form the distinctive seed-head structure of the various botanical tribes of the grass family, including the spike structure of *Lolium* spp. (Ghareeb et al. 2011). As far as is currently known, the fungal endophyte strictly transmits vertically by colonising vegetative meristem primordia, floral primordia, ovaries and embryos. Research has shown that a dense network of branching hyphae is formed among the cells of the shoot meristem (Christensen et al. 2007), and this point was confirmed in this study. With the initiation of the floral meristem, the endophyte hyphae have the potential to enter each branch meristem, spikelet meristem and floret meristem. However, the endophyte transmission is imperfect and can fail at any stage during the hierarchical branching and differentiation steps in the floral development process. Transmission might be mediated by host or endophyte genetics, causing variation in the endophyte seed-infection frequency in different host cultivars or genotypes (Ravel et al. 1997; Afkhami et al. 2008).

This research used real-time PCR to quantify the endophyte density in the shoot apex and used immunoblotting intensity analysis to estimate the endophyte density in the floral tissues. TPIB is widely employed to study the localisation of proteins, nucleic acids and soluble metabolites from newly-cut tissues (Ye et al. 1991; Taylor et al. 1993). The

transferred proteins are bound to the surface of the membrane, providing access to immunodetection reagents (Ni et al. 2016), with the intensity of the immunoblots corresponding positively to the amount of the specific protein in tissues (Chen et al. 2003; Ayliffe et al. 2013; Darkoh et al. 2014). Research has shown that there were significant positive correlations among disease incidence of Fusarium head bright (a disease caused by pathogens of *Fusarium graminearum*, *F. culmorum*, *F. avenaceum*, *F. poae*, *Microdochium nivale* and *M. majus*) and fungal biomass in wheat grains (Xu et al. 2007). Based on this established analytical procedure, the intensity of the immunoblots in this study can also estimate the density of endophyte-specific proteins. Therefore, the endophyte density between samples can be estimated and compared by analysing the intensities of the immunoblots. In this study, genotypes with higher endophyte density have higher endophyte infection frequency. However, the genotypes with lower endophyte density can still have higher endophyte infection frequency (Figures 5.2 and 5.3). The results strongly suggest that the endophyte density in the shoot apex might be one of the factors that can govern the endophyte infection frequency in seeds of the offspring. For genotypes 79 and 83, the immunoblot intensities were much lower in Stage I and Stage II than Stage III at the reproductive stage. However, there was no significant difference between genotypes 79 or 83 and the other genotypes in immunoblot intensity at Stage III (Figure 5.4). The immunoblot intensity at Stage III was very high for genotypes 79 and 83 and in these genotypes the endophyte hyphae were transmitted to nearly every floret. However, the endophyte infection frequencies differed in the offspring seeds, which indicates that the presence of endophyte during floral development does not guarantee transmission of endophyte to the mature seed. Ralphs et al. (2011) showed that the vertically-transmitted endophyte *Undifilum*

*oxytropis* in locoweed endophyte was transmitted to nearly all progeny of the tested locoweed species and varieties. However, the amount of endophyte in the progeny of low endophyte parent plants was lower than high endophyte ones. Therefore, even though the endophyte density were high at the base of each floret for genotype 79 and 83 at Stage III, the endophyte infection frequencies in the mature seeds were still low. This possibly means that the transmission speeds in these two genotypes were slower than the other genotypes. Other research by Cook et al. (2012) revealed that the endophyte content of *Oxytropis sericea* was higher in the full pod/mature seed stage than early flower and later flower stages in locoweed. Although the absolute endophyte density of the immature and mature seeds was not quantified in this study, there is sufficient evidence that the endophyte density in flowers at Stage III was higher than the earlier stages in the LT genotypes. It may be that the low hyphal density seen in the LT genotypes arises from a lower hyphal elongation rate. This is consistent with the deduction that hyphae reached florets but did not necessarily produce an endophyte-infected seed. The fact that plant genotypes differ in the transmission of the same endophyte strain suggests that the rate of hyphal ramification is influenced by host genotype. Another explanation is that since trehalose is critical for organelle protection, it is likely that the endophyte in the LT plant genotypes was incapable of fully protecting itself post-seed maturation.

This research estimated the endophyte density in developing floral tissues by using TPIB coupled with Photoshop software. However, this approach uses a different mechanism for determining the endophyte biomass, compared to real-time PCR. The endophyte density analysed by immunoblotting intensity analysis quantified the endophyte-specific

proteins while real-time PCR quantified the relative amounts of endophyte DNA in the plant-endophyte symbiosis (Young et al. 2005). Real-time PCR is sensitive in quantifying endophyte DNA even for samples with low endophyte density. However, the drawback is the complicated procedure for DNA extraction and high cost. There are other studies using ergosterol or secondary alkaloids to estimate the endophyte biomass (Bush et al. 1993; Richardson et al. 1997). However, these indexes also have limitations. Firstly, ergosterol is present in many microorganisms and is not specific for endophytes. Secondly, some research has shown that the alkaloid concentration and endophyte biomass are not necessarily positively correlated (Cook et al. 2009b). Possible reasons for this include alkaloid production varying with factors such as temperature, and some of the alkaloids produced upon endophyte infection being as yet unidentified. TPIB has been proved to be an accurate method in identifying endophytes in plant tissues (Koh et al. 2006). The quantification method derived from TPIB broadened its application. However, given the potential limitations of indirect methods such as TPIB for quantifying endophyte density, microscopy was also employed to visualise the hyphae in plant tissues. This study showed that both microscopy results on the shoot apex and ovaries at Stage I showed that the mycelium in HT genotypes is denser than the LT genotypes, as indicated by TPIB, which supports the validity of the method of immunoblotting intensity analysis. Future research could investigate the genetic basis for these differences in the host and in the symbiont, and whether or not a difference in the rate of mycelial growth is a factor in the differences in density of endophyte mycelium, between host genotypes.

# Chapter 6 Transcriptomic analysis of inflorescence tissues to explore the mechanisms underlying *Epichloë* transmission in perennial ryegrass

## 6.1 Abstract

Successful growth and performance of the main forage species in New Zealand, perennial ryegrass, is largely dependent on its association with symbiotic endophytic fungi of the genus *Epichloë*. *Epichloë* endophytes are vertically transmitted between perennial ryegrass generations *via* hyphal infection of the flower and seed tissues. However, as with many natural and/or synthetic grass-endophyte associations, this transmission process can at times be imperfect, creating a significant challenge for the commercialisation of endophyte products. In this study, the aim was to identify ryegrass candidate genes involved in the vertical transmission of endophyte within perennial ryegrass to reveal the underpinning molecular mechanisms involved. High-throughput sequencing of mRNA using RNA-Seq was used to measure the transcriptomes of high- (HT) and low-transmission (LT) genotypes. Two types of plant tissues were used for RNA-Seq; the inflorescence primordia and the ovary. This study showed that 102 genes were commonly or exclusively differentially-expressed between the HT and LT genotypes in the inflorescence primordia and/or the ovary. Functional enrichment analyses by agriGO showed that the gene ontology (GO) terms more highly enriched in the HT than LT genotypes were involved in *serine family amino acid metabolic process* (GO:0009069) and *cytoplasmic membrane-bounded vesicle* (GO:0016023) in both the inflorescence primordia and the ovary. More differentially-expressed genes (DEGs) coding for trehalose-6-phosphate phosphatase were induced in the ovary compared with the inflorescence primordia in the HT than the LT genotypes, consistent with a higher

demand for trehalose in the HT than the LT genotypes during transmission from the inflorescence primordia to the ovary. There were more DEGs related to salicylic acid metabolism repressed in the ovary compared to the inflorescence primordia in the HT than LT genotypes. There were more DEGs related to jasmonic acid metabolism induced in the ovary compared with the inflorescence primordia in the HT than the LT genotypes. This suggests that the lower salicylic acid and higher jasmonic acid metabolism in the HT genotypes might be related to the endophyte transmission efficiency.

## 6.2 Introduction

Asexual *Epichloë* endophytes are vertically-transmitted fungi exclusively found in grasses of the subfamily Poöideae, family Poaceae. *Epichloë* species can confer beneficial traits to their hosts, with the most frequently documented feature being the protection from insect herbivores *via* the production of secondary metabolites (Prestidge et al. 1988; Patchett et al. 2008). This feature is of great value to farming systems worldwide, especially to New Zealand where pasture utilisation is often impacted by damage from insects like Argentine stem weevil and black beetle (Breen 1994). In perennial ryegrass, novel endophytes such as AR1, AR5, AR37, NEA2 (all sharing the Latin name *E. festucae* var. *lolii*) and NEA12 (LpTG-3) are marketed with wide acceptance in New Zealand and Australia because of their effectiveness in insect-deterrence (Johnson et al. 2013). Perennial ryegrass infected with AR37 added an estimated $42 M NZD to New Zealand's economy between 2007 and 2011 (Fletcher 2010; Johnson et al. 2013).

*Epichloë* spp. also have other traits related to their life cycle that make them ideal biological control agents. One of the most important is their dissemination. However,

imperfect transmission (< 100% of seeds infected with endophytes) has been reported in almost all studied grass-endophyte associations, including those in the host species perennial ryegrass, tall fescue, *Poa alsodes*, *Elymus virginicus* and *Festuca subverticillata* (Gundel et al. 2008; Gundel et al. 2011b). The loss of endophyte transmission is firmly linked with the growth of the host plants (Gundel et al. 2012). Langer (1979) and Loveless (1984) have described the growth and development in grasses of the family Poaceae in detail. In brief, the aboveground portion of a mature perennial ryegrass plant consists of a number of tillers. During vegetative growth, an individual tiller is made up of a number of sub-units called phytomers which are initiated from the shoot apical meristem. The shoot apical meristem is located at the base of the aboveground tiller surrounded by layers of leaf sheath and is involved in forming leaves that comprise each tiller by cell division and differentiation. An axillary bud is formed in the axil of each leaf, with the capability of later forming a daughter tiller (tillering). Each vegetative meristem inside of the mature tiller has the potential to convert to a floral meristem upon vernalisation, which later develops to inflorescence primordia. Vernalisation is achieved by a prolonged exposure to low temperatures (a period of 12 to 14 weeks below 5°C), short photoperiods, or a combination of both, which ensures that plants flower during the following spring (Jensen et al. 2001). Then the apical meristem starts to expand and eventually forms groups of inflorescences (spikelets), each containing 3 to 10 floral meristems (Hannaway et al. 1999). Two spikelets are alternately embedded along the central axis. The ovary is the female reproductive tissue of a flower where fertilisation takes place and will further develop into a seed (Chapter 3). Since the asexual *Epichloë* endophytes investigated in this study are vertically transmitted (Figure 2.1), their dissemination is presumed to be largely mediated by the genetics of the seed parent

(Sampson 1933; Gundel et al. 2017; Zhang et al. 2017). Schardl et al. (2004) proposed that most of the asexual *Epichloë* species rely entirely on the ability of their hosts to achieve transmission to the shoot apical meristem, inflorescence primordia, ovaries and embryos since endophyte growth is strictly synchronised with grass plant growth. There are a few critical stages during which endophyte transmission fails. If the endophyte hyphae fail to infect an axillary bud, the tiller that develops from it will remain endophyte-free *ad infinitum*. Also, loss of endophyte can occur during the flowering stage when mycelium fails to infect the ovary or infects a location that does not result in transmission to the seedling upon germination (Afkhami et al. 2008). Gundel et al. (2011a) proposed that plant anthesis (the period during which a flower is fully open and functional) is a key stage at which events occur that are critical to the success of transmission to seeds. In the unfertilised ovary, endophyte mycelium is observed to be present between the ovary wall cells, between the nucellus cells and inside the embryo sac (attached to the antipodal cells) and further infects mature embryo (Zhang et al. 2017). With the onset of seed maturation, the ovary wall cells and the integument cells are condensed into a few layers of pericarp and seed coat cells, but the endophyte hyphae in these positions will not contribute to the transmission to the next generation.

The disaccharide trehalose is an osmoprotectant and a potential signal metabolite in plant interactions with microorganisms (Lunn et al. 2014). It has been shown that *Aspergillus nidulans* requires trehalose for long-term survival (Ni et al. 2007). Trehalose is likely to be one of the energy sources in carbon catabolism for the fungus (Thines et al. 2000; Foster et al. 2003). Trehalose synthesis and metabolism were required at different stages of plant infection by *Magnaporthe grisea* (Foster et al. 2003). In Chapter

4, it has been shown that the amount of trehalose significantly decreased with prolonged seed storage, suggesting trehalose may also be utilised by endophytes in seed storage as an energy source, implying the importance of trehalose to sustain endophyte viability.

Salicylic acid is a phenolic phytohormone with functions related to plant growth and development including regulation of photosynthesis, transpiration, ion uptake and transport. It is also involved in endogenous signalling, mediating in plant defence against pathogens (Loake et al. 2007). Salicylic acid plays a critical role in regulating the endophyte-conferred resistance against herbivores and could negatively impact endophytes and reduce the benefits endophytes would provide (Bastías et al. 2018). Jasmonic acid and its derivatives are lipid-based hormone signals that regulate a wide range of processes in plants, including signal functions in plant responses to abiotic and biotic stresses, plant growth and development (Wasternack 2007), as well as in plant-microbe interactions (Pozo et al. 2004).

To investigate the potential mechanisms that contribute to endophyte transmission in floral tissues, this study sought to compare the transcriptomes of HT and LT genotypes in two categories of tissue samples, the inflorescence primordia and the ovary. High-throughput DNA sequencing methods have developed very rapidly in recent years and are gaining wider adoption as their cost decreases, and data outputs increase. Using this platform for sequencing cDNA (known as RNA-Seq) enables effective determination of transcript abundances and identification of novel transcriptionally active regions (Wilhelm et al. 2010). RNA-Seq is widely used for measuring gene expression across samples, especially to investigate transcriptome responses to biotic and abiotic changes.

RNA-Seq has also been used in previous studies related to endophytes (Dupont et al. 2015; Dinkins et al. 2017). In terms of perennial ryegrass, infection of *Epichloë* induced 38% (n = 16,041) DEGs in the host transcriptome (Dupont et al. 2015). The percentage was much higher than infections by other microorganisms beneficial to their hosts, such as *Glomus intraradices* in rice (Güimil et al. 2005), *Funneliformis mosseae* in tomato (Zouari et al. 2014), *Laccaria bicolor* in California poplar (Plett et al. 2015), and *Trichoderma harzianum* in *A. thaliana* (Morán-Diez et al. 2012). The DEGs in perennial ryegrass were mostly related to enhanced resistance to drought and infection by fungal pathogens. By comparison, only 478 DEGs were identified when comparing endophyte-free and endophyte-infected transcriptomes in tall fescue (Dinkins et al. 2017). However, the author found no papers on the molecular mechanisms for endophyte transmission.

## 6.3 Materials and methods

### 6.3.1 Plant sample collection

Six genotypes (three HT genotypes: 11, 103, 107; three LT genotypes: 13, 79, 83) of perennial ryegrass were grown at the AgResearch Grasslands Research Centre, Palmerston North, New Zealand. The six genotypes were selected from a single population and were evaluated for their transmission capability by measuring the endophyte infection frequency of the offspring seeds for each genotype in two harvest seasons (2012-2013, 2014-2015) (Gagic et al. unpublished).

Inflorescence primordia and ovary tissues were collected for RNA-Seq in the spring-summer period of 2015-2016. Harvesting was conducted over a period of a week at a consistent time (solar noon ± 1 hr) to reduce variability owing to diurnal changes to the transcriptomes. The tillers from which the inflorescence primordia were dissected were

assessed for endophyte infection status by tissue-print immunoblotting as described by Hahn et al. (2003). Only the inflorescence primordia from the endophyte-infected tillers were used for RNA extraction. The photographs of the inflorescence primordia provide information about the developmental stage and condition of the inflorescence primordia at the time of harvest. Seven complete inflorescence primordia (Stage 6-7 by Zadok's scale, Figure 6.1) (Zadoks et al. 1974) of each genotype were selected and pooled into one tube for RNA isolation. Samples were immediately snap frozen in liquid nitrogen after collection, and then stored in a –80°C freezer until RNA extraction. At the ovary development stage, ovaries were collected at two developmental stages: before fertilisation, and after fertilisation (20 days after collection of the unfertilised ovaries) (Figure 6.2). Both unfertilised and fertilised ovaries were collected from three independent reproductive tillers of nearly the same emergence date. Unfertilised ovaries were collected from the reproductive tillers when the inflorescence (spike) was just fully emerged from the leaf sheath. Three ovaries were collected at each of three locations on each spike, namely, the top, the middle and the bottom. The fertilised ovaries were collected from the same spike as the unfertilised ovaries of a similar spread of location.

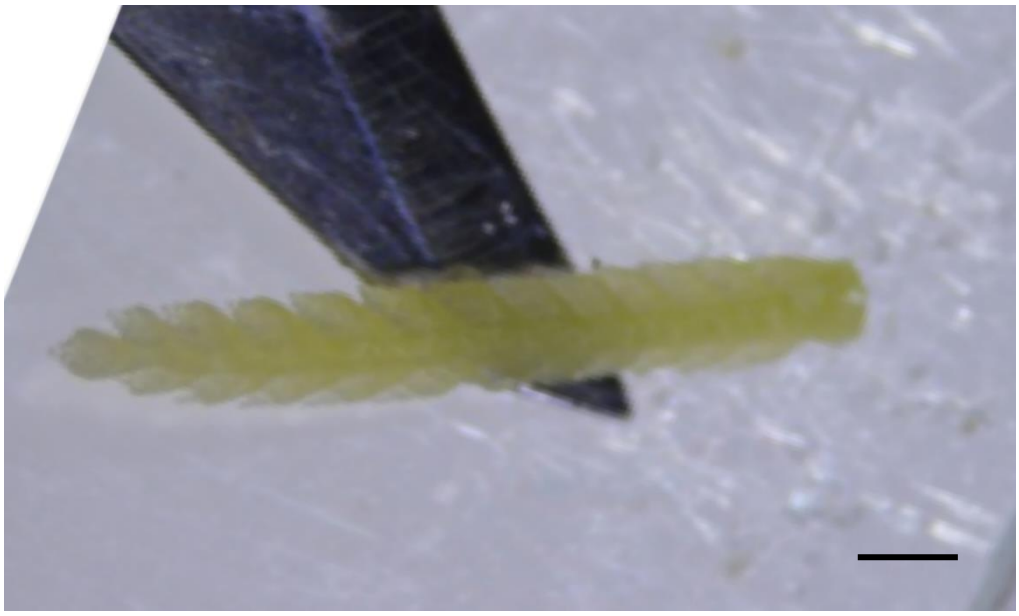

**Figure 6.1 Developmental status of Stage 6-7 inflorescence primordia (Zadok's scale) when harvested for RNA-Seq.** Scale bar = 200 µm.


**Figure 6.2 Morphology of the unfertilised and fertilised ovaries when harvested for RNA-Seq.** Fertilised ovaries were collected 20 days after the unfertilised ovaries. 'Top', 'Middle' and 'Bottom' panels show samples taken from spikelets located at the top, middle and bottom of one spike. From the left to right, in each 'Top', 'Middle' or 'Bottom' panel, the ovaries shown were extracted from the bottom, middle and top of a single spikelet. The samples in each yellow panel are the samples selected for RNA extraction from one tiller. Bar scale = 200 µm.

### 6.3.2 RNA extraction

The RNA extraction methods for the inflorescence primordia and the ovary tissue samples differed due to the accumulation of starch during seed development, especially towards maturity (Birtić et al. 2006). Each inflorescence primordia sample (~ 50 mg fresh weigh [fw]) was powdered in liquid nitrogen using a micropestle in a 1.5 mL tube. The RNA was extracted using 500 µL TRIzol (Thermo Fisher Scientific, Waltham, USA) followed by centrifuging at high speed. The supernatant was further extracted with chloroform (100 µL) by vigorous handshaking. The top layer (~ 200 µL) was then purified with an RNeasy MinElute Cleanup Kit (Qiagen, Valencia, USA) according to manufacturer's instructions. The purified RNA was stored in DNase-free water at –80°C until further use.

The unfertilised (n = 27, mass ≈ 2.7 mg fw) and fertilised ovaries (n = 27, mass ≈ 50 mg fw) were separately pooled into single samples which were then ground to fine powder quickly and thoroughly with an electric drill and a liquid nitrogen cooled plastic pestle that fitted 1.5 mL micro-centrifuge tubes under liquid nitrogen. The method for RNA extraction was optimised by combining a sodium dodecyl sulfate (SDS)/TRIzol method, and further purification with an RNeasy MinElute Cleanup Kit. Specifically, 0.4 mL RNA extraction buffer was added to the powder in a ribonuclease-free 1.5 mL tube. RNA extraction buffer was prepared by mixing 100 mM Tris-HCl (pH 9.0) and 2% β-mercaptoethanol (v/v) (prepared with autoclaved DEPC-treated MilliQ water), which was prepared just before use and stored at room temperature. The sample was mixed thoroughly by vortexing and incubated at room temperature for 15 min. Twenty microliters of 20% SDS was added into the suspension, inverted gently for five times and

incubated at room temperature for 5 min. The mixture was centrifuged at 12,000 *x*g for 10 min at 4°C. The aqueous phase was carefully transferred to a fresh tube, two volumes of TRIzol (0.8 mL) were added, mixed thoroughly using a vortexer and incubated at room temperature for 10 min. One-fifth volume of chloroform (240 µL) was added into the mixture and mixed with a vortexer. Then the tube was centrifuged at 12,000 *x*g for 10 min at 4°C. The aqueous phase (0.7 mL) was carefully transferred to a fresh tube with an equal volume of isopropanol added, followed by mixing by inversion several times. After 20 min precipitation at –20°C, the mixture was then centrifuged at 12,000 *x*g for 10 min at 4°C. After discarding the supernatant, the pellet was suspended gently in 400 µL DEPC-treated water, then an equal volume of citrate buffer saturated phenol (pH 4.3): chloroform (1:1) was added and mixed thoroughly. Afterwards, the mixture was centrifuged at 12,000 *x*g for 10 min at 4°C. The aqueous phase (400 µL) was carefully transferred to a fresh tube with a pipette, an equal volume of chloroform was added and mixed thoroughly by vortexing. The sample was then centrifuged at 12,000 *x*g for 10 min at 4°C. The liquid from the top layer (approximately 400 µL) was further purified to achieve the RNA for sequencing using RNeasy MinElute Cleanup kit according to manufacturer's instructions. The purified RNA was stored in RNase-free water at –80°C until further use.

### 6.3.3 Determination of RNA yield and purity

The concentration and purity of the total RNA samples were measured using the NanoDrop™ 1000 spectrophotometer (Thermo Scientific; Wilmington, USA). RNA purity was measured by the absorbance ratios of A260/A280 and A260/A230 from the NanoDrop™ 1000 spectrophotometer. RNA integrity number (RIN) was measured with

the Eukaryote Total RNA Nano Assay of the Agilent 2100 Bioanalyzer (Agilent Technologies; Santa Clara, USA).

### 6.3.4 RNA-Seq library preparation and sequencing

To construct the RNA-Seq library, greater than 2 μg of total RNA from each sample was used for RNA-Seq. RNA preparation (mRNA enrichment, fragment interruption, addition of adapters, size selection, and PCR amplification) and RNA-Seq on the inflorescence primordia and the ovaries were performed by New Zealand Genomics Ltd. (Dunedin, New Zealand) and Beijing Genomics Institute (Hong Kong, China), respectively. The cDNA libraries were constructed following the protocol of standard Illumina sample preparation (Illumina Inc.; San Diego, USA, Cat. # RS-100-0801). Specifically, mRNA, containing a long sequence of adenine nucleotides (poly [A]-tails, often several hundred) added to the 3' end, was isolated with a magnetic bead attached to a short sequence (16-20 nt) of deoxy-thymidine nucleotides (oligo[dT]). Then fragmentation buffer was used to break mRNA into short fragments, which were used as templates for synthesising the first-strand cDNA using reverse transcriptase and a random hexamer primer. The second-strand of cDNA was then synthesised with RNase H (a family of non-sequence-specific endonuclease enzymes that catalyse the cleavage of RNA in an RNA/DNA substrate via a hydrolytic mechanism) to remove the mRNA strand followed by dNTPs and DNA polymerase I to synthesise the second strand. After purifying the double-strand cDNA, blunt and phosphorylate DNA was repaired with T4 DNA polymerase and polynucleotide kinase. The repaired cDNA fragments were ligated to sequencing adapters and amplified using PCR and the final cDNA library was constructed. Paired-end (2 x 125 bp read length for the inflorescence primordia samples, 2 x 100 bp

read length for the ovary samples) sequencing of the cDNA libraries was performed on Illumina HiSeq™ 2500 and Illumina HiSeq™ 4000 systems (Illumina Inc.; San Diego, USA), respectively.

### 6.3.5 RNA-Seq data processing to identify DEGs

Figure 6.3 shows a schematic of the bioinformatics pipeline used to analyse the RNA-Seq data to identify DEGs between the HT and LT genotypes in the inflorescence primordia and ovary, and between the inflorescence primordia and ovary in the HT and LT genotypes. Trimmomatic version 0.36 software was used to remove low-quality regions (< Q 15: with an average quality score below 15) and sequencing adapters from the reads. This step removed reads < 36 bp after quality trimming and only kept properly paired reads. Each sample was mapped to the concatenated endophyte (Schardl et al. 2013) and plant genomes (Byrne et al. 2015) using STAR version 2.5.3a (Dobin et al. 2013), resulting in ~ 50–92 M (≈ 90%) mapped paired-end reads, of which ~49–90 M (≈ 85%) were uniquely mapped. STAR also generated counts of uniquely mapped pairs of reads that overlapped known genes on the genome. For each sample, these counts were compiled into a tab-delimited text file. Counts for each gene were analysed using the 'limma' version 3.30.13 package in R (version 3.3.3) with the voom method (Law et al. 2014) and trimmed mean of M-values (TMM) normalisation (Robinson et al. 2010). Fold changes between the HT and LT treatments, as well as between the inflorescence primordia and ovary were calculated using linear models. Empirical Bayes moderated t-tests were used to calculate p-values, which were corrected for multiple testing using FDR-corrected q-values. Fold changes, p-values and FDR values were imported into Excel

for further analysis. Genes exhibiting significant up- or down-regulation were identified using FDR < 0.05 and ≥ 1.5 fold change as cut-offs.

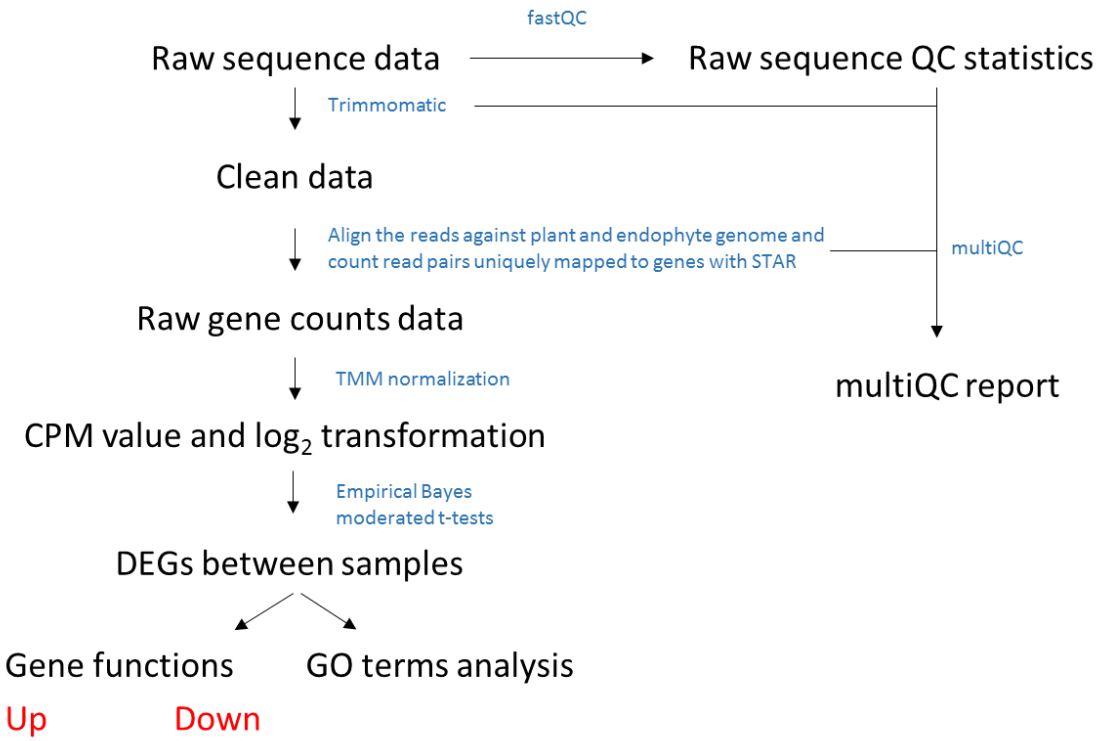


**Figure 6.3 Workflow of the bioinformatics analysis used in this study.**

### 6.3.6 Functional annotation of genes

The sequences of the predicted transcript and protein sequences of all genes were annotated using a comprehensive bioinformatics pipeline involving BLAST (Camacho et al. 2009), Interproscan (Quevillon et al. 2005) and Mercator databases (Lohse et al. 2014). The transcripts were searched against the NCBI nr nucleotide database using BLASTN with an e-value cut-off of 1e-20, while the proteins were searched against the NCBI nr protein and Kyoto Encyclopedia of Genes and Genomes (KEGG) (Kanehisa et al. 2000) databases using BLASTP with an e-value cut-off of 1e-20. Interproscan (Quevillon et al. 2005) was used to identify protein domains in the proteins while Mercator was used to annotate the protein sequences using homology to reference plant genomes. A

further search of the protein sequences using BLASTP against the NCBI non-redundant protein database was performed with an e-value of 1e-10. The output of this search was used as input to the Blast2GO suite is a tool to retrieve the GO annotations of the genes to describe their functions (molecular functions, biological processes and cellular components) (Conesa et al. 2008). Three sources including Blast2GO, KEGG and Interproscan were used to retrieve gene ontology (GO) terms for each gene. The GO terms with the DEGs were analysed with agriGO v2 (http://systemsbiology.cau.edu.cn/agriGOv2/index.php) (Tian et al. 2017). In agriGO, GO term enrichment was computed by singular enrichment analysis (SEA) on the selected genes by comparing with the reference set (the TAIR genome locus [TAIR10_2017]). The statistical method used was Fisher's test. The multi-test adjustment method used was Benjamini–Yekutieli (FDR under dependence) with a significance level of $p < 0.05$ (Benjamini et al. 2001). DEGs were screened for homology to plant sequences of *A. thaliana* and rice with Mercator. The functions of the homologue genes with rice were referenced from RiceNetDB (http://bis.zju.edu.cn/ricenetdb/).

Venn diagrams were built using Venny (version 2.1.0), an online tool available at http://bioinfogp.cnb.csic.es/tools/venny/. Heatmaps with cluster dendrograms were generated in R Bioconductor using the heatmap.2 function of the 'gplots' package within RStudio (version 0.99.903).

Validation by real-time PCR was not performed in this study for two reasons. One is the high sensitivity platform used for RNA-Seq. The second is that as there were three biological replicates (three genotypes) for each treatment, quantitative PCR validation was deemed unnecessary (Fang et al. 2011).

## 6.4 Results

### 6.4.1 RNA quality for RNA-Seq

The absorbance ratios of A260/280 and A260/230 were consistently greater than 1.8 (Table 6.1), which indicated that there was no major contamination of proteins, polysaccharides or salts in the isolated RNA. Values for the integrity of total RNA were greater than 7.9 in all samples, which showed that the RNA integrity was satisfactorily retained during the extraction process (Table 6.1).

**Table 6.1 Yield and purity of the total RNA isolated from the three tissue types.**

| Tissue type | Genotype | Yield (ng/μL) | RIN | rRNA ratio (28s/18s) | $A_{260}/A_{280}$ | $A_{260}/A_{230}$ |
|---|---|---|---|---|---|---|
| Inflorescence primordia | 11 | 251 | n.a. | n.a. | 1.9 | 2.4 |
| | 103 | 274 | n.a. | n.a. | 2.0 | 1.8 |
| | 107 | 277 | n.a. | n.a. | 2.0 | 2.2 |
| | 13 | 294 | n.a. | n.a. | 2.0 | 2.1 |
| | 79 | 289 | n.a. | n.a. | 1.9 | 2.2 |
| | 83 | 258 | n.a. | n.a. | 1.9 | 2.4 |
| Unfertilised ovary | 11 | 328 | 8.1 | 1.8 | 2.1 | 2.2 |
| | 103 | 186 | 8.8 | 1.8 | 2.0 | 1.9 |
| | 107 | 272 | 8.3 | 1.9 | 2.0 | 2.2 |
| | 13 | 237 | 8.0 | 2.0 | 2.1 | 2.0 |
| | 79 | 237 | 8.4 | 1.8 | 2.1 | 2.0 |
| | 83 | 205 | 8.6 | 1.6 | 2.0 | 1.9 |
| Fertilised ovary | 11 | 1,742 | 9.4 | 1.8 | 2.1 | 2.3 |
| | 103 | 280 | 8.8 | 2.3 | 2.1 | 2.2 |
| | 107 | 716 | 8.7 | 2.0 | 2.0 | 2.1 |
| | 13 | 1,169 | 7.9 | 1.5 | 2.1 | 2.4 |
| | 79 | 1,202 | 7.9 | 1.0 | 2.1 | 2.4 |
| | 83 | 1,480 | 8.9 | 1.8 | 2.0 | 2.4 |

### 6.4.2 Descriptions on the mappings to perennial ryegrass and endophyte genome

Table 6.2 shows that the number of the trimmed reads in the inflorescence primordia of the six genotypes ranged from 74,716,838 to 92,705,995, and in the unfertilised ovary ranged from 78,350,766 to 104,415,421. Among the trimmed reads, the number of reads in the inflorescence primordia of the six genotypes that matched with perennial ryegrass genome ranged from 62,890,280 to 81,006,854, among which 16,684 (0.03%) to 128,768 (0.17%) reads matched with the non-small subunit (non-SSU) AR37 genome.

The number of reads in the unfertilised ovary of the six genotypes ranged from 69,715,232 to 93,103,337, among which 88,525 (0.11%) to 456,499 (0.61%) reads uniquely mapped to non-SSU AR37 genome, which was, on average, higher than the inflorescence primordia. RNA-Seq analysis showed that all but one fertilised ovary sample (genotype 11) had a severe *Lolium* latent virus infection (56.5% – 67.2% reads mapped to the genome of *Lolium* latent virus), rendering them unsuitable for further analysis (Figure A6.1). Therefore, this chapter only discusses RNA-Seq results of the inflorescence primordia and the unfertilised ovary samples.

**Table 6.2 Summary of RNA-Seq reads and mapping information.**

| Tissue | Genotype | Trimmed reads | Number of uniquely mapped reads to endophyte and ryegrass genomes | Number of reads uniquely mapping to the AR37 genome | Number of reads uniquely mapping to non-SSU AR37 genome | % of uniquely mapped reads mapping to non-SSU AR37 genome |
|---|---|---|---|---|---|---|
| Inflorescence primordia | 11 | 88,853,890 | 76,542,977 | 162,911 | 128,768 | 0.17 |
| | 103 | 84,070,932 | 71,505,652 | 134,121 | 103,352 | 0.14 |
| | 107 | 92,705,995 | 81,006,854 | 74,091 | 47,504 | 0.06 |
| | 13 | 79,765,074 | 69,182,541 | 53,358 | 37,080 | 0.05 |
| | 79 | 74,716,838 | 62,890,280 | 47,634 | 16,684 | 0.03 |
| | 83 | 88,788,284 | 74,833,290 | 88,511 | 57,454 | 0.08 |
| Ovary | 11 | 95,491,762 | 84,335,925 | 348,382 | 335,112 | 0.40 |
| | 103 | 96,060,778 | 86,726,552 | 430,875 | 415,107 | 0.48 |
| | 107 | 104,415,421 | 93,103,337 | 250,309 | 241,483 | 0.26 |
| | 13 | 83,674,427 | 74,417,066 | 462,883 | 456,499 | 0.61 |
| | 79 | 86,089,240 | 77,113,915 | 92,479 | 88,525 | 0.11 |
| | 83 | 78,350,766 | 69,715,232 | 235,290 | 185,867 | 0.27 |

SSU rRNA: small subunit RNA
GC content: guanine-cytosine content

### 6.4.3 Global description of the DEGs in perennial ryegrass

By mapping the RNA-Seq reads to the genome of perennial ryegrass, 25,306 unique genes were identified. After filtering out the genes whose copies were less than 1 copy per million (CPM) for all replicates in at least 1 tissue/condition (inflorescence primordial: HT; inflorescence primordial: LT; ovary: HT; ovary: LT), 15,979 genes were normalised

for DEGs analysis. The expression level of genes in the transcriptome of perennial ryegrass was compared in two ways to identify DEGs: between the HT and LT genotypes separately for the inflorescence primordia and ovary tissues, and between the inflorescence primordia and ovary tissues separately for the HT and LT genotypes.

Comparing HT and LT genotypes, in the inflorescence primordia tissue, 78 (~ 0.48% of the total genes) DEGs were found between the HT and LT genotypes, with 35 genes induced and 43 genes repressed in the HT genotypes. In the unfertilised ovary tissue, there were 61 (~ 0.38% of the total genes) DEGs between the HT and LT genotypes, with 28 and 33 genes induced and repressed in the HT genotypes, respectively. There were 37 common DEGs in both tissues, with 13 and 24 of them induced and repressed in the HT genotypes, respectively (Figure 6.4A).

Comparing inflorescence primordia and ovary tissues, in the HT genotypes, 7,819 DEGs (~ 48.4% of the total genes) were found with 4,084 of these induced and 3,735 of them repressed in the ovary, compared to the inflorescence primordia. In the LT genotypes, 6,850 DEGs were found, with 3,588 induced and 3,262 of the DEGs repressed in the ovary, relative to the inflorescence primordia. Of the DEGs in both the HT and LT genotypes, 6,298 (~ 39.0% of the total genes) were DEGs in both tissues with 3,311 induced and 2,987 of them repressed in the ovary, respectively (Figure 6.4B).

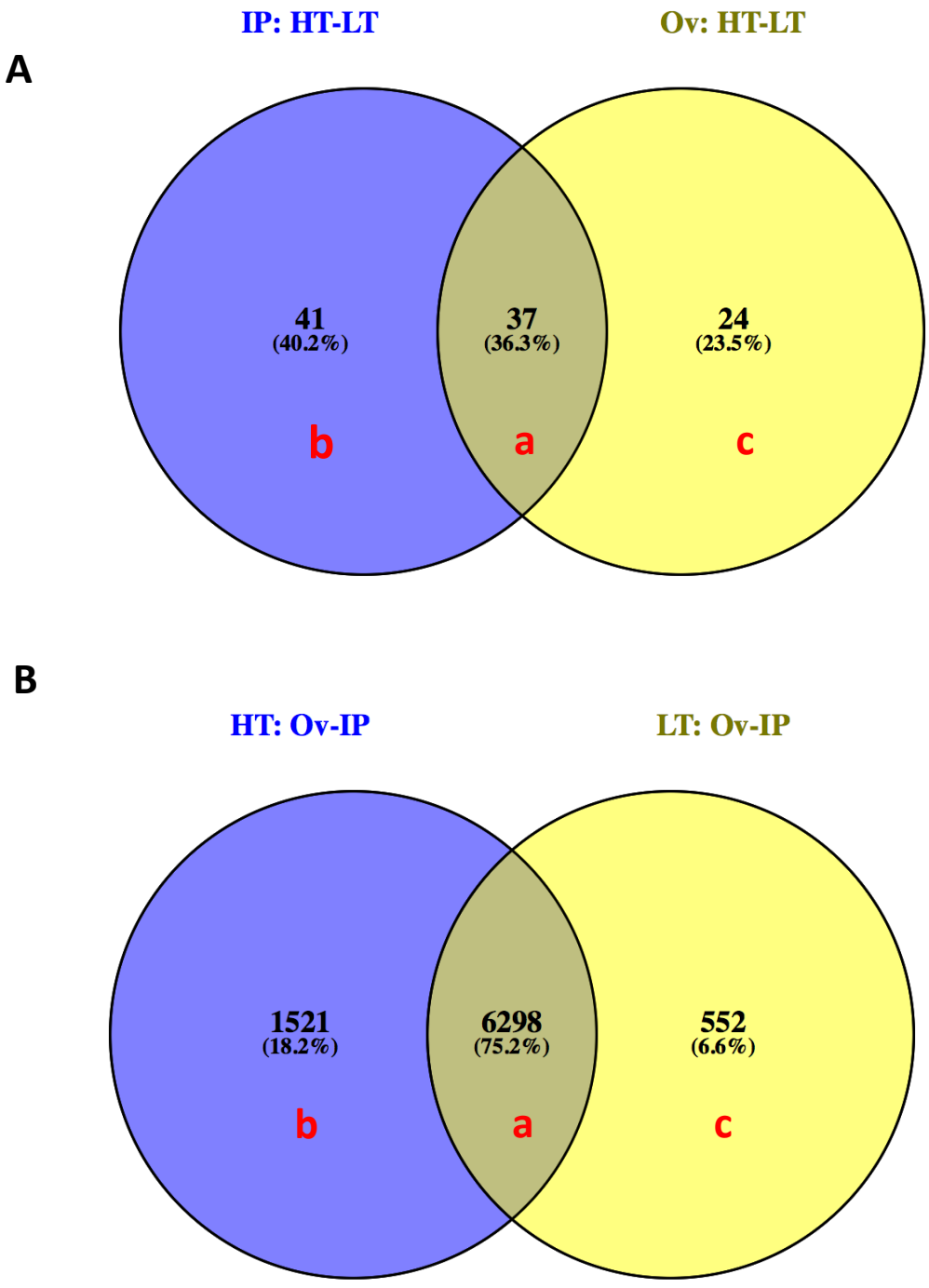


**Figure 6.4 Venn diagram representation of common and divergent DEGs in perennial ryegrass (A) comparing HT and LT genotypes in both the inflorescence primordia (blue) and ovary (yellow), and (B) comparing the inflorescence primordia and ovary in both the HT (blue) and LT genotypes (yellow).** IP = inflorescence primordia, Ov = ovary.

Heatmap analysis coupled with cluster analysis was performed on the gene expression profiles of the DEGs, which clearly showed that the three HT genotypes 11, 103 and 107 were clustered into one group while the three LT genotypes 13, 79 and 83 were clustered into another group, with this being found in both the inflorescence primordia and ovary tissues (Figure 6.5A and 6.5B). The corresponding analysis comparing DEG profiles of inflorescence primordia and ovary tissues showed that the DEGs in the inflorescence primordia differed from those in the ovary, with this result being consistent in both the HT (11, 103, 107) and LT genotypes (13, 79, 83) (Figure 6.6A and 6.6B).

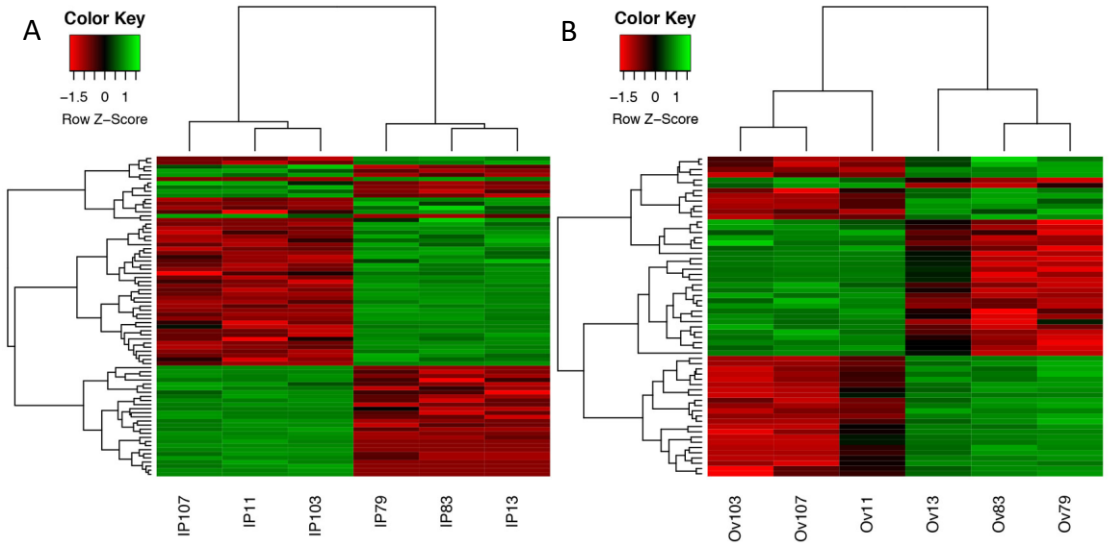


**Figure 6.5 Heatmaps of DEGs with hierarchical cluster trees comparing the HT genotypes (11, 103 and 107) and LT genotypes (11, 79 and 83) in both the inflorescence primordia (A) and the ovary (B) according to their expression patterns.** Each row in (A) and (B) separately represents one gene. The expression data were z-scored when generating the heatmaps, with green showing higher gene expression and red lower gene expression. IP = inflorescence primordia, Ov = ovary.

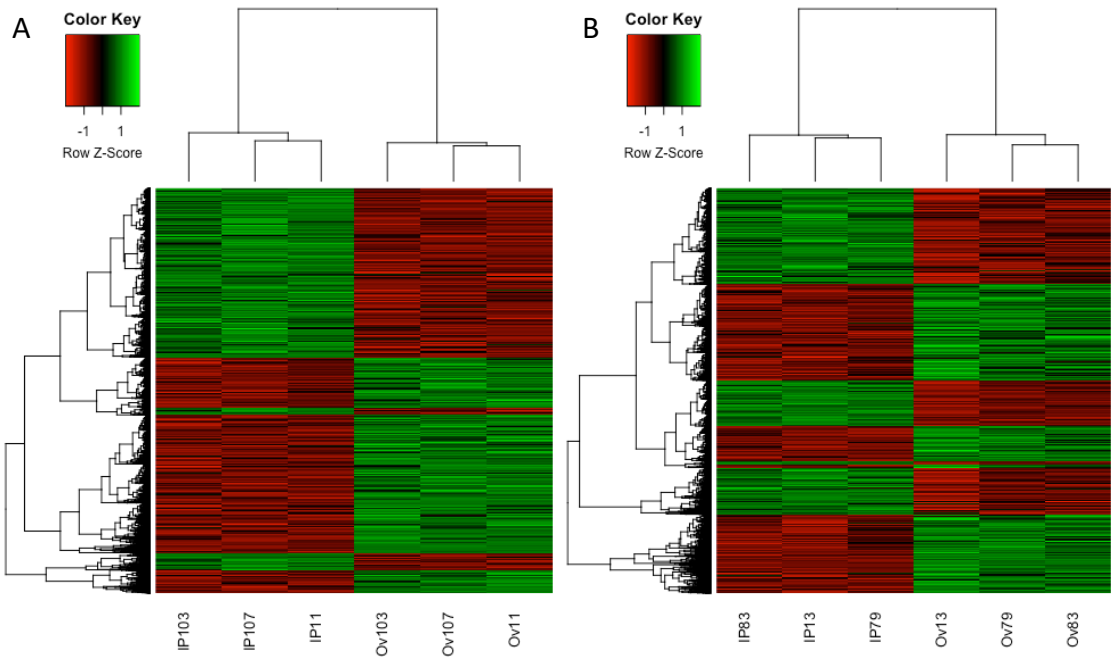


**Figure 6.6 Heatmaps of the DEGs with hierarchical cluster trees comparing the inflorescence primordia and the ovary tissues in both (A) HT genotypes (11, 103 and 107) and (B) LT genotypes (13, 79 and 83) according to their expression patterns.** Each row (A) and (B) separately represents one gene. The expression data were z-scored when generating the heatmaps, with green showing higher gene expression and red lower gene expression. IP = inflorescence primordia, Ov = ovary.

### 6.4.4 DEGs when comparing HT and LT genotypes

For the 37 DEGs found in both inflorescence primordia and ovary tissues when comparing the gene expression between the HT and LT genotypes (Fig 6.4A), 26 were found to have homologues with rice and/or *A. thaliana* (Table 6.3). For the 41 DEGs identified only in the inflorescence primordia tissue, 27 had a homologue with rice and/or *A. thaliana* (Table 6.4), and in the case of 24 DEGs found only in the ovary, 19 of them had a homologue with rice and/or *A. thaliana* (Figure 6.5). In terms of DEGs between HT and LT genotypes in only one tissue type (inflorescence primordia or ovary), their expression between HT and LT genotypes followed the same trend in the other tissue type but did not reach significance at FDR < 0.05. Most DEGs were putatively involved in lipid metabolism such as signalling related receptor-like kinase, RNA transcription and protein synthesis (Tables 6.3, 6.4 and 6.5).

**Table 6.3 List of the DEGs between the HT and LT genotypes that were identified as candidate genes involved in regulating endophyte transmission.**

26 out of 37 common DEGs in 'IP: HT-LT' and 'Ov: HT-LT' (matched with Figure 6.4A[a]):

| Gene | $Log_2^{FC}$ IP: HT-LT | Ov: HT-LT | HT: Ov-IP | LT: Ov-IP | Rice ID | Rice description | *Arabidopsis thaliana* ID | *A. thaliana* description | Function |
|---|---|---|---|---|---|---|---|---|---|
| ms_10051\|ref0018386-eeg-0.1 | **-12.00** | **-7.50** | 5.02 | 0.52 | loc_os10g34602.1 | csAtPR5 [p] [e] | — | — | — |
| ms_12167\|ref0018949-eeg-0.1 | **-10.21** | **-8.81** | 1.74 | 0.34 | loc_os02g47600.2 | soluble inorganic pyrophosphatase [p] [e] | AT2G46860.1 | pyrophosphorylase 3 | nucleotide metabolism. phosphotransfer and pyrophosphatases. |
| ms_6653\|ref0034203-eeg-0.0 | **-9.66** | **-6.33** | 2.60 | -0.73 | loc_os01g12870.1 | eukaryotic translation initiation factor 3 subunit E-interacting protein [p] [e] | AT5G25754.1 | RNA polymerase I-associated factor PAF67 | — |
| ms_2165\|ref0015751-eeg-0.3 | **-9.01** | **-6.82** | 2.29 | 0.10 | loc_os01g02800.1 | receptor-like kinase ARK1AS [p] [e] | AT1G67000.1 | protein kinase superfamily protein | lipid metabolism. lipid degradation. |
| ms_639\|ref0045347-eeg-0.1 | **-8.55** | **-5.53** | **3.09** | 0.07 | loc_os02g02590.2 | — | AT2G39230.1 | lateral organ junction | — |
| ms_12538\|ref0002228-eeg-0.1 | **-7.57** | **-6.56** | -0.27 | **-1.28** | loc_os02g15270.1 | tyrosine-protein phosphatase YVH1 [p] [e] | — | — | protein. postranslational modification. |
| ms_2270\|ref0020580-eeg-0.4 | **-5.96** | **-3.69** | 1.86 | -0.42 | loc_os07g47030.2 | expressed protein | — | — | — |
| ms_9055\|ref0019389-eeg-0.1 | **-5.42** | **-5.29** | -0.60 | -0.74 | loc_os08g28540.1 | resistance protein LR10 [p] [e] | AT3G46530.1 | NB-ARC domain-containing disease resistance protein | stress. biotic. |
| ms_4871\|ref0016800-eeg-0.3 | **-4.42** | **-3.67** | 1.03 | 0.29 | loc_os06g18820.2 | serine threonine kinase [p] [e] | — | — | — |
| ms_2270\|ref0020580-eeg-0.5 | **-4.41** | **-5.28** | -0.99 | -0.11 | loc_os07g47030.1 | expressed protein | — | — | — |
| ms_10216\|ref0033030-eeg-0.0 | **-3.81** | **-4.27** | -0.45 | 0.01 | loc_os01g01369.1 | 3-beta-hydroxysteroid-Delta-isomerase [p] [e] | — | — | — |
| ms_786\|ref0026877-eeg-0.5 | **-3.21** | **-3.02** | 0.81 | **0.61** | loc_os02g06460.1 | expressed protein | AT3G54190.1 | Transducin/WD40 repeat-like superfamily protein | signalling. G-proteins. |
| ms_4753\|ref0012634-eeg-0.1 | **-2.85** | **-3.47** | 0.06 | 0.68 | loc_os08g01940.1 | non-lysosomal glucosylceramidase [p] [e] | AT1G33700.2 | beta-glucosidase, GBA2 type family protein | — |
| ms_974\|ref0000436-eeg-0.0 | **-2.22** | **-1.52** | 0.61 | -0.09 | loc_os07g35050.1 | OsFBX237 - F-box domain containing protein [e] | AT5G49610.1 | F-box family protein | — |
| ms_2194\|ref0008300-eeg-0.0 | **-1.69** | **-1.29** | **0.78** | 0.38 | loc_os05g01330.1 | expressed protein | — | — | — |

Continued on the next page.

| Gene | $Log_2^{FC}$ IP: HT-LT | Ov: HT-LT | HT: Ov-IP | LT: Ov-IP | Rice ID | Rice description | *Arabidopsis thaliana* ID | *A. thaliana* description | Function |
|---|---|---|---|---|---|---|---|---|---|
| ms_1267\|ref0008191-eeg-0.2 | **-1.16** | **-1.15** | **-1.50** | **-1.51** | loc_os02g33540.1 | translational activator family protein [p] [e] | — | — | protein. synthesis. |
| ms_4689\|ref0044391-eeg-0.0 | **-0.88** | **-0.98** | **-0.82** | **-0.72** | loc_os03g08440.2 | ribosomal protein S2 [p] [e] | AT3G04770.2 | 40s ribosomal protein SA B | protein. synthesis. |
| ms_1663\|ref0005605-eeg-0.4 | **2.15** | **2.52** | -0.09 | -0.46 | loc_os04g43420.1 | PTAC5 [p] [e] | — | — | RNA. transcription. |
| ms_6726\|ref0037291-eeg-0.0 | **4.65** | **3.46** | 0.32 | 1.51 | loc_os05g06300.1 | 3-hydroxyacyl-CoA dehydrogenase [p] [e] | AT4G29010.1 | Enoyl-CoA hydratase/isomerase family | RNA. regulation of transcription. |
| ms_30251\|ref0010452-eeg-0.0 | **6.20** | **5.09** | -0.06 | 1.06 | loc_os04g34000.1 | digalactosyldiacylglycerol synthase, chloroplast precursor [p] [e] | AT4G00550.1 | digalactosyl diacylglycerol deficient 2 | lipid metabolism. lipid degradation. |
| ms_21621\|ref0011178-eeg-0.0 | **6.64** | **2.65** | -0.04 | **3.95** | loc_os01g66230.2 | csAtPR5 [p] [e] | — | — | — |
| ms_807\|ref0022598-eeg-0.0 | **7.55** | **6.70** | 0.46 | 1.31 | loc_os08g38620.1 | expressed protein | — | — | — |
| ms_23084\|ref0011235-eeg-0.0 | **7.75** | **4.84** | **-2.34** | 0.57 | loc_os03g02010.3 | — | — | — | — |
| ms_1060\|ref0014573-eeg-0.3 | **9.60** | **7.01** | 0.34 | 2.93 | loc_os07g02760.1 | OsFBD13 - F-box and FBD domain containing protein [e] | — | — | — |
| ms_17402\|ref0022797-eeg-0.0 | **9.80** | **7.38** | -0.20 | 2.22 | loc_os01g05420.1 | IWS1 C-terminus family protein [p] [e] | AT4G19000.1 | transcription elongation factor (TFIIS) family protein | lipid metabolism. glycolipid synthesis. |
| ms_1937\|ref0031964-eeg-0.1 | **11.51** | **7.04** | -0.74 | 3.73 | — | — | AT2G18760.1 | chromatin remodeling 8 | RNA. regulation of transcription. |

In the 'Gene' column, ms = maker-scaffold; eeg = exonerate_est2genome-gene.

[1]'$Log_2^{FC}$ IP: HT-LT' and '$Log_2^{FC}$ Ov: HT-LT' denote the $log_2$ fold change (FC) of the gene expression in the HT relative to LT genotype in the inflorescence primordia and ovary, respectively. '$Log_2^{FC}$ HT: Ov-IP' and '$Log_2^{FC}$ LT: Ov-IP' denote the $log_2^{FC}$ of the gene expression in the ovary relative to inflorescence primordia in the HT and LT genotypes, respectively. The genes with homologues with rice, *A. thaliana* or functions from Mercator are displayed, while those without any annotation are displayed in Table A6.1. The significantly up-regulated genes are marked bold red while the down-regulated genes are marked bold green. IP = inflorescence primordia, Ov = ovary, [u] = unclassified, [p] = putative, [e] = expressed.

**Table 6.4 List of the DEGs between the HT and LT genotypes that were identified as candidate genes involved in regulating endophyte transmission efficiency only in the inflorescence primordia[1].**

27 out of 41 elements included exclusively in 'IP: HT-LT' (matched with Figure 6.4A[b]):

| Gene | $Log_2^{FC}$ IP: HT-LT | Ov: HT-LT | HT: Ov-IP | LT: Ov-IP | Rice ID | Rice description | *Arabidopsis thaliana* ID | *A. thaliana* description | Function |
|---|---|---|---|---|---|---|---|---|---|
| ms_11723\|ref0041671-eeg-0.0 | **-6.56** | -6.22 | 0.23 | -0.11 | loc_os06g42420.1 | transposon protein [u] [p] [e] | AT2G27110.2 | FAR1-related sequence 3 | signalling. light. |
| ms_16777\|ref0035273-eeg-0.0 | **-5.68** | -3.82 | **3.35** | 1.49 | loc_os08g28010.1 | expressed protein | — | — | — |
| ms_9330\|ref0025972-eeg-0.4 | **-4.84** | -2.97 | 1.61 | -0.26 | loc_os01g70080.1 | NB-ARC domain containing protein [e] | AT3G46730.1 | NB-ARC domain-containing disease resistance protein | stress. biotic. |
| ms_1244\|ref0044124-eeg-0.3 | **-4.66** | -4.13 | -0.96 | **-1.49** | loc_os04g49270.1 | tRNA-splicing endonuclease positive effector-related [p] [e] | AT5G52090.1 | P-loop containing nucleoside triphosphate hydrolases superfamily protein | RNA. processing. splicing. |
| ms_639\|ref0045347-eeg-0.4 | **-4.20** | -3.07 | 1.30 | 0.16 | loc_os02g02590.2 | — | AT2G39230.1 | lateral organ junction | — |
| ms_4645\|ref0019413-eeg-0.0 | **-3.77** | -0.35 | **2.17** | -1.25 | loc_os02g09200.1 | cytochrome P450 71D10 [p] [e] | AT3G26180.1 | cytochrome P450, family 71, subfamily B, polypeptide 20 | secondary. metabolism. |
| ms_15690\|ref0009450-eeg-0.0 | **-3.46** | -2.15 | **1.41** | 0.11 | loc_os10g04700.2 | OsFBX361 - F-box domain containing protein [e] | — | — | — |
| ms_10051\|ref0018386-eeg-0.0 | **-3.10** | -2.81 | -0.73 | **-1.02** | loc_os10g34602.1 | csAtPR5 [p] [e] | — | — | — |
| ms_1559\|ref0000370-eeg-0.0 | **-2.19** | -1.83 | 0.52 | 0.16 | loc_os02g32610.3 | protein kinase domain containing protein [e] | AT4G24480.1 | protein kinase superfamily protein | protein. postranslational modification. |
| ms_5979\|ref0020965-eeg-0.0 | **-1.86** | -1.31 | 0.36 | -0.19 | loc_os10g11354.1 | MATE efflux family protein [p] [e] | AT2G34360.1 | MATE efflux family protein | transport. misc. |
| ms_7609\|ref0013234-eeg-0.1 | **-1.86** | -1.48 | -0.22 | -0.59 | loc_os10g24954.1 | ulp1 protease family, C-terminal catalytic domain containing protein [e] | — | — | — |
| ms_3546\|ref0025043-eeg-0.0 | **-1.16** | 1.02 | **-1.62** | **-3.81** | loc_os03g49050.1 | possible lysine decarboxylase domain containing protein [e] | AT3G53450.1 | putative lysine decarboxylase family protein | amino acid metabolism. degradation. |
| ms_18274\|ref0020425-eeg-0.0 | **-1.07** | 0.07 | **3.28** | **2.14** | loc_os08g27850.1 | endothelial differentiation-related factor 1 [p] [e] | AT3G58680.1 | multiprotein bridging factor 1B | hormone metabolism. ethylene. |
| ms_8315\|ref0014502-eeg-0.0 | **-0.90** | -0.49 | 0.00 | -0.40 | loc_os08g02120.1 | kinase, pfkB family [p] [e] | AT3G59480.1 | pfkB-like carbohydrate kinase family protein | major CHO metabolism. degradation. |

Continued on the next page.

| Gene | $Log_2^{FC}$ IP: HT-LT | $Log_2^{FC}$ Ov: HT-LT | $Log_2^{FC}$ HT: Ov-IP | $Log_2^{FC}$ LT: Ov-IP | Rice ID | Rice description | *Arabidopsis thaliana* ID | *A. thaliana* description | Function |
|---|---|---|---|---|---|---|---|---|---|
| ms_4964\|ref0009054-eeg-0.1 | **0.61** | 0.37 | -0.09 | 0.15 | loc_os04g37690.1 | RNA recognition motif containing protein [p] [e] | AT1G47490.1 | RNA-binding protein 47C | RNA. regulation of transcription. |
| ms_4522\|ref0038436-eeg-0.2 | **0.77** | 0.42 | -0.41 | -0.06 | loc_os04g51180.1 | GPR89A [p] [e] | AT4G27630.2 | GPCR-type G protein 2 | — |
| ms_13281\|ref0047557-eeg-0.1 | **0.83** | 0.31 | **-0.62** | -0.10 | loc_os02g45650.1 | peptidase [p] [e] | — | — | — |
| ms_1731\|ref0036760-eeg-0.2 | **0.86** | 0.66 | **-1.13** | **-0.92** | loc_os05g05440.1 | expressed protein | AT4G03130.1 | BRCT domain-containing DNA repair protein | RNA. regulation of transcription. |
| ms_2370\|ref0043188-eeg-0.1 | **0.92** | 0.28 | -0.24 | 0.40 | loc_os03g46770.2 | — | AT4G39260.3 | cold, circadian rhythm, and RNA binding 1 | RNA. regulation of transcription. |
| ms_8397\|ref0012762-eeg-0.1 | **0.97** | 0.72 | **-1.18** | **-0.93** | loc_os05g37980.1 | PSF1 - Putative GINS complex subunit [e] | — | — | — |
| ms_14538\|ref0034846-eeg-0.2 | **1.05** | 0.06 | **-3.00** | **-2.00** | loc_os01g13260.1 | cyclin-A1 [p] [e] | AT1G77390.1 | CYCLIN A1;2 | cell. cycle. |
| ms_11653\|ref0008384-eeg-0.0 | **1.90** | 0.94 | 0.32 | **1.29** | loc_os01g40750.1 | expressed protein | — | — | — |
| ms_16585\|ref0001680-eeg-0.1 | **2.33** | 0.93 | **-1.37** | 0.03 | loc_os02g16270.2 | xa1 [p] [e] | AT3G14460.1 | LRR and NB-ARC domains-containing disease resistance protein | protein. degradation. |
| ms_11093\|ref0014860-eeg-0.0 | **2.97** | 3.48 | **-2.68** | **-3.19** | loc_os01g31870.1 | natural resistance-associated macrophage protein [p] [e] | AT1G15960.1 | NRAMP metal ion transporter 6 | transport. metal. |
| ms_713\|ref0006958-eeg-0.0 | **4.18** | 1.14 | **-2.31** | 0.72 | loc_os03g61040.1 | GIL1 [p] [e] | — | — | stress. biotic. |
| ms_20995\|ref0017051-eeg-0.1 | **6.50** | 5.05 | -0.04 | 1.40 | loc_os06g40520.1 | TNP1 [p] [e] | — | — | — |
| ms_10394\|ref0014269-eeg-0.1 | **8.22** | 5.25 | -1.11 | 1.85 | loc_os08g10780.1 | transposon protein [u] [p] [e] | — | — | — |

In the 'Gene' column, ms = maker-scaffold; eeg = exonerate_est2genome-gene.

[1] '$Log_2^{FC}$ IP: HT-LT' and '$Log_2^{FC}$ Ov: HT-LT' denote the $log_2$ fold change (FC) of the gene expression in the HT relative to LT genotype in the inflorescence primordia and ovary, respectively. '$Log_2^{FC}$ HT: Ov-IP' and '$Log_2^{FC}$ LT: Ov-IP' denote the $Log_2^{FC}$ of the gene expression in the ovary relative to inflorescence primordia in the HT and LT genotypes, respectively. The genes with homologues with rice, *A. thaliana* or functions from Mercator are displayed, while those without any annotation are displayed in Table A6.2. The significantly up-regulated genes are marked bold red while the down-regulated genes are marked bold green. IP = inflorescence primordia, Ov = ovary, [u] = unclassified, [p] = putative, [e] = expressed.

**Table 6.5 List of DEGs between the HT and LT genotypes that were identified as candidate genes involved in regulating endophyte transmission efficiency only in the ovary[1].**

19 out of 24 elements included exclusively in 'Ov: HT-LT' (matched with Figure 6.4A[c]):

| Gene | $Log_2^{FC}$ IP: HT-LT | Ov: HT-LT | HT: Ov-IP | LT: Ov-IP | Rice ID | Rice description | *Arabidopsis thaliana* ID | *A. thaliana* description | Function |
|---|---|---|---|---|---|---|---|---|---|
| ms_639\|ref0045347-eeg-0.3 | -3.38 | **-6.35** | -2.98 | -0.01 | loc_os04g02680.1 | expressed protein | — | — | — |
| ms_6703\|ref0002616-eeg-0.1 | -1.23 | **-3.03** | **-2.89** | **-1.08** | loc_os06g04450.2 | Sec1 family transport protein [p] [e] | AT4G12120.1 | Sec1/munc18-like (SM) proteins superfamily | protein. targeting. |
| ms_11517\|ref0006436-eeg-0.0 | -1.15 | **-2.81** | **0.97** | 2.63 | loc_os07g17300.1 | expressed protein | — | — | — |
| ms_15380\|ref0020740-eeg-0.0 | -2.79 | **-2.57** | **2.55** | **2.33** | loc_os08g35160.2 | heat shock protein DnaJ [p] [e] | — | — | — |
| ms_7258\|ref0024859-eeg-0.0 | -2.01 | **-2.55** | **3.81** | **4.35** | loc_os02g18410.1 | salt stress root protein RS1 [p] [e] | — | — | protein. degradation. |
| ms_2767\|ref0015320-eeg-0.0 | -4.89 | **-1.99** | **8.63** | **5.74** | loc_os03g60509.2 | expressed protein | AT5G66230.2 | Chalcone-flavanone isomerase family protein | secondary metabolism. flavonoids. |
| ms_1304\|ref0035692-eeg-0.3 | -0.74 | **-1.07** | **1.29** | **1.62** | loc_os07g33310.1 | MATE efflux family protein [p] [e] | AT1G61890.1 | MATE efflux family protein | transport. misc. |
| ms_374\|ref0040306-eeg-0.2 | 0.94 | **1.19** | **1.14** | **0.88** | loc_os02g02350.3 | OsFBK2 - F-box domain and kelch repeat containing protein [e] | AT1G55270.1 | Galactose oxidase/kelch repeat superfamily protein | — |
| ms_16353\|ref0013246-eeg-0.0 | 0.19 | **1.79** | **9.37** | **7.76** | loc_os01g60770.1 | expansin precursor [p] [e] | AT2G03090.1 | expansin A15 | redox. glutaredoxins. |
| ms_53\|ref0019421-eeg-1.0 | -0.14 | **1.97** | **8.11** | **6.00** | loc_os11g42960.1 | integral membrane protein TIGR01569 containing protein [e] | — | — | — |
| ms_9793\|ref0028890-eeg-0.0 | -0.58 | **2.03** | **2.87** | 0.26 | loc_os04g38390.1 | wound/stress protein [p] [e] | AT2G22170.1 | lipase/lipooxygenase, PLAT/LH2 family protein | — |
| ms_6854\|ref0012592-eeg-0.2 | 1.37 | **2.18** | 0.47 | -0.34 | loc_os05g39410.2 | expressed protein | AT5G45840.2 | Leucine-rich repeat protein kinase family protein | signalling. receptor kinases. |
| ms_13717\|ref0005325-eeg-0.0 | 0.31 | **2.27** | **8.42** | **6.46** | loc_os08g01450.1 | cytochrome P450 [p] [e] | AT3G26300.1 | cytochrome P450, family 71, subfamily B, polypeptide 34 | cell wall. modification. |
| ms_8920\|ref0048067-eeg-0.1 | 2.25 | **2.35** | 0.64 | 0.54 | loc_os11g37340.1 | OsFBX426 - F-box domain containing protein [e] | — | — | — |

Continued on the next page

| Gene | $Log_2^{FC}$ IP: HT-LT | Ov: HT-LT | HT: Ov-IP | LT: Ov-IP | Rice ID | Rice description | *Arabidopsis thaliana* ID | *A. thaliana* description | Function |
|---|---|---|---|---|---|---|---|---|---|
| ms_3574\|ref0030282-eeg-0.2 | 3.06 | **2.45** | **6.46** | **7.07** | loc_os10g34170.1 | glutaredoxin domain containing protein [p] [e] | AT4G08550.1 | electron carriers; protein disulfide oxidoreductases | protein. degradation. |
| ms_9469\|ref0034926-eeg-0.0 | -1.69 | **2.88** | **4.85** | 0.28 | loc_os03g49600.1 | Os3bglu7 - beta-glucosidase, exo-beta-glucanse [e] | AT3G18070.1 | beta glucosidase 43 | misc. gluco-, galacto- and mannosidases. |
| ms_8541\|ref0030295-eeg-0.2 | 0.69 | **3.52** | **2.56** | -0.27 | loc_os02g04340.1 | NIN-like protein 2 [p] [e] | AT4G24020.1 | NIN like protein 7 | development. unspecified. |
| ms_6018\|ref0043257-eeg-0.2 | 1.69 | **4.00** | **6.52** | **4.21** | loc_os06g49020.1 | 26S proteasome non-ATPase regulatory subunit 14 [p] [e] | AT1G71230.1 | COP9-signalosome 5B | misc. cytochrome P450. |
| ms_7823\|ref0043153-eeg-0.0 | 2.54 | **4.80** | 0.94 | -1.32 | loc_os02g44770.1 | uncharacterized mscS family protein [p] [e] | AT1G53470.1 | mechanosensitive channel of small conductance-like 4 | signalling. unspecified |

In the 'Gene' column, ms = maker-scaffold; eeg = exonerate_est2genome-gene.

[1]'$Log_2^{FC}$ IP: HT-LT' and '$Log_2^{FC}$ Ov: HT-LT' denote the $log_2$ fold change (FC) of the gene expression in the HT relative to LT genotype in the inflorescence primordia and ovary, respectively. '$Log_2^{FC}$ HT: Ov-IP' and '$Log_2^{FC}$ LT: Ov-IP' denote the $log_2^{FC}$ of the gene expression in the ovary relative to inflorescence primordia in the HT and LT genotypes, respectively. The genes with homologues with rice, *A. thaliana* or functions from Mercator are displayed, while those without any annotation are displayed in Table A6.3. The significantly up-regulated genes are marked bold red while the down-regulated genes are marked bold green. IP = inflorescence primordia, Ov = ovary, [u] = unclassified, [p] = putative, [e] = expressed.

### 6.4.5 Ontology analysis for the DEGs between HT and LT genotypes

Since the number of DEGs was relatively low at the FDR < 0.05 significance threshold, GO enrichment analysis was based on a significance threshold of $p < 0.001$ for selecting the DEGs. AgriGO, with the SEA tool, was used to evaluate global gene expression.

With the cutoff of $p < 0.001$, the number of significant GO terms was higher in the inflorescence primordia than ovary. Analysis by agriGO revealed that 60 (51% of the total DEGs) and 58 (40% of the total DEGs) genes in the inflorescence primordia and ovary, respectively, had hits to GO terms, which were functionally classified into three main categories, *i.e.*, cellular component (the parts of a cell or its extracellular environment), molecular function (the elemental activities of a gene product at the molecular level, such as binding or catalysis and biological process) and biological process (operations or sets of molecular events with a defined beginning and end, pertinent to the functioning of integrated living units: cells, tissues, organs, and organisms). For the inflorescence primordia, there were 29, 18 and 32 significant GO terms belonging to cellular component, molecular function and biological process, respectively. AgriGO analysis revealed that the *serine family amino acid metabolic process* (GO:0009069) subcategory was the main biological process where the majority of the gene products from the DEGs are likely to belong (Figure 6.7A). *Adenyl ribonucleotide binding* (GO:0032559) and *purine ribonucleoside binding* (GO:0032550) functions were the main subcategories in the molecular function subcategory (Figure 6.7B). *Cytoplasmic membrane-bounded vesicle* (GO:0016023) functions were the highly-enriched subcategory for the cellular component category (Figure 6.7C). For the ovary, there were 21, 8 and 21 significant GO terms related to cellular component, molecular function and biological process,

respectively. Analysis by agriGO showed that *serine family amino acid metabolic process* (GO:0009069) functions were the enriched subcategory in biological process which was also enriched in the inflorescence primordia (Figure 6.8A). Furthermore, *cytoplasmic membrane-bounded vesicle* (GO:0016023) functions were the highly enriched subcategory in the cellular component category (Figure 6.8B).

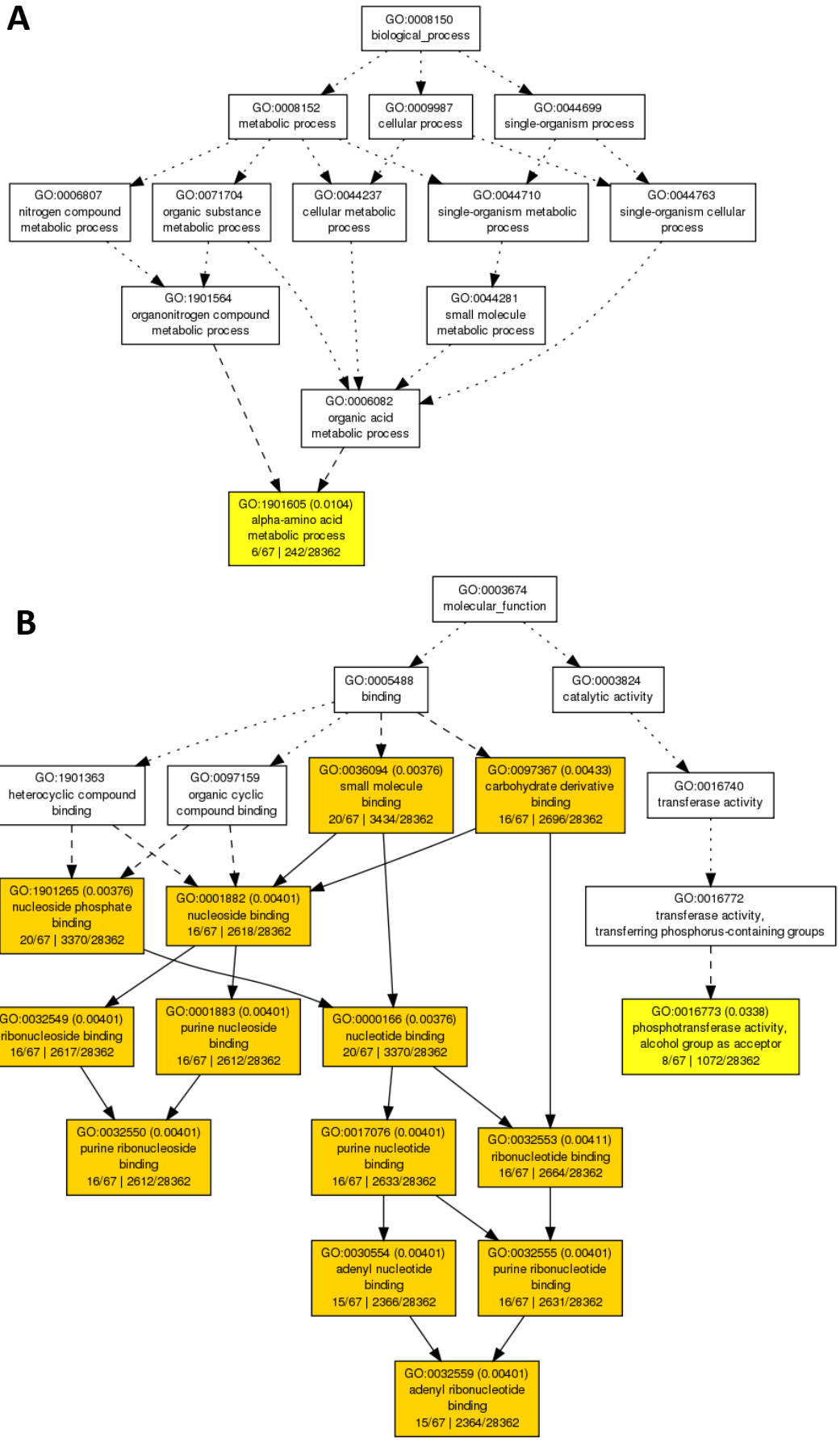
A
GO:0008150
biological_process
GO:0008152
metabolic process
GO:0009987
cellular process
GO:0044699
single-organism process
GO:0006807
nitrogen compound
metabolic process
GO:0071704
organic substance
metabolic process
GO:0044237
cellular metabolic
process
GO:0044710
single-organism metabolic
process
GO:0044763
single-organism cellular
process
GO:1901564
organonitrogen compound
metabolic process
GO:0044281
small molecule
metabolic process
GO:0006082
organic acid
metabolic process
GO:1901605 (0.0104)
alpha-amino acid
metabolic process
6/67 | 242/28362
B
GO:0003674
molecular_function
GO:0005488
binding
GO:0003824
catalytic activity
GO:1901363
heterocyclic compound
binding
GO:0097159
organic cyclic
compound binding
GO:0036094 (0.00376)
small molecule
binding
20/67 | 3434/28362
GO:0097367 (0.00433)
carbohydrate derivative
binding
16/67 | 2696/28362
GO:0016740
transferase activity
GO:1901265 (0.00376)
nucleoside phosphate
binding
20/67 | 3370/28362
GO:0001882 (0.00401)
nucleoside binding
16/67 | 2618/28362
GO:0016772
transferase activity,
transferring phosphorus-containing groups
GO:0032549 (0.00401)
ribonucleoside binding
16/67 | 2617/28362
GO:0001883 (0.00401)
purine nucleoside
binding
16/67 | 2612/28362
GO:0000166 (0.00376)
nucleotide binding
20/67 | 3370/28362
GO:0016773 (0.0338)
phosphotransferase activity,
alcohol group as acceptor
8/67 | 1072/28362
GO:0032550 (0.00401)
purine ribonucleoside
binding
16/67 | 2612/28362
GO:0017076 (0.00401)
purine nucleotide
binding
16/67 | 2633/28362
GO:0032553 (0.00411)
ribonucleotide binding
16/67 | 2664/28362
GO:0030554 (0.00401)
adenyl nucleotide
binding
15/67 | 2366/28362
GO:0032555 (0.00401)
purine ribonucleotide
binding
16/67 | 2631/28362
GO:0032559 (0.00401)
adenyl ribonucleotide
binding
15/67 | 2364/28362

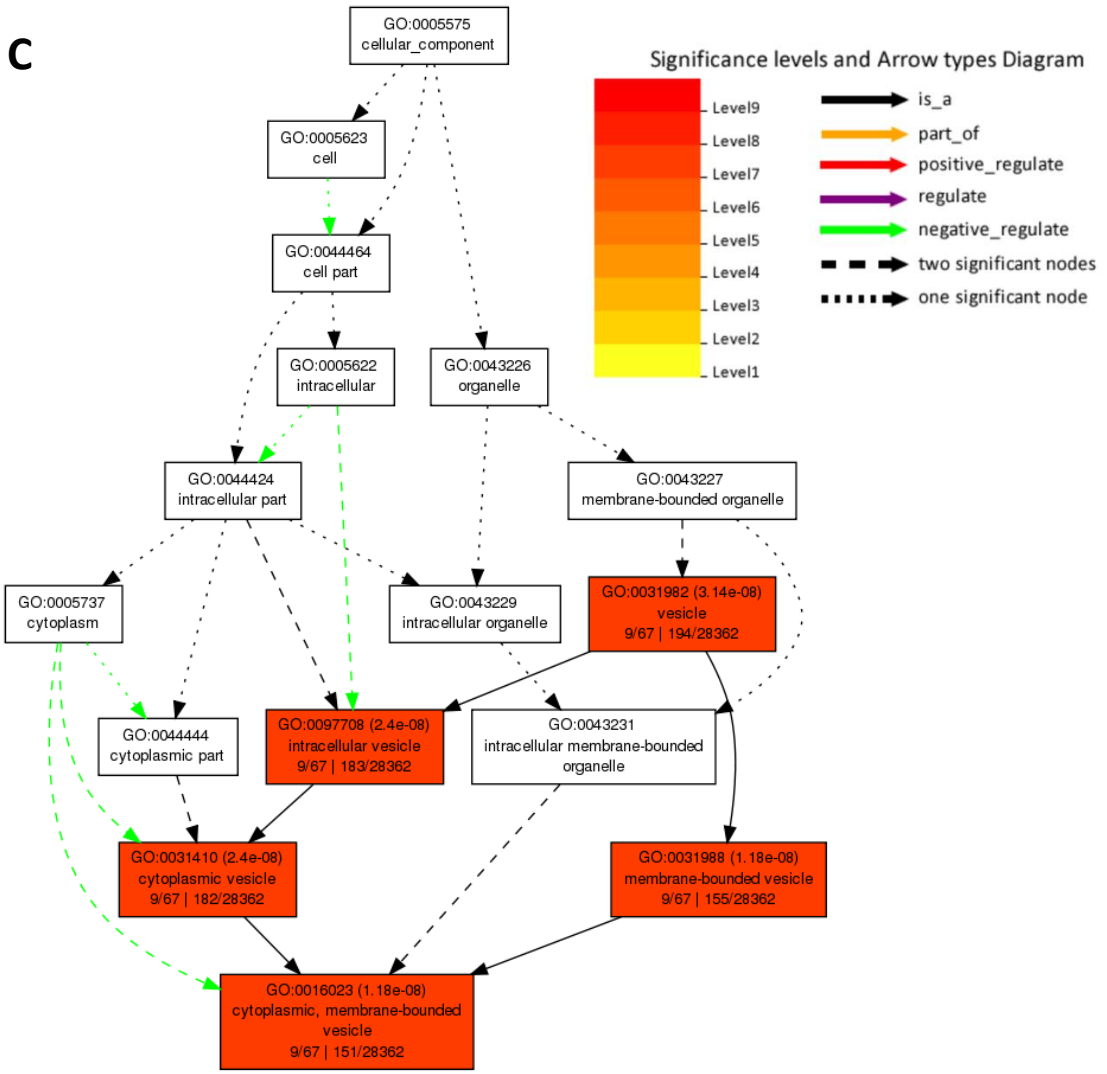


**Figure 6.7 Hierarchical tree graph of overrepresented GO terms in (A) biological process, (B) molecular function and (C) cellular component categories generated by SEA from agriGO analysis of transcriptomic results for samples from the inflorescence primordia.** Boxes in the graph represent GO terms labelled by their GO ID, term definition and statistical information. The significant (FDR < 0.05) terms are marked with colour. The degree of colour saturation of a box is positively correlated with the enrichment level of the term. Solid, dashed, and dotted lines represent two, one and zero enriched terms at both ends connected by the line, respectively. Green lines indicate down regulation. The rank direction of the graph is set from top to bottom. Significance values and arrow types are shown in the diagram.

**A**

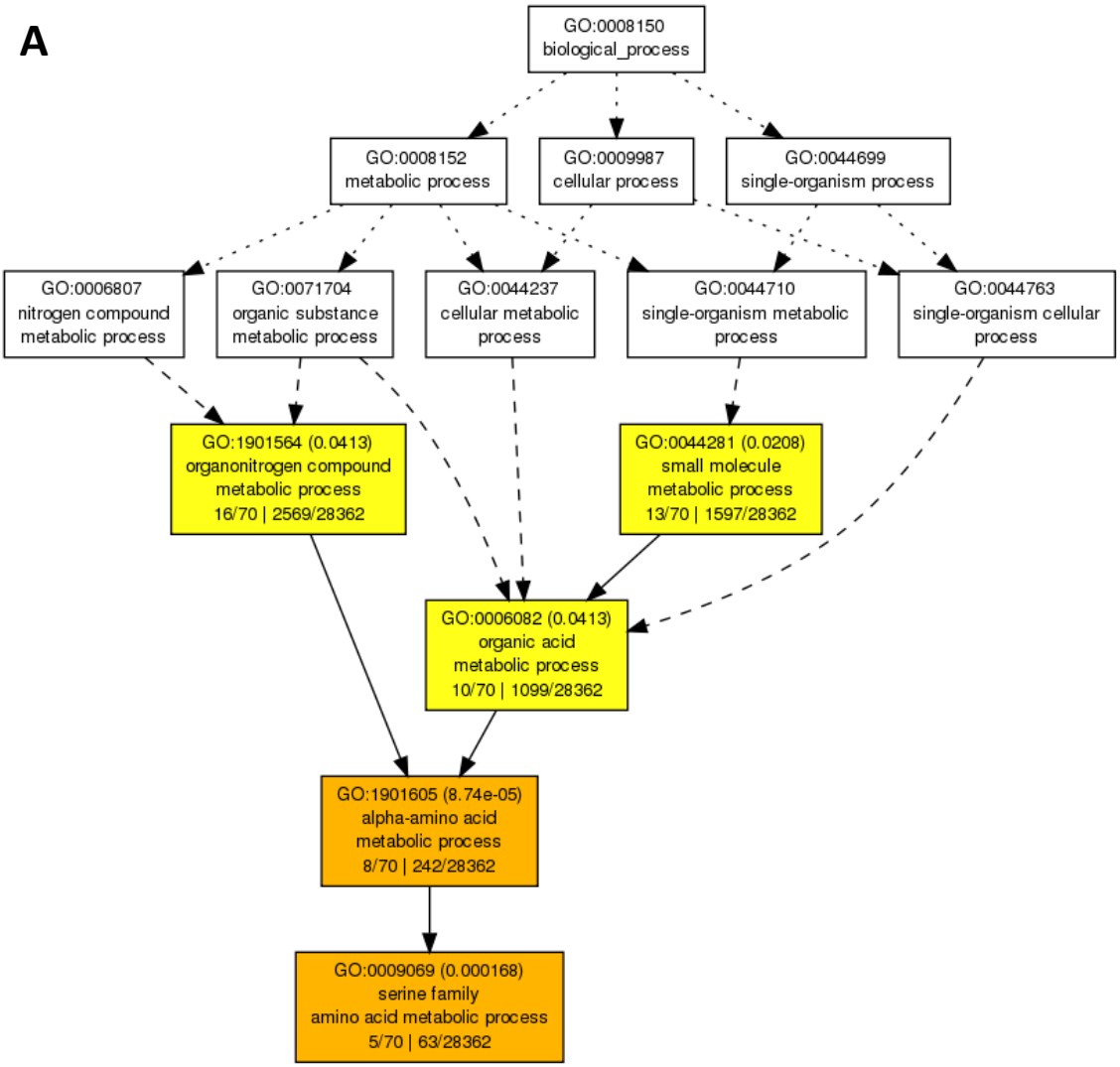
GO:0008150
biological_process
GO:0008152
metabolic process
GO:0009987
cellular process
GO:0044699
single-organism process
GO:0006807
nitrogen compound
metabolic process
GO:0071704
organic substance
metabolic process
GO:0044237
cellular metabolic
process
GO:0044710
single-organism metabolic
process
GO:0044763
single-organism cellular
process
GO:1901564 (0.0413)
organonitrogen compound
metabolic process
16/70 | 2569/28362
GO:0044281 (0.0208)
small molecule
metabolic process
13/70 | 1597/28362
GO:0006082 (0.0413)
organic acid
metabolic process
10/70 | 1099/28362
GO:1901605 (8.74e-05)
alpha-amino acid
metabolic process
8/70 | 242/28362
GO:0009069 (0.000168)
serine family
amino acid metabolic process
5/70 | 63/28362

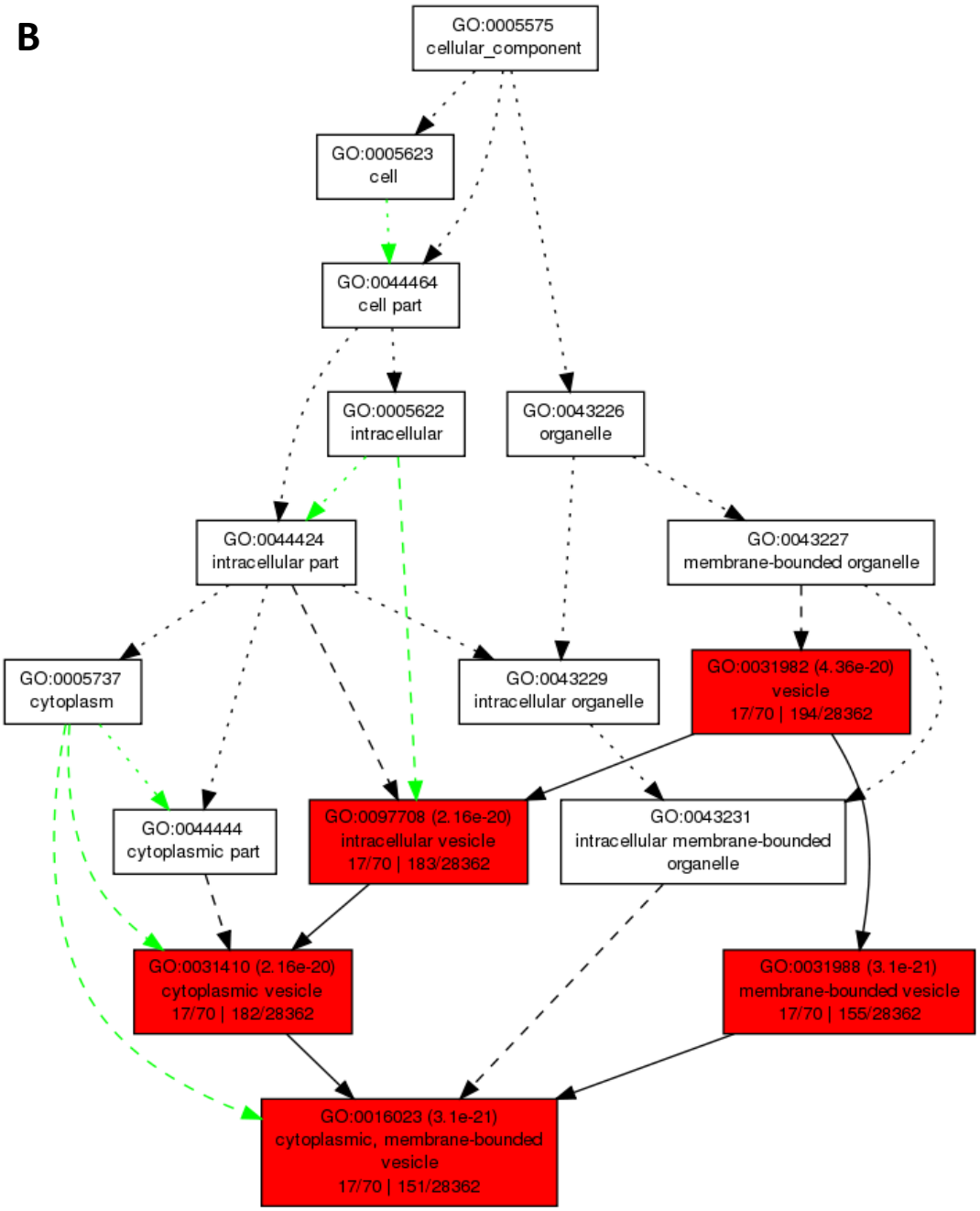


**Figure 6.8 Hierarchical tree graph of overrepresented GO terms in (A) biological process and (B) cellular component categories generated by SEA from agriGO in the ovary.** Boxes in the graph represent GO terms labelled by their GO ID, term definition and statistical information. The significant (FDR < 0.05) terms are marked with colour. The degree of colour saturation of a box is positively correlated with the enrichment level of the term. Solid, dashed, and dotted lines represent two, one and zero enriched terms at both ends connected by the line, respectively. Green lines indicate down regulation. The rank direction of the graph is set from top to bottom. Significance levels and arrow legands are shown in Figure 6.7.

### 6.4.6 DEGs between inflorescence primordia and ovary

As would be expected due to developmental differences, there was a high count of DEGs in the comparison between inflorescence primordia and ovary tissues. There were 6,298 DEGs between the inflorescence primordia and ovary in both the HT and LT genotypes. HT genotypes had more exclusive DEGs (1,521) than the LT genotypes (552) (Figure 6.4B).

The KEGG database was used to classify the common DEGs between the inflorescence primordia and the ovary in both HT and LT genotypes. KEGG analyses showed that 1,540 of the 6,298 common DEGs were involved in 317 pathways. Pathways with higher representation among the DEGs were involved in carbon metabolism (79 genes, 5.13%), plant hormone signal transduction (74 genes, 4.81%), starch and sucrose metabolism (70 genes, 4.55%), cell cycle (68 genes, 4.42%), biosynthesis of amino acids (64 genes, 4.16%), spliceosome (60 genes, 3.90%), purine metabolism (55 genes, 3.57%), ubiquitin mediated proteolysis (55 genes, 3.57%), phenylpropanoid biosynthesis (54 genes, 3.51%) and RNA transport (53 genes, 3.44%).

Furthermore, 378 of the 1,521 genes which were exclusively differentially-expressed in the HT genotypes in the inflorescence primordia and ovary tissues were involved in known KEGG pathways. These genes were involved in 260 pathways, among which the ten highly enriched pathways were ribosome (18 genes, 4.76%), ubiquitin mediated proteolysis (18 genes, 4.76%), carbon metabolism (17 genes, 4.50%), protein processing in the endoplasmic reticulum (17 genes, 4.50%), RNA transport (16 genes, 4.23%), spliceosome (16 genes, 4.23%), plant hormone signal transduction (16 genes, 4.23%), starch and sucrose metabolism (13 genes, 3.44%), biosynthesis of amino acids (13 genes, 3.44%) and Epstein-Barr virus infection (13 genes, 3.44%).

Of particular note in this study, 167 of the 552 genes which were exclusively differentially-expressed in the LT genotypes during development from the inflorescence primordia to the ovary were listed in KEGG pathways. These genes were more highly abundant in 233 pathways, among which the ten most enriched pathways were carbon metabolism (12 genes, 7.19%), the insulin signalling pathway (11 genes, 6.59%), phenylpropanoid biosynthesis (11 genes, 6.59%), the PI3K-Akt signaling pathway (10 genes, 5.99%), starch and sucrose metabolism (10 genes, 5.99%), biosynthesis of amino acids (9 genes, 5.39%), purine metabolism (8 genes, 4.79%), the mTOR signaling pathway (7 genes, 4.19%), protein processing in the endoplasmic reticulum (7 genes, 4.19%) and RNA transport (7 genes, 4.19%).

### 6.4.7 Expression profiling of trehalose metabolism

As concluded in Chapter 5, the loss of endophytes in the stored seeds was associated with a decrease in internal trehalose content. Therefore, we sought to understand the status of trehalose metabolism in the HT and LT genotypes of both the ovary and inflorescence primordia by analysing the starch and sucrose metabolism pathway. This pathway was indicated as induced by the exclusive DEGs (when comparing inflorescence primordia and ovary tissues) in both HT and LT genotypes (Figure 6.9). Comparing the gene expression patterns, two genes for coding trehalose 6-phosphate phosphatase (TPP) (EC:3.1.3.12) were significantly up-regulated (ovary > inflorescence primordia) in the HT genotypes but there were no significant differences in the LT genotypes. Moreover, one gene for coding trehalose-6-phosphate synthase (TPS) was also down-regulated (ovary < inflorescence primordia) in the LT genotypes (EC:2.4.1.15) but was not differentially expressed in the HT genotypes.

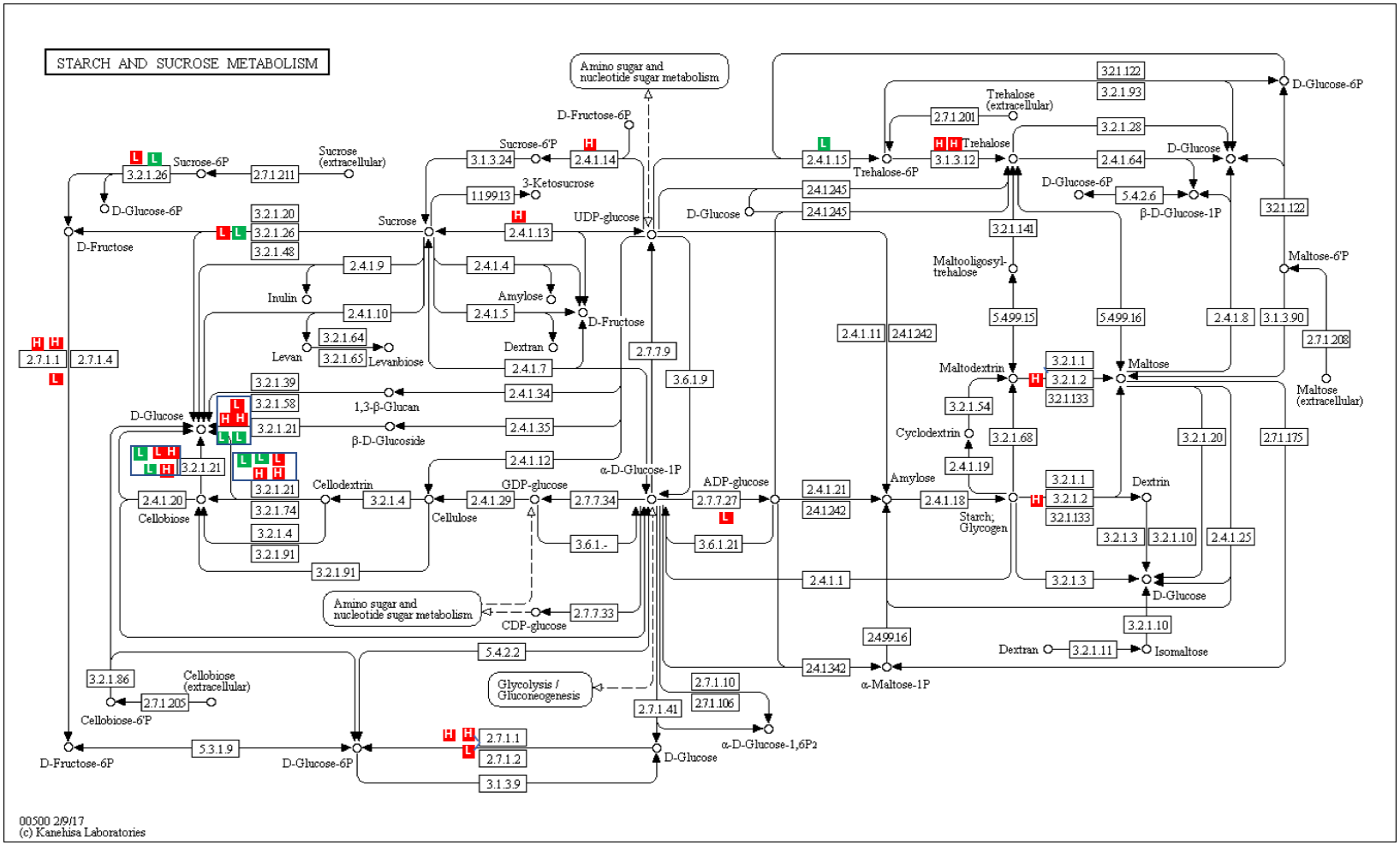


**Figure 6.9 KEGG pathway map of starch and sucrose metabolism.** Coloured squares show the exclusive DEGs between inflorescence primordia and ovary in HT (marked H inside the square) and LT genotypes (marked L inside the square), separately. Red colour signifies up-regulation (ovary > inflorescence primordia) while green colour shows down-regulation (ovary < inflorescence primordia) of the indicated genes.

The genes related to trehalose metabolism were also selected based on the gene annotations from Mercator. It was found that almost all of the genes linked to TPS were similarly expressed in the inflorescence primordia and ovary in both the HT and LT genotypes. Only one gene in the LT genotypes was significantly less abundantly expressed. Seven TPP genes were significantly more abundant in the ovary, compared to the inflorescence primordia, in the HT genotypes, among which five genes were also significantly up-regulated in the LT genotypes. The fold changes of the two common genes were also much higher in the HT than LT genotypes (underlined in Table 6.6).

**Table 6.6 Expression of genes related to trehalose metabolism in the HT compared to LT genotypes in the inflorescence primordia and the ovary; as well as in the ovary compared with inflorescence primordia in the HT and LT genotypes of perennial ryegrass[1].**

| Gene | Gene symbol | $Log_2^{FC}$ | | | |
|---|---|---|---|---|---|
| | | IP: HT-LT | Ov: HT-LT | HT: Ov-IP | LT: Ov-IP |
| ms_3053\|ref0033116-eeg-0.0 | TPS8 | -0.56 | 0.42 | -0.47 | **-1.44** |
| ms_12265\|ref0028712-eeg-0.0 | TPS2 | -0.81 | -0.97 | -0.94 | -0.78 |
| ms_2235\|ref0020919-eeg-0.0 | TPS2 | -0.36 | 0.02 | 0.22 | -0.16 |
| ms_1480\|ref0044477-eeg-0.1 | TPS5 | -0.28 | -0.32 | -0.18 | -0.14 |
| ms_2340\|ref0000205-eeg-0.0 | TPS5 | -0.41 | 0.27 | 0.14 | -0.55 |
| ms_5128\|ref0013887-eeg-0.0 | TPS5 | 0.15 | 0.11 | 0.05 | 0.09 |
| ms_5813\|ref0029399-eeg-0.0 | TPS5 | -0.29 | 0.33 | 0.52 | -0.10 |
| ms_8895\|ref0021743-eeg-0.2 | TPS5 | -0.32 | 0.11 | 0.51 | 0.08 |
| ms_2501\|ref0009238-eeg-0.0 | TPS9 | -0.61 | -0.32 | 1.60 | 1.31 |
| ms_479\|ref0026826-eeg-0.4 | TPPE | -2.05 | 0.24 | **7.16** | **4.87** |
| ms_3393\|ref0039787-eeg-0.0 | TPPH | 0.28 | 0.22 | **3.88** | **3.93** |
| ms_7867\|ref0018169-eeg-0.0 | TPPH | -0.46 | 0.29 | **3.04** | 2.29 |
| ms_5151\|ref0044420-eeg-0.2 | TPPI | -0.29 | -0.59 | **2.91** | **3.21** |
| ms_5439\|ref0015640-eeg-0.1 | TPPF | -0.31 | 0.14 | **2.19** | **1.73** |
| ms_9684\|ref0044411-eeg-0.1 | TPPG | 0.91 | 2.77 | **1.61** | -0.24 |
| ms_4925\|ref0034052-eeg-0.1 | TPPC | 0.41 | -0.12 | **0.98** | **1.52** |
| ms_13547\|ref0028015-eeg-0.0 | TPPE | -0.48 | 0.34 | 0.33 | -0.50 |
| ms_321\|ref0033184-eeg-0.2 | TPPG | -0.01 | -0.34 | 0.06 | 0.39 |
| ms_471\|ref0026820-eeg-0.5 | | 0.87 | 0.69 | -0.18 | 0.00 |
| ms_3425\|ref0047539-eeg-0.0 | TPPH | 0.16 | 0.39 | -0.19 | -0.43 |
| ms_17545\|ref0032790-eeg-0.0 | TPPH | -0.04 | -0.40 | -0.52 | -0.16 |
| ms_2536\|ref0027257-eeg-0.0 | TPPH | -0.51 | -0.08 | -0.71 | -1.14 |

In the 'Gene' column, ms = maker-scaffold; eeg = exonerate_est2genome-gene.

[1]Gene symbols of the genes with homology with *Arabidopsis thaliana* was shown. '$Log_2^{FC}$ IP: HT-LT' and '$Log_2^{FC}$ Ov: HT-LT' denote the $log_2$ $^{fold\ change\ (FC)}$ of the gene expression in HT relative to LT genotype in the inflorescence primordia and ovary, respectively. '$Log_2^{FC}$ HT: Ov-IP' and '$Log_2^{FC}$ LT: Ov-IP' denote the $log_2^{FC}$ of the gene expression in the Ov relative to IP in the HT and LT genotypes, respectively. Significantly up-regulated genes are marked bold red while down-regulated genes are marked bold green. Values are underlined when there is a significant difference between the ovary and IP in both the HT and LT genotypes, and when the FC is higher in the HT than LT genotypes. IP = inflorescence primordia, Ov = ovary.

### 6.4.8 Expression profiling of salicylic acid and jasmonic acid metabolism

The genes related to salicylic acid and jasmonic acid metabolism were also selected for more detailed investigation based on the gene annotation from Mercator. It was found that most of the genes related to jasmonic acid metabolism were up-regulated (ovary > inflorescence primordia) in the ovary compared to the inflorescence primordia, while those related to salicylic acid metabolism were down-regulated (ovary < inflorescence

primordia). In particular, three genes relative to salicylic acid metabolism were significantly down-regulated (ovary < inflorescence primordia) in the HT genotypes, among which two genes were also significantly down-regulated (ovary < inflorescence primordia) in the LT genotypes (Table 6.7). Conversely, ten genes related to jasmonic acid metabolism were significantly up-regulated (ovary > inflorescence primordia) in the HT genotypes, among which six genes were also significantly up-regulated (ovary > inflorescence primordia) in the LT genotypes. Also, the fold changes of the common six genes were higher in the HT than LT genotypes (underlined in Table 6.8).

**Table 6.7 Expression of genes related to salicylic acid metabolism in the HT compared to LT genotypes in the inflorescence primordia and ovary; and in the ovary compared with inflorescence primordia in the HT and LT genotypes of perennial ryegrass[1].**

| Gene | Gene symbol | $Log_2^{FC}$ | | | |
|---|---|---|---|---|---|
| | | IP: HT-LT | Ov: HT-LT | HT: Ov-IP | LT: Ov-IP |
| ms_1134\|ref0047379-eeg-0.0 | UGT74F1 | 0.43 | 0.54 | **-6.92** | **-4.50** |
| ms_16551\|ref0041347-eeg-0.0 | UGT74E2 | -0.24 | -0.07 | **-4.30** | **-4.64** |
| ms_3027\|ref0043252-eeg-0.1 | | 0.71 | 0.24 | **-1.19** | -0.72 |
| ms_1517\|ref0023937-eeg-0.2 | BSMT1 | 0.28 | -2.15 | **0.78** | **0.61** |
| ms_6346\|ref0010855-eeg-0.2 | | -0.85 | -0.80 | -0.93 | -0.98 |
| ms_15350\|ref0024553-eeg-0.0 | RFL9 | -0.79 | -0.92 | -0.68 | -0.55 |
| ms_4680\|ref0044386-eeg-0.3 | UGT74F1 | 0.04 | 0.00 | -0.39 | -0.35 |
| ms_3671\|ref0011082-eeg-0.1 | RFL2 | 0.18 | 0.11 | 0.09 | 0.16 |
| ms_1339\|ref0041032-eeg-0.2 | UGT74F1 | -0.23 | 0.12 | 0.11 | 0.00 |
| ms_2375\|ref0043193-eeg-0.0 | UGT74F1 | -0.44 | 0.07 | 0.11 | -0.40 |

In the 'Gene' column, ms = maker-scaffold; eeg = exonerate_est2genome-gene.

[1]Gene symbols of the genes with homologue with *Arabidopsis thaliana* was shown. '$Log_2^{FC}$ IP: HT-LT' and '$Log_2^{FC}$ Ov: HT-LT' denote the $log_2$ $^{fold\ change\ (FC)}$ of the gene expression in the HT relative to LT genotype in the inflorescence primordia and ovary, respectively. '$Log_2^{FC}$ HT: Ov-IP' and '$Log_2^{FC}$ LT: Ov-IP' denote the $log_2^{FC}$ of the gene expression in the Ov relative to IP in the HT and LT genotypes, respectively. Up-regulated genes are marked bold red while down-regulated genes are marked bold green. The values are underlined when there is a significant difference between the Ov and IP in both the HT and LT genotypes, and when the FC is higher in the HT than the LT genotypes. IP = inflorescence primordia, Ov = ovary.

**Table 6.8 Expression of genes related to jasmonic acid and in the HT compared to LT genotypes in the inflorescence primordia and ovary; and in the ovary compared with inflorescence primordia in the HT and LT genotypes of perennial ryegrass[1].**

| Gene | Gene symbol | $Log_2^{FC}$ | | | |
|---|---|---|---|---|---|
| | | IP: HT-LT | Ov: HT-LT | HT: Ov-IP | LT: Ov-IP |
| ms_9415\|ref0006109-eeg-0.0 | OPR2 | 0.08 | 0.88 | **8.84** | **8.03** |
| ms_7552\|ref0041371-eeg-0.1 | OPR2 | -1.16 | 0.15 | **5.22** | **3.91** |
| ms_2111\|ref0018533-eeg-0.0 | LOX6 | -1.87 | -0.19 | **4.89** | **3.21** |
| ms_7715\|ref0034244-eeg-0.1 | LOX6 | 0.23 | 0.55 | **3.86** | **3.53** |
| ms_3235\|ref0030072-eeg-0.0 | OPR2 | -1.38 | -0.59 | **2.99** | **2.19** |
| ms_5037\|ref0032359-eeg-0.0 | LOX4 | 0.14 | 0.18 | **2.95** | **2.90** |
| ms_5548\|ref0036016-eeg-0.3 | LOX4 | -0.93 | -0.03 | **2.10** | 1.20 |
| ms_7552\|ref0041371-eeg-0.0 | OPR2 | -1.34 | -0.75 | **1.45** | 0.86 |
| ms_14669\|ref0004090-eeg-0.0 | LOX4 | -0.44 | 0.21 | **1.45** | 0.80 |
| ms_2566\|ref0021833-eeg-0.0 | LOX4 | -0.48 | -0.12 | **0.99** | 0.64 |
| ms_2911\|ref0019974-eeg-0.4 | OPR1 | 1.65 | 0.91 | 3.35 | 4.09 |
| ms_8694\|ref0001888-eeg-0.0 | LOX6 | -0.74 | 0.44 | 0.78 | -0.40 |
| ms_5020\|ref0001773-eeg-0.1 | OPR1 | 0.28 | 0.46 | 0.41 | 0.24 |
| ms_3877\|ref0034879-eeg-0.1 | LOX5 | 0.15 | 0.23 | 0.05 | -0.04 |
| ms_6151\|ref0017538-eeg-0.0 | BSMT1 | 0.07 | -0.14 | 0.01 | 0.22 |
| ms_24\|ref0012210-eeg-2.3 | LOX3 | -0.39 | -0.11 | -0.35 | -0.63 |

In the 'Gene' column, ms = maker-scaffold; eeg = exonerate_est2genome-gene.

[1]Gene symbols of the genes with homologue with *Arabidopsis thaliana* was shown. '$Log_2^{FC}$ IP: HT-LT' and '$Log_2^{FC}$ Ov: HT-LT' denote the $log_2$ fold change (FC) of the gene expression in the HT relative to LT genotype in the inflorescence primordia and ovary, respectively. '$Log_2^{FC}$ HT: Ov-IP' and '$Log_2^{FC}$ LT: Ov-IP' denote the $log_2^{FC}$ of the gene expression in the Ov relative to IP in the HT and LT genotypes, respectively. Up-regulated genes are marked bold red while down-regulated genes are marked bold green. The values are underlined when there is a significant difference between the Ov and IP in both the HT and LT genotypes, and when the FC is higher in the HT than the LT genotypes. IP = inflorescence primordia, Ov = ovary.

## 6.5 Discussion

Isolating RNA of high quality and quantity is very important in molecular biology studies. Inflorescence primordia are mainly composed of small cells filled with dense contents (Kidston et al. 1920) and are assumed to have a comparatively simple chemical composition (Tupper-Carey et al. 1923; Whaley et al. 1960), which makes it easier to isolate total RNA from them. Forester et al. (unpublished) have successfully isolated high-quality RNA from the inflorescence primordia of perennial ryegrass using the RNA extraction method adopted in this study. Compared with the inflorescence primordia, the chemical structure of ovary is more complex and as seeds develop towards maturity, more starch is steadily deposited inside them. Seeds with high starch have proved to be hard to isolate RNA from (Li et al. 2005; Birtić et al. 2006). Wang et al. (2012) developed an appropriate method for isolating total RNA from cereal seeds. However, the weight of the seed material used by Wang et al. (2012) was 0.2 g which was too high for research with limited seed materials. In this study, 27 unfertilised ovaries weighed only about 2.7 mg while 27 fertilised ovaries weighed about 50 mg. Therefore, to isolate RNA from the ovary, this study modified the method of Wang et al. (2012) by applying part of the methodology from Wang et al. (2017) followed by purification with a commercial kit, which proved to be a suitable method for the lower tissue volumes in this study and can be used in other future studies. In the modified method, alkaline Tris buffer (pH 9.0) and SDS can effectively prevent the problem of solidification of sample homogenate during TRIzol extraction. SDS can promote cell lysis and quickly dissolve samples with a high amount of starch. Acid phenol was used to remove most of the polysaccharides, proteins and DNA.

The genotype of the plant host is a key factor influencing the transmission efficiency in many beneficial microorganisms. For example, in white clover (*Trifolium repens*) infected by mycorrhizal fungi, parental genotype significantly affected mycorrhizal infection rates (Eason et al. 2001). Similarly, tomato genotype was a key factor influencing the level of colonisation by mycorrhizal fungi of *Funneliformis mosseae* (Njeru et al. 2017). The genotypes of the host trees of Douglas-fir (*Pseudotsuga menziesii*) varied significantly in the infection frequency of a symptomless endophytic fungus, *Meria parkeri* (Todd 1988). This study used host genotypes of contrasting transmission efficiency based on screening by Gagic et al. (unpublished), whose study examined about 500 genotypes and assessed their endophyte transmission efficiency. The genotypes of the three HT and three LT genotypes used for RNA-Seq in this experiment have been assessed on the endophyte transmission efficiency of their seed progeny over two years of field trials and proved to have contrasting transmission efficiency.

Gene ontology enrichment analysis showed that the GO terms including response to chitin, respiratory burst during defence response and intracellular signal transduction were significantly overrepresented in endophyte-free leaf blades, compared with the endophyte-infected counterparts. By comparison, this study identified only 102 genes indicated as commonly or exclusively differentially expressed between HT and LT genotypes in the inflorescence primordia and/or ovary tissues, with the number of DEGs thus being much smaller than the transcriptome differences between endophyte-free and endophyte-infected hosts (Dupont et al. 2015; Dinkins et al. 2017). Further analysis to enhance understanding of the mechanisms of endophyte transmission is desirable. Manipulation by genetic engineering, especially for the genes with high fold changes

between HT and LT genotypes, could be beneficial. Most of the genes identified are related to signalling, RNA transcription and defence resistance, which have been reported to play roles in the symbiosis of some beneficial plant-microorganism associations. Receptor-like kinase has been reported to be involved in the plant and mycorrhizal fungi symbiosis (Calabrese et al. 2017). Transcription factors of KNAT3/4/5-like class 2 KNOX are involved in *Medicago truncatula* symbiotic nodule organ development (Di Giacomo et al. 2017).

The GO terms enriched by the DEGs between the HT and LT genotypes ($p < 0.001$) were mostly related to biotic or abiotic stress. GO terms for '*serine family amino acid metabolic process*' and '*cytoplasmic membrane-bounded vesicle*' were both enriched in both the inflorescence primordia and ovary tissues. The '*serine family amino acid metabolic process*' is often related to stress, such as cold stress (Shen et al. 2014), drought stress (Gupta et al. 2012; Bhardwaj et al. 2015), and salt stress (Skorupa et al. 2016; Wu et al. 2016). Vesicles are membrane-bound organelles that function to transport material (e.g., proteins) throughout the cell. The '*Cytoplasmic membrane-bounded vesicle*' was also enriched in barley roots when colonised by *Pochonia chlamydosporia* (Larriba et al. 2015), in mandarins seriously infected by '*Candidatus* Liberibacter asiaticus' (Xu et al. 2015), and in roots of *Taxodium* 'Zhongshanshan 405' in response to salinity stress (Yu et al. 2016).

Trehalose-6-phosphate synthase catalyses glucose-6-phosphate and UDP-glucose into trehalose-6-phosphate, whose related gene (TPS) did not change in the HT genotypes, and only one gene was significantly repressed in the LT genotype (Table 6.6). One possible explanation for this observation might be that the substrate for synthesising

trehalose was under less demand in the LT genotypes during development from the inflorescence primordia to ovary. However, this will require further investigation to confirm. Meanwhile, more genes coding for trehalose-6-phosphate phosphatase which catalyses trehalose-6-phosphate into trehalose were induced in the HT than the LT genotypes (Figure 6.9, Table 6.6). This implies that trehalose was required during development from the inflorescence primordia to the ovary for endophyte-infected hosts, as well as the higher demand for trehalose was in the HT genotypes during transmission from the inflorescence primordia to the ovary.

This research showed the DEGs related to salicylic acid metabolism were mostly down-regulated in the ovary relative to the inflorescence primordia in both HT and LT genotypes. Moreover, the observation that the fold changes of the DEGs were mostly lower in the HT than LT genotypes, suggests there was more down-regulation on the salicylic acid pathway in the inflorescence primordia relative to the ovary in the HT than in the LT genotypes (Table 6.7). Research from Bastías et al. (2018) showed that salicylic acid suppresses the endophyte, so reducing the production of fungal alkaloids. Therefore, this research indicated that HT genotypes, as well as having better transmission rates, should provide more benefits against herbivores than the LT genotypes.

The activation of the jasmonic acid pathway was assumed to be related to a plant mechanism that links to symbiosis with microorganisms, such as mycorrhizal fungi and rhizobial bacteria (Hause et al. 2002; Sun et al. 2006; Jung et al. 2012; Pozo et al. 2015). As reviewed by Bastías et al. (2017), endophytes prime jasmonic acid metabolism, which is effective against a broad spectrum of chewing insects. Transcriptome analysis by this

study also showed that the DEGs related to jasmonic acid metabolism were all up-regulated in the ovary compared with inflorescence primordia in both the HT and LT genotypes, and also the fold changes in most of DEGs were much higher in the HT than LT genotypes, indicating likely higher effectiveness against insects in the HT genotypes (Table 6.8). One of the 102 genes coding for 3-hydroxyacyl-CoA dehydrogenase which functions in jasmonic acid biosynthesis as well as catabolism in *A. thaliana* was induced in HT compared with LT genotypes, in both the inflorescence primordia and ovary (Koo 2017). The increased level of jasmonic acid seems to be involved in regulation of the development and functioning of the symbiont in mycorrhizal plants (Hause et al. 2002; Pozo et al. 2015). Considering the results showing higher induction of jasmonic acid metabolism in the HT genotypes from this study, how jasmonic acid relates to endophyte transmission is worth investigating further.

# Chapter 7 General discussion

## 7.1 Introduction

*Epichloë* endophytes are fungi that form symbiotic associations with certain species of grass within the family Poaceae. Many of these plant-endophyte associations have superior abiotic and biotic stress tolerance compared with endophyte-free plants. In the seed industry, the main problems with the commercialisation of endophyte-infected seeds are closely related to the viable endophyte percentage, which is directly related to endophyte transmission throughout the plant life cycle and seed storage. As noted in Section 2.4.2, endophyte viability problems can be divided into two categories, pre-zygotic and post-zygotic transmission failure. Pre-zygotic failure is where the fungus fails to successfully infect tillers, spikes, spikelets, ovules, embryos and seedlings. Post-zygotic failure is when the fungus dies within the seed (described by Gundel et al. 2008).

The research questions in this thesis were all based on the problems related to the failure of endophyte transmission: (1) how endophytes transmit from the unfertilised ovary to mature seeds; (2) the mechanisms for the failure of post-zygotic transmission from a storage carbohydrate perspective; (3) the relationship between endophyte hyphal density in host tissues and endophyte transmission; and (4) use of RNA-Seq to explore the molecular mechanisms underlying failure in pre-zygotic transmission.

## 7.2 Endophyte colonisation of ovule

The infection frequency of endophyte within seed can be assessed using multiple methods, utilising microscopy, immunological and PCR techniques (Latch et al. 1985; Gwinn et al. 1991; Doss et al. 1995). Comparison of the results from these tests on the

same seed batches has uncovered some interesting findings, for example the total endophyte infection frequencies in recently harvested seeds are sometimes higher than the viable endophyte infection frequencies when assessed by seed squash and tissue-print immunoblotting (TPIB), respectively (Card et al. 2014b). This could reflect a loss of endophyte viability in the short time between seed development and harvest and is seen in stored seed accessions or those seed accessions harvested from plants exposed to certain fungicide regimes (Card et al. 2011), but another possible explanation relates to the location of the endophyte hyphae within the seed tissues. It was demonstrated in Chapter 3 that the endophyte strain AR601 infects the embryo sac, the nucellus cells and ovary wall cells before fertilisation takes place. Therefore, the early and mature embryo cells are all colonised by endophyte hyphae, which will then transmit to the seedlings in appropriate conditions. AR601, an endophyte strain with high efficiency of transmission to the seeds (Pennell et al. 2010), was shown to have colonised the embryo sac before fertilisation takes place. However, confirmation is needed that this pattern of endophyte colonisation also applies to other endophyte strains. It is possible that in some cases, endophyte hyphae largely accumulate between nucellus cells and ovary wall cells (in later seed development compressed between the seed coat and the aleurone layer), with only very few hyphae in the embryo axis. In this case, use of a microscopy-based assessment technique, such as a seed squash (Latch et al. 1985), would still indicate that the seed contains endophyte mycelium but the endophyte would not be transmitted to the seedling as the hyphae would not be located in the embryo at a high enough density. Similarly, where endophyte hyphal biomass in the embryo axis is low, transmission of hyphae to the seedlings might not be ensured. This insight provides a potential explanation of why values from TPIB assessment of

endophyte transmission between plant generations can be lower than those from seed squash assessment, and also an explanation for enhanced transmission of endophyte strains with generally higher hyphal biomass within the host.

### 7.3 Post-zygotic transmission failure

Prolonged seed storage has long been recognised to reduce endophyte viability, and in that sense, seed storage is considered to be an adverse process for the endophyte. As noted above, for endophyte hyphae to achieve transmission between host generations, they must be located between cells of the embryos. In addition to storage duration, the viability of the fungus within the stored seed is greatly dependent on storage conditions (particularly temperature and humidity) (Hume et al. 2013). However, other factors may also affect the survival duration of the fungus during seed storage. For instance, tall fescue-endophyte associations are generally known to be less robust than perennial ryegrass-endophyte associations (Neill 1940; Neil 1942; Welty et al. 1987), while endophyte strains within a cultivar may differ in endophyte longevity. This may be related to the amounts, types and ratios of particular carbohydrates stored by the endophyte.

The temporary suspension of metabolic processes in seeds presents an extreme physiological environment and challenge for *Epichloë* endophytes. During this dormant state, it is unlikely that endophyte hyphae have access to the host plant's reserves for their metabolism and therefore the endophyte must rely on its own storage carbohydrates for its survival. This research (Chapter 4) showed that the concentration of trehalose was significantly higher in the endophyte-infected than in the endophyte-free embryos. In addition, the concentration of trehalose in the endophyte-infected

embryos significantly dropped after seed aging, which demonstrated that trehalose is a critical sugar for endophyte survival during seed storage and provides a further indication that the endophyte hyphae may be using internal reserves rather than accessing plant substrates during seed storage. RNA-Seq also showed that the genes for trehalose synthesis were more highly induced in the high-transmission (HT) than the low-transmission (LT) genotypes during the development of the ovary within the inflorescence primordium stage (Chapter 6), corroborating the indications that trehalose has a significant role in endophyte survival during seed storage.

In mycobacteria, glycogen can be degraded to trehalose with the catalysis of TreY/TreZ. Christensen (unpublished) showed that large deposits of amorphous storage polysaccharide product, probably glycogen had accumulated in the endophyte mycelium located between the seed embryo cells but not in the endophyte mycelium located between the seed coat and the aleurone layer. Glycogen is a long chain carbohydrate and used in fungi as their main energy substrate. These observations also support the hypothesis of trehalose involvement in retention of endophyte viability in seed storage, and it is of interest that glycogen accumulation was observed only in the endophyte hyphae located in the embryo cells, and responsible for the endophyte transmission.

In this thesis, an attempt was made to investigate differences in endophyte glycogen storage between endophyte-infected and endophyte-free seeds and also to determine how fungal glycogen levels change during seed aging. Glycogen in seeds was extracted with tricine buffer and analysed with a size-exclusive column (SEC) and HPLC (Powell et al. 2014). This experiment failed because phytoglycogen was present in significant

quantities and phytoglycogen and fungal glycogen were found to be so similar in structure that their HPLC elution peaks could not be separated sufficiently for differential quantification using the techniques employed. It is possible that refinement of the extraction methods might lead to the successful differentiation between plant and fungal glycogen.

### 7.4 Relationships between endophyte biomass and endophyte transmission

Pre-zygotic transmission represents the transmission loss from the fungus failing to successfully infect tillers, spikes, spikelets, ovules, embryos and seedlings (Gundel et al. 2008). Pre-zygotic transmission has been reported to be related to host/endophyte genetics and the environmental factors which impact the endophyte transmission during its lifecycle (Gundel et al. 2011a). In grasses, parent tillers keep generating daughter tillers which are initiated from the buds found in each leaf axil. If any particular bud was uninfected, the future daughter tiller developed from it will be an endophyte-free tiller (Gundel et al. 2008). Since axillary buds are initiated within the shoot apex tissues, endophyte biomass in the shoot apex is assumed to be related to endophyte transmission in the daughter tillers through tillering (Christensen et al. 2009). This study showed that the hyphal biomass in the shoot apex was not the only determinant in endophyte transmission. As shown in Chapter 5, not all the HT genotypes had higher hyphal biomass than the LT genotypes in the shoot apex tissues. Christensen et al. (2008) demonstrated that endophyte hyphal extension within leaf blades involves intercalary growth rather than tip extension as is normal for fungal growth in culture. Tan et al. (2001) showed that the number of hyphal strands significantly decreased from the leaf basal to the leaf tip, but there was no significant difference in hyphal counts in each leaf

section with developmental age. The explanation is that a developing leaf primordium has a basal meristem where cell division occurs, with subsequent cell elongation providing the mechanism for leaf extension. Hyphae continue to enter the leaf basal meristems from the tiller apical meristem with the basal meristems of the leaf primordia undergo cell division. Those hyphae that have already entered the basal meristem of a leaf primordium early in its development will be carried by the coordinated host leaf primordium cell expansion and intercalary hyphal growth so that they eventually reach the leaf tip; whereas those hyphae entering later will only colonise the base of the leaf, not yet developed at the time of hyphal entry to the leaf basal meristem. Since it was shown in Chapter 5 that the endophyte biomass in the shoot apex tissues differed between host genotypes (Figure 5.2), it would be logical to assume that the endophyte biomass in the leaf tissues produced from those shoot apex tissues also differed between host genotypes. If true this would increase herbivore dietary exposure to endophyte mycelium on HT genotypes, a point for possible future research.

Another point for consideration is that Rasmussen (2007) showed that adding nitrogen fertiliser decreased the endophyte biomass in perennial ryegrass host leaf tissues, which implies that nitrogen promoted the growth of the host more than the endophyte. In reproductive tillers, the meristem is elevated by internode elongation during the time between the transformation of the tiller apical meristem from vegetative to reproductive growth, and anthesis and pollination in the developed seed-head. If different genotypes of a host species differed in their inflorescence elongation rate and the amounts of hyphae that were carried to the inflorescences, it would be reasonable to expect that this might affect the endophyte biomass in the mature seeds. A question

for clarification by estimating the endophyte biomass in the florets over time in Chapter 5, was whether or not endophytes colonise the developing floral tissues more rapidly in the HT than the LT genotypes. The data did indeed confirm that a faster colonisation in the seeds is one of the reasons for the higher endophyte biomass in the seeds.

## 7.5 Mechanisms for pre-zygotic transmission

After vernalisation, some of the vegetative meristems become transformed into floral meristems. Inflorescence primordia develop from the floral meristems and as noted above, will move upwards along with the elongation of inflorescence internodes in the reproductive tiller (Mjolsness et al. 1999). The endophyte hyphae between the cells in the floral meristems are thus carried upwards with the developing inflorescence primordia, and have the potential to eventually infect mature seeds. The ovary is the main component inside the floret which will develop into a mature seed after successful fertilisation. Inflorescence primordia (Stage 6-7 in Zadok's scale, Figure 6.1) and unfertilised ovaries (Figure 6.2) were the two tissue types used for RNA-Seq studies. By comparing the number of reads mapped to the endophyte genome in the HT and LT genotypes from the RNA-Seq study, it was evident that the hyphal biomass in the floral apex was not the only determinant in endophyte transmission. For both inflorescence primordia and ovary tissues, two of the three HT genotypes had more reads mapped to the endophyte genome than the LT genotypes (Table 6.2), suggesting a possible role of endophyte gene activation in the transmission of those two genotypes.

As discussed by Gundel et al. (2011), one important piece of information for which data are unavailable in many studies is the variation in the rate of vertical transmission among host populations (or genotypes). Unpublished research by Gagic et al. (AgResearch)

showed that different genotypes of perennial ryegrass varied in their transmission efficiencies. RNA-Seq performed on the inflorescence primordia and ovary in Chapter 6 has identified a set of key genes with significant differences in expression between HT and LT genotypes. These are therefore candidate genes for deciphering the mechanisms for the failure of endophyte transmission from the host side. Most of the key genes are functioning in plant signalling and encode for receptor protein kinase, which has been reported to relate to the evolution of the plant symbiosis with microorganisms (Gómez-Gómez et al. 2000; Markmann et al. 2008).

The RNA-Seq work in Chapter 6 also found that more genes related to salicylic acid metabolism were significantly repressed while more genes related to jasmonic acid metabolism were significantly induced during development from the inflorescence primordia to the ovary in the HT compared to the LT genotypes (Tables 6.7 and 6.8). However, in terms of the gene expressions of salicylic acid and jasmonic acid metabolism in inflorescence primordia and ovary separately, there was no significant difference between the HT and LT genotypes (Tables 6.7 and 6.8). This result indicates that for the HT genotypes, salicylic acid metabolism is more repressed and jasmonic acid metabolism is more upregulated during seed maturation. It is highly possible that these metabolic changes have a role in the endophyte transmission from the inflorescence primordia to the ovaries. Bastías et al. (2017) showed that plants with symbiotic endophytes had lower concentrations of salicylic acid than the non-symbiotic counterparts, suggesting that endophyte repressed salicylic acid metabolism. Also, the same authors found that externally applying salicylic acid to the host plants reduced concentrations in the plants of alkaloids which are toxic to insects. In legume-*Rhizobium* associations, increased

exogenous salicylic acid has been observed to reduce the number of nodules in soybean and alfalfa (*Medicago sativa*) (Lian et al. 2000). In plant and mycorrhizal fungus associations, tomato roots infected with arbuscular mycorrhizal fungi of lower colonisation ability had higher concentrations of salicylic acid than the fungi with higher colonisation abilities (López-Ráez et al. 2010). A negative correlation was also observed between the levels of salicylic acid and the colonisation of arbuscular mycorrhizal fungi in pea and tobacco (*Nicotiana tabacum*) (Blilou et al. 1999; Medina et al. 2003). An increased jasmonic acid level has been reported to be related to the functionality of symbioses in many cases (Sun et al. 2006; Pozo et al. 2015). With the greater up-regulation of the genes related to jasmonic acid metabolism during development from the inflorescence primordia to the ovary in the HT genotypes, an investigation of the correlation between jasmonic acid metabolism and endophyte vertical transmission in the progenies would be interesting. It can be proposed from this study that host genotypes differing in the amounts of endogenous salicylic acid and jasmonic acid, might be negatively and positively correlated, respectively, with endophyte biomass and endophyte transmission. Since different genotypes have been shown to have different endogenous salicylic acid and jasmonic acid levels (Blilou et al. 1999), selecting genotypes with lower salicylic acid and higher jasmonic acid content might mean higher endophyte infection capabilities.

## 7.6 Summary of outcomes and further research

### 7.6.1 Summary of outcomes

This thesis investigated how *Epichloë* endophytes infect the seeds from the unfertilised ovary, which is one step of endophyte life cycle, and revealed that hyphae of *Epichloë*

*coenophiala* strain AR601 have colonised the embryo sac before host grass fertilisation. With respect to the transmission process, this study proved that endophyte biomass in host tissues is one of the factors that governs the success of transmission to the next generation. By using RNA-Seq, this study showed that the salicylic acid and jasmonic acid metabolism might underlie the mechanisms of endophyte transmission from the inflorescence primordia to the unfertilised ovary. Furthermore, during seed storage, reduction in internal trehalose levels is highly correlated with endophyte death.

### 7.6.2 Further research

In Chapter 3, this experiment only investigated the timing of embryo infection by *Epichloë* strain AR601 and it showed that endophytes have infected the embryo sac before fertilisation. To test whether this result is applicable to other endophyte strains, more plant-endophyte combinations can be tested using the method developed in this thesis.

To investigate the functions of glycogen inside endophyte hyphae within stored seeds, further research could be done to observe glycogen within the endophyte mycelium using a transmission electron microscope (TEM). Comparisons between freshly harvested seeds and seeds after long-term storage would be useful.

To more comprehensively investigate the pathways related to seed aging or seed imbibition, it would be of interest to measure, using GC-FID, the sugar intermediates in the various metabolic pathways. Likewise, GC coupled with mass spectrometry would be an even more ideal method to map the metabolites in seeds.

The key genes which were differentially expressed between the HT and LT genotypes in the inflorescence primordia and/or ovaries need to be further researched. Specifically, the expression of the key genes will be best explored comparing hosts of contrasting endophyte transmission capability.

Due to its out-crossing pollination pattern, perennial ryegrass shows genetic variation between genotypes. Therefore, setting up endophyte-free controls for each genotype and analysis of their transcriptomes is a useful step to elimination of the possibility that the DEGs identified arise from genetic differences in the host genotypes that are in fact not related to endophyte transmission. Another approach would be for the DEGs identified in this study to be verified by assessing their expression in other genotypes with similar variations in endophyte transmission efficiencies.

The expression of the endophyte genes within different host genotypes will be analysed in the next stage of this research. This study has identified differences in the expression of some particular genes between the HT and LT genotypes. By comparing the gene expression of the HT and LT endophyte genotypes within the hosts, some genes will probably be identified which were differentially expressed in response to the gene expression changes in the hosts that were identified in this study.

## Appendices

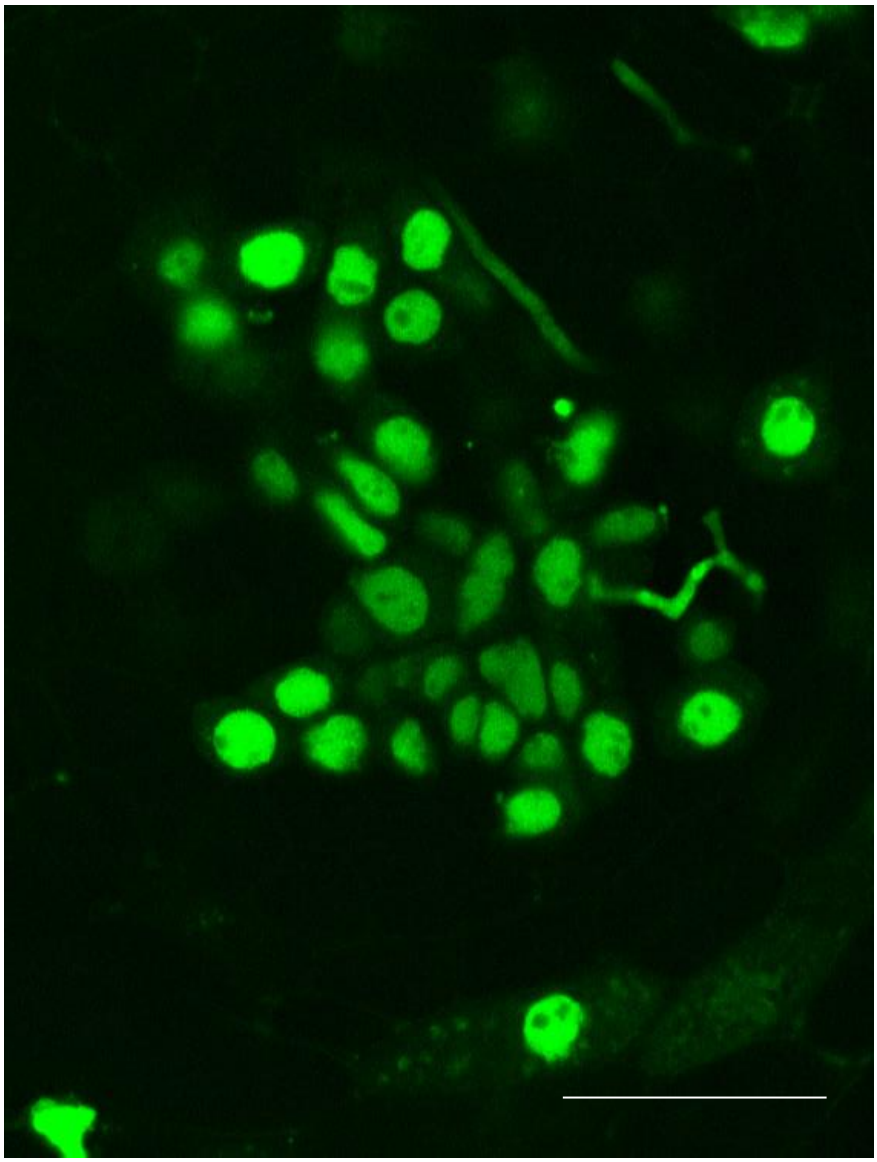

**Figure A2.1 Confocal image of a cross section of a mature seed embryo showing viable filamentous epichloid hyphae in embryo axis of seed which was stained with CMFDA (reproduced from Figure 2.1A).** Scale bar = 50 µm.

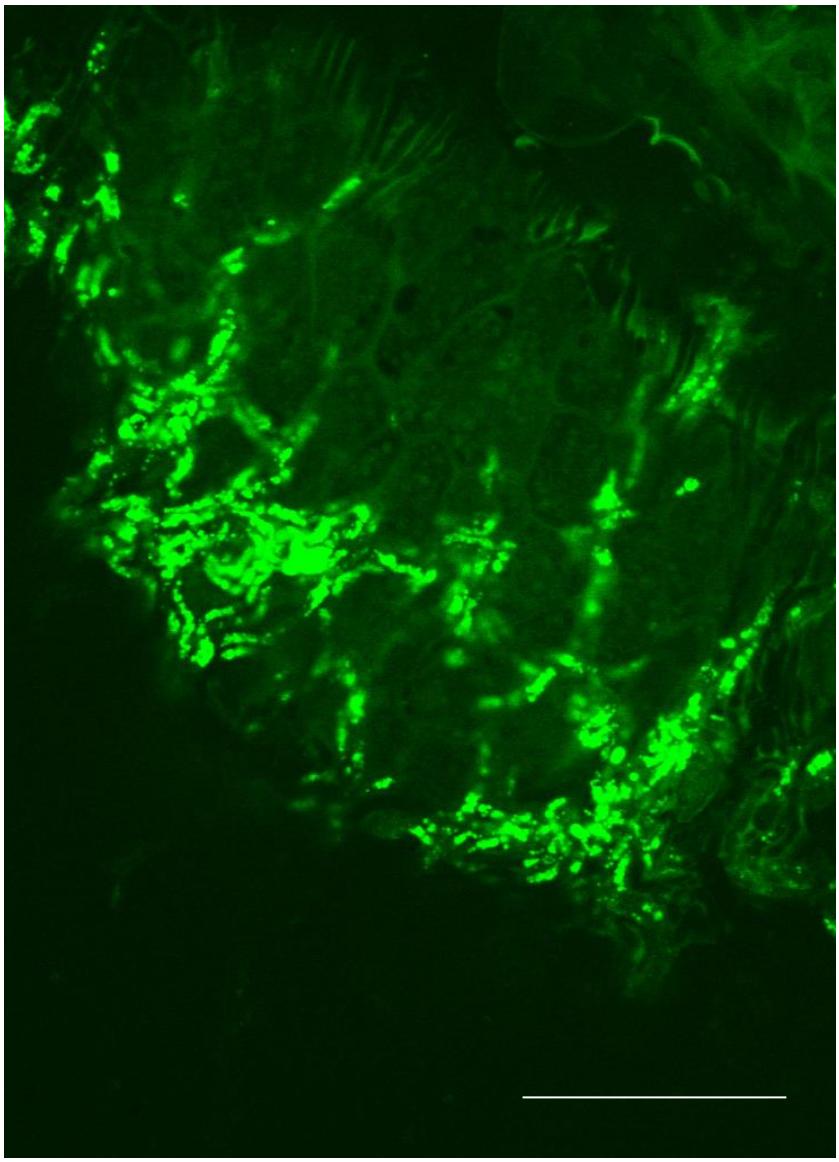

**Figure A2.2 Confocal image of the back side of a dissected seed embryo showing viable epichloid hyphae in the 'infection layer' (between embryo and endosperm), stained with CMFDA (reproduced from Figure 2.1B).** Scale bar = 50 µm.

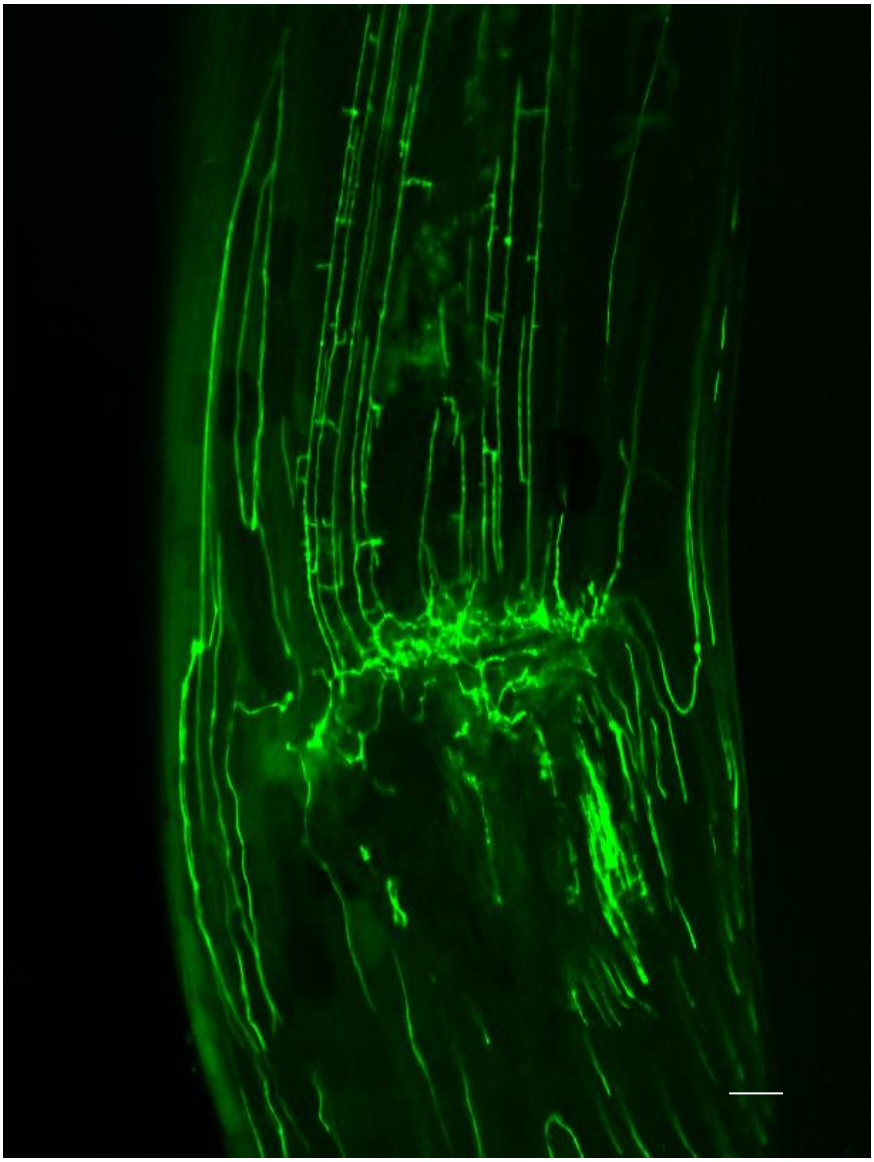

**Figure A2.3 Confocal image of a longitudinal section of a seedling showing GFP-labelled epichloid hyphae** (reproduced from Figure 2.1C). Scale bar = 50 µm.

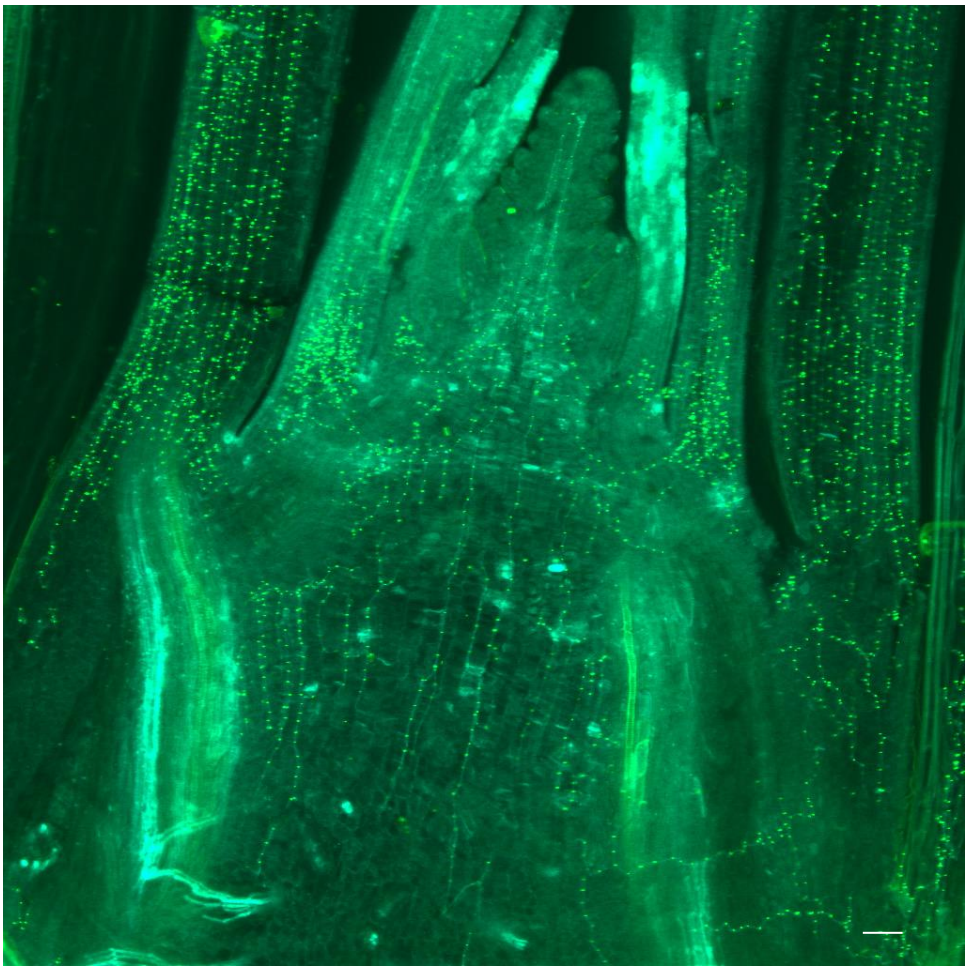

**Figure A2.4 Confocal image of a longitudinal section of the meristematic zone of the apex of a vegetative tiller with the epichloid hyphae stained with aniline blue and Alexa Fluor 488.** The dots on the filamentous hyphae show the hyphal septa stained with Alexa Fluor 488 (reproduced from Figure 2.1D). Scale bar = 50 µm.

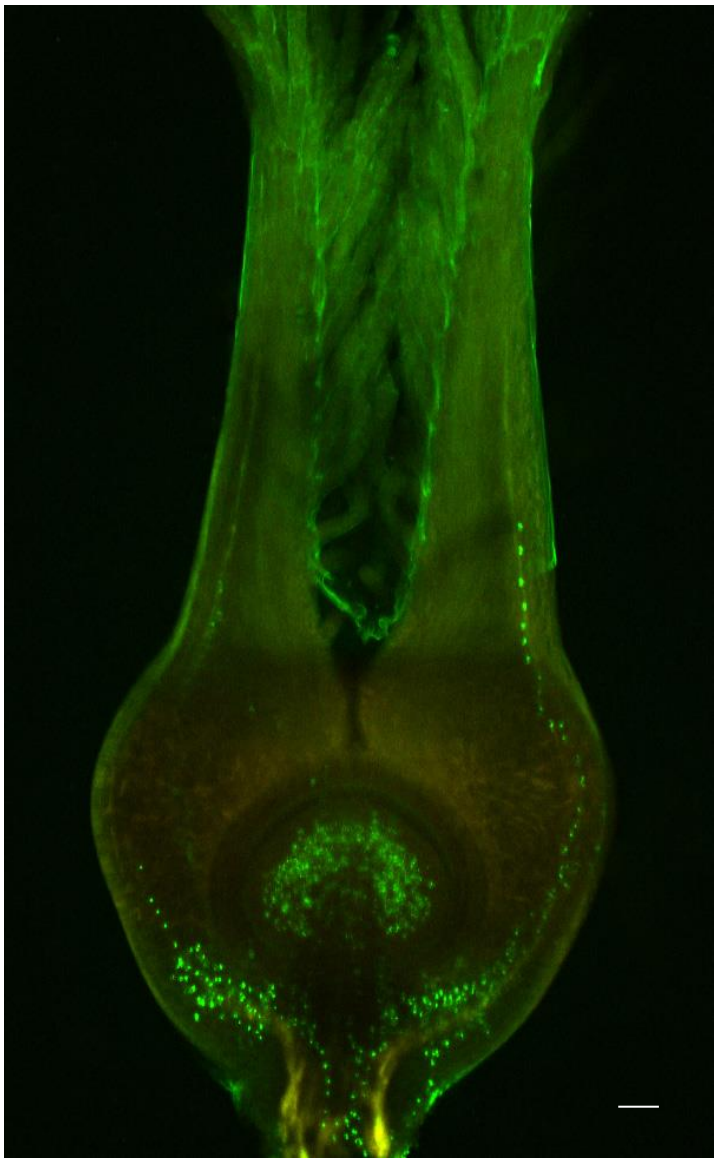

**Figure A2.5 Confocal image of a longitudinal section of an endophyte-infected unfertilised ovary with the epichloid hyphae stained with aniline blue and Alexa Flour 488.** The dots are the hyphal septa stained with Alexa Flour 488 (reproduced from Figure 2.1E). Scale bar = 50 µm.

**Table A4.1 Chemical formula and structures of the analysed sugars.**

| | | |
|---|---|---|
| D-arabitol $C_5H_{12}O_5$ 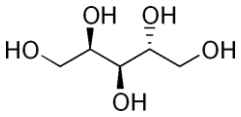 | Myo-inositol $C_6H_{12}O_6$ 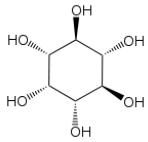 | Sorbitol $C_6H_{14}O_6$ 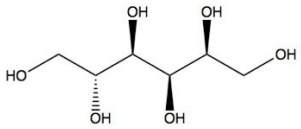 |
| DL-arabinose $C_5H_{10}O_5$ 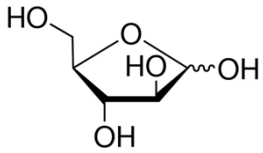 | Lactose $C_{12}H_{22}O_{11}$ 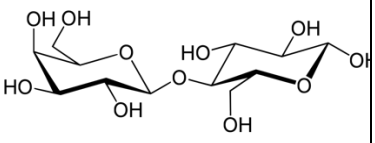 | Sucrose $C_{12}H_{22}O_{11}$ 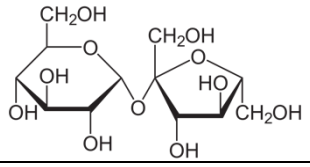 |
| Fructose $C_6H_{12}O_6$ 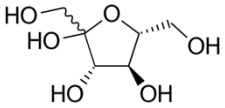 | Maltose $C_{12}H_{22}O_{11}$ 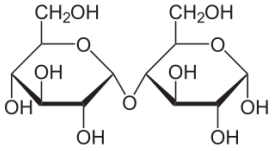 | Trehalose $C_{12}H_{22}O_{11}$ 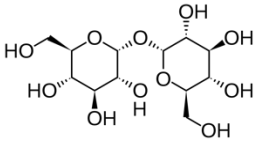 |
| Galactinol $C_{12}H_{22}O_{11}$ 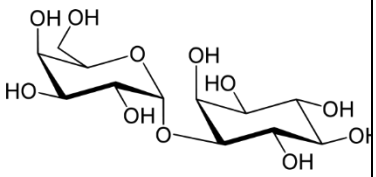 | Mannitol $C_6H_{14}O_6$ 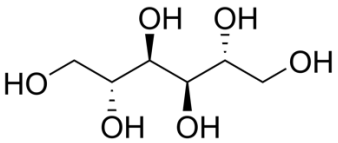 | Xylitol $C_5H_{12}O_5$ 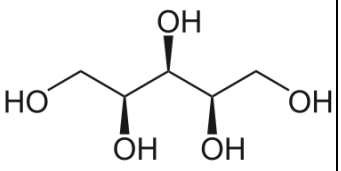 |
| D-galactose $C_6H_{12}O_6$ 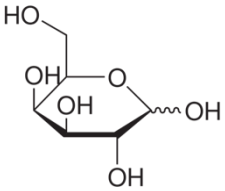 | Mannose $C_6H_{12}O_6$ 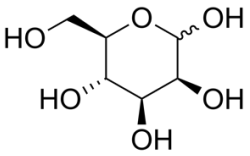 | Xylose $C_5H_{10}O_5$ 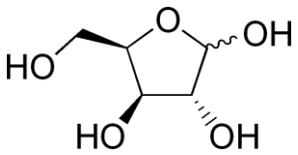 |
| Glucose $C_6H_{12}O_6$ 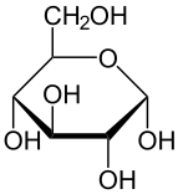 | Raffinose $C_{18}H_{32}O_{16}$ 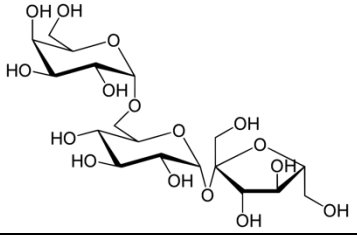 | |
| Glycerol $C_3H_8O_3$ 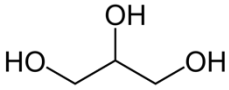 | Ribitol $C_5H_{12}O_5$ 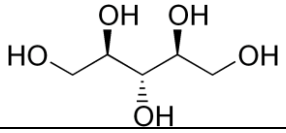 | |

**Table A4.2 Retention time of the standard compounds in GC-FID.** Different retention times of the same compound denotes different isomers of the same compound.

| Retention time (min) | | | |
|---|---|---|---|
| D-arabitol | 27.806 | 28.386 | 29.021 |
| DL-arabinose | 26.534 | | |
| Fructose | 31.008 | 31.210 | |
| Galactinol | 49.222 | | |
| D-galactose | 39.192 | | |
| Glucose | 31.513 | 31.877 | |
| Glycerol | 16.606 | | |
| Inositol | 35.244 | | |
| Lactose | 45.068 | 45.312 | |
| Maltose | 45.795 | 46.177 | |
| Mannitol | 32.158 | 33.135 | |
| Mannose | 31.300 | 31.574 | |
| Raffinose | 54.209 | | |
| Ribitol | 27.911 | | |
| Sorbitol | 32.291 | | |
| Sucrose | 44.332 | | |
| Trehalose | 45.874 | | |
| Xylitol | 27.494 | 28.452 | |
| Xylose | 26.141 | 26.368 | |

**Table A4.3 Mean (±SE) concentration of sugars (µmol/g of each sample in dw) from the embryo tissues of four grass accessions (endophyte-free, AR584, AR605, CT) under AA (0d, 4d) and state treatment (dry, imbibed)[1].**

| State | AA | Endo | Ara | DL-ara | Fru | Galacti | Gal | Glu | Gly | Ino | Lac | Mal | Manni | Man | Raf | Rib | Sor | Suc | Tre | Xyli | Xyl |
|---|---|---|---|---|---|---|---|---|---|---|---|---|---|---|---|---|---|---|---|---|---|
| Dry | 0d | E- | 0.689 | 0.088 | 2.706 | 15.387 | 0.138 | 1.156 | 2.999 | 33.850 | 0.044 | 0.064 | 0.611 | 0.065 | 0.326 | 0.000 | 0.058 | 299.257 | 0.249 | 0.030 | 0.000 |
| | | | 0.158 | 0.010 | 0.497 | 0.556 | 0.021 | 0.195 | 0.244 | 0.384 | 0.010 | 0.031 | 0.096 | 0.016 | 0.006 | 0.000 | 0.002 | 10.724 | 0.042 | 0.006 | 0.000 |
| | | AR584 | 1.038 | 0.074 | 2.354 | 13.335 | 0.149 | 1.088 | 2.978 | 37.678 | 0.060 | 0.077 | 3.119 | 0.103 | 0.315 | 0.311 | 0.047 | 265.820 | 2.135 | 0.036 | 0.008 |
| | | | 0.030 | 0.006 | 0.219 | 0.961 | 0.016 | 0.116 | 0.373 | 2.307 | 0.006 | 0.020 | 0.260 | 0.056 | 0.035 | 0.099 | 0.002 | 13.109 | 0.138 | 0.006 | 0.004 |
| | | AR605 | 1.604 | 0.074 | 1.784 | 11.664 | 0.120 | 0.947 | 2.635 | 34.615 | 0.049 | 0.095 | 3.726 | 0.041 | 0.319 | 0.632 | 0.046 | 281.564 | 2.033 | 0.056 | 0.000 |
| | | | 0.185 | 0.008 | 0.204 | 1.148 | 0.046 | 0.168 | 0.378 | 0.797 | 0.013 | 0.027 | 0.489 | 0.018 | 0.043 | 0.070 | 0.004 | 20.734 | 0.107 | 0.007 | 0.000 |
| | | CT | 1.546 | 0.081 | 2.494 | 14.348 | 0.123 | 1.093 | 2.919 | 31.968 | 0.046 | 0.073 | 2.453 | 0.024 | 0.338 | 0.899 | 0.063 | 286.225 | 2.569 | 0.045 | 0.000 |
| | | | 0.086 | 0.004 | 0.042 | 0.576 | 0.008 | 0.061 | 0.149 | 0.858 | 0.007 | 0.002 | 0.096 | 0.004 | 0.015 | 0.011 | 0.022 | 9.588 | 0.127 | 0.001 | 0.000 |
| | 4d | E- | 1.469 | 0.182 | 3.161 | 10.146 | 0.331 | 1.690 | 3.870 | 32.188 | 0.087 | 0.109 | 0.314 | 0.351 | 0.689 | 0.087 | 0.090 | 198.390 | 0.037 | 0.127 | 0.051 |
| | | | 0.175 | 0.011 | 0.170 | 0.544 | 0.050 | 0.085 | 0.015 | 0.575 | 0.046 | 0.020 | 0.038 | 0.121 | 0.050 | 0.001 | 0.015 | 3.170 | 0.005 | 0.007 | 0.004 |
| | | AR584 | 1.679 | 0.215 | 2.408 | 11.472 | 0.431 | 1.638 | 3.745 | 38.502 | 0.056 | 0.099 | 2.424 | 0.201 | 0.578 | 0.150 | 0.077 | 189.588 | 0.660 | 0.105 | 0.051 |
| | | | 0.226 | 0.015 | 0.270 | 0.254 | 0.079 | 0.062 | 0.306 | 1.911 | 0.007 | 0.002 | 0.200 | 0.082 | 0.069 | 0.070 | 0.016 | 8.371 | 0.156 | 0.032 | 0.006 |
| | | AR605 | 1.330 | 0.150 | 1.931 | 7.680 | 0.279 | 1.049 | 4.214 | 33.634 | 0.056 | 0.059 | 2.583 | 0.139 | 0.664 | 0.608 | 0.139 | 200.415 | 0.258 | 0.103 | 0.033 |
| | | | 0.064 | 0.011 | 0.170 | 0.143 | 0.052 | 0.066 | 0.103 | 0.962 | 0.003 | 0.005 | 0.122 | 0.101 | 0.026 | 0.070 | 0.012 | 8.306 | 0.009 | 0.005 | 0.008 |
| | | CT | 1.766 | 0.207 | 2.203 | 10.709 | 0.315 | 1.351 | 4.443 | 33.694 | 0.061 | 0.102 | 2.642 | 0.108 | 0.744 | 1.055 | 0.071 | 222.608 | 0.577 | 0.079 | 0.057 |
| | | | 0.137 | 0.019 | 0.229 | 0.636 | 0.056 | 0.114 | 0.197 | 1.571 | 0.003 | 0.034 | 0.121 | 0.043 | 0.062 | 0.089 | 0.011 | 11.126 | 0.040 | 0.016 | 0.007 |
| Imbibed | 0d | E- | 0.672 | 0.072 | 3.742 | 10.844 | 0.354 | 1.624 | 4.237 | 35.391 | 0.186 | 0.291 | 0.550 | 0.098 | 0.572 | 0.000 | 0.055 | 276.379 | 0.151 | 0.038 | 0.014 |
| | | | 0.103 | 0.015 | 0.870 | 0.354 | 0.139 | 0.343 | 0.713 | 2.407 | 0.125 | 0.055 | 0.060 | 0.044 | 0.046 | 0.000 | 0.002 | 14.565 | 0.010 | 0.013 | 0.014 |
| | | AR584 | 1.293 | 0.099 | 2.888 | 13.535 | 0.225 | 1.464 | 3.933 | 46.169 | 0.081 | 0.286 | 3.949 | 0.067 | 0.473 | 0.274 | 0.047 | 308.735 | 1.432 | 0.039 | 0.000 |
| | | | 0.177 | 0.006 | 0.446 | 0.895 | 0.049 | 0.068 | 0.481 | 3.149 | 0.012 | 0.030 | 0.302 | 0.014 | 0.086 | 0.018 | 0.013 | 17.518 | 0.074 | 0.004 | 0.000 |
| | | AR605 | 1.382 | 0.069 | 2.197 | 9.304 | 0.276 | 1.425 | 5.916 | 43.152 | 0.011 | 0.772 | 5.306 | 0.069 | 0.369 | 0.716 | 0.124 | 327.004 | 1.225 | 0.056 | 0.000 |
| | | | 0.248 | 0.008 | 0.389 | 2.026 | 0.088 | 0.275 | 0.842 | 4.226 | 0.016 | 0.150 | 0.900 | 0.046 | 0.123 | 0.057 | 0.084 | 42.843 | 0.112 | 0.014 | 0.000 |
| | | CT | 1.558 | 0.082 | 2.367 | 12.562 | 0.262 | 1.187 | 3.381 | 33.572 | 0.050 | 0.297 | 2.696 | 0.025 | 0.794 | 0.812 | 0.041 | 302.596 | 1.414 | 0.042 | 0.000 |
| | | | 0.094 | 0.013 | 0.340 | 1.112 | 0.098 | 0.051 | 0.451 | 0.867 | 0.027 | 0.051 | 0.127 | 0.014 | 0.125 | 0.035 | 0.004 | 4.952 | 0.090 | 0.007 | 0.000 |
| | 4d | E- | 0.729 | 0.047 | 2.857 | 6.424 | 0.513 | 0.776 | 2.412 | 43.178 | 0.103 | 0.327 | 0.051 | 0.082 | 0.395 | 0.000 | 0.067 | 296.733 | 0.302 | 0.028 | 0.024 |
| | | | 0.136 | 0.005 | 0.383 | 0.151 | 0.078 | 0.171 | 0.278 | 2.206 | 0.013 | 0.062 | 0.009 | 0.017 | 0.099 | 0.000 | 0.013 | 22.828 | 0.149 | 0.006 | 0.012 |
| | | AR584 | 1.328 | 0.056 | 1.797 | 8.510 | 0.582 | 0.523 | 2.105 | 44.307 | 0.089 | 0.158 | 2.793 | 0.010 | 0.730 | 0.305 | 0.056 | 207.241 | 0.358 | 0.020 | 0.043 |
| | | | 0.134 | 0.009 | 0.173 | 0.773 | 0.194 | 0.119 | 0.445 | 2.442 | 0.003 | 0.069 | 0.502 | 0.010 | 0.104 | 0.061 | 0.018 | 8.924 | 0.098 | 0.010 | 0.018 |
| | | AR605 | 1.029 | 0.041 | 2.134 | 4.947 | 0.410 | 0.480 | 1.603 | 40.155 | 0.076 | 0.229 | 4.063 | 0.025 | 0.383 | 0.765 | 0.044 | 281.208 | 0.359 | 0.027 | 0.007 |
| | | | 0.171 | 0.006 | 0.479 | 1.134 | 0.142 | 0.102 | 0.089 | 4.378 | 0.004 | 0.043 | 0.541 | 0.025 | 0.158 | 0.076 | 0.016 | 20.059 | 0.076 | 0.008 | 0.004 |
| | | CT | 1.221 | 0.055 | 1.870 | 7.120 | 0.581 | 0.558 | 2.359 | 43.514 | 0.454 | 0.225 | 2.715 | 0.477 | 0.487 | 1.080 | 0.025 | 279.316 | 0.296 | 0.042 | 0.002 |
| | | | 0.072 | 0.008 | 0.259 | 1.321 | 0.416 | 0.031 | 0.540 | 6.557 | 0.378 | 0.039 | 0.291 | 0.459 | 0.117 | 0.266 | 0.018 | 47.123 | 0.051 | 0.018 | 0.002 |

[1]The upper value in each cell means the average concentration of each sugar and the lower value denotes the standard error (SE). Endo = endophyte, CT = common-toxic, E- = endophyte-free, Ara = D-arabitol, DL-ara = DL-arabinose, Fru = fructose, Galacti = galactinol, Gal = D-galactose, Glu = glucose, Gly = glycerol, Ino = myo-inositol, Mal = maltose, Manni = mannitol, Raf = raffinose, Rib = ribitol, Sor = sorbitol, Suc = sucrose, Tre = trehalose, Xyli = xylitol, Xyl = xylose.

**Table A4.4 Mean (±SE) concentrations of the sugars (µmol/g of each sample in dw) from the endosperm tissues of four grass accessions (endophyte-free, AR584, AR605, CT) under AA (0d, 4d) and seed state treatment (dry, imbibed)[1].**

| State | AA | Endo | Ara | DL-ara | Fru | Galacti | Gal | Glu | Gly | Ino | Lac | Mal | Manni | Man | Raf | Rib | Sor | Suc | Tre | Xyli | Xyl |
|---|---|---|---|---|---|---|---|---|---|---|---|---|---|---|---|---|---|---|---|---|---|
| Dry | 0d | E- | 0.266 | 0.115 | 2.435 | 0.159 | 0.263 | 1.012 | 1.513 | 1.750 | 0.053 | 0.997 | 0.135 | 0.092 | 0.000 | 0.000 | 0.008 | 15.815 | 0.080 | 0.019 | 0.007 |
| | | | 0.150 | 0.013 | 0.874 | 0.046 | 0.034 | 0.333 | 0.041 | 0.236 | 0.033 | 0.220 | 0.079 | 0.026 | 0.000 | 0.000 | 0.001 | 3.108 | 0.010 | 0.006 | 0.004 |
| | | AR 584 | 0.168 | 0.130 | 4.102 | 0.185 | 0.260 | 1.770 | 1.657 | 1.859 | 0.033 | 0.723 | 1.332 | 0.094 | 0.011 | 0.110 | 0.019 | 14.887 | 0.216 | 0.015 | 0.000 |
| | | | 0.022 | 0.009 | 2.568 | 0.007 | 0.087 | 0.963 | 0.104 | 0.200 | 0.005 | 0.222 | 0.067 | 0.012 | 0.011 | 0.069 | 0.019 | 5.627 | 0.036 | 0.006 | 0.000 |
| | | AR 605 | 0.559 | 0.145 | 3.364 | 0.166 | 0.387 | 1.474 | 1.937 | 2.074 | 0.064 | 1.019 | 2.063 | 0.116 | 0.023 | 0.402 | 0.025 | 21.440 | 0.294 | 0.019 | 0.000 |
| | | | 0.081 | 0.018 | 1.248 | 0.033 | 0.077 | 0.489 | 0.439 | 0.113 | 0.016 | 0.069 | 0.191 | 0.014 | 0.012 | 0.022 | 0.006 | 5.322 | 0.042 | 0.001 | 0.000 |
| | | CT | 0.235 | 0.132 | 2.143 | 0.192 | 0.247 | 0.782 | 2.008 | 1.742 | 0.045 | 0.728 | 0.702 | 0.073 | 0.010 | 0.616 | 0.007 | 19.055 | 0.402 | 0.015 | 0.000 |
| | | | 0.074 | 0.013 | 0.947 | 0.016 | 0.049 | 0.315 | 0.442 | 0.217 | 0.005 | 0.145 | 0.069 | 0.016 | 0.010 | 0.007 | 0.007 | 2.418 | 0.075 | 0.008 | 0.000 |
| | 4d | E- | 0.300 | 0.291 | 4.524 | 0.100 | 0.447 | 2.059 | 1.765 | 1.481 | 0.029 | 0.492 | 0.173 | 0.141 | 0.047 | 0.000 | 0.041 | 15.067 | 0.004 | 0.020 | 0.049 |
| | | | 0.085 | 0.015 | 1.258 | 0.010 | 0.038 | 0.505 | 0.186 | 0.056 | 0.002 | 0.045 | 0.077 | 0.034 | 0.006 | 0.000 | 0.001 | 2.794 | 0.002 | 0.004 | 0.005 |
| | | AR 584 | 0.437 | 0.408 | 3.866 | 0.142 | 0.635 | 1.914 | 3.401 | 2.214 | 0.058 | 0.670 | 1.542 | 0.128 | 0.006 | 0.062 | 0.028 | 11.475 | 0.038 | 0.025 | 0.037 |
| | | | 0.065 | 0.073 | 1.608 | 0.017 | 0.090 | 0.541 | 1.126 | 0.590 | 0.010 | 0.080 | 0.287 | 0.016 | 0.006 | 0.034 | 0.010 | 2.200 | 0.017 | 0.003 | 0.017 |
| | | AR 605 | 0.810 | 0.296 | 2.177 | 0.072 | 0.479 | 1.254 | 1.469 | 1.849 | 0.066 | 0.466 | 2.001 | 0.084 | 0.025 | 0.340 | 0.039 | 10.306 | 0.058 | 0.014 | 0.048 |
| | | | 0.151 | 0.029 | 0.677 | 0.008 | 0.022 | 0.108 | 0.166 | 0.427 | 0.034 | 0.120 | 0.072 | 0.022 | 0.009 | 0.011 | 0.017 | 1.402 | 0.046 | 0.003 | 0.002 |
| | | CT | 1.063 | 0.564 | 6.173 | 0.150 | 1.107 | 3.333 | 2.710 | 2.195 | 0.055 | 0.652 | 1.625 | 0.171 | 0.037 | 0.503 | 0.138 | 19.971 | 0.020 | 0.032 | 0.067 |
| | | | 0.232 | 0.075 | 2.741 | 0.019 | 0.315 | 1.265 | 0.947 | 0.092 | 0.018 | 0.156 | 0.560 | 0.011 | 0.002 | 0.065 | 0.086 | 0.597 | 0.010 | 0.002 | 0.008 |
| Imbibed | 0d | E- | 0.071 | 0.131 | 0.792 | 0.042 | 0.381 | 0.750 | 0.716 | 1.292 | 0.090 | 1.335 | 0.152 | 0.145 | 0.000 | 0.000 | 0.002 | 11.069 | 0.039 | 0.004 | 0.003 |
| | | | 0.011 | 0.016 | 0.086 | 0.004 | 0.048 | 0.131 | 0.170 | 0.217 | 0.021 | 0.270 | 0.018 | 0.032 | 0.000 | 0.000 | 0.002 | 1.726 | 0.019 | 0.003 | 0.003 |
| | | AR 584 | 0.077 | 0.105 | 1.264 | 0.053 | 0.393 | 0.781 | 1.341 | 1.323 | 0.110 | 1.495 | 1.306 | 0.141 | 0.000 | 0.168 | 0.010 | 10.661 | 0.044 | 0.000 | 0.000 |
| | | | 0.044 | 0.022 | 0.141 | 0.006 | 0.073 | 0.103 | 0.432 | 0.130 | 0.009 | 0.092 | 0.368 | 0.038 | 0.000 | 0.019 | 0.005 | 0.773 | 0.015 | 0.000 | 0.000 |
| | | AR 605 | 0.108 | 0.122 | 1.244 | 0.061 | 0.470 | 1.087 | 2.317 | 1.335 | 0.103 | 1.597 | 1.500 | 0.221 | 0.000 | 0.358 | 0.003 | 10.883 | 0.082 | 0.000 | 0.000 |
| | | | 0.010 | 0.015 | 0.135 | 0.005 | 0.075 | 0.212 | 0.387 | 0.166 | 0.020 | 0.201 | 0.431 | 0.011 | 0.000 | 0.035 | 0.002 | 1.999 | 0.022 | 0.000 | 0.000 |
| | | CT | 0.111 | 0.088 | 0.808 | 0.047 | 0.299 | 0.550 | 1.390 | 1.393 | 0.067 | 0.914 | 0.706 | 0.060 | 0.000 | 0.439 | 0.003 | 11.923 | 0.048 | 0.000 | 0.000 |
| | | | 0.007 | 0.017 | 0.148 | 0.009 | 0.048 | 0.055 | 0.324 | 0.044 | 0.018 | 0.189 | 0.126 | 0.010 | 0.000 | 0.059 | 0.002 | 2.234 | 0.009 | 0.000 | 0.000 |
| | 4d | E- | 0.058 | 0.096 | 0.556 | 0.023 | 0.297 | 0.642 | 0.640 | 1.177 | 0.054 | 0.762 | 0.018 | 0.078 | 0.000 | 0.000 | 0.000 | 8.492 | 0.057 | 0.001 | 0.003 |
| | | | 0.022 | 0.005 | 0.072 | 0.005 | 0.036 | 0.073 | 0.153 | 0.179 | 0.011 | 0.097 | 0.018 | 0.004 | 0.000 | 0.000 | 0.000 | 0.587 | 0.008 | 0.001 | 0.001 |
| | | AR 584 | 0.165 | 0.137 | 1.142 | 0.018 | 0.492 | 0.785 | 1.424 | 1.336 | 0.076 | 1.025 | 0.901 | 0.091 | 0.000 | 0.140 | 0.023 | 7.155 | 0.033 | 0.003 | 0.029 |
| | | | 0.102 | 0.038 | 0.426 | 0.006 | 0.133 | 0.172 | 0.678 | 0.298 | 0.022 | 0.253 | 0.209 | 0.019 | 0.000 | 0.018 | 0.011 | 0.550 | 0.015 | 0.003 | 0.026 |
| | | AR 605 | 0.639 | 0.107 | 1.222 | 0.030 | 0.465 | 0.918 | 1.525 | 1.325 | 0.158 | 2.038 | 2.317 | 0.146 | 0.000 | 0.447 | 0.023 | 11.352 | 0.063 | 0.006 | 0.007 |
| | | | 0.501 | 0.014 | 0.464 | 0.016 | 0.108 | 0.282 | 0.522 | 0.155 | 0.048 | 0.558 | 1.014 | 0.054 | 0.000 | 0.105 | 0.012 | 3.233 | 0.014 | 0.006 | 0.004 |
| | | CT | 0.137 | 0.104 | 0.798 | 0.037 | 0.403 | 0.672 | 1.268 | 1.261 | 0.094 | 1.181 | 0.827 | 0.063 | 0.000 | 0.620 | 0.015 | 8.007 | 0.041 | 0.000 | 0.000 |
| | | | 0.037 | 0.016 | 0.238 | 0.023 | 0.085 | 0.208 | 0.567 | 0.087 | 0.022 | 0.239 | 0.313 | 0.012 | 0.000 | 0.202 | 0.005 | 1.838 | 0.005 | 0.000 | 0.000 |

The upper value in each cell means the average concentration of each sugar and the lower value denotes the standard error (SE). Endo = endophyte, E- = endophyte-free, CT = common-toxic, Ara = D-arabitol, DL-ara = DL-arabinose, Fru = fructose, Galacti = galactinol, Gal = D-galactose, Glu = glucose, Gly = glycerol, Ino = myo-inositol, Mal = maltose, Manni = mannitol, Raf = raffinose, Rib = ribitol, Sor = sorbitol, Suc = sucrose, Tre = trehalose, Xyli = xylitol, Xyl = xylose.

## Table A4.5 Heatmap for the effects of endophytes on selected metabolites in seed embryo and endosperm samples with fold changes and significance values[1].

Down-regulated $p \le 0.01$ $0.01 < p \le 0.05$ $0.05 < p \le 0.10$
Up-regulated $p \le 0.01$ $0.01 < p \le 0.05$ $0.05 < p \le 0.10$

| F1 | F2 | F3 | | | Ara | DL-ara | Fru | Galacti | Gal | Glu | Gly | Ino | Lac | Mal | Manni | Man | Raf | Rib | Sor | Suc | Tre | Xyli | Xyl |
|---|---|---|---|---|---|---|---|---|---|---|---|---|---|---|---|---|---|---|---|---|---|---|---|
| Dry | AA- | Embryo | AR584 | FC | 1.51 | 0.84 | 0.87 | 0.87 | 1.08 | 0.94 | 0.99 | 1.11 | 1.37 | 1.20 | 5.11 | 1.58 | 0.97 | n.a. | 0.81 | 0.89 | 8.58 | 1.20 | n.a. |
| | | | | p | 0.275 | 0.349 | 0.634 | 0.162 | 0.718 | 0.795 | 0.967 | 0.243 | 0.313 | 0.761 | 0.012 | 0.584 | 0.784 | 0.089 | 0.024 | 0.143 | 0.006 | 0.513 | 0.185 |
| | | | AR605 | FC | 2.33 | 0.84 | 0.66 | 0.76 | 0.87 | 0.82 | 0.88 | 1.02 | 1.13 | 1.48 | 6.10 | 0.63 | 0.98 | n.a. | 0.79 | 0.94 | 8.17 | 1.85 | n.a. |
| | | | | p | 0.033 | 0.377 | 0.336 | 0.062 | 0.742 | 0.503 | 0.478 | 0.451 | 0.759 | 0.534 | 0.025 | 0.396 | 0.891 | 0.012 | 0.070 | 0.504 | 0.001 | 0.066 | n.a. |
| | | | CT | FC | 2.24 | 0.92 | 0.92 | 0.93 | 0.89 | 0.95 | 0.97 | 0.94 | 1.05 | 1.14 | 4.02 | 0.37 | 1.04 | n.a. | 1.09 | 0.96 | 10.33 | 1.48 | n.a. |
| | | | | p | 0.041 | 0.631 | 0.744 | 0.285 | 0.629 | 0.809 | 0.806 | 0.139 | 0.881 | 0.818 | 0.001 | 0.247 | 0.498 | 0.000 | 0.830 | 0.461 | 0.003 | 0.246 | n.a. |
| | | Endosperm | AR584 | FC | 0.63 | 1.12 | 1.68 | 1.17 | 0.99 | 1.75 | 1.10 | 1.06 | 0.61 | 0.73 | 9.85 | 1.02 | n.a. | n.a. | 2.33 | 0.94 | 2.69 | 0.82 | 0.00 |
| | | | | p | 0.588 | 0.427 | 0.601 | 0.630 | 0.977 | 0.535 | 0.289 | 0.743 | 0.597 | 0.430 | 0.000 | 0.943 | 0.423 | 0.253 | 0.626 | 0.894 | 0.068 | 0.708 | 0.205 |
| | | | AR605 | FC | 2.11 | 1.25 | 1.38 | 1.04 | 1.47 | 1.46 | 1.28 | 1.19 | 1.20 | 1.02 | 15.26 | 1.26 | n.a. | n.a. | 3.03 | 1.36 | 3.66 | 1.03 | 0.00 |
| | | | | p | 0.184 | 0.256 | 0.575 | 0.906 | 0.238 | 0.479 | 0.438 | 0.304 | 0.793 | 0.934 | 0.003 | 0.479 | 0.189 | 0.003 | 0.122 | 0.429 | 0.038 | 0.923 | 0.205 |
| | | | CT | FC | 0.88 | 1.14 | 0.88 | 1.21 | 0.94 | 0.77 | 1.33 | 1.00 | 0.85 | 0.73 | 5.20 | 0.79 | n.a. | n.a. | 0.89 | 1.20 | 5.00 | 0.82 | 0.00 |
| | | | | p | 0.865 | 0.418 | 0.832 | 0.563 | 0.808 | 0.641 | 0.381 | 0.980 | 0.832 | 0.381 | 0.006 | 0.574 | 0.423 | 0.000 | 0.914 | 0.457 | 0.051 | 0.760 | 0.205 |
| | AA+ | Embryo | AR584 | FC | 1.14 | 1.18 | 0.76 | 1.13 | 1.30 | 0.97 | 0.97 | 1.20 | 0.65 | 0.91 | 7.72 | 0.57 | 0.84 | 1.79 | 0.85 | 0.96 | 17.74 | 0.83 | 1.01 |
| | | | | p | 0.505 | 0.157 | 0.100 | 0.114 | 0.366 | 0.648 | 0.724 | 0.087 | 0.574 | 0.674 | 0.009 | 0.366 | 0.259 | 0.445 | 0.575 | 0.398 | 0.058 | 0.577 | 0.928 |
| | | | AR605 | FC | 0.91 | 0.82 | 0.61 | 0.76 | 0.84 | 0.62 | 1.09 | 1.04 | 0.64 | 0.55 | 8.22 | 0.40 | 0.96 | 7.25 | 1.54 | 1.01 | 6.95 | 0.81 | 0.65 |
| | | | | p | 0.509 | 0.110 | 0.007 | 0.048 | 0.510 | 0.004 | 0.081 | 0.287 | 0.563 | 0.138 | 0.003 | 0.252 | 0.682 | 0.017 | 0.058 | 0.834 | 0.000 | 0.056 | 0.136 |
| | | | CT | FC | 1.20 | 1.14 | 0.70 | 1.06 | 0.95 | 0.80 | 1.15 | 1.05 | 0.70 | 0.94 | 8.41 | 0.31 | 1.08 | 12.58 | 0.78 | 1.12 | 15.51 | 0.62 | 1.13 |
| | | | | p | 0.252 | 0.333 | 0.028 | 0.538 | 0.842 | 0.076 | 0.102 | 0.434 | 0.630 | 0.887 | 0.003 | 0.201 | 0.528 | 0.008 | 0.346 | 0.171 | 0.005 | 0.072 | 0.485 |
| | | Endosperm | AR584 | FC | 1.46 | 1.40 | 0.85 | 1.43 | 1.42 | 0.93 | 1.93 | 1.49 | 2.00 | 1.36 | 8.89 | 0.91 | 0.13 | n.a. | 0.68 | 0.76 | 8.73 | 1.25 | 0.77 |
| | | | | p | 0.271 | 0.257 | 0.763 | 0.115 | 0.150 | 0.854 | 0.288 | 0.342 | 0.106 | 0.146 | 0.044 | 0.749 | 0.011 | 0.212 | 0.336 | 0.370 | 0.186 | 0.357 | 0.599 |
| | | | AR605 | FC | 2.70 | 1.02 | 0.48 | 0.72 | 1.07 | 0.61 | 0.83 | 1.25 | 2.25 | 0.95 | 11.54 | 0.60 | 7.19 | n.a. | 0.95 | 0.68 | 13.38 | 0.69 | 0.98 |
| | | | | p | 0.060 | 0.878 | 0.199 | 0.098 | 0.526 | 0.260 | 0.301 | 0.483 | 0.392 | 0.851 | 0.000 | 0.253 | 0.000 | 0.001 | 0.909 | 0.225 | 0.367 | 0.297 | 0.893 |
| | | | CT | FC | 3.54 | 1.94 | 1.36 | 1.50 | 2.47 | 1.62 | 1.54 | 1.48 | 1.87 | 1.33 | 9.36 | 1.22 | 0.79 | n.a. | 3.39 | 1.33 | 4.59 | 1.63 | 1.37 |
| | | | | p | 0.054 | 0.071 | 0.623 | 0.102 | 0.173 | 0.418 | 0.431 | 0.007 | 0.299 | 0.427 | 0.124 | 0.483 | 0.281 | 0.016 | 0.373 | 0.228 | 0.284 | 0.059 | 0.169 |
| Imbibed | AA- | Embryo | AR584 | FC | 1.92 | 1.37 | 0.77 | 1.25 | 0.64 | 0.90 | 0.93 | 1.30 | 0.44 | 0.98 | 7.18 | 0.68 | 0.83 | n.a. | 0.85 | 1.12 | 9.46 | 1.02 | 0.00 |
| | | | | p | 0.056 | 0.186 | 0.447 | 0.068 | 0.473 | 0.692 | 0.742 | 0.053 | 0.491 | 0.942 | 0.008 | 0.561 | 0.387 | 0.004 | 0.600 | 0.229 | 0.003 | 0.967 | 0.423 |
| | | | AR605 | FC | 2.06 | 0.96 | 0.59 | 0.86 | 0.78 | 0.88 | 1.40 | 1.22 | 0.06 | 2.65 | 9.65 | 0.71 | 0.65 | n.a. | 2.24 | 1.18 | 8.10 | 1.46 | 0.00 |
| | | | | p | 0.078 | 0.869 | 0.203 | 0.532 | 0.669 | 0.675 | 0.203 | 0.209 | 0.300 | 0.057 | 0.034 | 0.672 | 0.220 | 0.006 | 0.503 | 0.380 | 0.011 | 0.418 | 0.423 |
| | | | CT | FC | 2.32 | 1.14 | 0.63 | 1.16 | 0.74 | 0.73 | 0.80 | 0.95 | 0.27 | 1.02 | 4.90 | 0.26 | 1.39 | n.a. | 0.74 | 1.09 | 9.34 | 1.09 | 0.00 |
| | | | | p | 0.003 | 0.629 | 0.237 | 0.279 | 0.620 | 0.335 | 0.385 | 0.528 | 0.399 | 0.942 | 0.001 | 0.253 | 0.194 | 0.002 | 0.044 | 0.230 | 0.005 | 0.836 | 0.423 |
| | | Endosperm | AR584 | FC | 1.08 | 0.80 | 1.60 | 1.26 | 1.03 | 1.04 | 1.87 | 1.02 | 1.23 | 1.11 | 8.60 | 0.98 | n.a. | n.a. | 4.93 | 0.96 | 1.13 | 0.03 | 0.00 |
| | | | | p | 0.915 | 0.391 | 0.065 | 0.211 | 0.907 | 0.858 | 0.271 | 0.909 | 0.432 | 0.632 | 0.089 | 0.950 | n.a. | 0.013 | 0.244 | 0.843 | 0.844 | 0.205 | 0.423 |
| | | | AR605 | FC | 1.51 | 0.93 | 1.57 | 1.46 | 1.23 | 1.45 | 3.24 | 1.03 | 1.15 | 1.20 | 9.88 | 1.53 | n.a. | n.a. | 1.72 | 0.98 | 2.09 | 0.00 | 0.00 |
| | | | | p | 0.065 | 0.707 | 0.067 | 0.042 | 0.396 | 0.270 | 0.032 | 0.883 | 0.661 | 0.479 | 0.089 | 0.156 | n.a. | 0.009 | 0.654 | 0.947 | 0.216 | 0.197 | 0.423 |
| | | | CT | FC | 1.56 | 0.67 | 1.02 | 1.11 | 0.78 | 0.73 | 1.94 | 1.08 | 0.74 | 0.68 | 4.65 | 0.42 | n.a. | n.a. | 1.47 | 1.08 | 1.23 | 0.00 | 0.00 |
| | | | | p | 0.051 | 0.141 | 0.934 | 0.677 | 0.293 | 0.255 | 0.163 | 0.694 | 0.452 | 0.270 | 0.049 | 0.132 | n.a. | 0.018 | 0.725 | 0.777 | 0.690 | 0.197 | 0.423 |
| | AA+ | Embryo | AR584 | FC | 1.82 | 1.17 | 0.63 | 1.32 | 1.13 | 0.67 | 0.87 | 1.03 | 0.86 | 0.48 | 54.80 | 0.12 | 1.85 | n.a. | 0.84 | 0.70 | 1.18 | 0.73 | 1.81 |
| | | | | p | 0.035 | 0.494 | 0.086 | 0.118 | 0.763 | 0.292 | 0.600 | 0.749 | 0.381 | 0.141 | 0.032 | 0.036 | 0.081 | 0.038 | 0.669 | 0.035 | 0.775 | 0.561 | 0.436 |
| | | | AR605 | FC | 1.41 | 0.86 | 0.75 | 0.77 | 0.80 | 0.62 | 0.66 | 0.93 | 0.74 | 0.62 | 79.70 | 0.31 | 0.97 | n.a. | 0.67 | 0.95 | 1.19 | 0.96 | 0.29 |
| | | | | p | 0.242 | 0.441 | 0.304 | 0.326 | 0.571 | 0.234 | 0.109 | 0.581 | 0.181 | 0.258 | 0.018 | 0.141 | 0.951 | 0.010 | 0.338 | 0.636 | 0.756 | 0.926 | 0.309 |
| | | | CT | FC | 1.67 | 1.16 | 0.65 | 1.11 | 1.13 | 0.72 | 0.98 | 1.01 | 4.40 | 0.69 | 53.27 | 5.84 | 1.23 | n.a. | 0.37 | 0.94 | 0.98 | 1.49 | 0.06 |
| | | | | p | 0.050 | 0.470 | 0.100 | 0.653 | 0.887 | 0.336 | 0.936 | 0.966 | 0.452 | 0.253 | 0.012 | 0.481 | 0.583 | 0.056 | 0.135 | 0.761 | 0.973 | 0.517 | 0.204 |
| | | Endosperm | AR584 | FC | 2.87 | 1.43 | 2.05 | 0.78 | 1.66 | 1.22 | 2.22 | 1.14 | 1.40 | 1.34 | 51.26 | 1.17 | n.a. | n.a. | n.a. | 0.84 | 0.57 | 0.00 | 9.702 |
| | | | | p | 0.411 | 0.395 | 0.307 | 0.566 | 0.292 | 0.499 | 0.377 | 0.678 | 0.438 | 0.403 | 0.052 | 0.566 | n.a. | 0.017 | 0.189 | 0.172 | 0.242 | 0.423 | 0.414 |
| | | | AR605 | FC | 11.11 | 1.11 | 2.20 | 1.35 | 1.57 | 1.43 | 2.38 | 1.13 | 2.92 | 2.67 | 131.83 | 1.88 | n.a. | n.a. | n.a. | 1.34 | 1.10 | 11.01 | 2.309 |
| | | | | p | 0.366 | 0.505 | 0.292 | 0.684 | 0.279 | 0.444 | 0.245 | 0.565 | 0.170 | 0.153 | 0.151 | 0.332 | n.a. | 0.051 | 0.193 | 0.476 | 0.745 | 0.461 | 0.399 |
| | | | CT | FC | 2.38 | 1.08 | 1.44 | 1.62 | 1.36 | 1.05 | 1.98 | 1.07 | 1.73 | 1.55 | 47.07 | 0.82 | n.a. | n.a. | n.a. | 0.94 | 0.73 | 0.00 | 0.00 |
| | | | | p | 0.162 | 0.707 | 0.432 | 0.613 | 0.334 | 0.905 | 0.397 | 0.701 | 0.202 | 0.203 | 0.123 | 0.371 | n.a. | 0.092 | 0.094 | 0.825 | 0.177 | 0.423 | 0.042 |

[1]Fold changes (FC) were calculated as of the ratio of the amount of individual metabolite under the non-underlined treatment and the underlined treatment in Factor 3. n.a. in FC denotes that the denominator was zero in calculating the fold change of the metabolite. n.a. in p-value means that all the observations in of the related treatment were all zero. The meanings of the cells coloured were as above. F1 = factor 1, F2 = factor 2, F3 = factor 3, FC = fold change, E- = endophyte-free, CT = common toxic, Ara = D-arabitol, DL-ara = DL-arabinose, Fru = fructose, Galacti = galactinol, Gal = D-galactose, Glu = glucose, Gly = glycerol, Ino = myo-inositol, Mal = maltose, Manni = mannitol, Raf = raffinose, Rib = ribitol, Sor = sorbitol, Suc = sucrose, Tre = trehalose, Xyli = xylitol, Xyl = xylose.

## Table A4.6 Heatmap for the effects of AA on selected metabolites in seed embryo and endosperm samples with fold changes and significance values[1].

Down-regulated $p \le 0.01$ $0.01 < p \le 0.05$ $0.05 < p \le 0.10$
Up-regulated $p \le 0.01$ $0.01 < p \le 0.05$ $0.05 < p \le 0.10$

| F1 | F2 | F3 | | Ara | DL-ara | Fru | Galacti | Gal | Glu | Gly | Ino | Lac | Mal | Manni | Man | Raf | Rib | Sor | Suc | Tre | Xyli | Xyl |
|---|---|---|---|---|---|---|---|---|---|---|---|---|---|---|---|---|---|---|---|---|---|---|
| Embryo | Dry | E- | FC | 2.13 | 2.06 | 1.17 | 0.66 | 2.40 | 1.46 | 1.29 | 0.95 | 2.00 | 1.70 | 0.51 | 5.39 | 2.11 | n.a. | 1.55 | 0.66 | 0.15 | 4.17 | n.a. |
| | | | p | 0.045 | 0.008 | 0.546 | 0.007 | 0.038 | 0.242 | 0.174 | 0.096 | 0.451 | 0.351 | 0.213 | 0.145 | 0.018 | 0.001 | 0.161 | 0.070 | 0.124 | 0.002 | 0.007 |
| | | AR584 | FC | 1.62 | 2.89 | 1.02 | 0.86 | 2.88 | 1.51 | 1.26 | 1.02 | 0.95 | 1.29 | 0.78 | 1.96 | 1.83 | 0.48 | 1.63 | 0.71 | 0.31 | 2.88 | 6.64 |
| | | | p | 0.107 | 0.003 | 0.884 | 0.202 | 0.074 | 0.025 | 0.188 | 0.797 | 0.754 | 0.385 | 0.102 | 0.378 | 0.042 | 0.256 | 0.209 | 0.016 | 0.002 | 0.173 | 0.009 |
| | | AR605 | FC | 0.83 | 2.02 | 1.08 | 0.66 | 2.33 | 1.11 | 1.60 | 0.97 | 1.13 | 0.63 | 0.69 | 3.37 | 2.08 | 0.96 | 3.02 | 0.71 | 0.13 | 1.82 | n.a. |
| | | | p | 0.297 | 0.005 | 0.611 | 0.075 | 0.084 | 0.611 | 0.056 | 0.476 | 0.668 | 0.330 | 0.151 | 0.443 | 0.006 | 0.823 | 0.017 | 0.036 | 0.004 | 0.006 | 0.052 |
| | | CT | FC | 1.14 | 2.54 | 0.88 | 0.75 | 2.56 | 1.24 | 1.52 | 1.05 | 1.34 | 1.40 | 1.08 | 4.56 | 2.20 | 1.17 | 1.12 | 0.78 | 0.22 | 1.75 | n.a. |
| | | | p | 0.268 | 0.022 | 0.338 | 0.013 | 0.076 | 0.139 | 0.004 | 0.406 | 0.139 | 0.482 | 0.288 | 0.187 | 0.023 | 0.223 | 0.778 | 0.012 | 0.004 | 0.168 | 0.016 |
| Endosperm | | E- | FC | 1.13 | 2.52 | 1.86 | 0.63 | 1.70 | 2.03 | 1.17 | 0.85 | 0.55 | 0.49 | 1.28 | 1.53 | n.a. | n.a. | 4.96 | 0.95 | 0.05 | 1.06 | 6.78 |
| | | | p | 0.854 | 0.001 | 0.244 | 0.338 | 0.023 | 0.182 | 0.316 | 0.383 | 0.536 | 0.153 | 0.746 | 0.318 | 0.018 | n.a. | 0.000 | 0.867 | 0.016 | 0.874 | 0.003 |
| | | AR584 | FC | 2.59 | 3.14 | 0.94 | 0.77 | 2.44 | 1.08 | 2.05 | 1.19 | 1.77 | 0.93 | 1.16 | 1.35 | 0.58 | 0.57 | 1.45 | 0.77 | 0.17 | 1.63 | n.a. |
| | | | p | 0.060 | 0.063 | 0.943 | 0.101 | 0.040 | 0.905 | 0.263 | 0.626 | 0.110 | 0.836 | 0.550 | 0.169 | 0.740 | 0.582 | 0.716 | 0.612 | 0.021 | 0.246 | 0.164 |
| | | AR605 | FC | 1.45 | 2.05 | 0.65 | 0.44 | 1.24 | 0.85 | 0.76 | 0.89 | 1.03 | 0.46 | 0.97 | 0.72 | 1.09 | 0.85 | 1.55 | 0.48 | 0.20 | 0.71 | n.a. |
| | | | p | 0.240 | 0.022 | 0.465 | 0.110 | 0.371 | 0.703 | 0.393 | 0.661 | 0.965 | 0.028 | 0.782 | 0.306 | 0.899 | 0.088 | 0.505 | 0.180 | 0.019 | 0.218 | 0.002 |
| | | CT | FC | 4.53 | 4.27 | 2.88 | 0.78 | 4.48 | 4.26 | 1.35 | 1.26 | 1.20 | 0.90 | 2.31 | 2.34 | 3.61 | 0.82 | 18.90 | 1.05 | 0.05 | 2.12 | n.a. |
| | | | p | 0.077 | 0.030 | 0.299 | 0.161 | 0.114 | 0.189 | 0.549 | 0.150 | 0.674 | 0.741 | 0.244 | 0.007 | 0.124 | 0.224 | 0.267 | 0.748 | 0.037 | 0.188 | 0.016 |
| Embryo | Imbibed | E- | FC | 1.09 | 0.66 | 0.76 | 0.59 | 1.45 | 0.48 | 0.57 | 1.22 | 0.56 | 1.13 | 0.09 | 0.83 | 0.69 | n.a. | 1.21 | 1.07 | 2.00 | 0.73 | 1.72 |
| | | | p | 0.752 | 0.248 | 0.421 | 0.001 | 0.391 | 0.114 | 0.097 | 0.076 | 0.578 | 0.681 | 0.014 | 0.748 | 0.205 | n.a. | 0.471 | 0.507 | 0.420 | 0.526 | 0.615 |
| | | AR584 | FC | 1.03 | 0.56 | 0.62 | 0.63 | 2.59 | 0.36 | 0.54 | 0.96 | 1.10 | 0.55 | 0.71 | 0.14 | 1.54 | 1.11 | 1.20 | 0.67 | 0.25 | 0.52 | n.a. |
| | | | p | 0.881 | 0.028 | 0.107 | 0.013 | 0.216 | 0.006 | 0.049 | 0.665 | 0.590 | 0.187 | 0.143 | 0.026 | 0.132 | 0.678 | 0.698 | 0.014 | 0.001 | 0.174 | 0.138 |
| | | AR605 | FC | 0.74 | 0.59 | 0.97 | 0.53 | 1.48 | 0.34 | 0.27 | 0.93 | 6.83 | 0.30 | 0.77 | 0.37 | 1.04 | 1.07 | 0.36 | 0.86 | 0.29 | 0.48 | n.a. |
| | | | p | 0.308 | 0.050 | 0.924 | 0.157 | 0.481 | 0.048 | 0.036 | 0.648 | 0.056 | 0.074 | 0.322 | 0.461 | 0.950 | 0.632 | 0.455 | 0.404 | 0.003 | 0.176 | 0.239 |
| | | CT | FC | 0.78 | 0.67 | 0.79 | 0.57 | 2.21 | 0.47 | 0.70 | 1.30 | 9.06 | 0.76 | 1.01 | 18.94 | 0.61 | 1.33 | 0.62 | 0.92 | 0.21 | 1.00 | n.a. |
| | | | p | 0.046 | 0.169 | 0.310 | 0.034 | 0.533 | 0.002 | 0.220 | 0.272 | 0.399 | 0.323 | 0.955 | 0.429 | 0.146 | 0.422 | 0.488 | 0.672 | 0.002 | 0.997 | 0.423 |
| Endosperm | | E- | FC | 0.81 | 0.74 | 0.70 | 0.54 | 0.78 | 0.86 | 0.89 | 0.91 | 0.60 | 0.57 | 0.12 | 0.54 | n.a. | n.a. | 0.00 | 0.77 | 1.45 | 0.12 | 0.91 |
| | | | p | 0.618 | 0.184 | 0.103 | 0.051 | 0.234 | 0.526 | 0.757 | 0.704 | 0.229 | 0.139 | 0.006 | 0.176 | n.a. | n.a. | 0.423 | 0.293 | 0.448 | 0.246 | 0.941 |
| | | AR584 | FC | 2.16 | 1.31 | 0.90 | 0.33 | 1.25 | 1.00 | 1.06 | 1.01 | 0.69 | 0.69 | 0.69 | 0.64 | n.a. | 0.83 | 2.27 | 0.67 | 0.73 | 1.040 | n.a. |
| | | | p | 0.483 | 0.507 | 0.812 | 0.013 | 0.559 | 0.986 | 0.925 | 0.971 | 0.242 | 0.179 | 0.410 | 0.320 | n.a. | 0.354 | 0.389 | 0.021 | 0.609 | 0.994 | 0.372 |
| | | AR605 | FC | 5.94 | 0.88 | 0.98 | 0.50 | 0.99 | 0.84 | 0.66 | 0.99 | 1.53 | 1.28 | 1.54 | 0.66 | n.a. | 1.25 | 6.56 | 1.04 | 0.77 | n.a. | n.a. |
| | | | p | 0.400 | 0.512 | 0.968 | 0.201 | 0.972 | 0.658 | 0.290 | 0.968 | 0.371 | 0.511 | 0.512 | 0.305 | n.a. | 0.507 | 0.249 | 0.910 | 0.522 | 0.423 | 0.197 |
| | | CT | FC | 1.23 | 1.18 | 0.99 | 0.79 | 1.35 | 1.22 | 0.91 | 0.91 | 1.41 | 1.29 | 1.17 | 1.05 | n.a. | 1.41 | 4.92 | 0.67 | 0.85 | 0.966 | n.a. |
| | | | p | 0.560 | 0.532 | 0.975 | 0.719 | 0.365 | 0.628 | 0.864 | 0.269 | 0.395 | 0.430 | 0.743 | 0.863 | n.a. | 0.481 | 0.148 | 0.247 | 0.550 | 0.955 | n.a. |

F3: AA- (non-underlined), AA+ (underlined)

[1]Fold changes (FC) were calculated as of the ratio of the amount of individual metabolite under the non-underlined treatment and the underlined treatment in Factor 3. n.a. in FC denotes that the denominator was zero in calculating the fold change of the metabolite. n.a. in p-value means that all the observations in of the related treatment were all zero. The meanings of the cells marked were as above. F1 = factor 1, F2 = factor 2, F3 = factor 3, FC = fold change, E- = endophyte-free, CT = common-toxic, Ara = D-arabitol, DL-ara = DL-arabinose, Fru = fructose, Galacti = galactinol, Gal = D-galactose, Glu = glucose, Gly = glycerol, Ino = myo-inositol, Mal = maltose, Manni = mannitol, Raf = raffinose, Rib = ribitol, Sor = sorbitol, Suc = sucrose, Tre = trehalose, Xyli = xylitol, Xyl = xylose.

**Table A4.7 Heatmap for the effects of imbibition on selected metabolites in seed embryo and endosperm samples with fold changes and significance values[1].**

Down-regulated: $p \le 0.01$; $0.01 < p \le 0.05$; $0.05 < p \le 0.10$
Up-regulated: $p \le 0.01$; $0.01 < p \le 0.05$; $0.05 < p \le 0.10$

| F1 | F2 | F3 | | Ara | DL-ara | Fru | Galacti | Gal | Glu | Gly | Ino | Lac | Mal | Manni | Man | Raf | Rib | Sor | Suc | Tre | Xyli | Xyl |
|---|---|---|---|---|---|---|---|---|---|---|---|---|---|---|---|---|---|---|---|---|---|---|
| Embryo | AA- | Dry | FC | 0.97 | 0.82 | 1.38 | 0.70 | 2.56 | 1.41 | 1.41 | 1.05 | 4.25 | 4.55 | 0.90 | 1.51 | 1.75 | n.a | 0.95 | 0.92 | 0.61 | 1.26 | n.a. |
| | E- | | p | 0.934 | 0.428 | 0.377 | 0.020 | 0.264 | 0.321 | 0.242 | 0.592 | 0.374 | 0.037 | 0.643 | 0.528 | 0.033 | n.a. | 0.391 | 0.295 | 0.264 | 0.624 | 0.423 |
| | AR584 | | FC | 1.25 | 1.33 | 1.23 | 1.01 | 1.50 | 1.35 | 1.32 | 1.23 | 1.36 | 3.73 | 1.27 | 0.65 | 1.50 | 0.88 | 0.99 | 1.16 | 0.67 | 1.07 | 0.00 |
| | | | p | 0.292 | 0.042 | 0.361 | 0.887 | 0.282 | 0.068 | 0.192 | 0.095 | 0.205 | 0.010 | 0.106 | 0.595 | 0.188 | 0.751 | 0.984 | 0.121 | 0.021 | 0.746 | 0.185 |
| | AR605 | | FC | 0.86 | 0.93 | 1.23 | 0.80 | 2.31 | 1.50 | 2.25 | 1.25 | 0.23 | 8.14 | 1.42 | 1.69 | 1.16 | 1.13 | 2.68 | 1.16 | 0.60 | 0.99 | n.a. |
| | | | p | 0.513 | 0.681 | 0.417 | 0.385 | 0.213 | 0.234 | 0.038 | 0.186 | 0.132 | 0.047 | 0.221 | 0.605 | 0.737 | 0.404 | 0.456 | 0.410 | 0.007 | 0.975 | n.a. |
| | CT | | FC | 1.01 | 1.01 | 0.95 | 0.88 | 2.13 | 1.09 | 1.16 | 1.05 | 1.09 | 4.06 | 1.10 | 1.06 | 2.35 | 0.90 | 0.64 | 1.06 | 0.55 | 0.92 | n.a. |
| | | | p | 0.929 | 0.945 | 0.746 | 0.249 | 0.292 | 0.297 | 0.432 | 0.259 | 0.891 | 0.048 | 0.203 | 0.934 | 0.069 | 0.142 | 0.408 | 0.227 | 0.002 | 0.669 | n.a. |
| Endosperm | | | FC | 0.27 | 1.13 | 0.33 | 0.27 | 1.45 | 0.74 | 0.47 | 0.74 | 1.68 | 1.34 | 1.12 | 1.57 | n.a. | n.a. | 0.24 | 0.70 | 0.49 | 0.19 | 0.46 |
| | E- | | p | 0.326 | 0.508 | 0.202 | 0.129 | 0.116 | 0.517 | 0.045 | 0.226 | 0.418 | 0.386 | 0.856 | 0.275 | n.a. | n.a. | 0.079 | 0.274 | 0.146 | 0.111 | 0.490 |
| | AR584 | | FC | 0.46 | 0.81 | 0.31 | 0.29 | 1.51 | 0.44 | 0.81 | 0.71 | 3.37 | 1.29 | 0.98 | 1.50 | 0.00 | 1.53 | 0.52 | 0.72 | 0.21 | 0.01 | n.a. |
| | | | p | 0.157 | 0.358 | 0.385 | 0.000 | 0.307 | 0.415 | 0.551 | 0.110 | 0.005 | 0.049 | 0.950 | 0.360 | 0.423 | 0.502 | 0.686 | 0.534 | 0.022 | 0.128 | n.a. |
| | AR605 | | FC | 0.19 | 0.84 | 0.37 | 0.37 | 1.21 | 0.74 | 1.20 | 0.64 | 1.62 | 1.57 | 0.73 | 1.91 | 0.00 | 0.89 | 0.14 | 0.51 | 0.28 | 0.00 | n.a. |
| | | | p | 0.031 | 0.376 | 0.233 | 0.089 | 0.486 | 0.520 | 0.551 | 0.021 | 0.195 | 0.112 | 0.319 | 0.005 | 0.189 | 0.362 | 0.085 | 0.160 | 0.021 | 0.004 | n.a. |
| | CT | | FC | 0.47 | 0.67 | 0.38 | 0.24 | 1.21 | 0.70 | 0.69 | 0.80 | 1.46 | 1.40 | 1.01 | 0.83 | 0.00 | 0.71 | 0.40 | 0.63 | 0.12 | 0.00 | n.a. |
| | | | p | 0.238 | 0.103 | 0.298 | 0.004 | 0.491 | 0.545 | 0.322 | 0.255 | 0.385 | 0.478 | 0.980 | 0.553 | 0.423 | 0.097 | 0.619 | 0.096 | 0.043 | 0.194 | n.a. |
| Embryo | AA+ | Imbibed | FC | 0.50 | 0.26 | 0.90 | 0.63 | 1.55 | 0.46 | 0.62 | 1.34 | 1.18 | 3.02 | 0.16 | 0.23 | 0.57 | 0.00 | 0.74 | 1.50 | 8.13 | 0.22 | 0.47 |
| | E- | | p | 0.029 | 0.002 | 0.521 | 0.022 | 0.147 | 0.017 | 0.035 | 0.040 | 0.774 | 0.078 | 0.021 | 0.160 | 0.077 | 0.001 | 0.298 | 0.051 | 0.218 | 0.001 | 0.163 |
| | AR584 | | FC | 0.79 | 0.26 | 0.75 | 0.74 | 1.35 | 0.32 | 0.56 | 1.15 | 1.57 | 1.60 | 1.15 | 0.05 | 1.26 | 2.03 | 0.73 | 1.09 | 0.54 | 0.19 | 0.83 |
| | | | p | 0.275 | 0.003 | 0.153 | 0.068 | 0.523 | 0.004 | 0.039 | 0.135 | 0.027 | 0.481 | 0.543 | 0.146 | 0.311 | 0.171 | 0.448 | 0.223 | 0.201 | 0.129 | 0.692 |
| | AR605 | | FC | 0.77 | 0.27 | 1.11 | 0.64 | 1.47 | 0.46 | 0.38 | 1.19 | 1.37 | 3.85 | 1.57 | 0.18 | 0.58 | 1.26 | 0.32 | 1.40 | 1.39 | 0.26 | 0.21 |
| | | | p | 0.198 | 0.003 | 0.728 | 0.139 | 0.449 | 0.018 | 0.000 | 0.283 | 0.019 | 0.059 | 0.116 | 0.391 | 0.221 | 0.204 | 0.008 | 0.034 | 0.319 | 0.001 | 0.059 |
| | CT | | FC | 0.69 | 0.27 | 0.85 | 0.66 | 1.84 | 0.41 | 0.53 | 1.29 | 7.38 | 2.19 | 1.03 | 4.40 | 0.65 | 1.02 | 0.35 | 1.25 | 0.51 | 0.53 | 0.03 |
| | | | p | 0.039 | 0.005 | 0.390 | 0.092 | 0.591 | 0.021 | 0.036 | 0.283 | 0.409 | 0.077 | 0.830 | 0.508 | 0.146 | 0.936 | 0.119 | 0.362 | 0.012 | 0.189 | 0.017 |
| Endosperm | | | FC | 0.19 | 0.33 | 0.12 | 0.23 | 0.66 | 0.31 | 0.36 | 0.79 | 1.85 | 1.34 | 0.10 | 0.55 | 0.00 | n.a. | 0.00 | 0.56 | 13.19 | 0.03 | 0.06 |
| | E- | | p | 0.110 | 0.007 | 0.088 | 0.006 | 0.046 | 0.109 | 0.010 | 0.245 | 0.159 | 0.085 | 0.187 | 0.204 | 0.018 | n.a. | 0.001 | 0.148 | 0.023 | 0.039 | 0.014 |
| | AR584 | | FC | 0.38 | 0.34 | 0.30 | 0.12 | 0.77 | 0.41 | 0.42 | 0.60 | 1.30 | 1.53 | 0.58 | 0.71 | 0.00 | 2.25 | 0.81 | 0.62 | 0.86 | 0.11 | 0.78 |
| | | | p | 0.110 | 0.046 | 0.243 | 0.020 | 0.423 | 0.185 | 0.230 | 0.276 | 0.517 | 0.312 | 0.146 | 0.210 | 0.423 | 0.141 | 0.743 | 0.197 | 0.828 | 0.005 | 0.808 |
| | AR605 | | FC | 0.79 | 0.36 | 0.56 | 0.42 | 0.97 | 0.73 | 1.04 | 0.72 | 2.40 | 4.37 | 1.16 | 1.74 | 0.00 | 1.31 | 0.59 | 1.10 | 1.09 | 0.46 | 0.15 |
| | | | p | 0.775 | 0.010 | 0.309 | 0.101 | 0.910 | 0.347 | 0.928 | 0.332 | 0.191 | 0.110 | 0.785 | 0.363 | 0.107 | 0.419 | 0.485 | 0.786 | 0.927 | 0.378 | 0.002 |
| | CT | | FC | 0.13 | 0.18 | 0.13 | 0.25 | 0.36 | 0.20 | 0.47 | 0.57 | 1.71 | 1.81 | 0.51 | 0.37 | 0.00 | 1.23 | 0.11 | 0.40 | 2.09 | 0.00 | 0.00 |
| | | | p | 0.059 | 0.027 | 0.190 | 0.020 | 0.163 | 0.174 | 0.282 | 0.002 | 0.241 | 0.161 | 0.302 | 0.003 | 0.002 | 0.637 | 0.286 | 0.025 | 0.165 | 0.003 | 0.016 |

[1]Fold changes (FC) were calculated as of the ratio of the amount of individual metabolite under the non-underlined treatment and the underlined treatment in Factor 3. n.a. in FC denotes that the denominator was zero in calculating the fold change of the metabolite. n.a. in p-value means that all the observations in of the related treatment were all zero. The meanings of the cells marked were as above. F1 = factor 1, F2 = factor 2, F3 = factor 3, E- = endophyte-free, FC = fold change, CT = common-toxic, Ara = D-arabitol, DL-ara = DL-arabinose, Fru = fructose, Galacti = galactinol, Gal = D-galactose, Glu = glucose, Gly = glycerol, Ino = myo-inositol, Mal = maltose, Manni = mannitol, Raf = raffinose, Rib = ribitol, Sor = sorbitol, Suc = sucrose, Tre = trehalose, Xyli = xylitol, Xyl = xylose.

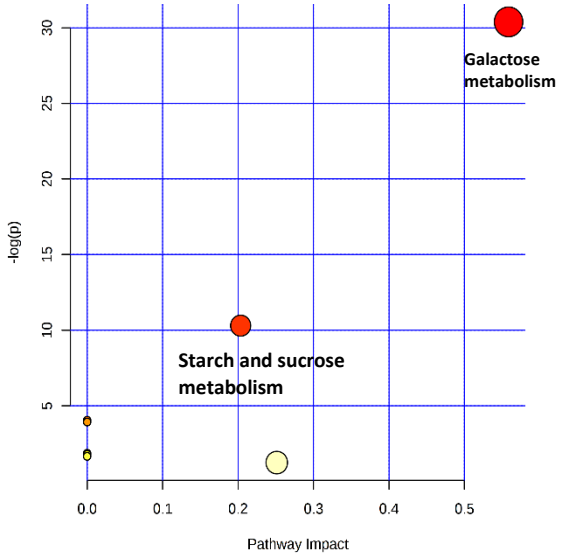


**Figure A4.1 Metabolite enrichment analysis using all the sugar metabolites analysed in this study with Metaboanalyst.** The two pathways labelled are the ones with most sugars measured in this study.

**a**

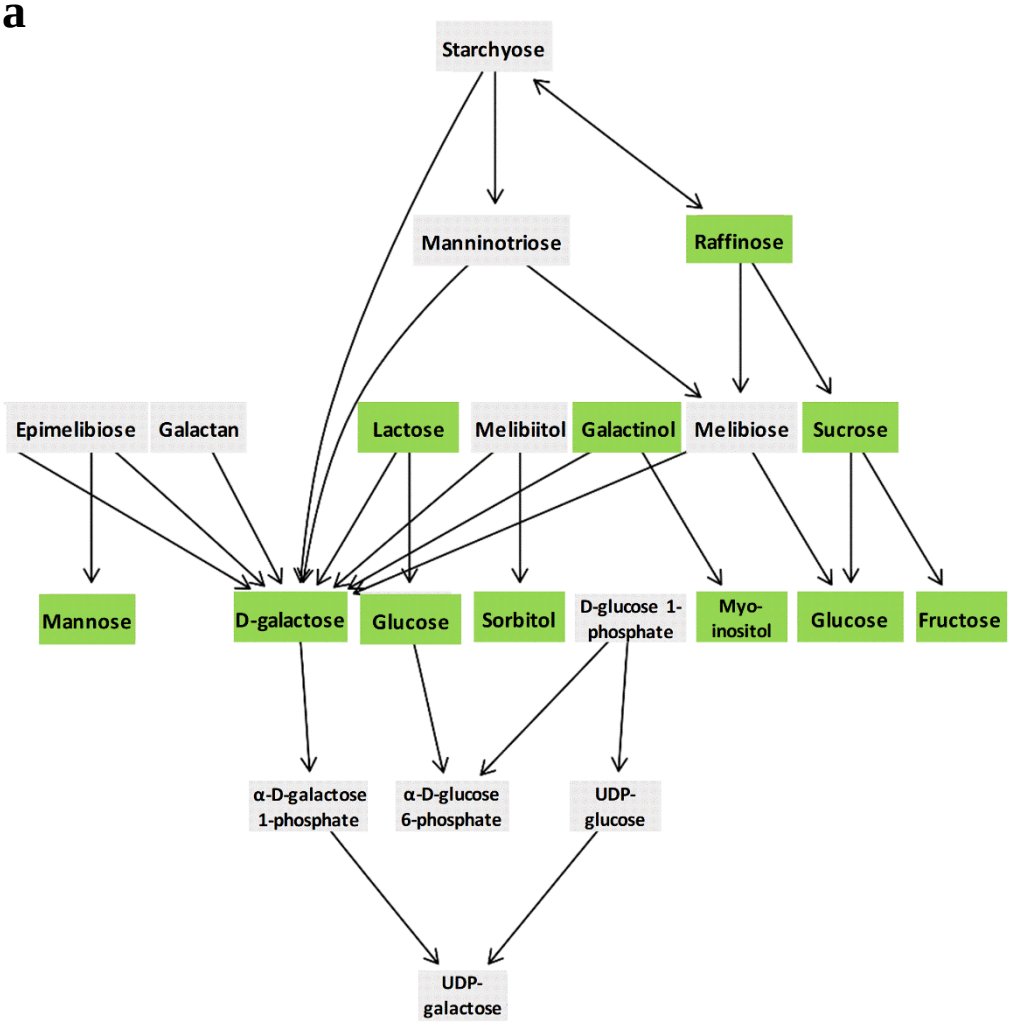
Starchyose
Manninotriose
Raffinose
Epimelibiose
Galactan
Lactose
Melibiitol
Galactinol
Melibiose
Sucrose
Mannose
D-galactose
Glucose
Sorbitol
D-glucose 1-phosphate
Myo-inositol
Glucose
Fructose
α-D-galactose 1-phosphate
α-D-glucose 6-phosphate
UDP-glucose
UDP-galactose

**b**

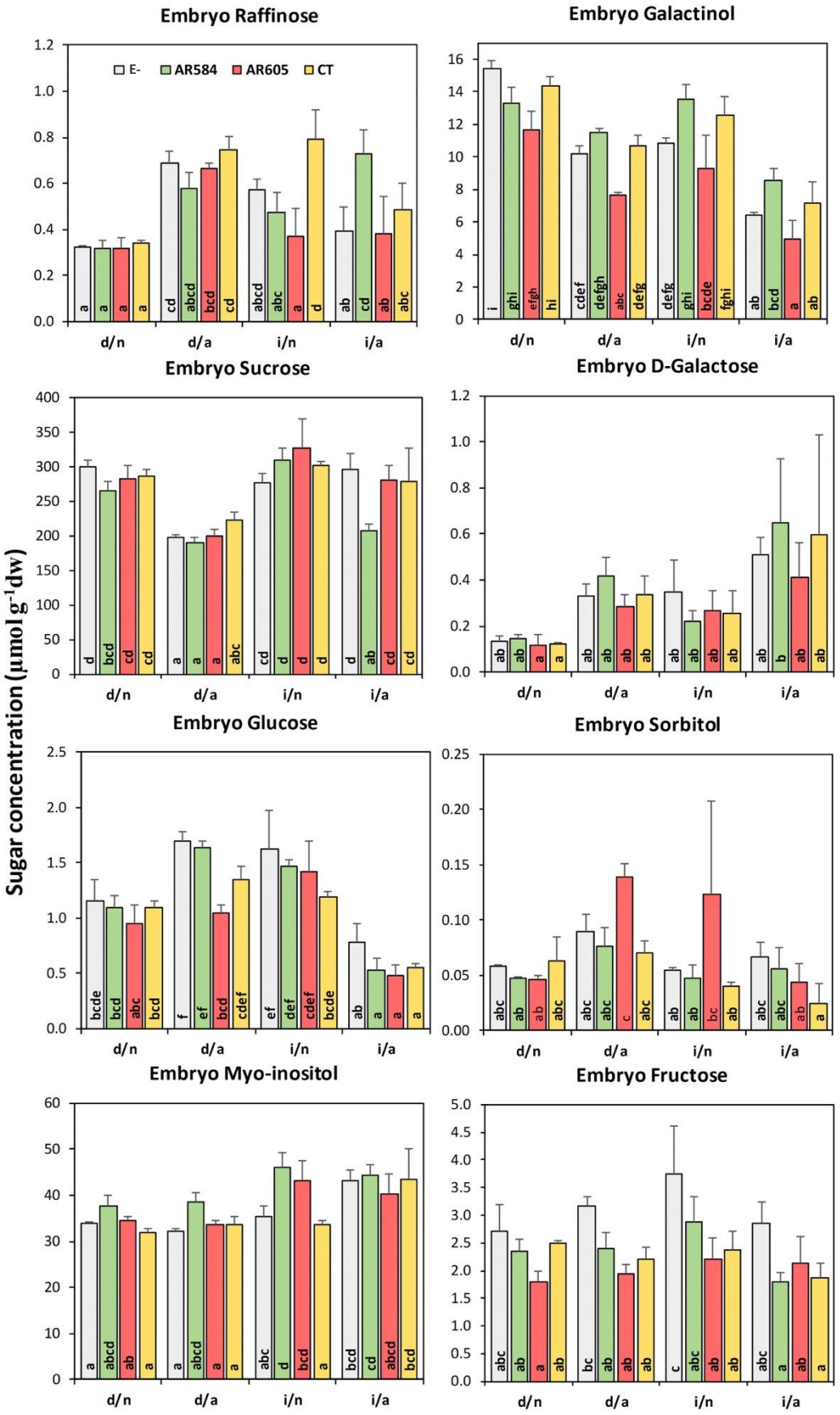
Embryo Raffinose
Embryo Galactinol
Embryo Sucrose
Embryo D-Galactose
Embryo Glucose
Embryo Sorbitol
Embryo Myo-inositol
Embryo Fructose
E-
AR584
AR605
CT
Sugar concentration (µmol g-1dw)
d/n
d/a
i/n
i/a

**c**

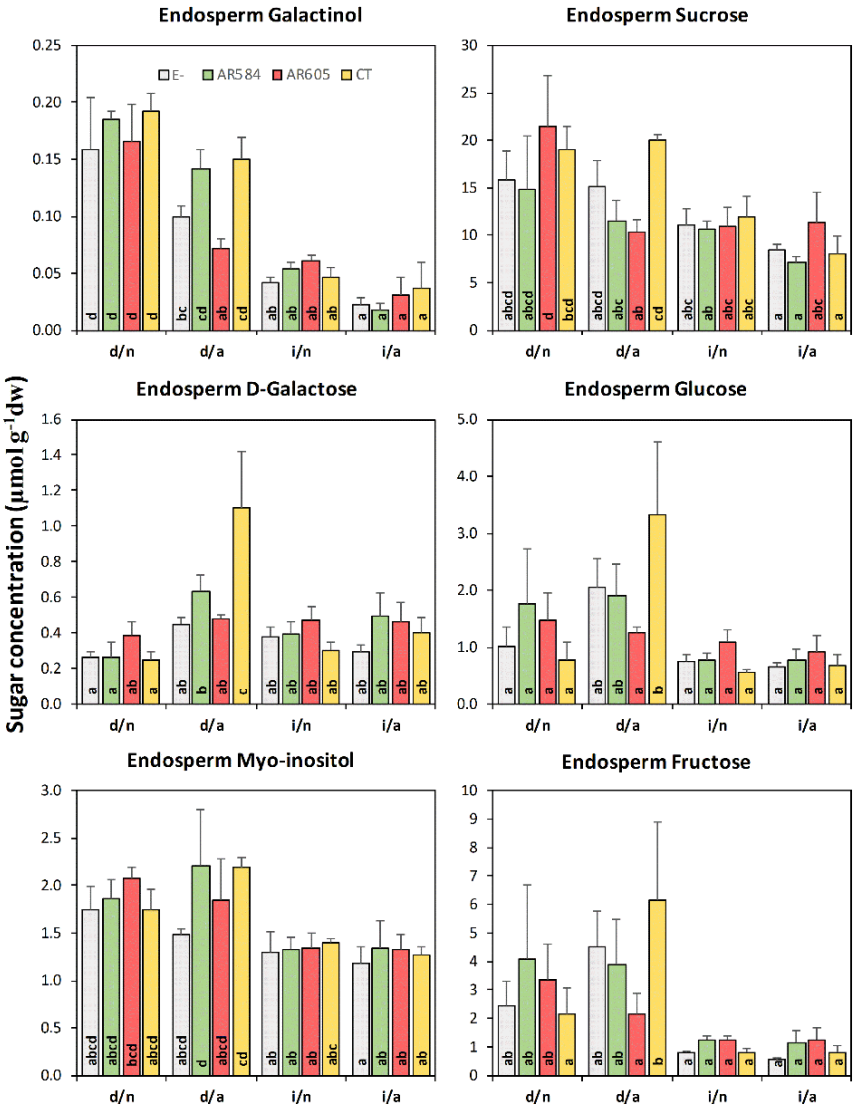


**Figure A4.2 a) Pathway of galactose metabolism obtained from Metaboanalyst with modification. b) Changes in selected metabolites inside the embryo tissues under different treatments.** Sugars of lactose and mannose were not shown due to their low concentrations and minimal changes with treatment. **c) Changes in selected metabolites inside the endosperm tissues under different treatments.** Each bar chart implies the amount of each sugar under different treatments. Sugars of lactose, mannose, sorbitol and raffinose were not shown due to their low concentrations and minimal changes with treatment. Different letters inside the bar imply multiple comparisons between different treatments by using Duncan's analysis. X axis denotes of treatment combinations and y axis shows the concentration of each sugar. E- = endophyte-free, CT = common-toxic; d = dry, i = imbibed; n = non-accelerated aging treatment, a = accelerated aging treatment.

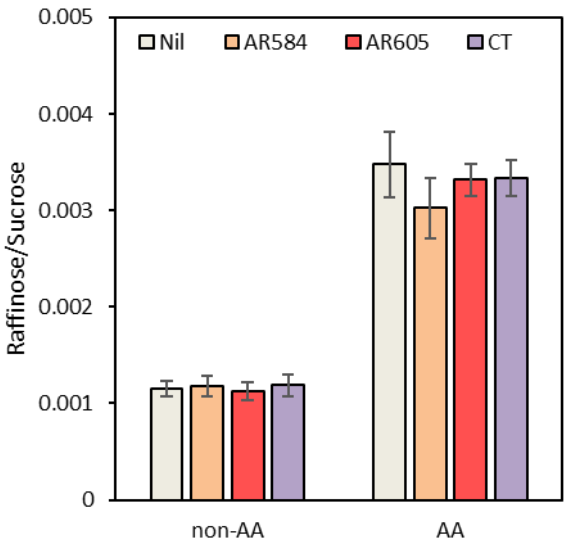


**Figure A4.3 Changes in the raffinose/sucrose ratio in non-AA and AA-treated dry embryo tissues from tall fescue seeds.** Y axis shows the ratio of raffinose concentration (µmol $g^{-1}$ dw) to sucrose concentration (µmol $g^{-1}$ dw). Error bars imply standard error of the replicates in each treatment. Non-AA = non-accelerated aging. AA = accelerated aging.

## A4.1 Investigating the effects of endophyte infection, accelerated aging and seed state on the sugar metabolites in seeds using multivariate analysis of variance (MANOVA) and canonical discriminant analysis (CDA).

### A4.1.1 Results of MANOVA on the soluble sugars in the embryo tissues

Three-way MANOVA on the sugar profiles in the embryo tissues revealed significant effects of all the main factors (State, Aging, Endophyte) and their two-way and three-way interactions (Table A4.8) ($p < 0.05$). The three-way interaction indicated that the changes in the interactions between State and Aging were not the same for different endophyte strains.

**Table A4.8 Three-way MANOVA (State x Aging x Endophyte) results for the sugar profiles in the embryo tissues.**

| Factor | Df | Wilks | F value | p-value | Significance |
|---|---|---|---|---|---|
| Endophyte | 3 | 0.00002 | 27.39 | < 0.0001 | *** |
| Aging | 1 | 0.01779 | 37.78 | < 0.0001 | *** |
| State | 1 | 0.01518 | 44.40 | < 0.0001 | *** |
| Aging x Endophyte | 3 | 0.00389 | 3.77 | < 0.0001 | *** |
| State x Endophyte | 3 | 0.01368 | 2.24 | 0.0044 | ** |
| State x Aging | 1 | 0.02342 | 28.53 | < 0.0001 | *** |
| State x Aging x Endophyte | 3 | 0.00703 | 3.00 | 0.0002 | *** |

Significance codes: ***: < 0.001, **: < 0.01, *: < 0.05.
Df: numerator degrees of freedom; p-value: probability

### A4.1.2 Results of the CDA on the sugar metabolites in the embryo tissues

With the presence of the significant three-way interaction from the MANOVA test, the canonical discriminant plots on two-way interactions or single factors were not self-explanatory. Based on the CDA plot of the three-way interaction, the first canonical discriminant function which accounted for 48.7% of the total variation separated the group including four CT-infected (d:n:c, dry x non-AA x CT; d:a:c, dry x AA x CT; i:n:c,

imbibed x non-AA x CT; i:a:c, imbibed x AA x CT) and one AR605-infected treatment (d:a:6, dry x AA x AR605) from the group including four endophyte-free treatment (i:a:0, imbibed x AA x endophyte-free; d:n:0, dry x non-AA x endophyte-free; i:n:0, imbibed x non-AA x endophyte-free, d:a:0, dry x AA x endophyte-free) and two AR584-infected treatment (d:a:5, dry x AA x AR584; i:n:5, imbibed x non-AA x AR584). The sugars with higher levels in the former group included D-arabitol and ribitol while in the latter group was fructose. The second canonical discriminant function captured 34.7% of the total variation which separated the group including three endophyte-free treatments (i:a:0, imbibed x AA x endophyte-free; d:n:0, dry x non-AA x endophyte-free; i:n:0, imbibed x non-AA x endophyte-free) and several endophyte-infected treatments (d:a:5, dry x AA x AR584; d:a:c, dry x AA x CT; d:n:6, dry x non-AA x AR605; d:a:6, dry x AA x AR605; d:n:5, dry x non-AA x AR584; d:a:CT, dry x AA x CT; d:n:5, dry x non-AA x CT). Fructose, maltose and sucrose were highly loaded in the first group, whilst D-arabitol, DL-arabinose, mannitol, ribitol, trehalose and xylitol were highly concentrated in the second group. Also, the separation caused by the second canonical discriminant function showed that CT-infected embryo tissues had higher levels of ribitol and trehalose than the other two endophyte-infected strains. The concentration of sucrose significantly decreased in the endophyte-free embryo tissues with the process of AA (Figure A4.4a, Table A4.9).

The first canonical discriminant function (47.6% of the total variation) from the biplot of the interaction between seed state and endophyte showed that with imbibition, myo-inositol and mannitol increased in AR584, AR605 and CT-infected embryo tissues while galactinol decreased in the embryo tissues infected by endophytes. Furthermore, D-arabitol, maltose, mannitol, ribitol and trehalose were higher in the embryo tissues with

endophyte infection than endophyte-free, whose results were explained by the second canonical discriminant function (33.9% of the total variation) (Figure A4.4b, Table A4.9).

By analysing the two canonical discriminant functions (explaining 74.1% and 21.3% of the total variation, respectively) in the biplot of aging and endophyte interaction, it was shown that trehalose significantly decreased with AA in the embryo tissues of three endophyte strains. The first canonical discriminant function also showed that D-arabitol and mannitol were highly accumulated in endophyte-infected embryo tissues under both non-AA and AA treatment (Figure A4.4c, Table A4.9).

CDA plot on the single factor of endophytes was very general due to the presence of two-way and three-way interactions. The two canonical discriminant functions (explained 63.6% and 32.4% of the total variation, respectively) showed that D-arabitol and ribitol were also abundant in the three endophyte-infected embryo tissues but were more abundant in AR605 and CT-infected embryo tissues than AR584. Moreover, the first canonical discriminant function showed that mannitol was abundant in AR584 and AR605-infected embryo tissues compared with AR605 and endophyte-free, with the concentration higher in the embryo tissues infected by AR605 than AR584 (Figure A4.4d, Table A4.9).

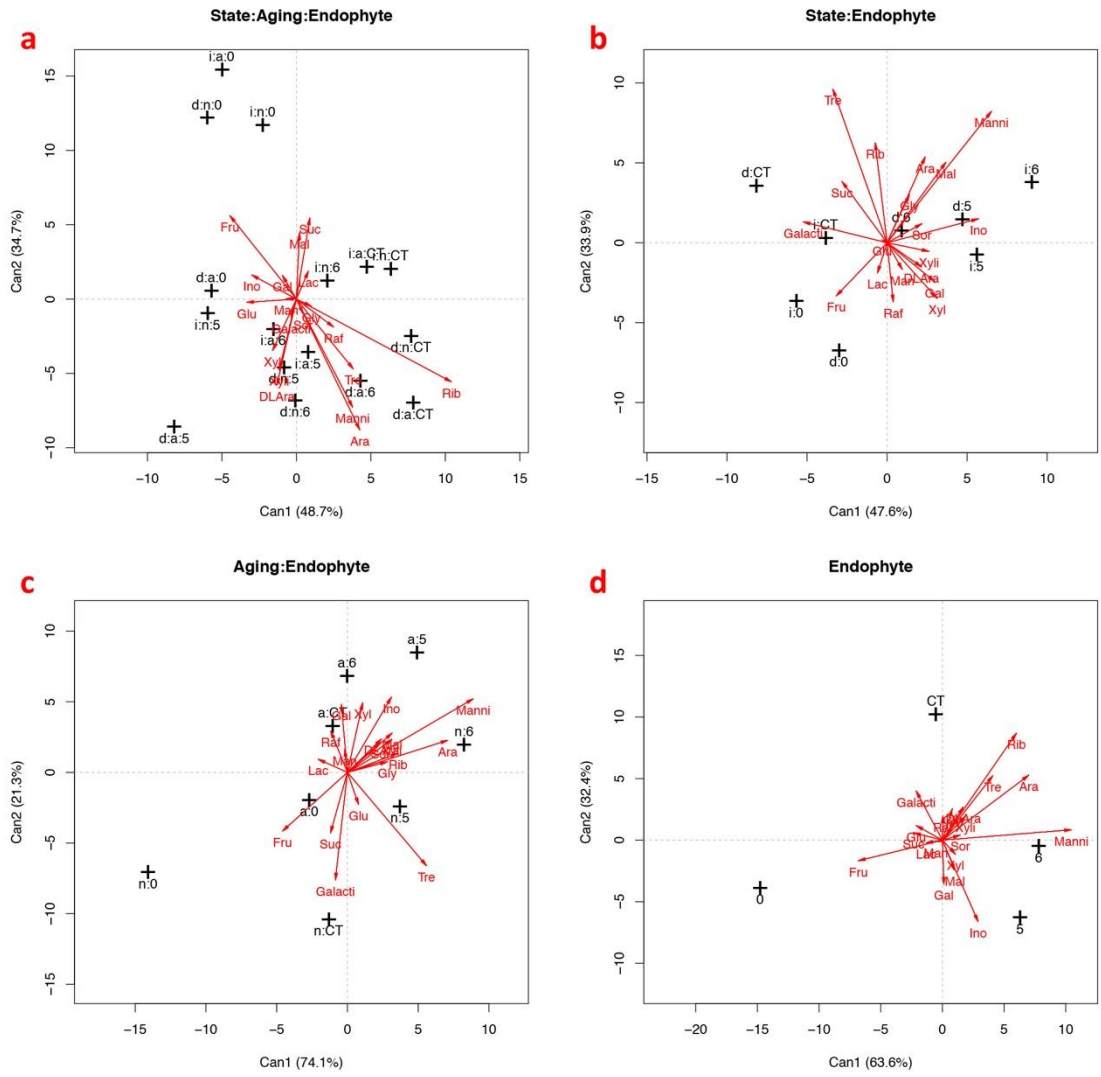


**Figure A4.4 Biplot graph showing the first two canonical functions (Can1 and Can2) obtained in a CDA of the sugar profiles in the embryo tissues applied to (a) State x Aging x Endophyte interaction, (b) State x Endophyte interaction, (c) Aging x Endophyte interaction, (d) Endophyte.** Vectors illustrate variables that strongly loaded for each treatment and + sign is the centroid of each treatment score. In (a) and (b), the first letter under the + sign denotes the seed state (d = dry, i = imbibed). The second letter in (a) and the first letter in (c) under the + sign denote the AA factor (n = non-accelerated aged, a = accelerated aged). The last letter in (a), (b) and (c) and only letter in (d) under the + sign denote different endophyte treatment (0: endophyte-free, 5: AR584, 6: AR605, CT: common-toxic). Ara = D-arabitol, DLAra = DL-arabinose, Fru = fructose, Galacti = galactinol, Gal = D-galactose, Glu = glucose, Gly = glycerol, Ino = myo-inositol, Mal = maltose, Manni = mannitol, Raf = raffinose, Rib = ribitol, Sor = sorbitol, Suc = sucrose, Tre = trehalose, Xyli = xylitol, Xyl = xylose.

The CDA plot of the State x Aging interaction and the main effects of the seed state and aging only has one canonical function since there is only one degree of freedom in each factor. Irrespective of the endophyte effects, CDA analysis revealed a separation of the dry and AA embryo tissues from the other three groups. The sugars which are abundant in the dry and AA groups are D-arabitol, DL-arabinose, xylitol and xylose while myo-inositol and sucrose are present in lower amounts (Figure A4.5a, A4.5b, A4.5c; Table A4.9).

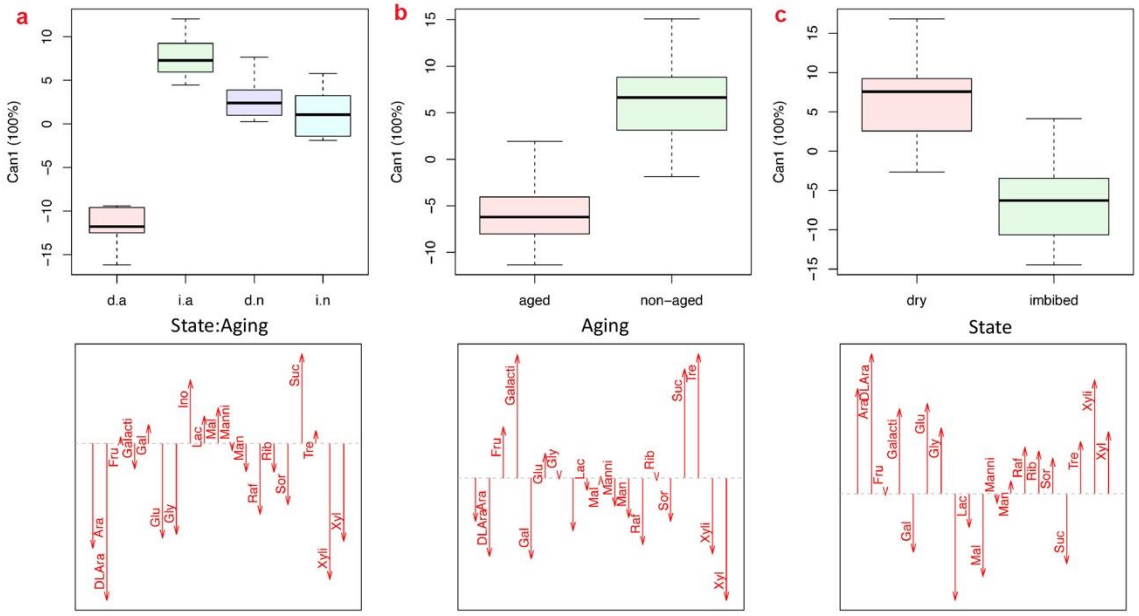


**Figure A4.5 CDA for the State x Aging interaction and the main effects of Aging and State on the sugar profiles in the embryo tissues.** The upper panel shows the canonical scores under each treatment while the lower panel shows the structure coefficients of each sugar variant in the embryo tissues. The first letter in (a) on the x-axis denotes seed state (d = dry, i = imbibed). The second letter in (a) denotes AA treatment (n = non-accelerated aged, a = accelerated aged). Ara = D-arabitol, DLAra = DL-arabinose, Fru = fructose, Galacti = galactinol, Gal = D-galactose, Glu = glucose, Gly = glycerol, Ino = myo-inositol, Mal = maltose, Manni = mannitol, Raf = raffinose, Rib = ribitol, Sor = sorbitol, Suc = sucrose, Tre = trehalose, Xyli = xylitol, Xyl = xylose.

**Table A4.9 Results of the structure coefficients ($r_s$) in the CDA of each significant experimental factor and the significant two-way or three-way interactions based on CDA of selected sugar metabolites in the embryo tissues.** For emphasis, structure coefficients above |0.30|% were underlined.

| | State x Aging x Endophyte | | | State x Endophyte | | | Aging x Endophyte | | | Endophyte | | | State x Aging | State | Aging |
|---|---|---|---|---|---|---|---|---|---|---|---|---|---|---|---|
| | $r_s$ 1 | $r_s$ 2 | $r_s$ 3 | $r_s$ 1 | $r_s$ 2 | $r_s$ 3 | $r_s$ 1 | $r_s$ 2 | $r_s$ 3 | $r_s$ 1 | $r_s$ 2 | $r_s$ 3 | $r_s$ 1 | $r_s$ 1 | $r_s$ 1 |
| Variation (%) | 48.7 | 34.7 | 16.6 | 47.6 | 33.9 | 18.5 | 74.1 | 21.3 | 4.6 | 63.6 | 32.4 | 4.0 | 100 | 100 | 100 |
| D-arabitol | 0.327 | -0.677 | 0.406 | 0.183 | 0.414 | 0.661 | 0.545 | 0.175 | -0.247 | 0.538 | 0.406 | -0.382 | -0.611 | 0.580 | -0.215 |
| DL-arabinose | -0.101 | -0.445 | 0.002 | 0.165 | -0.116 | 0.351 | 0.185 | 0.182 | -0.678 | 0.130 | 0.208 | -0.474 | -0.914 | 0.771 | -0.389 |
| Fructose | -0.344 | 0.432 | -0.323 | -0.244 | -0.256 | -0.507 | -0.353 | -0.320 | -0.118 | -0.524 | -0.128 | -0.102 | 0.039 | -0.009 | 0.255 |
| Galactinol | -0.028 | -0.096 | -0.121 | -0.403 | 0.100 | -0.045 | -0.065 | -0.586 | -0.050 | -0.164 | 0.307 | -0.756 | -0.148 | 0.470 | 0.613 |
| D-galactose | -0.072 | 0.122 | -0.010 | 0.229 | -0.187 | -0.041 | -0.033 | 0.370 | -0.183 | 0.009 | -0.274 | 0.363 | 0.110 | -0.322 | -0.401 |
| Glucose | -0.256 | -0.017 | -0.016 | -0.023 | 0.014 | -0.145 | 0.061 | -0.175 | -0.317 | -0.163 | 0.091 | -0.420 | -0.552 | 0.498 | 0.123 |
| Glycerol | 0.077 | -0.037 | 0.167 | 0.108 | 0.233 | 0.072 | 0.216 | 0.057 | -0.039 | 0.062 | 0.196 | -0.077 | -0.528 | 0.361 | -0.004 |
| Myo-inositol | -0.230 | 0.125 | 0.311 | 0.439 | 0.115 | -0.123 | 0.239 | 0.410 | 0.200 | 0.223 | -0.509 | 0.419 | 0.371 | -0.587 | -0.261 |
| Lactose | 0.062 | 0.144 | -0.071 | -0.046 | -0.145 | -0.075 | -0.159 | 0.072 | 0.131 | -0.102 | -0.017 | 0.208 | 0.159 | -0.185 | -0.061 |
| Maltose | 0.016 | 0.343 | 0.310 | 0.283 | 0.388 | -0.216 | 0.243 | 0.214 | 0.446 | 0.078 | -0.187 | 0.569 | 0.208 | -0.456 | 0.008 |
| Mannitol | 0.290 | -0.559 | 0.663 | 0.502 | 0.633 | 0.566 | 0.684 | 0.401 | 0.467 | 0.804 | 0.065 | 0.130 | -0.041 | -0.052 | -0.139 |
| Mannose | -0.053 | 0.002 | 0.030 | 0.073 | -0.128 | -0.027 | -0.014 | 0.124 | -0.086 | -0.041 | -0.009 | 0.059 | -0.163 | 0.070 | -0.196 |
| Raffinose | 0.192 | -0.145 | -0.225 | 0.030 | -0.284 | 0.259 | -0.091 | 0.225 | -0.525 | 0.003 | 0.151 | -0.057 | -0.412 | 0.257 | -0.331 |
| Ribitol | 0.801 | -0.428 | 0.247 | -0.057 | 0.480 | 0.722 | 0.275 | 0.104 | 0.479 | 0.462 | 0.668 | 0.101 | -0.165 | 0.235 | -0.012 |
| Sorbitol | 0.035 | -0.076 | 0.172 | 0.167 | 0.092 | 0.096 | 0.180 | 0.163 | -0.171 | 0.112 | 0.032 | 0.066 | -0.356 | 0.196 | -0.216 |
| Sucrose | 0.070 | 0.419 | 0.004 | -0.216 | 0.295 | -0.321 | -0.092 | -0.330 | 0.754 | -0.180 | 0.046 | 0.253 | 0.523 | -0.386 | 0.543 |
| Trehalose | 0.294 | -0.361 | 0.455 | -0.260 | 0.739 | 0.216 | 0.430 | -0.508 | 0.420 | 0.314 | 0.402 | -0.571 | 0.076 | 0.288 | 0.618 |
| Xylitol | -0.089 | -0.366 | 0.154 | 0.201 | -0.041 | 0.230 | 0.241 | 0.180 | -0.524 | 0.143 | 0.149 | -0.275 | -0.793 | 0.627 | -0.377 |
| Xylose | -0.123 | -0.266 | -0.063 | 0.241 | -0.268 | 0.251 | 0.083 | 0.379 | -0.796 | 0.081 | -0.088 | -0.155 | -0.568 | 0.341 | -0.608 |

### A4.1.3 Results of MANOVA on the soluble sugars in the endosperm tissues

Three-way MANOVA on the endosperm sugar profiles revealed significant effects of all the main factors (State, Aging, Endophyte) and their two-way interactions (Table A4.10) with all p-values smaller than 0.05.

**Table A4.10 Three-way MANOVA (State x Aging x Endophyte) results for the sugar profiles in the endosperm tissues.**

| Factor | Df | Wilks | F value | p-value | Significance |
|---|---|---|---|---|---|
| Endophyte | 1 | 0.01972 | 36.63 | < 0.0001 | *** |
| Aging | 1 | 0.01853 | 39.03 | < 0.0001 | *** |
| State | 3 | 0.00569 | 3.48 | < 0.0001 | *** |
| Aging x Endophyte | 1 | 0.02285 | 31.52 | < 0.0001 | *** |
| State x Endophyte | 3 | 0.01503 | 2.31 | 0.0026 | ** |
| State x Aging | 3 | 0.01114 | 2.63 | 0.0007 | *** |
| State x Aging x Endophyte | 3 | 0.04068 | 1.44 | 0.1082 | |

Significance codes: ***: < 0.001, **: < 0.01, *: < 0.05.
Df: numerator degrees of freedom; p-value: probability

### A4.1.4 Results of the CDA on the sugar metabolites in the endosperm tissues

Based on the CDA plot of the interaction between state and endophyte in the sugars of the endosperm tissues, the first two canonical discriminant functions (accounted for 74.0% and 18.3% of the total variation, respectively) separated the dry endosperm tissues infected by the three endophytes from imbibed ones. The sugars which were abundant in dry endophyte-infected endosperm tissues included D-arabitol, DL-arabinose, fructose, galactose, glucose, myo-inositol, raffinose, sorbitol, xylitol and xylose, whereas maltose was highly concentrated in the imbibed endosperm tissues of both endophyte-free and endophyte-infected (Figure A4.6a, Table A4.11).

The two canonical discriminant functions (explained 57.4% and 28.1 of the total variation, respectively) from the interactions between aging and endophyte state

separated aged endophyte-free and endophyte-infected endosperm tissues from non-aged endophyte-free and endophyte-infected endosperm tissues. The two-dimension CDA plot revealed that there were more maltose and trehalose in the non-aged and more DL-arabinose, fructose, glucose, myo-inositol, raffinose, xylitol and xylose in the aged endosperm tissues (Figure A4.6b, Table A4.11).

CDA plot on the main effect of endophytes showed that there were more mannitol and ribitol in the endophyte-infected compared to the endophyte-free endosperm tissues (Figure A4.6c, Table A4.11).

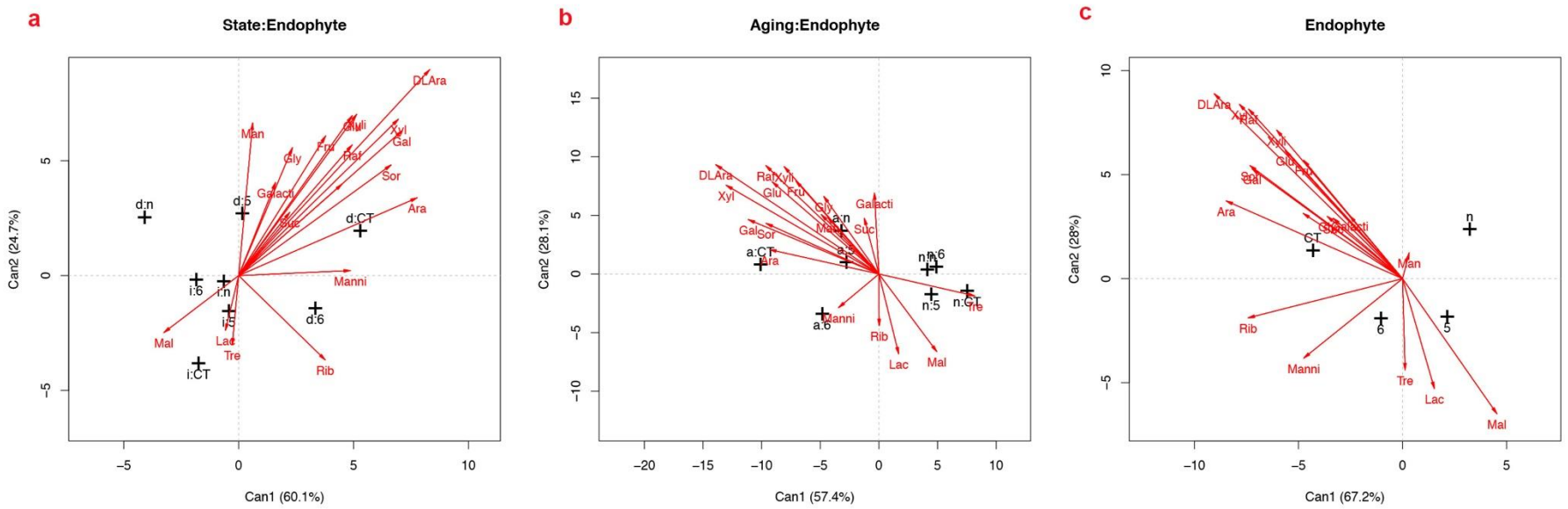


**Figure A4.6 Biplot graph showing the first two canonical functions (Can1 and Can2) obtained in a CDA of the sugar profiles in the endosperm tissues applied to (a) State x Endophyte interaction, (b) Aging x Endophyte interaction and (c) Endophyte.** Vectors illustrate variables that strongly loaded for each treatment and + sign is the centroid of each treatment score. In (a), the first letter under the + sign denotes the seed state (d = dry, i = imbibed). In (b), the first letter under the + sign denotes AA (n = non-accelerated aged, a = accelerated aged). The second letter in (a) and (b), and the only letter in (c) under the + sign denote different endophyte treatment (0: endophyte-free, 5: AR584, 6: AR605, CT: common-toxic). Ara = D-arabitol, DLAra = DL-arabinose, Fru = fructose, Galacti = galactinol, Gal = D-galactose, Glu = glucose, Gly = glycerol, Ino = myo-inositol, Mal = maltose, Manni = mannitol, Raf = raffinose, Rib = ribitol, Sor = sorbitol, Suc = sucrose, Tre = trehalose, Xyli = xylitol, Xyl = xylose.

CDA plot on the State x Aging interaction and the main effects of the seed state and aging revealed a separation of dry and AA groups of endosperm tissues from the other three groups. The sugars which were highly loaded in the dried-AA groups included D-arabitol, DL-arabinose, fructose, D-galactose, glucose, glycerol, myo-inositol, raffinose, sorbitol, xylitol and xylose, but were lack in maltose and trehalose (Figure A4.7a, A4.7b and A4.7c; Table A4.11).

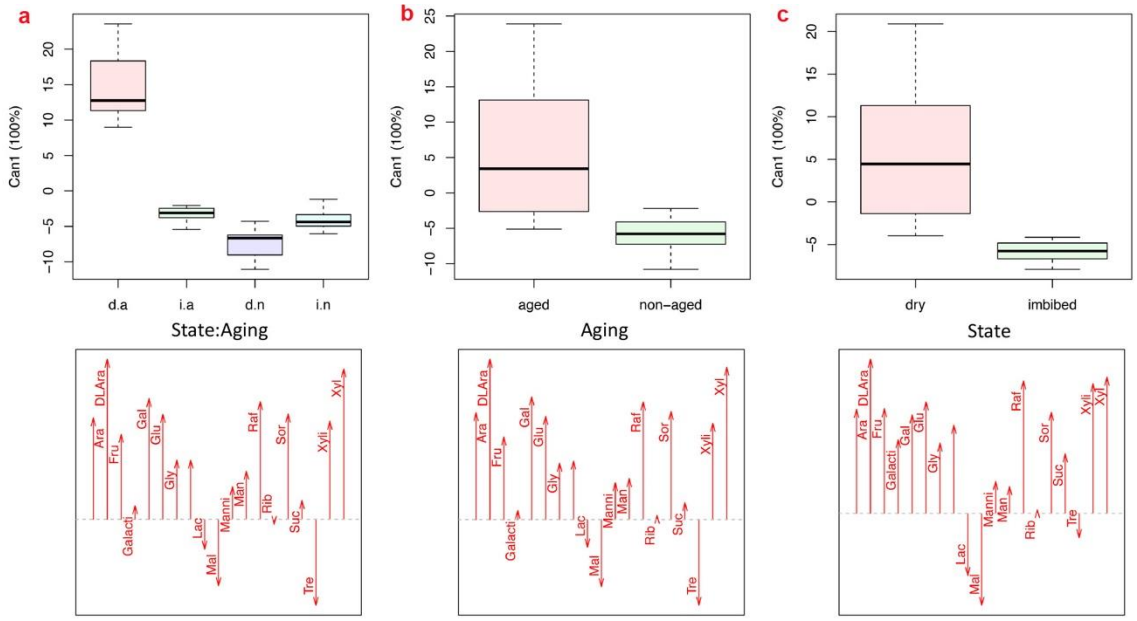


**Figure A4.7 CDA for the State x Aging interaction and the main effects of aging and state on the sugar profiles in the endosperm tissues.** The upper panel shows the canonical scores under each treatment while the lower panel shows the structure coefficients of each sugar variant in the embryo tissues. The first letter in (a) and the only letter in (c) on the x-axis denotes seed state (d = dry, i = imbibed). The second letter in (a) and the only letter in (b) denotes AA treatment (n = non-accelerated aged, a = accelerated aged). Ara = D-arabitol, DLAra = DL-arabinose, Fru = fructose, Galacti = galactinol, Gal = D-galactose, Glu = glucose, Gly = glycerol, Ino = myo-inositol, Mal = maltose, Manni = mannitol, Raf = raffinose, Rib = ribitol, Sor = sorbitol, Suc = sucrose, Tre = trehalose, Xyli = xylitol, Xyl = xylose.

**Table A4.11 Results of the structure coefficients ($r_s$) in the CDA of each significant experimental factor and the significant two-way interactions based on CDA of selected sugar metabolites in the endosperm tissues.** For emphasis, structure coefficients above |0.30|% were underlined.

| | State x Endophyte | | | Aging x Endophyte | | | Endophyte | | | State x Aging | State | Aging |
|---|---|---|---|---|---|---|---|---|---|---|---|---|
| | $r_s$ 1 | $r_s$ 2 | $r_s$ 3 | $r_s$ 1 | $r_s$ 2 | $r_s$ 3 | $r_s$ 1 | $r_s$ 2 | $r_s$ 3 | $r_s$ 1 | $r_s$ 1 | $r_s$ 1 |
| Variation (%) | 60.1 | 24.7 | 15.2 | 73.7 | 21.8 | 4.5 | 61.2 | 34.9 | 3.9 | 100 | 100 | 100 |
| D-arabitol | 0.647 | 0.282 | -0.555 | -0.582 | 0.130 | -0.497 | -0.652 | 0.287 | 0.106 | 0.559 | 0.602 | 0.583 |
| DL-arabinose | 0.692 | 0.747 | -0.795 | -0.869 | 0.583 | -0.543 | -0.696 | 0.684 | 0.437 | 0.881 | 0.890 | 0.873 |
| Fructose | 0.315 | 0.507 | -0.432 | -0.443 | 0.496 | -0.521 | -0.365 | 0.438 | 0.422 | 0.468 | 0.605 | 0.450 |
| Galactinol | 0.134 | 0.338 | -0.007 | -0.024 | 0.432 | -0.448 | -0.195 | 0.232 | 0.767 | 0.075 | 0.426 | 0.050 |
| D-galactose | 0.592 | 0.525 | -0.642 | -0.696 | 0.290 | -0.264 | -0.556 | 0.405 | 0.171 | 0.665 | 0.569 | 0.668 |
| Glucose | 0.411 | 0.580 | -0.534 | -0.568 | 0.491 | -0.497 | -0.434 | 0.473 | 0.337 | 0.578 | 0.644 | 0.562 |
| Glycerol | 0.195 | 0.464 | -0.241 | -0.294 | 0.414 | -0.237 | -0.278 | 0.230 | 0.393 | 0.327 | 0.406 | 0.307 |
| Myo-inositol | 0.374 | 0.331 | -0.230 | -0.307 | 0.317 | -0.380 | -0.367 | 0.241 | 0.559 | 0.326 | 0.509 | 0.319 |
| Lactose | -0.048 | -0.198 | 0.125 | 0.105 | -0.425 | 0.347 | 0.118 | -0.406 | -0.468 | -0.165 | -0.358 | -0.150 |
| Maltose | -0.271 | -0.207 | 0.308 | 0.309 | -0.414 | 0.486 | 0.349 | -0.500 | -0.473 | -0.366 | -0.530 | -0.366 |
| Mannitol | 0.405 | 0.018 | -0.142 | -0.215 | -0.179 | -0.290 | -0.365 | -0.294 | -0.030 | 0.179 | 0.185 | 0.200 |
| Mannose | 0.051 | 0.554 | -0.267 | -0.273 | 0.301 | -0.023 | 0.025 | 0.095 | -0.185 | 0.265 | 0.155 | 0.224 |
| Raffinose | 0.411 | 0.474 | -0.700 | -0.603 | 0.578 | -0.823 | -0.569 | 0.627 | 0.103 | 0.648 | 0.766 | 0.641 |
| Ribitol | 0.314 | -0.306 | -0.038 | 0.001 | -0.275 | -0.237 | -0.571 | -0.145 | -0.074 | -0.028 | 0.022 | 0.023 |
| Sorbitol | 0.553 | 0.402 | -0.597 | -0.601 | 0.270 | -0.433 | -0.564 | 0.418 | 0.217 | 0.580 | 0.584 | 0.589 |
| Sucrose | 0.185 | 0.229 | -0.125 | -0.078 | 0.298 | -0.401 | -0.256 | 0.223 | 0.384 | 0.104 | 0.345 | 0.092 |
| Trehalose | -0.023 | -0.251 | 0.477 | 0.511 | -0.117 | -0.196 | 0.009 | -0.337 | 0.429 | -0.474 | -0.140 | -0.467 |
| Xylitol | 0.428 | 0.585 | -0.477 | -0.505 | 0.572 | -0.553 | -0.465 | 0.549 | 0.598 | 0.540 | 0.750 | 0.524 |
| Xylose | 0.579 | 0.567 | -0.836 | -0.814 | 0.473 | -0.522 | -0.603 | 0.645 | 0.162 | 0.828 | 0.787 | 0.830 |

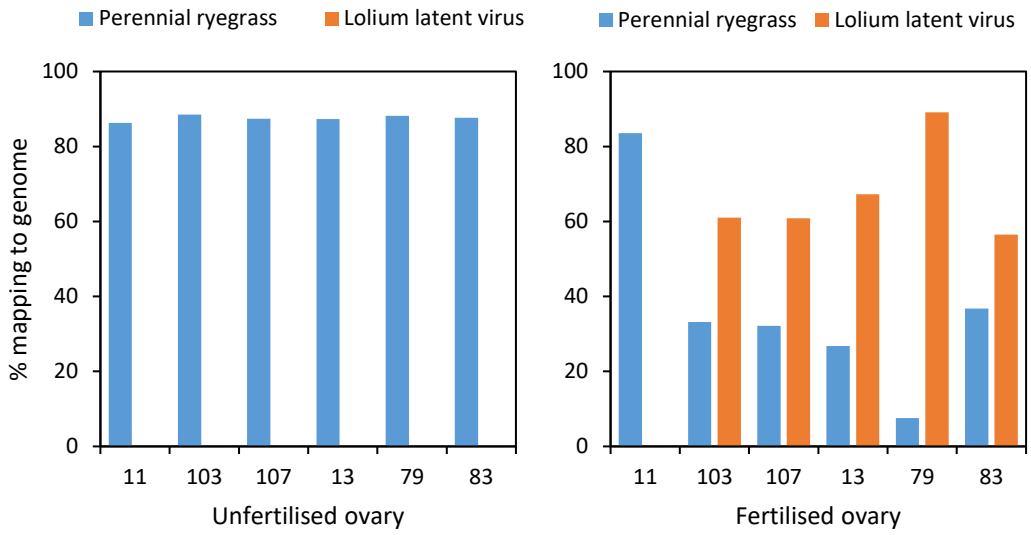


**Figure A6.1 Proportions of reads mapping to the genome of perennial ryegrass and *Lolium* latent virus in unfertilised and fertilised ovary tissues.**

**Table A6.1 List of DEGs between the HT and LT genotypes that can be considered as candidate genes involved in response to endophyte transmission efficiency in both the inflorescence primordia and ovary but have no annotations with rice or *Arabidopsis thaliana*[1].**

11 out of 37 common elements in 'IP: HT-LT' and 'Ov: HT-LT':

| | $Log_2^{FC}$ | | | |
|---|---|---|---|---|
| Gene | IP: HT-LT | Ov: HT-LT | HT: Ov-IP | LT: Ov-IP |
| ms_80\|ref0023173-eeg-1.1 | **-9.90** | **-7.88** | 2.05 | 0.03 |
| ms_14024\|ref0036536-eeg-0.1 | **-7.17** | **-6.88** | 0.38 | 0.09 |
| ms_18650\|ref0017274-eeg-0.0 | **-6.92** | **-6.62** | 0.24 | -0.06 |
| ms_16780\|ref0028190-eeg-0.0 | **-6.80** | **-5.68** | 1.05 | -0.07 |
| ms_7817\|ref0012680-eeg-0.0 | **-5.86** | **-3.67** | **4.36** | **2.17** |
| ms_21050\|ref0039844-eeg-0.0 | **-5.10** | **-3.92** | 2.08 | 0.90 |
| ms_2473\|ref0029525-eeg-0.1 | **-3.00** | **-2.87** | 0.87 | 0.75 |
| ms_518\|ref0037018-eeg-0.0 | **6.89** | **4.83** | 0.19 | 2.25 |
| ms_15332\|ref0037037-eeg-0.0 | **7.08** | **3.31** | -0.59 | **3.18** |
| ms_1752\|ref0026070-eeg-0.3 | **8.65** | **6.52** | 0.48 | 2.62 |
| ms_454\|ref0014069-eeg-0.2 | **11.70** | **6.95** | 0.03 | **4.78** |

In the 'Gene' column, ms = maker-scaffold; eeg = exonerate_est2genome-gene.

[1]'$Log_2^{FC}$ IP: HT-LT' and '$Log_2^{FC}$ Ov: HT-LT' denote the $log_2$ $^{fold\ change\ (FC)}$ of the gene expression in the high-transmission (HT) relative to low-transmission (LT) genotype in the inflorescence primordia (IP) and ovary (Ov), respectively. '$Log_2^{FC}$ HT: Ov-IP' and '$Log_2^{FC}$ LT: Ov-IP' denote the $log_2^{FC}$ of the gene expression in the Ov relative to IP in the HT and LT genotypes, respectively. The significantly up-regulated genes were marked bold red while the down-regulated genes were marked bold green.

**Table A6.2 List of DEGs that can be considered as candidate genes involved in response to endophyte transmission efficiency in only the inflorescence primordia but have no annotations with rice or *Arabidopsis thaliana*[1].**

14 out of 41 elements included exclusively in 'IP: HT-LT':

| Gene | $Log_2^{FC}$ | | | |
|---|---|---|---|---|
| | IP: HT-LT | Ov: HT-LT | HT: Ov-IP | LT: Ov-IP |
| ms_813\|ref0040416-eeg-0.1 | **-10.06** | -6.69 | 2.99 | -0.37 |
| ms_3044\|ref0007391-eeg-0.5 | **-7.68** | -5.72 | 1.50 | -0.45 |
| ms_9900\|ref0010501-eeg-0.0 | **-6.99** | -4.04 | 2.49 | -0.46 |
| ms_13974\|ref0019127-eeg-0.2 | **-6.00** | -3.28 | **2.46** | -0.26 |
| ms_6498\|ref0037249-eeg-0.0 | **-1.34** | -0.73 | **1.35** | **0.74** |
| ms_16646\|ref0040011-eeg-0.0 | **3.60** | 4.04 | **-1.55** | -1.99 |
| ms_37632\|ref0011570-eeg-0.0 | **5.17** | 2.14 | -0.77 | **2.27** |
| ms_8207\|ref0040444-eeg-0.1 | **6.27** | 3.83 | -1.47 | 0.98 |
| ms_4075\|ref0004435-eeg-0.1 | **7.73** | 5.11 | -0.83 | 1.79 |
| ms_4075\|ref0004435-eeg-0.0 | **7.88** | 4.32 | **-2.73** | 0.84 |
| ms_32444\|ref0035426-eeg-0.0 | **8.13** | 5.45 | **-1.66** | 1.02 |
| ms_2562\|ref0030976-eeg-0.1 | **9.72** | 7.09 | -0.15 | 2.47 |
| ms_4681\|ref0044387-eeg-0.2 | **10.22** | 5.53 | **-3.24** | 1.45 |
| ms_4681\|ref0044387-eeg-0.1 | **11.90** | 6.71 | **-1.35** | 3.83 |

In the 'Gene' column, ms = maker-scaffold; eeg = exonerate_est2genome-gene.
[1]'$Log_2^{FC}$ IP: HT-LT' and '$Log_2^{FC}$ Ov: HT-LT' denote the $log_2$ fold change (FC) of the gene expression in the high-transmission (HT) relative to low-transmission (LT) genotype in the inflorescence primordia (IP) and ovary (Ov), respectively. '$Log_2^{FC}$ HT: Ov-IP' and '$Log_2^{FC}$ LT: Ov-IP' denote the $log_2^{FC}$ of the gene expression in the Ov relative to IP in the HT and LT genotypes, respectively. The significantly up-regulated genes were marked bold red while the down-regulated genes were marked bold green.

**Table A6.3 List of DEGs that can be considered as candidate genes involved in response to endophyte transmission efficiency in only the ovary but have no annotations with rice or *Arabidopsis thaliana*[1].**

5 out of 24 elements included exclusively in 'Ov: HT-LT':

| Gene | $Log_2^{FC}$ | | | |
|---|---|---|---|---|
| | IP: HT-LT | Ov: HT-LT | HT: Ov-IP | LT: Ov-IP |
| ms_4127\|ref0021745-eeg-0.2 | -3.32 | **-3.21** | **1.49** | 1.39 |
| ms_48\|ref0001314-eeg-1.3 | -1.97 | **-2.01** | **1.44** | **1.48** |
| ms_1445\|ref0021161-eeg-0.1 | 2.03 | **2.35** | **1.76** | **1.45** |
| ms_5692\|ref0000054-eeg-0.0 | -0.14 | **4.19** | **9.09** | **4.76** |
| ms_8426\|ref0009331-eeg-0.0 | -0.14 | **5.35** | **9.86** | **4.37** |

In the 'Gene' column, ms = maker-scaffold; eeg = exonerate_est2genome-gene.
[1]'$Log_2^{FC}$ IP: HT-LT' and '$Log_2^{FC}$ Ov: HT-LT' denote the $log_2$ fold change (FC) of the gene expression in the high-transmission (HT) relative to low-transmission (LT) genotype in the inflorescence primordia (IP) and ovary (Ov), respectively. '$Log_2^{FC}$ HT: Ov-IP' and '$Log_2^{FC}$ LT: Ov-IP' denote the $log_2^{FC}$ of the gene expression in the Ov relative to IP in the HT and LT genotypes, respectively. The significantly up-regulated genes were marked bold red while the down-regulated genes were marked bold green.

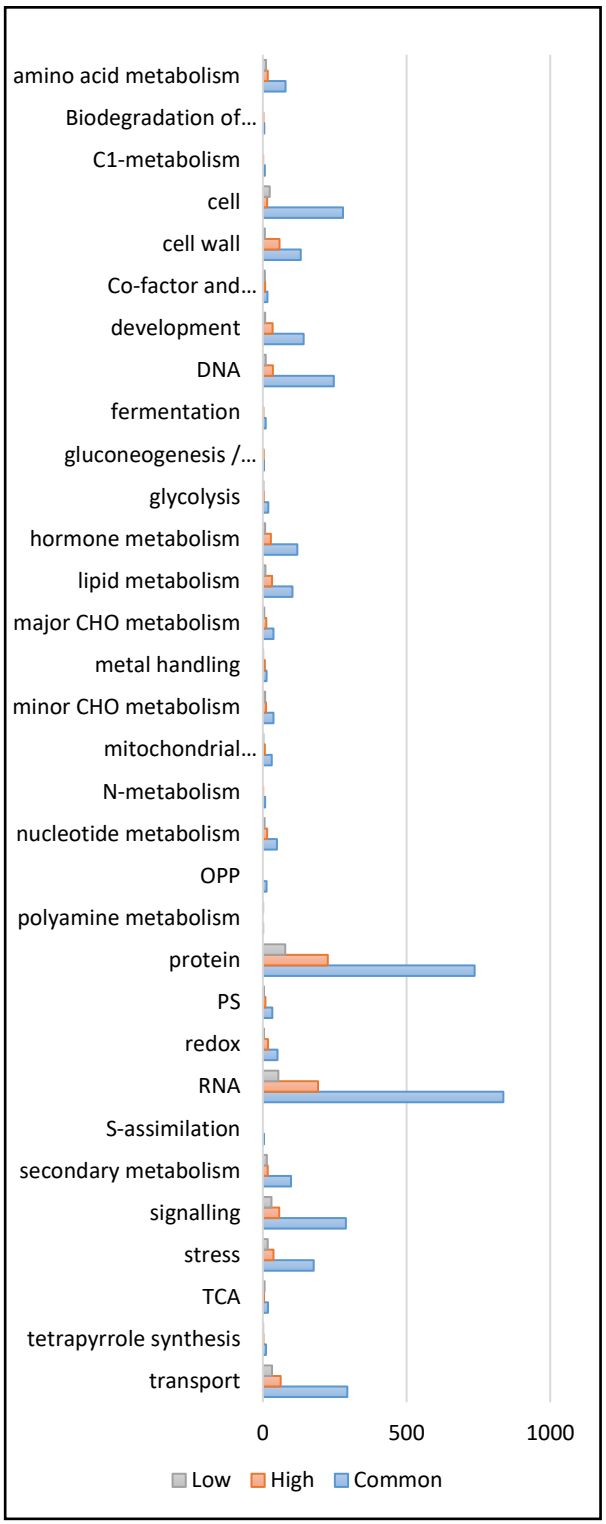


**Figure A6.2 Mercator analysis on the DEGs between the inflorescence primordia and ovary in both the HT and LT genotypes (blue column), only in HT genotype (orange column), and only in LT genotypes (grey column).**

## References


Abdul-Baki AA, Anderson JD 1970. Viability and leaching of sugars from germinating barley. Crop Science 10: 31-34.

Afkhami ME, Rudgers JA 2008. Symbiosis lost: imperfect vertical transmission of fungal endophytes in grasses. The American Naturalist 172: 405-416.

Alderman S, Pfender W, Welty R et al. 1997. First report of choke, caused by *Epichloë typhina*, on orchardgrass in Oregon. Plant Disease 81: 1335-1335.

Alkan N, Gadkar V, Yarden O, Kapulnik Y 2006. Analysis of quantitative interactions between two species of arbuscular mycorrhizal fungi, *Glomus mosseae* and *G. intraradices*, by real-time PCR. Applied and Environmental Microbiology 72: 4192-4199.

Ambrose KV, Belanger FC 2012. SOLiD-SAGE of endophyte-infected red fescue reveals numerous effects on host transcriptome and an abundance of highly expressed fungal secreted proteins. PLoS One 7: e53214.

Anderson L 1973. Relative performance of the late-flowering tetraploid red clover 'Grasslands 4706', five diploid red clovers, and white clover. New Zealand Journal of Experimental Agriculture 1: 233-237.

Anderson L 1982. 'Grasslands Roa' tall fescue (*Festuca arundinacea* Schreb.). New Zealand Journal of Experimental Agriculture 10: 269-273.

Aoki N, Scofield GN, Wang X-D, Offler CE, Patrick JW, Furbank RT 2006. Pathway of sugar transport in germinating wheat seeds. Plant Physiology 141: 1255-1263.

Assuero SG, Matthew C, Agnusdei MG. 2001. Leaf elongation rate of mediterranean and temperate tall fescue cultivars under water deficit. In: International Grassland Congress. Sao Paulo, Brazil.

Ayliffe M, Periyannan SK, Feechan A et al. 2013. A simple method for comparing fungal biomass in infected plant tissues. Molecular Plant-Microbe Interactions 26: 658-667.

Bacon CW 1993. Abiotic stress tolerances (moisture, nutrients) and photosynthesis in endophyte-infected tall fescue. Agriculture, Ecosystems & Environment 44: 123-141.

Bacon CW, White J 2000. Microbial Endophytes. New York, USA, Marcel Dekker.

Badaruddin M, Holcombe LJ, Wilson RA, Wang Z, Kershaw MJ, Talbot NJ 2013. Glycogen metabolic genes are involved in trehalose-6-phosphate synthase-mediated regulation of pathogenicity by the rice blast fungus *Magnaporthe oryzae*. PLoS Pathogens 9: e1003604.

Bago B, Pfeffer PE, Abubaker J et al. 2003. Carbon export from arbuscular mycorrhizal roots involves the translocation of carbohydrate as well as lipid. Plant Physiology 131: 1496-1507.

Bailly C 2004. Active oxygen species and antioxidants in seed biology. Seed Science Research 14: 93-107.

Ball O-P, Barker G, Prestidge R, Lauren D 1997. Distribution and accumulation of the alkaloid peramine in *Neotyphodium lolii*-infected perennial ryegrass. Journal of Chemical Ecology 23: 1419-1434.

Barrow J 2003. Atypical morphology of dark septate fungal root endophytes of *Bouteloua* in arid southwestern USA rangelands. Mycorrhiza 13: 239-247.

Bastías DA, Martínez-Ghersa MA, Ballaré CL, Gundel PE 2017. *Epichloë* fungal endophytes and plant defenses: not just alkaloids. Trends in Plant Science 22: 939-948.

Bastías DA, Alejandra Martínez-Ghersa M, Newman JA, Card SD, Mace WJ, Gundel PE 2018. The plant hormone salicylic acid interacts with the mechanism of anti-herbivory conferred by fungal endophytes in grasses. Plant, Cell & Environment 41: 395-405.

Bell W, Klaassen P, Ohnacker M et al. 1992. Characterization of the 56-kDa subunit of yeast trehalose-6-phosphate synthase and cloning of its gene reveal its identity with the

product of CIF1, a regulator of carbon catabolite inactivation. The FEBS Journal 209: 951-959.
Benaroudj N, Lee DH, Goldberg AL 2001. Trehalose accumulation during cellular stress protects cells and cellular proteins from damage by oxygen radicals. Journal of Biological Chemistry 276: 24261-24267.
Benjamini Y, Yekutieli D 2001. The control of the false discovery rate in multiple testing under dependency. Annals of Statistics 29: 1165-1188.
Bernal-Lugo I, Leopold AC 1992. Changes in soluble carbohydrates during seed storage. Plant Physiology 98: 1207-1210.
Bernier G, Périlleux C 2005. A physiological overview of the genetics of flowering time control. Plant Biotechnology Journal 3: 3-16.
Berry D, Takach JE, Schardl CL, Charlton ND, Scott B, Young CA 2015. Disparate independent genetic events disrupt the secondary metabolism gene perA in certain symbiotic *Epichloë* species. Applied and Environmental Microbiology 81: 2797-2807.
Bhardwaj AR, Joshi G, Kukreja B et al. 2015. Global insights into high temperature and drought stress regulated genes by RNA-Seq in economically important oilseed crop *Brassica juncea*. BMC Plant Biology 15: 9.
Birtić S, Kranner I 2006. Isolation of high-quality RNA from polyphenol-, polysaccharide- and lipid-rich seeds. Phytochemical Analysis 17: 144-148.
Blanche C, Elam W, Hodges J 1990. Accelerated aging of *Quercus nigra* seed: biochemical changes and applicability as a vigor test. Canadian Journal of Forest Research 20: 1611-1615.
Blilou I, Ocampo JA, García-Garrido JM 1999. Resistance of pea roots to endomycorrhizal fungus or *Rhizobium* correlates with enhanced levels of endogenous salicylic acid. Journal of Experimental Botany 50: 1663-1668.
Bluett S, Thom E, Clark D, Macdonald K, Minneé E 2005. Effects of perennial ryegrass infected with either AR1 or wild endophyte on dairy production in the Waikato, New Zealand Journal of Agricultural Research 48: 197-212.
Böhm J, Hahn A, Schubert R et al. 1999. Real-time quantitative PCR: DNA determination in isolated spores of the mycorrhizal fungus *Glomus mosseae* and monitoring of *Phytophthora infestans* and *Phytophthora citricola* in their respective host plants. Journal of Phytopathology 147: 409-416.
Bouton J, Latch G, Hill N et al. 2002. Reinfection of tall fescue cultivars with non-ergot alkaloid-producing endophytes. Agronomy Journal 94: 567-574.
Breen J 1994. *Acremonium* endophyte interactions with enhanced plant resistance to insects. Annual Review of Entomology 39: 401-423.
Brenner S, Johnson M, Bridgham J et al. 2000. Gene expression analysis by massively parallel signature sequencing (MPSS) on microbead arrays. Nature Biotechnology 18: 630.
Brock J 1983. 'Grasslands Roa'tall fescue: a review. Proceedings of New Zealand Grassland Association 44: 56-60.
Brosi GB, McCulley RL, Bush LP, Nelson JA, Classen AT, Norby RJ 2011. Effects of multiple climate change factors on the tall fescue–fungal endophyte symbiosis: infection frequency and tissue chemistry. New Phytologist 189: 797-805.
Brundrett MC 2006. Understanding the roles of multifunctional mycorrhizal and endophytic fungi. In: Schulz B, Boyle C, Sieber T ed. Microbial Root Endophytes. Berlin, Germany, Springer. Pp. 281-298.
Bultman TL, Leuchtmann A 2008. Biology of the *Epichloë–Botanophila* interaction: an intriguing association between fungi and insects. Fungal Biology Reviews 22: 131-138.
Bush L, Fannin F, Siegel M, Dahlman D, Burton H 1993. Chemistry, occurrence and biological effects of saturated pyrrolizidine alkaloids associated with endophyte-grass interactions. Agriculture, Ecosystems & Environment 44: 81-102.

Bylin A, Card S, Hume D, Lloyd-West C, Huss-Danell K 2016. Endophyte storage and seed germination of *Epichloë*-infected meadow fescue. Seed Science and Technology 44: 138-155.

Byrne SL, Nagy I, Pfeifer M et al. 2015. A synteny-based draft genome sequence of the forage grass *Lolium perenne*. The Plant Journal 84: 816-826.

Calabrese S, Kohler A, Niehl A, Veneault-Fourrey C, Boller T, Courty P-E 2017. Transcriptome analysis of the *Populus trichocarpa–Rhizophagus irregularis* mycorrhizal symbiosis: regulation of plant and fungal transportomes under nitrogen starvation. Plant and Cell Physiology 58: 1003-1017.

Camacho C, Coulouris G, Avagyan V et al. 2009. BLAST+: architecture and applications. BMC Bioinformatics 10: 421.

Card SD, Rolston M, Park Z, Cox N, Hume D 2011. Fungal endophyte detection in pasture grass seed utilising the infection layer and comparison to other detection techniques. Seed Science and Technology 39: 581-592.

Card SD, Tapper B, Lloyd-West C, Wright K 2013. Assessment of fluorescein-based fluorescent dyes for tracing *Neotyphodium* endophytes in planta. Mycologia 105: 221-229.

Card SD, Johnson L, de Bonth A et al. 2014a. *Epichloë* endophytes from cool season grasses–reaping the rewards from a well-tuned bio-prospecting pipeline. The 10th International Mycological Congress.

Card SD, Rolston MP, Lloyd-West C, Hume DE 2014b. Novel perennial ryegrass-*Neotyphodium* endophyte associations: relationships between seed weight, seedling vigour and endophyte presence. Symbiosis 62: 51-62.

Card SD, Faville MJ, Simpson WR et al. 2014c. Mutualistic fungal endophytes in the Triticeae–survey and description. FEMS Microbiology Ecology 88: 94-106.

Card SD 2015. Sowing the seeds for success: utilization of endophytes in the future of agriculture. BIT's 6th World Gene Convention. Qingdao, China.

Card SD, Johnson LJ, Teasdale S, Caradus J 2016. Deciphering endophyte behaviour: the link between endophyte biology and efficacious biological control agents. FEMS Microbiology Ecology 92: fiw114.

Carvalhais LC, Dennis PG, Fedoseyenko D, Hajirezaei MR, Borriss R, von Wirén N 2011. Root exudation of sugars, amino acids, and organic acids by maize as affected by nitrogen, phosphorus, potassium, and iron deficiency. Journal of Plant Nutrition and Soil Science 174: 3-11.

Chanway C 1996. Endophytes: they're not just fungi!. Canadian Journal of Botany 74: 321-322.

Charlton J, Stewart A 1999. Pasture species and cultivars used in New Zealand-a list. Proceedings of New Zealand Grassland Association 61: 147-166.

Charlton ND, Craven KD, Mittal S, Hopkins AA, Young CA 2012. *Epichloë canadensis*, a new interspecific epichloid hybrid symbiotic with Canada wildrye (*Elymus canadensis*). Mycologia 104: 1187-1199.

Chaves MM, Maroco JP, Pereira JS 2003. Understanding plant responses to drought—from genes to the whole plant. Functional Plant Biology 30: 239-264.

Chen N, Hsiang T, Goodwin P 2003. Use of green fluorescent protein to quantify the growth of *Colletotrichum* during infection of tobacco. Journal of Microbiological Methods 53: 113-122.

Chen Y, Ji Y, Yu H, Wang Z 2009. A new *Neotyphodium* species from *Festuca parvigluma* Steud. grown in China. Mycologia 101: 681-685.

Cheplick G 2007. Costs of fungal endophyte infection in *Lolium perenne* genotypes from Eurasia and North Africa under extreme resource limitation. Environmental and Experimental Botany 60: 202-210.

Cheplick GP 2017. Persistence of endophytic fungi in cultivars of *Lolium perenne* grown from seeds stored for 22 years. American Journal of Botany 104: 627-631.

Christensen MJ 1996. Antifungal activity in grasses infected with *Acremonium* and *Epichloë* endophytes. Australasian Plant Pathology 25: 186-191.
Christensen MJ, Bennett RJ, Schmid J 2002. Growth of *Epichloë*/*Neotyphodium* and p-endophytes in leaves of *Lolium* and *Festuca* grasses. Mycological Research 106: 93-106.
Christensen MJ, Voisey C R 2007. The biology of the endophyte/grass partnership. Proceedings of the 6th International Symposium on Fungal Endophytes of Grasses. Pp. 123-133.
Christensen MJ, Bennett R, Ansari H et al. 2008. *Epichloë* endophytes grow by intercalary hyphal extension in elongating grass leaves. Fungal Genetics and Biology 45: 84-93.
Christensen MJ, Voisey CR 2009. Tall fescue–endophyte symbiosis. USA, American Society of Agronomy, Crop Science of America, Soil Science Society of America. 251-272 p.
Chung K-R, Schardl CL 1997. Sexual cycle and horizontal transmission of the grass symbiont, *Epichloë typhina*. Mycological Research 101: 295-301.
Chynoweth R, Rolston M, Kelly M, Grbavac N 2012. Control of blind seed disease (*Gloeotinia temulenta*) in perennial ryegrass (*Lolium perenne*) seed crops and implications for endophyte transmission. Agronomy New Zealand 42: 141-148.
Clark S, Harris C 2009. Summer dormancy in Australian perennial grasses: Historical background, a simulation study, and current research. Crop Science 49: 2328-2334.
Clay K, Cheplick GP, Marks S 1989. Impact of the fungus *Balansia henningsiana* on *Panicum agrostoides*: frequency of infection, plant growth and reproduction, and resistance to pests. Oecologia 80: 374-380.
Clay K, Holah J 1999. Fungal endophyte symbiosis and plant diversity in successional fields. Science 285: 1742-1744.
Clay K, Schardl C 2002. Evolutionary origins and ecological consequences of endophyte symbiosis with grasses. The American Naturalist 160: S99-S127.
Clay K, Holah J, Rudgers JA 2005. Herbivores cause a rapid increase in hereditary symbiosis and alter plant community composition. Proceedings of the National Academy of Sciences of the United States of America 102: 12465-12470.
Conesa A, Götz S 2008. Blast2GO: A comprehensive suite for functional analysis in plant genomics. International Journal of Plant Genomics 2008: 619832.
Cook D, Gardner DR, Welch KD, Roper JM, Ralphs MH, Green BT 2009a. Quantitative PCR method to measure the fungal endophyte in locoweeds. Journal of Agricultural and Food Chemistry 57: 6050-6054.
Cook D, Gardner DR, Ralphs MH, Pfister JA, Welch KD, Green BT 2009b. Swainsoninine concentrations and endophyte amounts of *Undifilum oxytropis* in different plant parts of *Oxytropis sericea*. Journal of Chemical Ecology 35: 1272.
Cook D, Shi L, Gardner DR et al. 2012. Influence of phenological stage on swainsonine and endophyte concentrations in *Oxytropis sericea*. Journal of Chemical Ecology 38: 195-203.
Cookson W, Rowarth J, Sedcole J 2001. Seed vigour in perennial ryegrass (*Lolium perenne* L.): effect and cause. Seed Science and Technology 29: 255-270.
Coulter DB, Aronson JM 1977. Glycogen and other soluble glucans from Chytridiomycete and Oomycete species. Archives of Microbiology 115: 317-322.
Crowe JH, Crowe LM 1986. Stabilization of membranes in anhydrobiotic organisms. In: Leopold AC ed. Membranes, Metabolism and Dry Organisms. New York, USA, Comstock Publishing Associates. Pp. 188-209.
Cruz-Castillo J, Ganeshanandam S, MacKay B, Lawes G, Lawoko C, Woolley D 1994. Applications of canonical discriminant analysis in horticultural research. HortScience 29: 1115-1119.
Cunningham IJ 1958. Non-toxicity to animals of ryegrass endophyte and other endophytic fungi of New Zealand grasses. New Zealand Journal of Agricultural Research 1: 489-497.
Darkoh C, Comer L, Zewdie G, Harold S, Snyder N, DuPont HL 2014. Chemotactic chemokines are important in the pathogenesis of irritable bowel syndrome. PLoS One 9: e93144.
De Bary A 1866. Morphologie und physiologie der pilze, flechten und myxomyceten. Leipzig, Germany, Engelmann.

de Bonth A, Card S, Briggs L et al. 2015. Fungal foray: the pursuit of beneficial endophyte strains for Australasian pastures. 9th International Symposium on Fungal Endophytes of Grasses (ISFEG 2015) and International Symposium on Plant Microbiomes (ISPM 2015). Melbourne, Australia.

Di Giacomo E, Laffont C, Sciarra F, Iannelli MA, Frugier F, Frugis G 2017. KNAT3/4/5-like class 2 KNOX transcription factors are involved in *Medicago truncatula* symbiotic nodule organ development. New Phytologist 213: 822-837.

Ding H, Xu R 1999. Differentiation of beef and kangaroo meat by visible/near-infrared reflectance spectroscopy. Journal of Food Science 64: 814-817.

Dinkins RD, Barnes A, Waters W 2010. Microarray analysis of endophyte-infected and endophyte-free tall fescue. Journal of Plant Physiology 167: 1197-1203.

Dinkins RD, Nagabhyru P, Graham MA, Boykin D, Schardl CL 2017. Transcriptome response of *Lolium arundinaceum* to its fungal endophyte *Epichloë coenophiala*. New Phytologist 213: 324-337.

do Valle Ribeiro MA 1993. Transmission and survival of *Acremonium* and the implications for grass breeding. Agriculture, Ecosystems & Environment 44: 195-213.

Dobin A, Davis CA, Schlesinger F et al. 2013. STAR: ultrafast universal RNA-seq aligner. Bioinformatics 29: 15-21.

Dos Reis SF, Pessôa LM, Strauss RE 1990. Application of size-free canonical discriminant analysis to studies of geographic differentiation. Revista Brasileira de Genética 13: 509-520.

Doss R, Clement SL, Kuy SR, Welty RE 1995. A PCR-based technique for detection of Neotyphodium endophytes in diverse accessions of tall fescue. Plant Disease 82: 738-740.

Dupont PY, Eaton CJ, Wargent JJ et al. 2015. Fungal endophyte infection of ryegrass reprograms host metabolism and alters development. New Phytologist 208: 1227-1240.

Eason WR, Webb K, Michaelson-Yeates T et al. 2001. Effect of genotype of *Trifolium repens* on mycorrhizal symbiosis with *Glomus mosseae*. The Journal of Agricultural Science 137: 27-36.

Easton H 1983. Ryegrasses. In: Wratt G, Smith H ed. Plant Breeding in New Zealand. Wellington, New Zealand, Butterworths/DSIR. Pp. 229-236.

Easton H, Lane G, Tapper B et al. 1996. Ryegrass endophyte-related heat stress in cattle. Proceedings of the New Zealand Grassland Association 57: 37-41.

Easton H 1999. Endophyte in New Zealand ryegrass pastures, an overview. In: Woodfield D, Matthew C ed. Ryegrass Endophyte: an Essential New Zealand Symbiosis. Grassland Research and Practice Series 7. Pp. 1-9.

Easton H, Fletcher L 2007. The importance of endophyte in agricultural systems–changing plant and animal productivity. In: Popay A, Thom E ed. Proceedings of the 6th International Symposium on Fungal Endophytes in Grasses. Pp. 25-28.

Eisvand H, Tavakkol-Afshari R, Sharifzadeh F, Maddah Arefi H, Hesamzadeh Hejazi S 2010. Effects of hormonal priming and drought stress on activity and isozyme profiles of antioxidant enzymes in deteriorated seed of tall wheatgrass (*Agropyron elongatum* Host). Seed Science and Technology 38: 280-297.

El-Bashiti T, Hamamcı H, Öktem HA, Yücel M 2005. Biochemical analysis of trehalose and its metabolizing enzymes in wheat under abiotic stress conditions. Plant Science 169: 47-54.

Elbein AD, Pan Y, Pastuszak I, Carroll D 2003. New insights on trehalose: a multifunctional molecule. Glycobiology 13: 17R-27R.

Fang Z, Cui X 2011. Design and validation issues in RNA-seq experiments. Briefings in Bioinformatics. 12: 280-287.

Felitti S, Shields K, Ramsperger M et al. 2006. Transcriptome analysis of *Neotyphodium* and *Epichloë* grass endophytes. Fungal Genetics and Biology 43: 465-475.

Fletcher LR, Harvey I 1981. An association of a *Lolium* endophyte with ryegrass staggers. New Zealand Veterinary Journal 29: 185-186.

Fletcher LR 2010. Novel endophytes in New Zealand grazing systems: the perfect solution or a compromise? In: Young CA, Aiken GE, McCulley RL, Strickland JR, Schardl CL ed. Epichloae, Endophytes of Cool Season Grasses: Implications, Utilization and Biology. Proceedings of the 7th International Symposium on Fungal Endophytes of Grasses, Lexington, USA, Samuel Roberts Noble Foundation.

Foster AJ, Jenkinson JM, Talbot NJ 2003. Trehalose synthesis and metabolism are required at different stages of plant infection by *Magnaporthe grisea*. The EMBO Journal 22: 225-235.

Freeman EM 1904. The seed-fungus of *Lolium temulentum*, L., the Darnel. Philosophical Transactions of the Royal Society of London. Series B 196: 1-27.

Freitas P 2017. Crossing the species barrier: Investigating vertical transmission of a fungal endophyte from tall fescue within a novel ryegrass asscoiation. PhD thesis, Lincoln University.

Garcia Parisi PA, Casas C, Gundel PE, Omacini M 2012. Consequences of grazing on the vertical transmission of a fungal *Neotyphodium* symbiont in an annual grass population. Austral Ecology 37: 620-628.

Ghareeb HA, Becker A, Iven T, Feussner I, Schirawski J 2011. *Sporisorium reilianum* infection changes inflorescence and branching architectures of maize. Plant Physiology 156: 2037–2052.

Gibert A, Hazard L 2013. Genetically based vertical transmission drives the frequency of the symbiosis between grasses and systemic fungal endophytes. Journal of Ecology 101: 743-752.

Gladyshev MI, Artamonova VS, Makhrov AA, Sushchik NN, Kalachova GS, Dgebuadze YY 2017. Triploidy does not decrease contents of eicosapentaenoic and docosahexaenoic acids in filets of pink salmon *Oncorhynchus gorbuscha*. Food Chemistry 216: 66-69.

Goel A, Goel AK, Sheoran IS 2003. Changes in oxidative stress enzymes during artificial ageing in cotton *Gossypium hirsutum* L. seeds. Journal of Plant Physiology 160: 1093-1100.

Gómez-Gómez L, Boller T 2000. FLS2: an LRR receptor–like kinase involved in the perception of the bacterial elicitor flagellin in *Arabidopsis*. Molecular Cell 5: 1003-1011.

Granath G, Vicari M, Bazely DR, Ball JP, Puentes A, Rakocevic T 2007. Variation in the abundance of fungal endophytes in fescue grasses along altitudinal and grazing gradients. Ecography 30: 422-430.

Groppe K, Steinger T, Sanders I, Schmid B, Wiemken A, Boller T 1999. Interaction between the endophytic fungus *Epichloë bromicola* and the grass *Bromus erectus*: effects of endophyte infection, fungal concentration and environment on grass growth and flowering. Molecular Ecology 8: 1827-1835.

Güimil S, Chang H-S, Zhu T et al. 2005. Comparative transcriptomics of rice reveals an ancient pattern of response to microbial colonization. Proceedings of the National Academy of Sciences 102: 8066-8070.

Gundel PE, Maseda P, Vila-Aiub M, Ghersa C, Benech-Arnold R 2006. Effects of *Neotyphodium* fungi on *Lolium multiflorum* seed germination in relation to water availability. Annals of Botany 97: 571-577.

Gundel PE, Landesmann J, Martínez-Ghersa M, Ghersa C 2007. Effects of *Neotyphodium* endophyte infection on seed viability and germination vigor in *Lolium multiflorum* under accelerated ageing conditions. In: Popay A, Thom E ed. Proceedings of the 6th International Symposium on Fungal Endophytes of Grasses'. Grassland Research and Practice Series No. 13. Christchurch, New Zealand, New Zealand Grassland Association. Pp. 277–280.

Gundel PE, Batista WB, Texeira M, Martínez-Ghersa MA, Omacini M, Ghersa CM 2008. *Neotyphodium* endophyte infection frequency in annual grass populations: relative

importance of mutualism and transmission efficiency. Proceedings of the Royal Society of London B: Biological Sciences 275: 897-905.
Gundel PE, Martínez-Ghersa M, Garibaldi L, Ghersa C 2009a. Viability of *Neotyphodium* endophytic fungus and endophyte-infected and noninfected *Lolium multiflorum* seeds. Botany 87: 88-96.
Gundel PE, Garibaldi L, Tognetti P, Aragón R, Ghersa C, Omacini M 2009b. Imperfect vertical transmission of the endophyte *Neotyphodium* in exotic grasses in grasslands of the Flooding Pampa. Microbial Ecology 57: 740-748.
Gundel PE, Rudgers J, Ghersa C 2011a. Incorporating the process of vertical transmission into understanding of host–symbiont dynamics. Oikos 120: 1121-1128.
Gundel PE, Garibaldi L, Martínez-Ghersa M, Ghersa C 2011b. *Neotyphodium* endophyte transmission to *Lolium multiflorum* seeds depends on the host plant fitness. Environmental and Experimental Botany 71: 359-366.
Gundel PE, Martínez-Ghersa M, Omacini M et al. 2012. Mutualism effectiveness and vertical transmission of symbiotic fungal endophytes in response to host genetic background. Evolutionary Applications 5: 838-849.
Gundel PE, Rudgers JA, Whitney KD 2017. Vertically transmitted symbionts as mechanisms of transgenerational effects. American Journal of Botany 104: 787-792.
Guo F-Q, Crawford NM 2005. Arabidopsis nitric oxide synthase1 is targeted to mitochondria and protects against oxidative damage and dark-induced senescence. The Plant Cell 17: 3436-3450.
Gupta S, Bharalee R, Bhorali P et al. 2012. Identification of drought tolerant progenies in tea by gene expression analysis. Functional & Integrative Genomics 12: 543-563.
Gwinn KD, Collins-Shepard MH, Reddick BB 1991. Tissue print-immunoblot, an accurate method for the detection of *Acremonium coenophialum* in tall fescue. Phytopathology 81: 747-748.
Gwinn KD, Fribourg HA, Waller JC, Saxton AM, Smith MC 1998. Changes in *Neotyphodium coenophialum* infestation levels in tall fescue pastures due to different grazing pressures. Crop Science 38: 201-204.
Hahn H, Huth W, Schöberlein W, Diepenbrock W, Weber W 2003. Detection of endophytic fungi in *Festuca* spp. by means of tissue print immunoassay. Plant Breeding 122: 217-222.
Hair JF, Black WC, Babin BJ, Anderson RE, Tatham RL 1998. Multivariate data analysis. Upper Saddle River, USA, Prentice Hall.
Hannaway D, Fransen S, Cropper JB et al. 1999. Perennial ryegrass (*Lolium perenne* L.). Corvallis, USA, Oregon State University.
Hassid W, McCready R 1941. The molecular constitution of glycogen and starch from the seed of sweet corn (*Zea mays*). Journal of the American Chemical Society 63: 1632-1635.
Hause B, Maier W, Miersch O, Kramell R, Strack D 2002. Induction of jasmonate biosynthesis in arbuscular mycorrhizal barley roots. Plant Physiology 130: 1213-1220.
He L 2016. Drought tolerance of perennial ryegrass (*Lolium perenne* L.) and the role of *Epichloë* endophyte. PhD thesis, Massey University.
Hernández-Agramonte IM, Semmartin M 2016. The role of grazing intensity and preference on grass-fungal endophyte symbiosis in a Patagonian steppe. Journal of Arid Environments 134: 122-124.
Hiatt E, Hill N, Bouton J, Stuedemann J 1999. Tall fescue endophyte detection: commercial immunoblot test kit compared with microscopic analysis. Crop Science 39: 796-799.
Hilhorst HW 2007. Definitions and hypotheses of seed dormancy. In: Bradford K, Nonogaki H ed. Annual Plant Reviews Volume 27: Seed Development, Dormancy and Germination. Oxford, UK, Blackwell Publishing Ltd. Pp. 50-71.
Hill NS, Roach PK 2009. Endophyte survival during seed storage: endophyte-host interactions and heritability. Crop Science 49: 1425-1430.

Hinton D, Bacon C 1985. The distribution and ultrastructure of the endophyte of toxic tall fescue. Canadian Journal of Botany 63: 36-42.

Hooper T, Parrish CC 2009. Profiling neutral lipids in individual fish larvae by using short-column gas chromatography with flame ionization detection. Limnology and Oceanography: Methods 7: 411-428.

Hume DE, Barker DJ 2005. Growth and management of endophytic grasses in pastoral agriculture. *Neotyphodium* in Cool-Season Grasses. Iowa, USA, Blackwell Publishing Professional. Pp. 201-226.

Hume DE, Schmid J, Rolston M, Vijayan P, Hickey M 2011. Effect of climatic conditions on endophyte and seed viability in stored ryegrass seed. Seed Science and Technology 39: 481-489.

Hume DE, Card SD, Rolston MP 2013. Effects of storage conditions on endophyte and seed viability in pasture grasses. 22nd International Grassland Congress. Sydney, Australia. Pp. 405-408.

Hyde K, Soytong K 2008. The fungal endophyte dilemma. Fungal Diversity 33: e73.

Iannone LJ, Cabral D, Schardl CL, Rossi MS 2009. Phylogenetic divergence, morphological and physiological differences distinguish a new *Neotyphodium* endophyte species in the grass *Bromus auleticus* from South America. Mycologia 101: 340-351.

Iglesias AA, Preiss J 1992. Bacterial glycogen and plant starch biosynthesis. Biochemical Education 20: 196-203.

Jensen AMD, Roulund N 2004. Occurrence of *Neotyphodium* endophytes in permanent grassland with perennial ryegrass (*Lolium perenne*) in Denmark. Agriculture, Ecosystems & Environment 104: 419-427.

Jensen CS, Salchert K, Nielsen KK 2001. A TERMINAL FLOWER1-like gene from perennial ryegrass involved in floral transition and axillary meristem identity. Plant Physiology 125: 1517-1528.

Ji Y-l, Zhan L-h, Kang Y, Sun X-h, Yu H-s, Wang Z-w 2009. A new stromata-producing *Neotyphodium* species symbiotic with clonal grass *Calamagrostis epigeios* (L.) Roth. grown in China. Mycologia 101: 200-205.

Johnson HE, Lloyd AJ, Mur LA, Smith AR, Causton DR 2007. The application of MANOVA to analyse *Arabidopsis thaliana* metabolomic data from factorially designed experiments. Metabolomics 3: 517-530.

Johnson LJ, de Bonth AC, Briggs LR et al. 2013. The exploitation of epichloae endophytes for agricultural benefit. Fungal Diversity 60: 177-188.

Ju H, Hill N, Abbott T, Ingram K 2006. Temperature influences on endophyte growth in tall fescue. Crop Science 46: 404-412.

Jung SC, Martinez-Medina A, Lopez-Raez JA, Pozo MJ 2012. Mycorrhiza-induced resistance and priming of plant defenses. Journal of Chemical Ecology 38: 651-664.

Jürgens G, Ruiz RAT, Laux T, Mayer U, Berleth T 1994. Early events in apical-basal pattern formation in *Arabidopsis*. In: Coruzzi G, Puigdomènech P ed. Plant Molecular Biology. Berlin, Heidelberg, Springer. Pp. 95-103.

Kanehisa M, Goto S 2000. KEGG: kyoto encyclopedia of genes and genomes. Nucleic Acids Research 28: 27-30.

Kang Y, Ji Y, Zhu K, Wang H, Miao H, Wang Z 2011. A new *Epichloë* species with interspecific hybrid origins from *Poa pratensis* ssp. *pratensis* in Liyang, China. Mycologia 103: 1341-1350.

Kemp P, Matthew C, Lucas R 1999. Pasture species and cultivars. New Zealand Pasture and Crop Science 83-100.

Kidston R, Lang WH 1920. On Old Red Sandstone plants showing structure, from the Rhynie Chert Bed, Aberdeen-shire, Part IV. Restorations of the vascular cryptogams and discussion of their bearing on the general morphology of the Pteridophyta and the origin

of the organization of land-plants. Earth and Environmental Science Transactions of The Royal Society of Edinburgh 52: 603-627.
Kirkby K, Pratley J, Hume D, An M, Wu H 2011. Viability of seed and endophyte (*Neotyphodium occultans*) in annual ryegrass (*Lolium rigidum*) when buried and in long term storage. Seed Science and Technology 39: 452-464.
Koh S, Vicari M, Ball J et al. 2006. Rapid detection of fungal endophytes in grasses for large-scale studies. Functional Ecology 20: 736-742.
Koh S, Hik DS 2007. Herbivory mediates grass–endophyte relationships. Ecology 88: 2752-2757.
Koo AJ 2017. Metabolism of the plant hormone jasmonate: a sentinel for tissue damage and master regulator of stress response. Phytochemistry Reviews: 1-30.
Korb J, Aanen DK 2003. The evolution of uniparental transmission of fungal symbionts in fungus-growing termites (Macrotermitinae). Behavioral Ecology and Sociobiology 53: 65-71.
Kuldau G, Bacon C 2008. Clavicipitaceous endophytes: their ability to enhance resistance of grasses to multiple stresses. Biological Control 46: 57-71.
Kulkarni RK, Nielsen BD 1986. Nutritional requirements for growth of a fungus endophyte of tall fescue grass. Mycologia 78: 781-786.
Lahuta LB, Górecki RJ, Zalewski K, Hedley CL 2007. Sorbitol accumulation during natural and accelerated ageing of pea (*Pisum sativum* L.) seeds. Acta Physiologiae Plantarum 29: 527-534.
Lam CK, Belanger FC, White Jr JF, Daie J 1994. Mechanism and rate of sugar uptake by *Acremonium typhinum*, an endophytic fungus infecting *Festuca rubra*: evidence for presence of a cell wall invertase in endophytic fungi. Mycologia 86: 408-415.
Lancashire J 2006. The value of exotic germplasm to the NZ livestock industry. In: Mercer CF ed. Proceedings of the 13th Australasian Plant Breeding Conference. Christchurch, New Zealand, New Zealand Grassland Association. Pp 1431-1041.
Langer RHM 1979. How grasses grow. London, UK, Edward Arnold Ltd.
Larriba E, Jaime MD, Nislow C, Martín-Nieto J, Lopez-Llorca LV 2015. Endophytic colonization of barley (*Hordeum vulgare*) roots by the nematophagous fungus *Pochonia chlamydosporia* reveals plant growth promotion and a general defense and stress transcriptomic response. Journal of Plant Research 128: 665-678.
Larson L 1968. The effect soaking pea seeds with or without seedcoats has on seedling growth. Plant Physiology 43: 255-259.
Latch G 1983. Incidence of endophytes in seed lines and their control with fungicides. Proceedings of the New Zealand Grassland Association 44: 251-253.
Latch G, Christensen M 1985. Artificial infection of grasses with endophytes. Annals of Applied Biology 107: 17-24.
Law CW, Chen Y, Shi W, Smyth GK 2014. Voom: precision weights unlock linear model analysis tools for RNA-seq read counts. Genome Biology 15: R29.
Lee DK, Ahn S, Cho HY et al. 2016. Metabolic response induced by parasitic plant-fungus interactions hinder amino sugar and nucleotide sugar metabolism in the host. Scientific Reports 6: 37434.
Lehner A, Mamadou N, Poels P, Côme D, Bailly C, Corbineau F 2008. Changes in soluble carbohydrates, lipid peroxidation and antioxidant enzyme activities in the embryo during ageing in wheat grains. Journal of Cereal Science 47: 555-565.
Leopold AC 1980. Temperature effects on soybean imbibition and leakage. Plant Physiology 65: 1096-1098.
Leuchtmann A 1993. Systematics, distribution, and host specificity of grass endophytes. Natural Toxins 1: 150-162.
Leuchtmann A, Schardl CL, Siegel MR 1994. Sexual compatibility and taxonomy of a new species of *Epichloë* symbiotic with fine fescue grasses. Mycologia 86: 802-812.

Leuchtmann A, Schmidt D, Bush L 2000. Different levels of protective alkaloids in grasses with stroma-forming and seed-transmitted *Epichloë*/*Neotyphodium* endophytes. Journal of Chemical Ecology 26: 1025-1036.
Leuchtmann A, Oberhofer M 2013. The *Epichloë* endophytes associated with the woodland grass *Hordelymus europaeus* including four new taxa. Mycologia 105: 1315-1324.
Leuchtmann A, Bacon CW, Schardl CL, White Jr JF, Tadych M 2014. Nomenclatural realignment of *Neotyphodium* species with genus *Epichloë*. Mycologia 106: 202-215.
Leyronas C, Raynal G 2001. Presence of *Neotyphodium*-like endophytes in European grasses. Annals of Applied Biology 139: 119-127.
Li X, Zhou Y, Zhu M, Qin J, Ren A, Gao Y 2015. Stroma-bearing endophyte and its potential horizontal transmission ability in *Achnatherum sibiricum*. Mycologia 107: 21-31.
Li Z, Trick HN 2005. Rapid method for high-quality RNA isolation from seed endosperm containing high levels of starch. Biotechniques 38: 872.
Lian B, Zhou X, Miransari M, Smith D 2000. Effects of salicylic acid on the development and root nodulation of soybean seedlings. Journal of Agronomy and Crop Science 185: 187-192.
Liu F, Jenssen T-K, Trimarchi J et al. 2007. Comparison of hybridization-based and sequencing-based gene expression technologies on biological replicates. BMC Genomics 8: 153.
Liu H, Heckman JR, Murphy JA 1996. Screening fine fescues for aluminum tolerance. Journal of Plant Nutrition 19: 677-688.
Loake G, Grant M 2007. Salicylic acid in plant defence—the players and protagonists. Current Opinion in Plant Biology 10: 466-472.
Lohse M, Nagel A, Herter T et al. 2014. Mercator: a fast and simple web server for genome scale functional annotation of plant sequence data. Plant, Cell & Environment 37: 1250-1258.
López MF, Männer P, Willmann A, Hampp R, Nehls U 2007. Increased trehalose biosynthesis in Hartig net hyphae of ectomycorrhizas. New Phytologist 174: 389-398.
López-Ráez JA, Verhage A, Fernández I et al. 2010. Hormonal and transcriptional profiles highlight common and differential host responses to arbuscular mycorrhizal fungi and the regulation of the oxylipin pathway. Journal of Experimental Botany 61: 2589-2601.
Loveless A 1984. Consider the grasses. Journal of Biological Education 18: 156-160.
Lunn JE, Delorge I, Figueroa CM, Van Dijck P, Stitt M 2014. Trehalose metabolism in plants. The Plant Journal 79: 544-567.
Magi B, Liberatori S 2005. Immunoblotting techniques. Immunochemical Protocols 295: 227-254.
Majewska-Sawka A, Nakashima H 2004. Endophyte transmission via seeds of *Lolium perenne* L.: immunodetection of fungal antigens. Fungal Genetics and Biology 41: 534-541.
Malinowski DP, Belesky DP 1999. Tall fescue aluminum tolerance is affected by *Neotyphodium coenophialum* endophyte. Journal of Plant Nutrition 22: 1335-1349.
Malone JH, Oliver B 2011. Microarrays, deep sequencing and the true measure of the transcriptome. BMC Biology 9: 34.
Markmann K, Giczey G, Parniske M 2008. Functional adaptation of a plant receptor-kinase paved the way for the evolution of intracellular root symbioses with bacteria. PLoS Biology 6: e68.
Marks S, Clay K 1990. Effects of $CO_2$ enrichment, nutrient addition, and fungal endophyte-infection on the growth of two grasses. Oecologia 84: 207-214.
Mc Cargo PD, Iannone LJ, Vignale MV, Schardl CL, Rossi MS 2014. Species diversity of *Epichloë* symbiotic with two grasses from southern Argentinean Patagonia. Mycologia 106: 339-352.
McCallum H, Barlow N, Hone J 2001. How should pathogen transmission be modelled? Trends in Ecology & Evolution 16: 295-300.
McDonald M 1999. Seed deterioration: physiology, repair and assessment. Seed Science and Technology 27: 177-237.
McLennan JC 1920. Helium: its production and uses. Journal of the Chemical Society, Transactions 117: 923-947.

Medina JH, Gagnon H, Piché Y, Ocampo JA, Garcí JM, Vierheilig H 2003. Root colonization by arbuscular mycorrhizal fungi is affected by the salicylic acid content of the plant. Plant Science 164: 993-998.

Miao M, Li R, Jiang B, Cui SW, Lu K, Zhang T 2014. Structure and digestibility of endosperm water-soluble α-glucans from different sugary maize mutants. Food Chemistry 143: 156-162.

Milne G 2001. Tall fescue-dramatic changes. Proceedings of the 42nd Annual Conference of the Grassland Society of Victoria. Mornington, Australia, Grassland Society of Victoria. Pp. 60-69.

Miller DM, Redmonda CT, Flytheb MD, Potter DA 2017. Evaluation of 'Jackal' AR601 (Avanex) and Kentucky-31 endophytic tall fescues for suppressing types of invertebrates that contribute to bird strike hazard at airports. Crop, Forage & Turfgrass Management 3: In press.

Missaoui AM, Hill NS 2015. Use of accelerated aging as a surrogate phenotyping approach to improve endophyte survival during storage of tall fescue seed. Field Crops Research 183: 43-49.

Mjolsness E, Meyerowitz E, Gor V, Mann T 1999. Morphogenesis in plants: modeling the shoot apical meristem, and possible applications. Proceedings of the First NASA/DoD Workshop on Evolvable Hardware. Pasadena, USA. Pp. 139-144.

Moon CD, Scott B, Schardl CL, Christensen MJ 2000. The evolutionary origins of *Epichloë* endophytes from annual ryegrasses. Mycologia 92: 1103-1118.

Moon CD, Miles CO, Järlfors U, Schardl CL 2002. The evolutionary origins of three new *Neotyphodium* endophyte species from grasses indigenous to the Southern Hemisphere. Mycologia 94: 694-711.

Moon CD, Craven K, Leuchtmann A, Clement S, Schardl CL 2004. Prevalence of interspecific hybrids amongst asexual fungal endophytes of grasses. Molecular Ecology 13: 1455-1467.

Moon CD, Guillaumin JJ, Ravel C, Li C, Craven KD, Schardl CL 2007. New *Neotyphodium* endophyte species from the grass tribes Stipeae and Meliceae. Mycologia 99: 895-905.

Morán-Diez E, Rubio B, Domínguez S, Hermosa R, Monte E, Nicolás C 2012. Transcriptomic response of *Arabidopsis thaliana* after 24h incubation with the biocontrol fungus *Trichoderma harzianum*. Journal of Plant Physiology 169: 614-620.

Morita RY 1982. Starvation-survival of heterotrophs in the marine environment. In: Marshall KC ed. Advances in Microbial Ecology. Boston, USA, Springer. Pp. 171-198.

Morris DL, Morris CT 1939. Glycogen in the seed of *Zea mays* (variety golden bantam). Journal of Biological Chemistry 130: 535-544.

Morscher F, Kranner I, Arc E, Bailly C, Roach T 2015. Glutathione redox state, tocochromanols, fatty acids, antioxidant enzymes and protein carbonylation in sunflower seed embryos associated with after-ripening and ageing. Annals of Botany 116: 669-678.

Moy M, Belanger F, Duncan R et al. 2000. Identification of epiphyllous mycelial nets on leaves of grasses infected by clavicipitaceous endophytes. Symbiosis 28: 291-302.

Müller J, Boller T, Wiemken A 1995. Trehalose and trehalase in plants: recent developments. Plant Science 112: 1-9.

Mumford R, Walsh K, Barker I, Boonham N 2000. Detection of *Potato mop top virus* and *Tobacco rattle virus* using a multiplex real-time fluorescent reverse-transcription polymerase chain reaction assay. Phytopathology 90: 448-453.

Musgrave D, Fletcher L 1984. The development and application of ELISA detection of *Lolium* endophyte in ryegrass staggers research. Proceedings of the New Zealand Society of Animal Production 44: 185-188.

Nagabhyru P, Dinkins RD, Wood CL, Bacon CW, Schardl CL 2013. Tall fescue endophyte effects on tolerance to water-deficit stress. BMC Plant Biology 13: 127.

Nagalakshmi U, Waern K, Snyder M 2010. RNA-Seq: a method for comprehensive transcriptome analysis. Current Protocols in Molecular Biology: 4-11.

Nehls U 2008. Mastering ectomycorrhizal symbiosis: the impact of carbohydrates. Journal of Experimental Botany 59: 1097-1108.
Nehls U, Göhringer F, Wittulsky S, Dietz S 2010. Fungal carbohydrate support in the ectomycorrhizal symbiosis: a review. Plant Biology 12: 292-301.
Neill J 1940. The endophyte of Rye-Grass (*Lolium perenne*). New Zealand Journal of Science and Technology, Section A 21: 280-291.
Neill J 1942. The endophytes of *Lolium* and *Festuca*. New Zealand Journal of Science and Technology 23: 185-193.
New Zealand Plant Breeding and Research Association. 2016. NFVT Perennial ryegrass results - NZ. http://www.nzpbra.org/wp-content/uploads/2016-perennial-ryegrass-graphs.pdf
Ni D, Xu P, Gallagher S 2016. Immunoblotting and immunodetection. Current Protocols in Molecular Biology. Pp. 10.8. 1-10.8. 37.
Ni M, Yu J-H 2007. A novel regulator couples sporogenesis and trehalose biogenesis in *Aspergillus nidulans*. PLoS One 2: e970.
Njeru EM, Bocci G, Avio L et al. 2017. Functional identity has a stronger effect than diversity on mycorrhizal symbiosis and productivity of field grown organic tomato. European Journal of Agronomy 86: 1-11.
Nkoa R, Owen MD, Swanton CJ 2015. Weed abundance, distribution, diversity, and community analyses. Weed Science 63: 64-90.
Nomura T, Kono Y, Akazawa T 1969. Enzymic mechanism of starch breakdown in germinating rice seeds II. Scutellum as the site of sucrose synthesis. Plant Physiology 44: 765-769.
Novas MV, Collantes M, Cabral D 2007. Environmental effects on grass-endophyte associations in the harsh conditions of south Patagonia. FEMS Microbiology Ecology 61: 164-173.
Patchett B, Chapman R, Fletcher L, Gooneratne S 2008. Root loline concentration in endophyte-infected meadow fescue (*Festuca pratensis*) is increased by grass grub (*Costelytra zealandica*) attack. New Zealand Plant Protection 61: 210-214.
Pautler M, Tanaka W, Hirano H-Y, Jackson D 2013. Grass meristems I: shoot apical meristem maintenance, axillary meristem determinacy and the floral transition. Plant and Cell Physiology 54: 302-312.
Pennell C, Rolston P, De Bonth A, Simpson WR, Hume DE 2010. Development of a bird-deterrent fungal endophyte in turf tall fescue. New Zealand Journal of Agricultural Research 53: 145-150.
Pennell C, Rolston P 2011. AVANEX™ endophyte-infected grasses for the aviation industry now a reality. Bird Strike North America Conference. Canada: Niagara Falls, Birdstrike Committee.
Pennell C, Popay A, Rolston M, Townsend R, Lloyd-West C, Card SD 2015. Avanex Unique Endophyte Technology–a biological deterrent for the aviation industries. Environmental Entomology 45: 101-108.
Pennell C, Rolston M, Van Koten C, Hume D, Card SD 2017a. Reducing bird numbers at New Zealand airports using a unique endophyte product. New Zealand Plant Protection 70: 224-234.
Pennell C, Rolston M, Baird D, Hume D, McKenzie C, Card SD 2017b. Using novel-grass endophyte associations as an avian deterrent. New Zealand Plant Protection 70: 255-264.
Perreta MG, Ramos JC, Vegetti AC 2009. Development and structure of the grass inflorescence. The Botanical Review 75: 377-396.
Petrini O 1991. Fungal endophytes of tree leaves. In: Andrews J, Hirano S ed. Microbial Ecology of Leaves. Springer, New York, USA. Pp. 179-197.
Philipson MN, Christey MC 1986. The relationship of host and endophyte during flowering, seed formation, and germination of *Lolium perenne*. New Zealand Journal of Botany 24: 125-134.

Plett JM, Tisserant E, Brun A et al. 2015. The mutualist *Laccaria bicolor* expresses a core gene regulon during the colonization of diverse host plants and a variable regulon to counteract host-specific defenses. Molecular Plant-Microbe Interactions 28: 261-273.

Popay A, Hume D, Baltus J et al. 1999. Field performance of perennial ryegrass (*Lolium perenne*) infected with toxin-free fungal endophytes (*Neotyphodium* spp.). In: Woodfield D, Matthew C ed. Ryegrass Endophyte: an Essential New Zealand Symbiosis. Grassland Research and Practice Series 7. Pp. 113-122.

Popay A, Hume D 2011. Endophytes improve ryegrass persistence by controlling insects. In: Mercer CF ed. Pasture Persistence Symposium. Grassland Research and Practice Series 15. Pp 149–156.

Portarena S, Baldacchini C, Brugnoli E 2017. Geographical discrimination of extra-virgin olive oils from the Italian coasts by combining stable isotope data and carotenoid content within a multivariate analysis. Food Chemistry 215: 1-6.

Powell PO, Sullivan MA, Sweedman MC, Stapleton DI, Hasjim J, Gilbert RG 2014. Extraction, isolation and characterisation of phytoglycogen from su-1 maize leaves and grain. Carbohydrate Polymers 101: 423-431.

Pozo MJ, Van Loon L, Pieterse CM 2004. Jasmonates-signals in plant-microbe interactions. Journal of Plant Growth Regulation 23: 211-222.

Pozo MJ, López-Ráez JA, Azcón-Aguilar C, García-Garrido JM 2015. Phytohormones as integrators of environmental signals in the regulation of mycorrhizal symbioses. New Phytologist 205: 1431-1436.

Prestidge R, Gallagher R 1988. Endophyte fungus confers resistance to ryegrass: Argentine stem weevil larval studies. Ecological Entomology 13: 429-435.

Priestley DA 1986. Seed Aging: Implications for Seed Storage and Persistence in the Soil. Ithaca, USA, Comstock Publishing Associates.

Pukacka S, Ratajczak E 2007. Age-related biochemical changes during storage of beech (*Fagus sylvatica* L.) seeds. Seed Science Research 17: 45-53.

Quevillon E, Silventoinen V, Pillai S et al. 2005. InterProScan: protein domains identifier. Nucleic Acids Research 33: W116-W120.

Ralphs M, Cook D, Gardner D, Grum D 2011. Transmission of the locoweed endophyte to the next generation of plants. Fungal Ecology 4: 251-255.

Rasmussen S, Parsons A, Bassett S et al. 2007. High nitrogen supply and carbohydrate content reduce fungal endophyte and alkaloid concentration in *Lolium perenne*. New Phytologist 173: 787-797.

Rasmussen S, Parsons AJ, Fraser K, Xue H, Newman JA 2008. Metabolic profiles of *Lolium perenne* are differentially affected by nitrogen supply, carbohydrate content, and fungal endophyte infection. Plant Physiology 146: 1440-1453.

Ravel C, Michalakis Y, Charmet G 1997. The effect of imperfect transmission on the frequency of mutualistic seed-borne endophytes in natural populations of grasses. Oikos 80: 18-24.

Ren A, Li C, Gao Y 2011. Endophytic fungus improves growth and metal uptake of *Lolium arundinaceum* Darbyshire ex. Schreb. International Journal of Phytoremediation 13: 233-243.

Reza Sabzalian M, Mirlohi A 2010. *Neotyphodium* endophytes trigger salt resistance in tall and meadow fescues. Journal of Plant Nutrition and Soil Science 173: 952-957.

Richardson MD, Chapman G, Hoveland C, Bacon C 1992. Sugar alcohols in endophyte-infected tall fescue under drought. Crop Science 32: 1060-1061.

Richardson MD, Logendra S 1997. Ergosterol as an indicator of endophyte biomass in grass seeds. Journal of Agricultural and Food Chemistry 45: 3903-3907.

Robinson MD, Oshlack A 2010. A scaling normalization method for differential expression analysis of RNA-seq data. Genome Biology 11: R25.

Rolston M, Hare M, Moore K, Christensen M 1986. Viability of *Lolium* endophyte fungus in seed stored at different moisture contents and temperatures. New Zealand Journal of Experimental Agriculture 14: 297-300.

Rolston M, Agee C 2007. Delivering quality seed to specification-the USA and NZ novel endophyte experience. In: Popay A, Thom E ed. Proceedings of the 6th International Symposium on Fungal Endophytes of Grasses. Dunedin, New Zealand, New Zealand Grassland Association. Pp. 229-231.

Rowan DD, Gaynor DL 1986a. Isolation of feeding deterrents against Argentine stem weevil from ryegrass infected with the endophyte *Acremonium loliae*. Journal of Chemical Ecology 12: 647-658.

Rowan DD, Hunt MB, Gaynor DL 1986b. Peramine, a novel insect feeding deterrent from ryegrass infected with the endophyte *Acremonium loliae*. Journal of the Chemical Society, Chemical Communications: 935-936.

Rudgers JA, Fischer S, Clay K 2010. Managing plant symbiosis: fungal endophyte genotype alters plant community composition. Journal of Applied Ecology 47: 468-477.

Saikkonen K, Wäli PR, Helander M 2010. Genetic compatibility determines endophyte-grass combinations. PLoS One 5: e11395.

Saito K, Kuga-Uetake Y, Saito M, Peterson RL 2006. Vacuolar localization of phosphorus in hyphae of *Phialocephala fortinii*, a dark septate fungal root endophyte. Canadian Journal of Microbiology 52: 643-650.

Sampson K 1933. The systemic infection of grasses by *Epichloe typhina* (Pers.) Tul. Transactions of the British Mycological Society 18: 30-47.

Sardouie-Nasab S, Mohammadi-Nejad G, Nakhoda B 2014. Field screening of salinity tolerance in Iranian bread wheat lines. Crop Science 54: 1489-1496.

Schardl CL 2001. *Epichloë festucae* and related mutualistic symbionts of grasses. Fungal Genetics and Biology 33: 69-82.

Schardl CL, Leuchtmann A, Spiering M 2004. Symbioses of grasses with seedborne fungal endophytes. Annual Review of Plant Biology 55: 315-340.

Schardl CL, Leuchtmann A 2005. The *Epichloë* endophytes of grasses and the symbiotic continuum. In: Dighton J, White Jr J, White J, Oudemans F ed. The Fungal Community: Its Organization and Role in the Ecosystem. New Delhi, India, Taylor & Francis. Pp. 475-503.

Schardl CL, Craven KD, Speakman S, Stromberg A, Lindstrom A, Yoshida R 2008. A novel test for host-symbiont codivergence indicates ancient origin of fungal endophytes in grasses. Systematic Biology 57: 483-498.

Schardl CL, Young CA, Hesse U et al. 2013. Plant-symbiotic fungi as chemical engineers: multi-genome analysis of the Clavicipitaceae reveals dynamics of alkaloid loci. PLoS Genetics 9: e1003323.

Schiestl FP, Steinebrunner F, Schulz C et al. 2006. Evolution of 'pollinator'-attracting signals in fungi. Biology Letters 2: 401-404.

Secks ME, Richardson MD, West CP, Marlatt ML, Murphy JB 1999. Role of trehalose in desiccation tolerance of endophyte-infected tall fescue. Horticultural Studies 475: 134.

Shachar-Hill Y, Pfeffer PE, Douds D, Osman SF, Doner LW, Ratcliffe RG 1995. Partitioning of intermediary carbon metabolism in vesicular-arbuscular mycorrhizal leek. Plant Physiology 108: 7-15.

Shen C, Li D, He R et al. 2014. Comparative transcriptome analysis of RNA-seq data for cold-tolerant and cold-sensitive rice genotypes under cold stress. Journal of Plant Biology 57: 337-348.

Siegel MR, Latch GCM, Johnson MC 1985. *Acremonium* fungal endophytes of tall fescue and perennial ryegrass: significance and control. Plant Disease 69: 179-181.

Simpson W, Schmid J, Singh J, Faville M, Johnson R 2012. A morphological change in the fungal symbiont *Neotyphodium lolii* induces dwarfing in its host plant *Lolium perenne*. Fungal Biology 116: 234-240.

Skorupa M, Gołębiewski M, Domagalski K et al. 2016. Transcriptomic profiling of the salt stress response in excised leaves of the halophyte *Beta vulgaris* ssp. *maritima*. Plant Science 243: 56-70.

Smith K, Bacon C, Luttrell E 1985. Reciprocal translocation of carbohydrates between host and fungus in bahiagrass infected with *Myriogenospora atramentosa*. Phytopathology 75: 407-411.

Stewart A 2006. Genetic origins of New Zealand perennial ryegrass (*Lolium perenne*) cultivars. In: Mercer C ed. Proceedings of the 13th Australasian Plant Breeding Conference. Christchurch, New Zealand. Pp. 11-20.

Sun J, Cardoza V, Mitchell DM, Bright L, Oldroyd G, Harris JM 2006. Crosstalk between jasmonic acid, ethylene and Nod factor signaling allows integration of diverse inputs for regulation of nodulation. The Plant Journal 46: 961-970.

Sun WQ, Leopold AC 1993. The glassy state and accelerated aging of soybeans. Physiologia Plantarum 89: 767-774.

Sun WQ, Leopold AC 1995. The Maillard reaction and oxidative stress during aging of soybean seeds. Physiologia Plantarum 94: 94-104.

Tadych M, Bergen MS, White Jr JF 2014. *Epichloë* spp. associated with grasses: new insights on life cycles, dissemination and evolution. Mycologia 106: 181-201.

Tan Y, Spiering M, Scott V, Lane G, Christensen M, Schmid J 2001. In planta regulation of extension of an endophytic fungus and maintenance of high metabolic rates in its mycelium in the absence of apical extension. Applied and Environmental Microbiology 67: 5377-5383.

Tanaka A, Tapper BA, Popay A, Parker EJ, Scott B 2005. A symbiosis expressed non-ribosomal peptide synthetase from a mutualistic fungal endophyte of perennial ryegrass confers protection to the symbiotum from insect herbivory. Molecular Microbiology 57: 1036-1050.

Tanaka A, Takemoto D, Chujo T, Scott B 2012. Fungal endophytes of grasses. Current Opinion in Plant Biology 15: 462-468.

Tanaka Y, Ito T, Akazawa T 1970. Enzymic mechanism of starch breakdown in germinating rice seeds III. α-Amylase isozymes. Plant Physiology 46: 650-654.

Taylor R, Inamine G, Anderson JD 1993. Tissue printing as a tool for observing immunological and protein profiles in young and mature celery petioles. Plant Physiology 102: 1027-1031.

Thines E, Weber R, Talbot N 2000. MAP kinase and protein kinase A–dependent mobilization of triacylglycerol and glycogen during appressorium turgor generation by *Magnaporthe grisea*. The Plant Cell Online 12: 1703-1718.

Thom ER, Popay AJ, Hume DE, Fletcher LR 2013. Evaluating the performance of endophytes in farm systems to improve farmer outcomes–a review. Crop and Pasture Science 63: 927-943.

Thrower L, Lewis D 1973. Uptake of sugars by *Epichloe typhina* (Pers. Ex Fr.) Tul. in culture and from its host, *Agrostis stolonifera* L. New Phytologist 72: 501-508.

Tian P, Le T, Smith K, Forster J, Guthridge K, Spangenberg G 2013. Stability and viability of novel perennial ryegrass host–*Neotyphodium* endophyte associations. Crop and Pasture Science 64: 39-50.

Tian T, Liu Y, Yan H et al. 2017. agriGO v2. 0: a GO analysis toolkit for the agricultural community, 2017 update. Nucleic Acids Research 45: W122–W129.

Tibbett M, Sanders F, Cairney J 2002. Low-temperature-induced changes in trehalose, mannitol and arabitol associated with enhanced tolerance to freezing in ectomycorrhizal basidiomycetes (*Hebeloma* spp.). Mycorrhiza 12: 249-255.

Todd D 1988. The effects of host genotype, growth rate, and needle age on the distribution of a mutualistic, endophytic fungus in Douglas-fir plantations. Canadian Journal of Forest Research 18: 601-605.
Tracey TJ, Ellickson JL, Sherry P 1989. Reactance in relation to different supervisory environments and counselor development. Journal of Counseling Psychology 36: 336.
Tupper-Carey R, Priestley J 1923. The composition of the cell-wall at the apical meristem of stem and root. Proceedings of the Royal Society of London Series B 95: 109-131.
Ulrich E, Perkins L 2014. *Bromus inermis* and *Elymus canadensis* but not *Poa pratensis* demonstrate strong competitive effects and all benefit from priority. Plant Ecology 215: 1269-1275.
Vandemark G, Barker B, Gritsenko M 2002. Quantifying *Aphanomyces euteiches* in alfalfa with a fluorescent polymerase chain reaction assay. Phytopathology 92: 265-272.
Velculescu VE, Zhang L, Vogelstein B, Kinzler KW 1995. Serial analysis of gene expression. Science 270: 484.
Vertucci CW 1989. The kinetics of seed imbibition: controlling factors and relevance to seedling vigor. Seed Moisture. Madison, USA, Crop Science Society of America. Pp. 93-115.
Vogl A 1898. Mehl und die anderen Mehlprodukte der Cerealien und Leguminosen. Zeitschrift Nahrungsmittle Untersuchung Hyg Warenkunde 12: 25-29.
Wang G, Wang G, Zhang X, Wang F, Song R 2012. Isolation of high quality RNA from cereal seeds containing high levels of starch. Phytochemical Analysis 23: 159-163.
Wang M 2014. The effect of applications of different nitrogen types and potassium on seed quality and AR37 endophyte presence at different spikelet and floret positions of perennial ryegrass cv. Halo. Masters thesis, Massey University.
Wang Z, Gerstein M, Snyder M 2009. RNA-Seq: a revolutionary tool for transcriptomics. Nature Reviews Genetics 10: 57-63.
Wasternack C 2007. Jasmonates: an update on biosynthesis, signal transduction and action in plant stress response, growth and development. Annals of Botany 100: 681-697.
Watkin B 1975. The performance of pasture species in Canterbury. Proceedings of the New Zealand Grassland Association 36: 180-190.
Weinberger F, Pohnert G, Berndt M-L, Bouarab K, Kloareg B, Potin P 2005. Apoplastic oxidation of L-asparagine is involved in the control of the green algal endophyte *Acrochaete operculata* Correa & Nielsen by the red seaweed *Chondrus crispus* Stackhouse. Journal of Experimental Botany 56: 1317-1326.
Welty R, Azevedo M, Cooper T 1987. Influence of moisture content, temperature, and length of storage on seed germination and survival of endophytic fungi in seeds of tall fescue and perennial ryegrass. Phytopathology 77: 893-900.
Wettlaufer SH, Leopold AC 1991. Relevance of Amadori and Maillard products to seed deterioration. Plant Physiology 97: 165-169.
Whaley WG, Mollenhauer HH, Leech JH 1960. The ultrastructure of the meristematic cell. American Journal of Botany: 401-449.
Wheatley W, Kemp H, Simpson W et al. 2007. Viability of endemic endophyte (*Neotyphodium lolii*) and perennial ryegrass (*Lolium perenne*) seed at retail and wholesale outlets in south-eastern Australia. Seed Science and Technology 35: 360-370.
White Jr JF, Chambless DA 1991. Endophyte-host associations in forage grasses. XV. Clustering of stromata-bearing individuals of *Agrostis hiemalis* infected by *Epichloe typhina*. American Journal of Botany 78: 527-533.
White Jr JF, Morgan-Jones G, Morrow A 1993. Taxonomy, life cycle, reproduction and detection of *Acremonium* endophytes. Agriculture, Ecosystems & Environment 44: 13-37.
Wiemken A 1990. Trehalose in yeast, stress protectant rather than reserve carbohydrate. Antonie van Leeuwenhoek 58: 209-217.
Wilhelm BT, Marguerat S, Goodhead I, Bähler J 2010. Defining transcribed regions using RNA-seq. Nature Protocols 5: 255-266.

Wilson A 1996. Resources and testing of endophyte-infected germplasm in national grass repository collections. In: Redlin S, Carris L ed. Endophytic Fungi in Grasses and Woody Plants. St. Paul, USA, APS Press. Pp. 179-195.

Wilson WA, Roach PJ, Montero M et al. 2010. Regulation of glycogen metabolism in yeast and bacteria. FEMS Microbiology Reviews 34: 952-985.

Wu Y, Guo J, Cai Y et al. 2016. Genome-wide identification and characterization of *Eutrema salsugineum* microRNAs for salt tolerance. Physiologia Plantarum 157: 453-468.

Xia J, Sinelnikov IV, Han B, Wishart DS 2015. MetaboAnalyst 3.0—making metabolomics more meaningful. Nucleic Acids Research 43: W251-W257.

Xu G, Singh S, Barnaby J, Buyer J, Reddy V, Sicher R 2016. Effects of growth temperature and carbon dioxide enrichment on soybean seed components at different stages of development. Plant Physiology and Biochemistry 108: 313-322.

Xu M, Li Y, Zheng Z, Dai Z, Tao Y, Deng X 2015. Transcriptional analyses of mandarins seriously infected by '*Candidatus* Liberibacter asiaticus'. PLoS One 10: e0133652.

Xu X, Monger W, Ritieni A, Nicholson P 2007. Effect of temperature and duration of wetness during initial infection periods on disease development, fungal biomass and mycotoxin concentrations on wheat inoculated with single, or combinations of, *Fusarium* species. Plant Pathology 56: 943-956.

Ye Z-H, Varner JE 1991. Tissue-specific expression of cell wall proteins in developing soybean tissues. The Plant Cell 3: 23-37.

Yin L, Ren A, Wei M et al. 2014. *Neotyphodium coenophialum*-infected tall fescue and its potential application in the phytoremediation of saline soils. International Journal of Phytoremediation 16: 235-246.

Yin X, He D, Gupta R, Yang P 2015. Physiological and proteomic analyses on artificially aged *Brassica napus* seed. Frontiers in Plant Science 6: article 112.

Young C, Bryant M, Christensen M, Tapper B, Bryan G, Scott B 2005. Molecular cloning and genetic analysis of a symbiosis-expressed gene cluster for lolitrem biosynthesis from a mutualistic endophyte of perennial ryegrass. Molecular Genetics and Genomics 274: 13-29.

Yu C, Xu S, Yin Y 2016. Transcriptome analysis of the *Taxodium* 'Zhongshanshan 405'roots in response to salinity stress. Plant Physiology and Biochemistry 100: 156-165.

Zadoks JC, Chang TT, Konzak CF 1974. A decimal code for the growth stages of cereals. Weed Research 14: 415-421.

Zhang W, Card SD, Mace WJ, Christensen MJ, McGill CR, Matthew C 2017. Defining the pathways of symbiotic *Epichloë* colonization in grass embryos with confocal microscopy. Mycologia 109: 153-161.

Zhang X, Ren A, Ci H, Gao Y 2010. Genetic diversity and structure of *Neotyphodium* species and their host Achnatherum sibiricum in a natural grass–endophyte system. Microbial Ecology 59: 744-756.

Zhou M, Baudry M 2006. Developmental changes in NMDA neurotoxicity reflect developmental changes in subunit composition of NMDA receptors. The Journal of Neuroscience 26: 2956-2963.

Zhou R, Quebedeaux B 2003. Changes in photosynthesis and carbohydrate metabolism in mature apple leaves in response to whole plant source-sink manipulation. Journal of the American Society for Horticultural Science 128: 113-119.

Zhou Y, Bradshaw R, Johnson R, Hume D, Simpson W, Schmid J 2014. Detection and quantification of three distinct *Neotyphodium lolii* endophytes in *Lolium perenne* by real time PCR of secondary metabolite genes. Fungal Biology 118: 316-324.

Zouari I, Salvioli A, Chialva M et al. 2014. From root to fruit: RNA-Seq analysis shows that arbuscular mycorrhizal symbiosis may affect tomato fruit metabolism. BMC Genomics 15: 221.